GROUNDWATER 1

Studies in Hydrogeology

AUSTRALIA

HYDROGEOCHEMISTRY OF THE UPPER HUNTER RIVER VALLEY, NSW

J. K. KELLETT, B. G. WILLIAMS & J. K. WARD

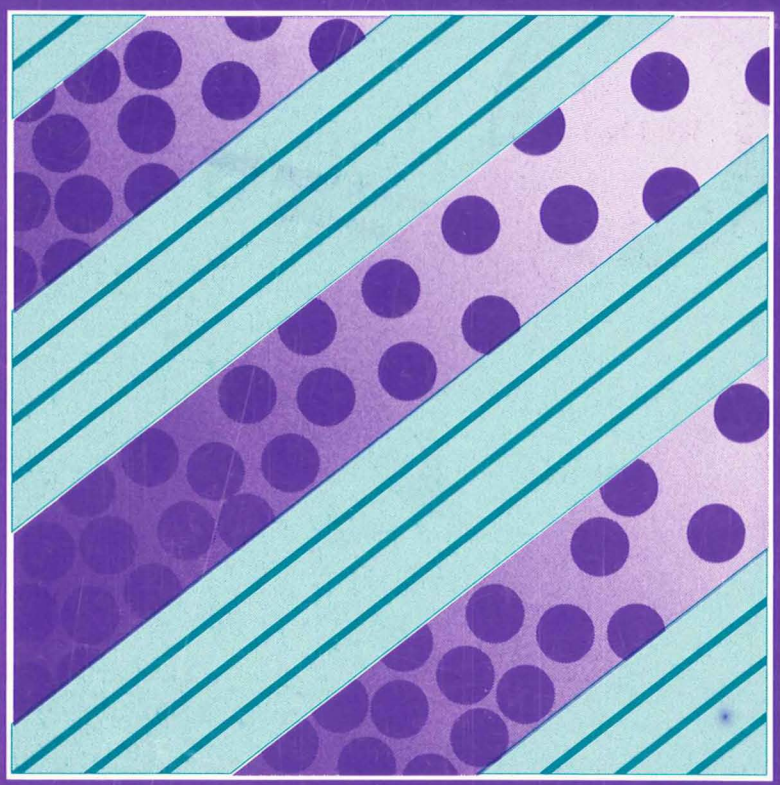

BUREAU OF MINERAL RESOURCES, GEOLOGY & GEOPHYSICS

DIVISION OF CONTINENTAL GEOLOGY

RECORD 1987/23

1987/23
Copy 3

DEPARTMENT OF RESOURCES & ENERGY

BUREAU OF MINERAL RESOURCES, GEOLOGY AND GEOPHYSICS

RECORD 1987/23

Hydrogeochemistry of the upper Hunter River valley, New South Wales

J.R.. Kellett[1], B.G. Williams[2] & J.K. Ward[2]

1. BMR Division of Continental Geology
2. CSIRO Department of Water and Land Resources

Note: This item contains some inconsistencies in pagination.

FOREWORD

This is the first of a new series of groundwater reports produced by the Hydrogeology Group of the BMR Division of Continental Geology. The need for the new series is a reflection of the increasing importance of groundwater at the national level. In attempting to respond to this high priority BMR has allocated increased resources to groundwater research and additional funds have also been provided through the Federal Water Resources Assistance Program (FWRAP).

Most of BMR's groundwater efforts must of necessity be directed toward the Murray Basin and therefore in this respect this first report is somewhat atypical of the majority of the reports that will be produced in the next few years.

However, there are many parts of Australia where there are major groundwater resources where supplies are becoming under increasing stress or where there are potential or actual environmental problems related to groundwater. The Hunter Valley is one such area.

The upper Hunter Valley area is one of Australia's most important mining, industrial and agricultural regions. The demand of these three activites on the groundwater resources of the area are adversely affecting groundwater resources and their quality.

Unless these water resources are carefully managed in the future it is evident that there may be increasing problems with providing adequate supplies of good quality water to the region. Coupled with this, there are emerging problems with increasing land and river salinity.

Future management options will require detailed information on the hydrogeology of the region including data on fluxes, flow paths and residence times of groundwater. With this in mind, the BMR and CSIRO undertook a major hydrochemical study of the upper Hunter Valley. This report documents the results of that study and clearly demonstrates that whilst man's activities are having and will continue to have, a profound effect on water quality in the region, it must also be recognized that saline groundwaters are a natural phenomenon of the Central Lowlands region and that they will continue to contribute a significant quantity of salt into the total groundwater and associated surface water systems.

It is clear that future salinity control measures will require even more detailed information on the chemistry of the Hunter River and that of the return water flows to it in order to safeguard this area of enormous economic importance and great natural beauty.

Peter J. Cook
Chief,
Division of Continental Geology.

CONTENTS

TABLES

12. Principal components extracted from covariance and correlation matrices of upper Hunter River valley hydrochemical provinces.

13. Comparison of chemical facies from significant $Y_3(S)$ loadings for upper Hunter River valley hydrochemical province.

14. Correlations of principal components from pooled covariance matrix of upper Hunter River valley hydrochemical provinces.

15. Comparison of chemical facies from significant $Y_3(R)$ loadings from upper Hunter River valley hydrochemical provinces.

16. Correlations of principal component scores from pooled correlation matrix of upper Hunter River valley hydrochemical provinces.

17. Angles between corresponding sets of principal components derived from S and R matrices of six $\log_{10}$- transformed variables, upper Hunter valley groundwaters.

FIGURES

18a Longitudinal variations in concentrations of major ions, Bowmans Creek; 13, 14/8/82

18b Longitudinal variations in concentrations of major ions, Swamp Creek; 15/8/82

18c Longitudinal variations in concentrations of major ions, Muscle Creek; 20/8/82

18d Longitudinal variation in concentrations of major ions, Stringybark Creek; 20/6/83

18e Longitudinal variations in concentrations of major ions and decline in HCO_3^-/Cl^- ratio, Goorangoola Creek; 16/8/82

19a Longitudinal variations in concentrations of major ions, Main Creek; 17/8/82

19b Longitudinal variations in concentrations of major ions, Loder Creek; 9, 10/8/82

20a Longitudinal variations in concentrations of major ions, Spring Creek; 11-12/8/82

20b Longitudinal variations in concentrations of major ions, Big Flat Creek; 29/6/83

21 Distribution of Disequilibrium Indices for the simple carbonate minerals calcite, magnesite and natron in Upper Hunter groundwaters

22 Distribution of calcite and magnesite and natron Disequilibrium Indices by hydrochemical province

33a) The effect on calcite Disequilibrium Index values for WO and
33b) GM groundwaters upon reaching equilibrium with atmospheric carbon dioxide

33c) The effect of sepiolite Disequilibrium Index values for WO
33b) and GM groundwaters upon reaching equilibrium with atmospheric carbon dioxide

34. Stability fields of some minerals in the Ca-Al-Si-H_2O system at 25°C as a function of Ca^{2+}, H^+ and soluble SiO_2. Points are from the upper Hunter Valley groundwaters and boundaries are from thermodynamic data of Stumm and Morgan (1970).

35. The relationship between the calcite Disequilibrium Index and the tendency for Ca-montmorillonite to form a stable phase in the upper Hunter Valley groundwaters.

36. Stability fields of some minerals in the Na-Al-Si-H_2O system at 25°C as a function of Na^+, H^+ and soluble SiO_2. Points are from the upper Hunter Valley groundwaters and boundaries (a) from thermodynamic data of Rai and Lindsay (1975) and (b) Stumm and Morgan (1970)

37. Stability fields of some minerals in the K-Al-Si-H_2O system at 25°C as a function of K^+, H^+ and soluble SiO_2. Points are from upper Hunter Valley groundwaters and boundaries (a) from thermodynamic data of Garrels and Christ (1965) and (b) from Rai and Lindsay (1975).

38. Canonical variate plot showing salinity and facies variations of upper Hunter Valley groundwaters. Based on six $\log_{10}$- transformed variables. Ninety-five per cent confidence circles shown

39. Canonical variate plot showing facies and silicate dissolution variations of upper Hunter Valley groundwaters. Based on 6 $\log_{10}$- transformed variables. Ninety-five per cent confidence circles shown

40. Complete linkage dendrogram of upper Hunter Valley hydrochemical provinces based on 6 $\log_{10}$- tranformed variables

41. Canonical variate plot showing salinity and facies variations of 25 subgroups of upper Hunter Valley groundwaters. Based on 6 $\log_{10}$- transformed variables. Ninety-five per cent confidence circles shown.

42. Complete linkage dendrogram of 25 subgroups of upper Hunter Valley groundwaters based on 6 $\log_{10}$- transformed variables

43a CARB-TRIAS)
43b WO)
43c HFP1) Clustering by principal component scores of
43d HFP2) salinity and facies variations for 670
43e WI1) individuals of upper Hunter Valley ground-
43f WI2) waters. Based on 6 $\log_{10}$- transformed
43g GM) variables. Principal components from pooled correlation matrix
43h Hydrochemical processes represented by principal component scores. Mean scores of hydrochemical provinces shown.

44a HFP1) Discrimination of zones of hydrodynamic mixing of
44b HFP2) Upper Hunter Valley groundwaters by principal
44c WO) component scores. Based on 6 $\log_{10}$- transformed
44d WI1) variables measured on 670 individuals. Principal components from pooled correlation matrix. Mean scores of hydrochemical provinces shown

PLATES

ABSTRACT

The chemistry of groundwaters in the regional recharge zones of Triassic and Carboniferous rocks in the upper Hunter River valley of New South Wales is strongly influenced by the processes of silicate and carbonate dissolution/precipitation reactions, ion exchange and dispersion of aerosols in infiltrated rainfall. The Wollombi Coal Measures and Jerrys Plains Subgroup of the Wittingham Coal Measures west of the Muswellbrook Anticline constitute the regional groundwater transmission zones, and the processes which exert the greatest influence on the chemistry of their waters include dissolution/precipitation reactions and oxidation of coals. The semi-confined aquifers of the Greta Coal Measures, Maitland Group, Dalwood Group and Wittingham Coal Measures in the eastern and southern parts of the valley discharge into unconfined sand and gravel aquifers of the Hunter River floodplain. These Permian rocks are the source of the most saline waters in the valley, and the chemical make-up of their groundwaters is largely determined by oxidation of sulphides and molecular diffusion of connate marine salts, a legacy of periodic immersion by Permian ocean waters. Disequilibrium indices for calcite, dolomite and dawsonite indicate that these carbonates are being precipitated today in the groundwater of the Central Lowlands provinces; they are being dissolved in the southern and western groundwater recharge zones and are in equilibrium with waters of the northern recharge zone. The iron carbonates, siderite and ankerite are a product of a palaeohydrochemical regime characterised by saline alkaline waters rich in dissolved iron disseminated from gels originally accumulated in the Permian peat swamps, but these minerals are not being precipitated in modern Upper Hunter valley groundwaters. The sulphate minerals, gypsum, thenardite and bloedite, occur extensively in salt efflorescences in the Permian rocks of the Central Lowlands but their disequilibrium indices show that none of the minerals can be precipitated in the contemporary upper Hunter groundwaters by processes other than evaporative concentration. Models based on incongruent dissolution of feldspars allocate many of the upper Hunter groundwaters to the kaolinite stability field which is consistent with the observed abundance of kaolinite as an

authigenic mineral in the fractured rock aquifers. Silica and cations leached from the fractured rocks are accumulating in the groundwater sinks around the margins of the Hunter River floodplain as indicated by the large proportion of groundwaters in these areas which are in equilibrium with Ca-montmorillonite. Concentrations of Ca^{2+}, SiO_2 and HCO_3^- ions in upper Hunter groundwaters approach log-normal distributions and these species are most highly identified with continental hydrochemical processes. In contrast the four 'elements' comprising the bulk of solutes in ocean water - Cl^-, Na^+, SO_4^{2-} and Mg^{2+}, are distributed in two modes: the low-concentration primary modes representing the dissemination of these species from the continental solute store, and the secondary high-concentration modes reflecting diffusion and oxidation of marine inputs. On a province-wide scale, composition diagrams of solute behaviour identify the Wittingham Coal Measures to the east and south of Muswellbrook Anticline, Greta Coal Measures and the Maitland and Dalwood Groups as systems which can be approximated by simple linear mixing models between meteoric and oceanic waters. Composition diagrams for the floodplain hydrochemical provinces show that the alluvial aquifers can be represented as mixing systems between Hunter River surface waters and groundwaters of the fractured-rock aquifers. Principal components analyses describe the chemical evolution of upper Hunter groundwaters from the Permian marine transgression through to the present continental leaching regime - for similar positions along flow lines in discharge zones, groundwaters of the Greta Coal Measures, Maitland Group and Wittingham Coal Measures east of the Muswellbrook Anticline have not advanced past the first stage of the evolutionary sequence Na^+-Cl^- → Na^+-HCO_3^- → Ca^{2+}-HCO_3^-; groundwaters of the Wittingham Coal Measures west of the Muswellbrook Anticline have attained the second stage of this evolution as a consequence of a longer history of flushing by meteoric waters and prior thermal mobilisation of interstitial fluids in areas peripheral to Tertiary dolerite intrusives. Discrimination of hybrids according to their first and second principal component scores shows that in the floodplain alluvium, significant inputs of groundwaters with the chemical signature of Maitland Group rocks emanate from the Aberdeen and Hunter Thrust Faults, the Hilliers Creek Valley and the Neotsfield area. Inputs of groundwaters from the Wittingham Coal Measures occur at Jerrys Plains and Alcheringa; the latter mixing zone is of special significance because the source is sufficiently strong to overprint the

role of the Hunter River as a dividing streamline for groundwater flow. The strongest sources of Wittingham groundwaters are those upwelling along the northern end of the Mount Ogilvie Fault. Their dispersion into the groundwaters of the Triassic rocks and Wollombi Coal Measures is reflected by saline pulse in baseflow chemistry of Big Flat Creek and Spring Creek, and by the shift in principal component scores of nearby bores and wells. Canonical variates analyses confirm that geology is the dominant control in the chemistry of the upper Hunter valley. It should be recognised that high background salinities in groundwaters of the Central Lowlands are natural phenomena which will persist for the foreseeable future.

INTRODUCTION

The upper Hunter River valley area of New South Wales (Fig.1) contains the largest exploitable deposits of Permian bituminous coal in the Sydney Basin. Raw coal production in 1983 was 23.3 million tonnes, mostly by open-cut mining. In recent years the upper Hunter has assumed increasing importance as a centre of power generation and associated industrial development. The valley is also a prime area of agricultural production, and as rural land has gradually been modified by industrial development, there has been an increasing demand on water resources as well as general concern about future water quality.

By the year 2000, it is estimated (Garman, 1982) that 46 per cent of water demands above Maitland will be for industrial consumption compared with 26 per cent for irrigated agriculture. Furthermore, much of the industrial activity centres around coal mining, which involves the interception, use, and disposal of groundwater. Similarly, power-generation industries require cooling water, resulting in evaporative concentration of soluble salts, which need to be disposed of at some stage of the operation. Apparently, no attempts have been made on a regional scale to determine salt returns to surface water from agricultural activities, but soluble salt concentrations in surface run-off from 'natural' pasture and mine-spoil materials are both in the concentration range of 140-1260 mg/L (Gates & Kalf, 1983). They also note that groundwater in spoil piles is likely to have considerably higher salt concentrations than in the surrounding undisturbed rocks.

Detailed monitoring of surface water indicates that baseflow contributions have a marked effect on quality. Under dry-weather conditions, electrical conductivity values of the Hunter River increase from about 400 μScm^{-1} just below the Glenbawn Dam (Fig. 1) to 1000 μScm^{-1} at Maitland, about 250 km downstream. At least part of this increase is due to geological influences on groundwater quality (Garman, 1982). To a large extent, water quality in the Hunter River is controlled by releases of stored surface water and the disposal of industrial waste waters under high-flow conditions, which are subject to legislative controls.

It is clear that future control measures will require even more detailed information on the chemistry of the Hunter River and that of the return flows to it. This report is designed to indicate various approaches to the interpretation of groundwater chemistry that may be useful in analysing the system, particularly in defining the chemical signature of various water sources. Restricted access to a number of mine sites for groundwater samples has, however, limited detailed interpretation in some areas.

PHYSIOGRAPHY AND CLIMATE

The groundwater survey covers the central portion of the Hunter-Goulburn River valley system, and therefore includes the major geomorphic regime of the catchment (Fig. 2). The physiography is dominated by the Central Lowlands (Story et al, 1963), which are traversed by the Hunter River and its major tributaries, and are surrounded by steep slopes and rugged ranges, which are broken in places by elevated plateaus.

The physiography is strongly controlled by the underlying geology (see Fig.2 and Pl. 1). The Southern Mountains region consists of rugged Triassic sandstone mountains with elevations up to 1000 m and deeply incised valleys; soils are generally shallow because of the strong resistance to chemical weathering by the Triassic sandstones. At the junction of this region with the Central Lowlands, discontinuous sheets of quartzose sands fan out from the foothills for a distance of 1-2 km.

In the west, the Central Goulburn valley region is similar; it is underlain by Triassic sandstones and shales, and consists of irregular steep-sided hills and plateaus and deeply incised rivers.The Merriwa Plateau region in the northwest consists of rolling to hilly terrain developed as a planation surface on extensive Tertiary basalt flows. Lavas have partially filled pre-existing valleys,and post-volcanic streams have incised on either side of the flows, forming sub-parallel valleys that reflect the pre-basalt drainage. The degree of incision has been controlled by uplift, and by marked variations in relative sea level during the Cainozoic.

Resistant folded Devonian and Carboniferous lavas and sedimentary rocks form the Northeastern Mountains-rugged, dissected terrain, which diminishes in relief towards the Central Lowlands. This region is fringed to the northeast by the Liverpool and Mount Royal ranges, and the Barrington Tops, which comprise rugged basaltic terrain interspersed with small plateaus in the narrow, steep-sided crests and valleys.

In contrast, the Central Lowlands have a gently undulating terrain developed on easily eroded Permian sedimentary rocks on which deep soils have developed. The region is therefore important agriculturally, but is also important economically for its mineable coal deposits. The Hunter River and its tributaries are bounded by alluvial flats 1-6 km wide.

Rainfall varies markedly with elevation and distance from the coast; the total annual precipitation increases with elevation away from the Central Lowlands, reaching a maximum of about 1500 mm in the higher reaches of the Barrington Tops Region. Average annual rainfall ranges from 580 mm at Denman in the western part of the study area (Pl. 1) to 1000 mm near the coast. The distribution of rainfall is fairly uniform throughout the year, although monthly means are highly variable ranging from 50 to 80-per cent.

In the Central Lowlands (Jerrys Plains) average temperatures range from 24°C in summer to 11°C in winter, the yearly average being 17.8°C; in the higher areas frosts are common in winter.

In the Central Lowlands soil moisture deficits of 10-50 mm per month are frequent during the period October-March, and little, if any, surplus occurs during the winter period. The Southern and Northwestern Mountains have average annual soil moisture surpluses ranging from 10-250 mm, depending on elevation. Base flow of the Hunter River and its major tributary streams is thus very dependent on the physiography and climate of the surrounding highlands.

GENERAL GEOLOGY

The map area incorporates the southwestern tip of the New England Fold Belt and the northwestern half of the Hunter Valley Dome Belt (Fig. 3) (Branagan & others, 1975) in the northern division of the Sydney Basin

(Fig. 1). Important recent works on the evolution and stratigraphy of the Sydney Basin are those of Mayne & others (1974), Branagan & others (1975) and Herbet & Helby (1980), and the Permian stratigraphy of the upper Hunter River valley is described in detail by Britten (1975).

The upper Hunter River valley is underlain by a sequence of alternating shallow marine and continental Permo-Triassic sedimentary rocks, which dip gently (<10°) to the southwest and are capped by Tertiary basalts in the north and west (see Plate 1 and Table 1); the total thickness of these Permo-Triassic rocks is in excess of 4 km. Basement is generally considered to be the Late Carboniferous glacigene sedimentary rocks derived from the Lachlan Fold Belt to the south, which are intercalated with volcaniclastics and lava flows from the New England Fold Belt to the north.

In the study area, the northeastern boundary of the Hunter River valley is clearly defined by the Hunter Thrust Fault (Pl.1 and Fig.3), which separates the Permian rocks of the valley floor and foot slopes from the northern overthrust Carboniferous rocks in the higher country of the southern New England Fold Belt; these Carboniferous rocks comprise sandstones, conglomerates, and tuffs of the lower Carboniferous Gilmore Volcanics and Wallaringa Formation, and remnants and down-faulted blocks of upper Carboniferous fluvioglacial sediments and volcaniclastics are preserved in some areas.

The western and southern boundaries of the upper Hunter River valley coincide with an escarpment formed by (Lower) Triassic rocks of the Narrabeen Group; these comprise interbedded sandstones and shales overlying basal fanglomerates. The southeastern boundary coincides with the unconformity in the Lochinvar Anticline about 14 km southeast of the map sheet (Fig. 3), where the coal seams and interbedded sediments of the Singleton Super-group wedge out (Britten, 1975).

The major geological structures (Pl. 1) which are hydrogeologically significant consist of a series of meridional faults with numerous associated cross-faults and doubly-plunging folds or domes oblique to the Hunter Thrust Fault. Many of these folds and parallel faults developed

Page numbering sequence does not include page 5.

contemporaneously with the Hunter Thrust Fault during the mid-Permian Hunter-Bowen Orogeny, and these structures apparently had an important effect on the distribution of Late Permian coal seams and sediments (Herbet & Helby, 1980). The curvilinear traces of the major fold axes (Pl.1) suggest that a minor subsequent phase of folding along an east-trending axis caused buckling of the existing folds and produced the dome and basin structures of the valley. In any event, tectonism had ceased by the time Eocene basalts were extruded in the northern and western parts of the map area. A renewed period of small- scale tectonism associated with Cainozoic uplift is indicated by variations in thickness of alluvium in the upper Hunter River floodplain (Williamson, 1958); these imply that the Mount Ogilvie Fault at the hinge of the valley in the western part of the map area (Pl. 1) was reactivated during the late Cainozoic.

The alternating shallow marine and continental depositional environments during the Permian are indicated in Table 1. The Greta and Wittingham Coal Measures formed as peat swamps on alluvial fans close to the sea. Within the Wittingham Coal Measures two brief marine transgressions are recorded by laminites of the Bulga and Denman Formations, which Britten (1975) used to define the tops of the Vane and Jerrys Plains Subgroups respectively. The Wollombi Coal Measures show the least marine influence of the Permian deposits. The coal seams are mostly interbedded with tuffaceous and terrigenous sedimentary rocks. Continental sedimentation continued into the Triassic with the deposition of a basal fanglomerate (Widden Brook Conglomerate) overlain by interbedded sandstones and shales of the Narrabeen Group. No coal seams are present in the Triassic rock types.

Eocene basalts of the Liverpool and Barrington Volcanoes (Wellman & McDougall, 1974) form a prominent planation surface to the north and west of the study area; Galloway (1971) considered that most of the Triassic rocks in the western half of the study area were formerly capped by basalts. Miocene basalts of the Dubbo Province are largely conformable with the contemporary landsurface in the western Goulburn River valley (Galloway, 1971), indicating that uplift and incision of the upper Hunter River valley west of the Mount Ogilvie Fault occurred between the Eocene and Miocene.

The major known Tertiary dolerite sills of the upper Hunter River valley are shown in Plate 1; numerous dyke swarms are not represented, owing to their small areal extent. Most dolerites occur to the west of a line extending south-southeastwards from the hinge of the Muswellbrook Anticline towards Broke. The dolerite intrusions have in places burnt the coal or converted it to cinders, and thus they have an important influence on the viability of coal exploitation. The present study shows that the line dividing intruded Wittingham coals in the west from essentially non-intruded equivalent units in the east coincides with a differentiation of natural hydrochemistry based on ionic proportions, which suggests that additional unexposed intrusives are present in the western part of the study area.

The only Cainozoic sediments of hydrogeological importance in the map area are the unconsolidated alluvial deposits of the Hunter River floodplain and, to a lesser extent, the alluvial terraces of the major tributary streams. These deposits are generally composed of basal gravels and boulders overlain by an upward-fining sequence of sands, silts, and clays with sporadic shoestring gravels. Secondary pedogenetic pore-filling of the Cainozoic sediments becomes significant because of reduced porosity on the oldest (and highest) terraces.

HYDROGEOLOGY

Previous and current Work

Several hydrogeological investigations have been conducted in different parts of the study area: Williamson (1958) compiled an inventory of groundwater resources of the alluvial aquifers in the Hunter River Floodplain above Denman, and in the Dart Brook valley. Griffin (1960) summarised the groundwater resources of the Wollombi Brook catchment in the south, with special reference to alluvial aquifers. Surface water quality of the Hunter River valley has been investigated by Garman (1980). Records of groundwater quality for the past twenty years are maintained by the NSW Water Resources Commission (WRC).

Some information on groundwaters in the Wittingham Coal Measures is contained in environmental impact statements prepared by the coal-mining companies.

At the time of writing three major hydrogeological research projects were in progress in the upper Hunter valley: WRC were continuing their surface water and groundwater quality monitoring over the entire Hunter River catchment; the Environmental Geology Subsection of the NSW Geological Survey were researching the hydrochemical characteristics of the Permian rocks in the valley; and the effect of coal mining on groundwater resources in the Permian sequence of the Hunter River valley was being analysed by Australian Groundwater Consultants Pty Ltd on behalf of the NSW Coal Association. The study described in this report was part of a CSIRO multi-disciplinary major research program in the upper Hunter River valley.

Regional hydrodynamics

The study area is roughly bisected by the Hunter River floodplain, which is a regional groundwater sink for the Permo-Triassic fractured-rock aquifers; bed underflow of the Hunter River represents a dividing streamline for groundwater flow, apart from a few important mixing zones. Contrasts in permeability and porosity between the alluvial and fractured-rock aquifers indicate that most groundwater in the upper Hunter River valley is stored in and transmitted through the floodplain sediments; the multivariate statistical analyses used in this study show that a strong chemical signature from the Carboniferous provenance is maintained through to Singleton in wells of the floodplain which are hydraulically connected to the Hunter River. These wells induce recharge from the Hunter River when their cones of depression during pumping intersect saturated sediments peripheral to the river. At the time of sampling (August 1982), withdrawal of groundwaters from wells on the floodplain was exceptionally heavy because of prolonged drought.

Several surface reservoirs in the map area act as plane sources for groundwater recharge; they also tend to impede lateral throughflow from up-gradient groundwater stores, and in some areas create springs and artesian conditions. The largest reservoir is Lake Liddell (148 000 ML capacity) which is filled with a mixture of water pumped from the Hunter River, and runoff, interflow and groundwaters from the 75 km^2 upper catchment of the Baywater Creek; this catchment drains Maitland Group rocks on the eastern limb of the Muswellbrook Anticline. In August 1982, the water chemistry of the lake margin was slightly closer to the mean composition of groundwater of the Hunter floodplain than to groundwaters in the Maitland Group rocks.

On a regional scale, groundwaters of the fractured-rock aquifers constitute only a minor proportion of storage and transmission. Their reserves are most important during times of low-flow regime of the Hunter River and its tributaries; however, groundwaters in Permian fractured-rock aquifers are very important in the coal-mining industry.

Alluvial aquifers

Basal gravels and overlying sands of the floodplain alluvium of the

Hunter River and its major tributaries are by far the most permeable aquifers in the study area. In many places groundwater yields are sufficient to permit intensive crop irrigation (see Table 2). In general, wells in floodplains of the Wollombi Brook, Goulburn River, and Hunter River do not extend to bed rock, although more than half the wells in the other tributary valleys listed in Table 2 do.

TABLE 2. MEAN YIELD AND DEPTH OF WELLS IN THE HUNTER RIVER AND MAJOR TRIBUTARY FLOODPLAINS

Location	Number	Mean Yield (L/sec)	Mean depth (m)
Hunter River Floodplain (Rouchel to Muswellbrook)	11	18.4 ± 4.6	11.7 ± 1.9
Hunter River Floodplain (Muswellbrook to Denman)	12	12.2 ± 6.2	12.5 ± 3.8
Hunter River Floodplain (Denman to Loder Creek)	26	12.3 ± 9.6	13.5 ± 2.6
Hunter River Floodplain (Loder Creek to Neotsfield)	25	13.4 ± 7.5	14.3 ± 2.1
Goulburn River (Sandy Hollow to Hunter River junction)	9	11.9 ±10.8	14.6 ± 6.3
Wybong Creek	6	13.5 ± 8.4	13.6 ± 4.9
Dart Brook	9	8.6 ± 4.8	12.6 ± 3.9
Martindale Creek	29	12.7 ± 7.9	12.9 ± 2.8
Wollombi Brook (Broke to Warkworth)	31	8.8 ± 3.4	9.4 ± 4.1
Milbrodale Brook	21	6.9 ± 3.1	6.6 ± 1.9
Hayes, Wambo, North Wambo and Appletree Creeks	20	5.8 ± 3.7	7.0 ± 2.6

Source: (1) WRC boremaster records
(2) Griffin (1960)

Fractured-rock aquifers

The permeability of a fractured-rock aquifer depends mainly on the spacing, interconnections and apertures of the fractures. In an interbedded sequence of coals and more competent rocks, cleats in the coal seams will always be more closely spaced than joints formed in competent rocks under the same stress field, because of the ability of coals to store higher strain energy. The ratio of cleat to joint spacing depends on the Young's modulus and Poisson's ratio of the respective rock units; in coals these parameters are related to rank. In addition, fracture spacing is inversely proportional to bed thickness; therefore, under a given regional stress field, the highest frequency of brittle fractures occurs in the coal seams, which are generally thinner than adjacent sandstone and shale interbeds.

The importance of fracture aperture is expressed in the cubic flow law derived by integration of the Navier Stokes equation of laminar flow between parallel planes. This law states that the rate of flux of fluid through a smooth open fracture is proportional to the cube of the fracture aperture. If groundwaters that are super-saturated with respect to a particular mineral are transmitted through rocks fractures, then precipitation of that mineral will occur in the fracture, provided that the appropriate thermo-dynamic conditions are attained; precipitation commences on the fracture face since the fluid velocity is minimised at the boundary layer, and in time accretes inwards, layer by layer, towards the centre of the fracture or void. Therefore, under conditions of constant effective stress the transmissivity of a fractured-rock aquifer may decline in time if the fracture (joint) apertures are decreased by precipitation of minerals. In the study area most groundwaters in the Permian rocks have exceeded calcite, dawsonite, and dolomite saturation, which is consistent with the abundance of healed carbonate fractures in the coal seems and interbedded sedimentary rocks.

The most transmissive fractured-rock aquifers are therefore likely to be those with the greatest frequency of open youngest tension fractures - the likelihood of lining or infilling with mineral precipitates increases with age. Shear planes (conjugate shear joints and faults) are likely to form impermeable barriers to groundwater flow since displacement is

parallel to the plane, but tension fractures oblique to faults may be capable of considerable groundwater storage. However, the effective stress of any fractured rock mass is rarely constant for a sustained length of time, and subsequent rotations in principal stress direction may promote jostling along previously tight shear planes to induce displacement oblique to the planes and thereby enhance the fracture permeability of the rock.

The orientation and location of the youngest tension fractures may be estimated by considering the regional stress history of the upper Hunter River valley since uplift of the Permo-Triassic rocks. The maximum principal stress direction would have been near vertical within a few hundred metres of ground surface owing to gravitational loading, irrespective of whether initial conditions were hydrostatic or whether there were residual stress components due to thrusting (Price, 1966). Tension fractures in the rock mass formed under these stress conditions would have been high-angle sets parallel to the plane of the maximum and intermediate principal stress directions. These first-stage tension fractures are clearly visible along the face of the escarpment of Triassic rocks, and in the Permian rocks of the Hunter River valley floor the fractures are most conspicuous as intersecting sets of closely-spaced cleats perpendicular to bedding in the coal seams.

Erosional unloading by entrenchment of the Hunter River and its tributaries resulted in rotation of the maximum principal stress equivalent to the confining pressure of the adjacent rock mass,to a subhorizontal direction, in the eroded section of the valley. The minimum principal stress would have rotated to a vertical direction - approximately orthogonal to the newly formed land surface. A second generation of tension fractures would therefore have developed subparallel to the land surface, but these would have formed only in the lower eroded section of the Hunter River valley where the unloading effects would have been greatest. In gently-dipping rocks stress relief would have been manifested by parting along bedding planes rather than by the formation of new fractures. Consequently, the most permeable fracture sets should be the youngest, low-angle joints and bedding plane separations in the Permian rocks of the valley floor.

The preferential development of closely spaced cleats in coals

increases their potential for transmitting groundwaters with the bedding plane separations and low-angle tension fracures forming the major conduits. Furthermore, the highest permeabilities within a sequence of coals of equal rank will occur close to the ground surface because this is where the difference between the maximum and minimum principal stresses is greatest; this stress difference is most pronounced in exhumed coal seams of the Early Permian Greta Coal Measures (Table 1) which were more deeply buried and therefore subjected to greater load stress than the other coal measures.

Several phases of deformation - lateral stretching of uplifted folds and domes (e.g., Muswellbrook Anticline), and slip along the Mount Ogilvie Fault which was related to early Tertiary igneous activity - were superimposed on structures in the map area. In anticlinal folds flexural slip-folding about the fold axes produced two sets of primary tension fractures parallel and perpendicular to the fold axes, whereas in synclinal folds the most prominent fractures were conjugate shear joints symmetric about a plane orthogonal to the fold axis. The hinge areas and limbs of anticlines are therefore generally considered to be the zones of highest fracture permeability, provided that the tension joints have remained open and the rock fabric has not been unduly deformed by cleavage. Subsequent uplift of domal structures may have resulted in further displacement of these tension fractures due to lateral extension. AGC (1982) quote enhanced groundwater yields from fractured rocks of the Muswellbrook Anticline zone.

Tension fracture patterns associated with the dolerite intrusions are almost impossible to predict; within the dolerites extension cooling joints are commonly symmetrical about the contact zones, but these joint patterns generally do not extend into the surrounding country rock.

Groundwater flow rates

Groundwater velocity represents an important constraint for assessing the applicability of equilibrium models in water chemistry to natural conditions. Estimates of regional groundwater velocities for the major lithological units in the upper Hunter River valley (Table 3) are intended only as a guide to relative velocities on a regional scale - they are for

unconfined flow. In particular, the estimates of velocities in fractured-rock aquifers are likely to be substantially in error on the scale of individual catchments because transmissivity may be highly anisotropic.

TABLE 3. ESTIMATED REGIONAL GROUNDWATER VELOCITIES FOR UNCONFINED FLOW IN THE MAJOR LITHOLOGICAL UNITS OF THE UPPER HUNTER RIVER VALLEY.

Unit	Mean hydraulic conductivity (m/day)	Mean effective porosity	Mean hydraulic gradient	Mean velocity (m/day)
Alluvial aquifers in Hunter River floodplain (no pumping)	250	0.15	0.0015	2.50
Narrabeen Group	0.01	0.02	0.25	0.13
Wollombi Coal Measures	0.05	0.03	0.05	0.08
Wittingham Coal Measures (west of the Muswellbrook Anticline)	0.08	0.04	0.03	0.06
Wittingham Coal Measures (east of the Muswellbrook Anticline)	0.10	0.05	0.02	0.04
Greta Coal Measures and Maitland Group rocks of the Muswellbrook Anticline	0.15	0.05	0.03	0.08
Carboniferous rocks	0.01	0.02	0.20	0.10

Source: AGC; company reports; and WRC records

Calculated results indicate groundwater velocities in the floodplain alluvium are at the very least an order of magnitude higher than in the

fractured rocks (Table 3). In addition, the highest velocities in the fractured-rock aquifers occur in the least permeable Narrabeen Group and Carboniferous rocks, where the large hydraulic gradients overshadow the limiting effects of minimal fracture permeability.

The applicability of chemical equilibrium models for the upper Hunter River system may now be assessed in the light of these results. In the Hunter River floodplain the mean contact time between a mineral grain - say 2 mm diameter - and groundwater is about 1 minute; in fractured-rock aquifers mean contact times for similar grain sizes range from about 20 minutes in the Narrabeen Group rocks to over an hour in the Wittingham Coal Measures. Reaction rates for sulphide oxidation, and simple dissolution/precipitation in carbonate and sulphate systems are measured in minutes,but silicate dissolution times are normally measured in days; therefore, the use of carbonate equilibrium models would be realistic in the fractured-rock aquifers but only of limited value in the alluvial aquifers. On a regional scale the groundwater velocities in all provinces are too high for silicate dissolution/precipitation reaction to be adequately explained by equilibrium models but this may not necessarily be true on the scale of individual catchments.

HYDROGEOCHEMISTRY

Hydrogeochemical survey and compilation of database

The data (chemical analyses) on which this report is based comprise 673 samples (see Pl.2 and Appendix 1) of which 340 were collected at the end of a prolonged drought during August 1982 - 21 from stream baseflow and springs, 71 from shallow wells, and 56 from fractured-rock bores - and the remainder are published chemical analyses of groundwaters from wells and bores.

Electricity conductivity (EC) was measured in the field with a portable meter, and in the laboratory on a direct-reading digital conductivity meter; pH was measured on unfiltered samples prior to the HCO_3^- titration.

Prior to analysis for Ca^{2+}, Mg^{2+}, Na^+, K^+, Cl^-, SO_4^{2-}, and SiO_2, the

samples were filtered through a 0.45 μm cellulose nitrate membrane filter, then stored at -20°C. When required for analysis the filtered samples were thawed, then acidified with nitric acid to a sample concentration of 1% in order to reconstitute the precipitates.

HCO_3^- was determined by titration; Ca^{2+}, Mg^{2+}, Na^+, and K^+ by atomic absorption spectrometry; and Cl^-, SO_4^{2-}, and SiO_2 colorimetrically using an auto-analyser; the detection limit for the Cl^-, SO_4^{2-}, and SiO_2 methods was 0.2 mg/L. An air-acetylene flame was used for the cation determination; strontium chloride to a final concentration of 1500 mg/L was added to samples and standards to suppress ionisation. The sensitivities for these determinations were 0.021 mg/L for Ca^{2+} at 422.7 nm, 0.003 mg/L for Mg^{2+} at 285.2 nm, 0.003 mg/L for Na^+ at 589.0 nm, and 0.01 mg/L for K^+ at 766.5 nm.

100 samples were analysed by inductively coupled plasma for Al and Fe and the trace elements B, Cu, Mn, Zn, Co, and P; the detection limit was less than 0.01 mg/L for each element.

Correlation and distribution of dissolved salts

TABLE 4. CORRELATION MATRIX OF SIX MAJOR IONS IN UPPER HUNTER RIVER VALLEY GROUNDWATERS. (n = 670)

HCO_3^-	1					
Cl^-	0.50	1				
SO_4^{2-}	0.18	0.51	1			
Ca^{2+}	0.15	0.43	0.65	1		
Mg^{2+}	0.43	0.86	0.72	0.66	1	
Na^+	0.62	0.96	0.56	0.35	0.81	1

All correlation coefficients in Table 4 are non-zero at the 95% significance level, and all are positively correlated. The most highly correlated pair of ions ($r>0.8$) is Na^+ - Cl^-, followed by Mg^{2+} - Cl^-; both associations give the commutative high correlation Na^+ - Mg^{2+}. The lowest correlations ($r<0.2$) are Ca^{2+} - HCO_3^- and HCO_3^- - SO_4^{2-}. SiO_2 and K^+ are not included in Table 4 owing to the large number of missing values for these elements (Appendix 1).

Sampling distributions of the major ions and SiO_2 lumped over the complete data set are all right-skewed; K^+ showed a lesser conformity. Although the asymmetric distributions arise partly from biased sampling, the main reasons are due to system constraints because the ranges of concentrations of elements fall within a lower bound slightly greater than zero set by laboratory detection limits, and an indefinite upper bound dependent upon saturation of the waters with respect to a particular suite of minerals.

Much of the skewness in the HCO_3^-, Ca^{2+}, and SiO_2 distributions (Fig. 4) is removed by transforming the data to $\log_{10}$ class intervals. Although these three distributions actually contradict the hypothesis of log-normality in rigorous goodness-of-fit tests at a level of significance of 0.05, it is quite apparent that they approach unimodel log-normal distributions. This indicates that the concentrations of HCO_3^-, Ca^{2+}, and SiO_2 are the products and not the sums of many small interdependent causes in a statistically homogeneous system; dissolution and precipitation of carbonate and silicate minerals are important influences on HCO_3^-, Ca^{2+}, and SiO_2 concentrations in the upper Hunter River valley groundwaters, as discussed later.

The polymodal distributions of Cl^-, SO_4^{2-}, Na^+, and Mg^{2+} (Fig. 4) can be partitioned into discrete modes which individually approach log-normality. Although the effects are again a consequence of the products of many multivariate causes within a particular mode the sample space can no longer be considered as statistically homogeneous. Figure 4 shows that the secondary modes of the Cl^-, SO_4^{2-}, Na^+, and Mg^{2+} distributions comprise dominantly samples from the Vane subgroup of the lower Wittingham Coal Measures, the Greta Coal Measures, and the Maitland Group rocks; the processes - diffusion of connate marine salts, oxidation of sulphides, and dissolution of evaporite minerals - which concentrate these solutes are much more intense in groundwaters of these rock types.

Figure 4 shows that K^+ approaches a uniform distribution, implying that there is a mechanism controlling K^+ concentrations which is not operative for other major elements in this system.

Hydrochemical provinces

Groundwaters of the upper Hunter River valley have been divided into eight hydrochemical provinces (Table 5; Plate 2). A hydrochemical province is here used to mean a region characterised by groundwaters of distinctive chemical composition stored in and transmitted through particular rock and/or soil associations. Hence a province comprises a lithological sequence and its associated groundwaters, though for convenience in this report it is commonly referred to by the relevant geological term, for example Wollombi Coal Measures WO (Table 5, Plate 2).

Most CARB province samples in the northeast of the study area are baseflow because the mountains of the southern New England Fold Belt are well endowed with surface waters and therefore very few bores have been drilled. The hydrochemical characteristics described for the CARB group in this report are representative only of a 10 km-wide strip of Carboniferous rocks adjacent to the Hunter Thrust Fault; within this zone, recycled salts are introduced from the Permian strata of the valley floor - as shown by proportional increases in HCO_3^-/Cl^- and Ca^{2+}/Na^+ ratios with increased distance from the Permian rocks.

The TRIAS province consists of fractured rocks of the Narrabeen Group. In the northwest of the map area the Triassic rocks are capped by Tertiary basalts, which are part of an extensive basaltic surface extending westwards for almost 100 km. The TRIAS province samples are from shallow wells, baseflow, and springs; no boreholes have been drilled in the rocks of the Triassic escarpment because of the ruggedness of the terrain. Groundwater characteristics (Na^+, Mg^{2+} - Cl^-) for this province are restricted to a 10 km-wide zone marginal to the Permian-Triassic boundary, although HCO_3^- is present, and even dominant, in groundwaters near the Tertiary basalts.

The Permian fractured rocks are subdivided into four hydrochemical provinces: WO, WI1, WI2 and GM. The WO province comprises the Wollombi Coal Measures; ionic proportions in groundwaters of these rocks are similar to those of the waters of the overlying Narrabeen Group rocks, but mean concentrations are almost twice those in the TRIAS group. The Wittingham Coal Measures are subdivided into the WI1 and WI2 hydrochemical provinces; the boundary between them is a line projected from the hinge of the Muswellbrook Anticline to Broke, and as noted earlier this line also

divides intruded rocks in the west forming the WI1 province from non-intruded rocks of the WI2 province in the east. In the central part of the valley, the WI1-WI2 boundary follows a 2 km-wide buffer zone adjacent to the Maitland Group rocks on the western limb of the Muswellbrook Anticline until it intersects the Hunter River about 5 km southwest of Muswellbrook; northwards to Aberdeen, the WI1-WI2 boundary is defined by the subcrop of the Bayswater seam.

A comparison of the WI1 and WI2 provinces shows several significant differences in environments and groundwater properties: the WI1 province contains scattered Tertiary intrusions; WI1 province comprises shallow-dipping and relatively undeformed, gently folded rocks, whereas in the WI2 province the rocks dip at higher angles and are extensively folded and faulted, particularly east of the Muswellbrook Anticline; WI1 province rocks are everywhere younger than the Vane Subgroup (Table 1) and except in the northern area, generally consist of rocks younger than the Mount Arthur seam. Concentrations of total dissolved salts (TDS) in groundwaters of the WI2 province are more than double those of the WI1 province for similar residence times and distances down flow lines; and the proportion of SO_4^{2-} in anion concentrations is significantly greater in the WI2 province. However, SiO_2 constitutes the most useful solute for distinguishing the Wittingham subprovinces from each other - as discussed later.

An outlier of the WI2 province represented by a line of sporadic salt springs above Big Flat Creek occurs along the surface trace of a diagonal fault that truncates the northern end of the Mount Ogilvie Fault; waters from these springs are allocated to the WI2 group by a linear discriminant function.

The GM province incorporates groundwaters of the Greta Coal Measures, and Maitland, and Dalwood Group rocks. These waters are distinguished from the WO, WI1 and WI2 groups by their high SO_4^{2-}/Cl^- and SO_4^{2-}/HCO_3^- ratios.

The HFP1 and HFP2 provinces - coincident with the upper and lower reaches respectively of the Hunter River floodplain (Plate 2) - show several differences; increased proportion of Cl^- in the anions of the HFP2 province (probably owing to increased contact time with Permian rocks); and diminution in mean grainsize of the aquifers away from the Carboniferous

rocks.

Mean and standard deviations of solute concentrations for each of the hydrochemical provinces are shown in Table 6.

TABLE 6. SOLUTE CONCENTRATIONS (meq/L) IN UPPER HUNTER RIVER VALLEY HYDROCHEMICAL PROVINCES.

Hydrochemical province	HCO_3^-		Cl^-		SO_4^{2-}		SiO_2	
	$\bar{c}$	s	$\bar{c}$	s	$\bar{c}$	s	$\bar{c}$	s
CARB	4.62	1.85	6.78	4.57	0.78	0.44	0.24	0.13
TRIAS	2.92	2.83	6.41	5.73	0.55	0.58	0.20	0.08
WO	5.00	4.09	11.01	11.63	0.71	1.18	0.46	0.51
HFP1	5.17	1.69	3.76	3.14	0.64	0.47	0.27	0.24
HFP2	5.87	2.36	5.73	3.37	0.90	0.64	0.49	0.37
WI1	11.42	10.89	22.93	22.01	0.99	1.15	0.58	0.81
WI2	13.98	8.60	68.14	59.62	10.83	8.59	0.26	0.24
GM	9.41	4.84	40.39	39.84	20.29	25.99	0.27	0.22
	Ca^{2+}		Mg^{2+}		Na^+		K^+	
	$\bar{c}$	s	$\bar{c}$	s	$\bar{c}$	s	$\bar{c}$	s
CARB	3.05	1.33	3.30	2.12	5.76	3.17	0.07	0.08
TRIAS	1.64	1.68	3.50	3.30	4.32	2.68	0.14	0.05
WO	2.38	2.16	4.51	4.74	10.33	10.17	0.21	0.18
HFP1	2.96	1.52	3.53	1.91	3.14	2.42	0.07	0.11
HFP2	3.31	1.44	4.16	1.98	5.37	3.12	0.09	0.06
WI1	2.94	2.26	8.83	8.05	25.37	23.93	0.26	0.18
WI2	5.06	3.70	19.38	15.47	66.78	53.42	0.56	0.60
GM	10.34	6.77	20.25	16.98	37.40	37.66	0.41	0.36

Solute behaviour in the hydrochemical provinces

Some fundamental differences in behaviour of the major elements in groundwaters of the hydrochemical provinces are evaluated by means of composition diagrams (Fig. 5-12); more refined analyses using multivariate statistical methods are considered later.

The behaviour of solutes is assessed by regression equations and variables are log-transformed; for example, the equation for Cl^- behaviour in the CARB - TRIAS provinces (Fig. 5a) is:

$$\log [Cl] = -0.58 + 1.02 \log [\Sigma \text{ major ions}]$$

or $[Cl] = 0.263 [\Sigma \text{ major ions}]^{1.02}$ - in terms of the untransformed variables.

Regression lines of the hydrogeochemical provinces are compared to a simple non-evaporative mixing line between the end-members - standard mean ocean water (SMOW), and mean annual rainfall composition (MUHR) of the upper Hunter River valley (NSWSPCC - pers. comm.) The MUHR-SMOW mixing line (Figs. 5a and b) defines an upper limit to which all regressions are either subparallel or asymptotic; simple mixing between the MUHR and SMOW end-members seems to explain the observed Cl concentrations in this system.

The regression coefficients for each hydrochemical province indicate the mean rate of enrichment of the Y species with respect to a concentration factor (X) within that province. Figure 5a shows that the rate of accretion of Cl^- is highest in the floodplain alluvium, but only over the range of sampled values; a quadratic regression would probably be asymptotic to the MUHR-SMOW line for higher X values, if indeed they exist in the HFP provinces.

The sample space in Figures 5a and 5b can be partitioned into two environment divisions: the fractured-rock environments (CARB-TRIAS, WO, WI1-2 and GM provinces) and the Hunter River floodplain alluvium (HFP1-2 provinces). The rate of Cl^- enrichment in the fractured-rock environments is not significantly different from that of the MUHR-SMOW mixing line, whereas the corresponding rate in the floodplain alluvium is significantly

greater. Furthermore, mixing of groundwaters in the floodplain alluvium is defined by different end-members: surface waters of the Hunter River, which plot around the lower region of the HFP regression line; and groundwaters of wells where there is considerable upward and lateral seepage of groundwaters from the Permian rocks - these sites are identified later by principal components based on the concentrations of the six major ions.

The high correlation coefficients (Figures 5 a and b) demonstrate the conservative nature of Cl^- within the range of concentrations of the upper Hunter River valley groundwaters; the maximum is still well below halite saturation or any other chloride minerals for that matter. Cl^- is therefore the ideal element in this system to use as a standard concentration factor, and the behaviour of all other elements may be compared with it (cf.Eugster & Jones, 1979); in all subsequent composition diagrams Cl^- concentrations are plotted as X-variables.

In HCO_3^-- Cl^- concentration relationships (Figs. 6 a and b), there are very few samples in which HCO_3^- values could be explained by concentration along flow lines in a linear MUHR-SMOW mixing system. The regression coefficients show that the rate of uptake of HCO_3^- is highest in the CARB-TRIAS groups (b=0.65); for the CARB province alone b=0.74. In this group the principal mechanisms responsible for HCO_3^- enrichment are carbonate and silicate mineral dissolution . Rates of HCO_3^- accretion higher than that for the MUHR-SMOW mixing system occur in the WO and WI1 province owing to dissolution of silicates in the dolerite intrusives; in the WO group north of the Goulburn River, an additional source of HCO_3^- is provided by weathering of basalts. A low rate of HCO_3^- enrichment with respect to Cl^- occurs in the HFP province (Fig. 6a); this contrasts with the high rate of enrichment of Cl^- in the floodplain alluvium mentioned previously. The HFP regression line defines mixing between the two end-members - the Hunter River surface waters, and groundwaters of Permian fractured rocks. A similar low rate of HCO_3^- enrichment occurs in the GM group (Fig. 6b), but this is accompanied by an enrichment in SO_4^{2-}.

SO_4^{2-}-Cl^- concentration relationships (Figs. 7 a and b) show that if SO_4^{2-} behaved as a perfectly conserved species, the MUHR-SMOW linear mixing system would be sufficient to account for SO_4^{2-} concentrations in all hydrochemical provinces, apart from the GM group. Evidently other processes of SO_4^{2-} enrichment are present in this group, the most important being oxidation of sulphides, and dissolution of sulphate minerals; however, SO_4^{2-} cannot be regarded as a conservative element because of its tendency to form ion pairs and complexes, and its affinity for surface adsorption on alumino-silicate gels: this is shown by the very low gradient of the CARB-TRIAS regression line (Fig. 7a). In the CARB-TRIAS provinces

aerosols constitute the primary source of both SO_4^{2-} and Cl^-, but much of the SO_4^{2-} is absorbed down flow lines. Some SO_4^{2-} losses are also incurred from H_2S springs in the Wollombi Brook valley section of the WI2 province; therefore, the similarity of the WI2 regression coefficient with the gradient of the MUHR-SMOW line should not necessarily be taken as an indication that the simple process of mixing between meteoric and oceanic waters alone accounts for observed SO_4^{2-} concentrations in the WI2 province. A more correct interpretation would be that the WI2 regression coefficient represents the residual rate of SO_4^{2-} enrichment which is controlled by the combined effects of flushing of connate marine salts by meteoric waters, sulphide oxidation, and sulphate mineral dissolution - less the effects of sulphate reduction, adsorption, and possibly precipitation.

Cl^--normalized SO_4^{2-} concentration relationships (Figs 7c and d) show that in the WO and WI1 provinces, samples with very low, constant SO_4^{2-} concentrations but with increasing Cl^- concentrations are defined by the line - $\log (SO_4^{2-}/Cl^-) = -1 - \log (Cl^-)$ - these points mainly consist of baseflow samples in streams with a substantial part of their catchments in the Triassic rocks. The concentration clusters outlined in Figures 7c and 7d mostly represent groundwaters from shallow wells, whereas samples with the highest SO_4^{2-}/Cl^- ratios - in the WI1 and WO provinces - are from bores in fractured rocks and deep wells which bottom on bedrock. The clusters of shallow wells concentrations can therefore be considered as mixing zones between the two end-members: interflow/surface runoff from the Triassic rocks; and deeper waters from fractured rocks within the same province. In addition, Figure 7c shows that the mean rate of change of the SO_4^{2-}/Cl^- ratio is highest in the Hunter River floodplain alluvium; when compared with Figures 5 a and 7 a this high rate of change reflects the higher-than-average increase in the rate of Cl^- enrichment in the HFP provinces.

The behaviour of SiO_2 relative to Cl^- (Fig. 8a and b) is probably the most useful method of differentiating between the individual Permian hydrochemical provinces. SiO_2 concentration increases sympathetially with Cl^- in the WO and WI1 groups, but decreases with increasing Cl^- in the WI2 and GM provinces. The decline in SiO_2 with increased salinity (TDS) in the latter groups is not due to precipitation of amorphous silica or silicate minerals such as sepiolite since the majority of WI2 and GM waters are undersaturated with respect to these minerals. Rather it represents

precipitation of alumino-silicates, dominantly montmorillonites, with a concurrent progressive decline in silica solubilities in the alkaline Cl-rich solutions of the WI2 and GM provinces.

The M-D-JP triangle curves (Figs 8a and b) describe high SiO_2-enrichment rates in wells and bores within, and adjacent to a triangle with apices at Muswellbrook (M), Denman (D), and Jerrys Plains (JP); these samples are all saturated with respect to amorphous silica and sepiolite, presumably because of the numerous local dolerite intrusions, which generated the high SiO_2 background. Analyses of well-waters in the Hunter River floodplain at Alcheringa form a distinct cluster enriched in SiO_2 (Fig. 8a); it will subsequently be shown the principal components based on the major ions alone indicate that the locality is an important mixing zone between groundwaters of the alluvium and the underlying Wittingham Coal Measures.

The relationships of Cl^- to Ca^{2+}, Mg^{2+} and Na^+ concentrations (Figs 9, 10 and 11) show that the sources of the divalent cations must be other than by mixing of meteoric and oceanic waters - as indicated by comparisons of the regression lines with the the MUHR-SMOW mixing lines; however, the MUHR-SMOW mixing system could explain the Na^+ concentrations in about half of the samples (Figs. 11a and b).

The diversity of sources of the major cations in the recharge zones is related to their total variance at low Cl^- concentrations: Ca^{2+} has the greatest dispersion of data points (Figs. 9a and b), and hence the greatest diversity of sources; Mg^{2+} has a lower variance (Figs. 10a and b) and therefore a more restricted number of sources; and Na^+ has the lowest variance (Figs. 11a and b) and least number of sources. Silicate mineral dissolution is an important source of these cations (Ca^+, Mg^{2+}, Na^+) but dissolution of carbonate minerals is also a prominent source of Ca^{2+}, and and probably even provides small amounts of Mg^{2+}.

Comparison of regression coefficients (Figs 9, 10 and 11) indicates that Ca^{2+} has the lowest rate of enrichment of the three cations despite having the greatest diversity of sources. In low-salinity groundwaters the principal mechanism of Ca^{2+}-depletion is probably cation exchange; in the Permian rocks Ca^{2+} is lost by precipitation of calcite and other

carbonates. Again, the composition diagrams for the divalent cations segregate the HFP provinces (Figs. 9a and 10a) on the basis of unusually low rates of Ca^{2+} and Mg^{2+} enrichment.

Figs. 11a and b show that Na^{+} is the most conservative of the cations. The rate of Na-enrichment in the CARB-TRIAS, HFP, and WO provinces is significantly lower than the MUHR-SMOW mixing system. Given that these groups have never been trangressed by ocean waters, the rates of Na^{+} enrichment shown by their regression coefficients probably reflect dissolution of sodium silicates. However, flushing and mixing of connate marine salts by meteoric waters could account for observed Na^{+} concentrations in the majority of samples in the WI1, WI2 and GM provinces (Fig. 11b).

The behaviour of K^{+} (Figs 12a and b) is quite different from the other major cations. The correlation between K^{+} and Cl^{-} concentrations in the HFP and CARB-TRIAS provinces is not significantly different from zero owing to the resistance to weathering of sanidines and muscovites in the CARB rocks, and the permanent incorporation of K^{+} present in circulating groundwaters into clay lattices. The apparently random behaviour of K^{+} concentrations in HFP provinces (Fig. 12a) which is reflected in the almost uniform K^{+} distribution (Fig. 4)) over the total sample space, is partly the result of the application of fertilizers to the floodplain soils. In contrast, the rates of K^{+} enrichment in the groundwaters of the Permian rocks are all significantly greater than zero; the coal measures may have been an important source of K^{+}.

Mineralogy and geochemistry

Framework grains in the Permo-Triassic sedimentary rocks of the upper Hunter River valley are dominantly quartz, feldspar, and volcanogenic rock fragments; however, cements and authigenic minerals yield some important information on hydrochemical systems, and knowledge of the paragenesis of these constituents facilitates evaluation of the present and palaeohydrogeochemical regimes.

In the Permian rocks carbonates are the most abundant cement and replacement minerals, whereas in the Lower Triassic rocks silica and clay

minerals are co-dominant with carbonates in the rock matrix.

The most common carbonate mineral is calcite ($CaCO_3$) which occurs as a cement, replacement mineral, and grain-cutan material in both marine and continental sedimentary rocks. In the Permian coal seams calcite invariably lines cleat faces, and fills numerous subsidiary joints and veins; in some of the high vitrinite coals there has been substantial replacement of coal by calcite (Kemezys & Taylor, 1964). Calcite frequently replaces sodic plagioclase and rock fragments in the Permian sediments and feldspars and pyroxene in dolerite intrusions (Mayne & others, 1974). Complete replacement of claystone bands by fibrous calcite exhibiting fine-scale cone-in-cone structure has been described in the Liddell area by Bunny (1967).

Siderite ($FeCO_3$) is widely distributed as a microcrystalline cement throughout the Wittingham and Wollombi Coal Measures, but it occurs mainly i n thin beds and lenses of concentrically-zoned nodules within the coal seam (Kemezys & Taylor (1964); siderite nodules tend to occur to the exclusion of pyrite and are most abundant in coal seams which are not overlain by marine rocks.

Pure dolomite ($CaMg(CO_3)_2$) is rare in the non-marine rocks in the upper Hunter River valley area (Kemezys & Taylor, 1964) because there is generally some Fe substitution for Mg to form the mineral ankerite ($Ca(Fe,Mg)(CO_3)_2$). The mode of occurrence of ankerite and dolomite is identical to that of calcite, and like calcite and other complex carbonates, ankerite and dolomite are considered to be of recent origin in coals distant from marine rocks; an exception occurs in some coal seams proximal to marine sediments where dolomitic lenses replacing clays appear to have formed during early diagenesis.

Dawsonite ($NaAl(CO_3)(OH)_2$) is particularly interesting because its formation ranges from very early diagenesis to the present. It is ubiquitous throughout the Permo-Triassic sedimentary sequence of the upper Hunter River valley area and reaches a maximum concentration in the Middle Permian rocks. The mode of occurrence of dawsonite ranges from geologically recent precipitation on cleat faces to cements, replacement minerals, and joint and vein fillings; in the Mulbring Siltstone (Table 1) it forms spherulites in dolomitic lenses (Loughnan & Goldbery, 1972). In

some places the spherulites are replaced by calcite and kaolinite which are incipiently altered to nordstrandite ($Al(OH)_3$ - a polymorph of gibbsite) around aggregate margins (Loughnan & Goldbery, 1972). Precipitation of dawsonite requires high pH values in sodic solutions enriched in Al relative to Si. These conditions are commonly satisfied in present groundwaters of many of the Permian fractured rocks (see Appendix 1), and apparently have always been throughout the evolution of the upper Hunter River valley groundwaters.

Primary and authigenic sulphate minerals are relatively sparse in the upper Hunter River valley aquifers and are mostly confined to the Permian rocks earlier than the Wittingham Coal Measures. Acicular gypsum crystals occur in joint and cleat faces in the Greta Coal Measures and are formed by the reaction of Ca-carbonate minerals and acids released from sulphide oxidation. The former abundance of primary sulphate minerals is recorded by glendonites in the Mulbring Siltstone: glendonites are stellate aggregates of euhedral crystals which, in the upper Hunter River valley area, are mostly composed of calcite pseudomorphs after glauberite ($Na_2Ca(SO_4)_2$); Loughnan & Goldbery (1972) also describe less-common dolomite, gypsum ($CaSO_4.2H_2O$)and dawsonite pseudomorphs, and Conybeare & Crook (1968) describe glendonites in the equivalent Ulladulla Mudstone in the southern Sydney Basin as siderite pseudomorphs after glauberite. However, the nature of the primary mineral in glendonites is controversial. Australian literature on glendonites in the Sydney Basin has always cited glauberite as the primary mineral - in keeping with the definitive work by David & others (1905) - whereas Kemper & Schmitz (1975) conclude that thenardite (Na_2SO_4) was most likely the primary mineral. In any event, the genesis of glenonites is not in doubt: they form below the surface of marine muds in marginal basins or embayments characterised by dense highly saline waters in which there is restricted mixing with the open sea (Conybeare & Crook, 1968). Glauberite precipitates in super-chilled solutions below 0°C, but Kemper & Schmitz (1975) conclude that under specific conditions thenardite glendonites also form at these very low temperatures - as indicated by their contemporary formation in semi-isolated polar marine basins such as the White Sea.

Sulphide minerals occur in every Permian coal seam and marine sediment in the upper Hunter River valley area, but their distribution is highly

variable; we are not aware of any reported occurrences of sulphides in the Triassic or Carboniferous rocks. In the Permian rocks sulphides are most abundant in the Greta Coal Measures, Maitland Group, and the Vane Subgroup and Denman Formation of the Wittingham Coal Measures. Pyrite is the dominant sulphide - especially in coal seams adjacent to marine beds - followed by marcasite (FeS_2) and accessory sphalerite ((Zn,Fe)S). Arsenopyrite (FeAsS) has been reported in a well-mineralised sandstone below the Bayswater seam at Saxonvale (Croft and Associates, 1979).

The mode of occurrence of pyrite ranges from infilled cell-lumens and mineral replacements in vitrinite coals to small spherical nodules which coat bedding planes at coal-band interfaces through to interlocking mosaics of anhedral crystals; concentrations of massive euhedral crystals at the top of the Greta Coal Measures impart the "brassy tops" characteristic for which these coals are renowned (Kemezys & Taylor, 1964). Sulphide content in the coals is highly correlated with total sulphur content; from sulphur isotope fractionation studies Smith & Batts (1974) conclude that much of the pyritic sulphur in the upper seams of the Greta Coal Measures formed by reduction of marine sulphate which diffused downwards into the system during the transgressive phase of the Maitland Group sediments. They also conclude that diffusion of marine sulphate into the Greta coals occurred while the biogenic mass was still active; sulphide enrichment involved the direct reaction of oceanic sulphates with organic compounds and precipitation by sulphate-reducing bacteria. On a smaller scale, it appears that the biomass in the peat which formed the Wynn seam of the Vane Subgroup was apparently reactive during marine transgression and deposition of the overlying Bulga Formation.

A strong link between total sulphur and the proximity of marine sediments (Fig. 13) is clearly shown in the coal seams of the Wittingham and Greta Coal Measures in the Mount Arthur and Saxonvale areas; unfortunately a composite section for the entire Permian coal sequence is not available at present. Trends in SO_4^{2-} and Cl^- concentrations of oxidised coal extracts from the Jerrys Plains Subgroup at Saxonvale (Fig. 13) indicate that, in the Wollombi Brook valley, a similar enrichment in sulphide probably occurred in the Whybrow seam underlying the Denman Formation (the final marine transgression); however, this trend is not apparent in the Mount Arthur area.

In the contemporary hydrochemical environment of the upper Hunter River valley area sulphides are readily oxidised to sulphates in near-surface groundwaters. The upper end-member of the GM province mixing system (Fig. 7b) is enriched in SO_4^{2-} relative to seawater, which can be explained by preferential biogenic sulphate sieving from marine waters resulting in enrichment of sulphides by reactive peats before the onset of coalification; in the present oxidising environment these initially high sulphide concentrations are being returned to the leaching groundwater system as sulphates. A similar explanation is pertinent to the high-sulphate groundwaters of the Vane Subgroup of the WI2 province (Fig. 7b). At the other end of the scale the equivalent end-member in the WO mixing system (Fig. 7a) is the continental sulphate store in the original Wollombi peat swamps because these sediments have never been inundated by marine waters. Average total sulphur in the Wollombi coals ranges from 0.3% to 0.5% and is mostly organically bound; there are no pronounced vertical concentration gradients typical of the older Permian coals.

Although carbonates and sulphur-bearing minerals constitute the main authigenic minerals of hydrochemical importance in the study area, silica and certain phyllosilicate minerals have an important influence on the chemistry of local groundwaters within individual catchments, and particularly in areas containing basic igneous intrusions. The most common form of authigenic silica in the Permian rocks is chalcedony which appears to have crystallized mainly from globular masses of amorphous silica (Kemezys & Taylor, 1964) in lenses essentially conformable with bedding and in cell cavity infills. The authors also note that the frequency of vein chalcedony in coal seams is highest in areas adjacent to igneous intrusions, and conclude that these occurrences are genetically related to the intrusions. Kaolinite ($Al_2Si_2O_5(OH)_4$) is the most abundant authigenic silicate in the coal seams. Kemezys & Taylor (1964) describe extensive kaolinite petrifactions composed of uncollapsed coalified plant cell walls filled with finely crystalline kaolinite. In the interseam beds, kaolinite, illite-montmorillonite ($KAl_2(AlSi_3)O_{10}(OH)_2$ - $Na_{0.33}(Al_{1.67}Mg_{0.33})Si_4O_{10}(OH)_2$), and chlorite ($Mg_5Al_2Si_3O_{10}(OH)_8$) occur extensively as weathering products and primary matrix materials. Kaolinite and illite-montmorillonite are the dominant minerals in claystones which occur intermittently throughout the Wittingham and Wollombi Coal Measures. Some

of these layers are derived from in-situ weathering of ash-fall tuffs (e.g., Fairford Claystone); others are detrital in origin. Analcite ($NaAlSi_2O_6.H_2O$) forms up to 35% of the volume of sediments in the Newcastle Coal Measures (Loughnan, 1966), which are the eastern equivalent of the Wollombi Coal Measures - the mineralogy of these measures is virtually unknown because the Wollombi coals have not been exploited in view of the high content of tuffaceous material which makes them sub economic. The analcite deposits in the Newcastle Coal Measures formed by devitrification of volcanic glasses in tuffaceous sediments under a highly alkaline and Na-enriched groundwater regime. It is therefore highly probable that zeolites such as analcite would be present in appreciable quantities in the tuffaceous interbeds of the Wollombi Coal Measures.

In the upper Hunter River valley the most detailed geochemical studies have been done on the coal seams and interbeds of the Jerrys Plain Subgroup at Saxonvale, and Mount Thorley in the Wollombi Brook valley (Croft and Associates 1979; ibid,1981). In general, the non-marine interseam beds have a low salinity status (mean TDS less than 1500 mg/L), and HCO_3^- is the dominant anion; conversely, the coal seams have an average TDS concentration of 5000 mg/L, and Cl^- is the dominant anion, exceeding HCO_3^- concentrations by an average of 15:1. Groundwater compositions reflect these variations in soluble salt concentrations; piezometers set at varying depths invariably encounter the most saline groundwaters in the coal seams, which are also the major aquifers in the Permian fractured rocks. Saline groundwaters with high Cl^- and SO_4^{2-} concentrations are also intercepted in the Denman and Bulga Formations (Table 1) and in the Mulbring Siltstone, although the permeability of these rocks is at least an order of magnitude lower than that of the coal seams. As there are no primary chloride minerals in the Wittingham Coal Measures, the chemical composition of groundwaters in the coal seams can only be explained by a significant input of marine salts, either by direct infiltration into peats during marine transgressions, or by subsequent translocation of connate marine salts at some stage during the diagenesis.

An interesting result of the Saxonvale and Mount Thorley studies is that the coarse-grained rocks most closely associated with high-energy fluvial depositional environments (lithic sandstones and conglomerates) have consistently higher soluble salt concentrations (mainly NaCl) than the

finer-grained interseam siltstones and mudstones. The coarse-grained rocks form secondary salt stores because in contrast to the argillaceous sediments, they have greater void space which is filled with connate marine salts in fluids expelled from adjacent coal seams; conversely, these reservoir rocks would also leach at a much faster rate under the appropriate field conditions. The initial expulsion of connate fluids would have resulted from the volume reduction caused by coalification processes; the effects would have been optimum in sediments adjacent to the coal seams which were originally porous peat deposits saturated with marine waters and salts. Modern processes responsible for transmitting connate marine salts include molecular diffusion driven by concentration gradients, and upward convection and dispersion of waters from the semi-confined coal seams in response to differences in groundwater potentials. However, the quantity of solutes transferred by these processes in the present groundwater regime is minor in comparison to the historical expulsion of connate fluids from the original peat deposits during burial and coalification; the transition from peat to bituminous coal represents a porosity decrease from over 80% to between 5% and 10%.

Salt efflorescences

During the severe drought conditions of August 1982 banks and low terraces in the lower reaches of almost every minor stream draining the WI2 and GM provinces were coated by surface salt encrustations (efflorescences); bulk mineralogy of some efflorescence samples was determined by X-ray diffraction (Table 7) - the semi-quantitative ranking of mineral proportions is based on adjusted diffraction peak areas: major indicates that a particular mineral is most abundant regardless of its absolute percentage, and two or more major minerals indicate that they are present in approximately equal amounts; minor indicates that the mineral constitutes above about 10% of the sample but is present in significantly lower amounts than the major mineral(s); and trace is indicative of amounts less than roughly 10% of the bulk samples.

Pagination does not include 33 to 35 in original.

Table 7. Mineralogy of Salt Effluorescences, Upper Hunter Valley

Sample site (see Fig 6)	Location	Description	Mineralogy Major	Minor	Trace
46	Fordwich Creek	Surface encrustation on sand terrace.	H		
		Nodules in B horizon of grey solodic.	D, Q	C, F	
		Crystallaria in lower B horizon.	H		D
48	Fordwich Creek	Surface encrustation on stream bank.	H		T
		Nodules in lower B horiz. of solodic.	H, Q	F	C
		Joint plane infills in lower B horiz.	H		C
51	Salt Pan Flat	Surface encrustation on alluvial flats.	H, B, Q	T	K
		Infill in bedding plane separation, laminated siltstone (Denman Fm?)	H,T,I-M	K	
54	Loder Creek	Surface encrustation on sands.	H		T
		Precipitate from subsolum seepages of buried soil.	H		D,Q
		Nodules in subsolum of buried soil.	D,Q		F
		Soluble salts in B horizon of buried soil.	H		
55	Loder Creek	Surface encrustation on sands.	H		
		Carbonate joint infills in fine sandstone.	D,Q	F	
56	The Salt Flats	Surface encrustation on outwash sands.	H, T	B	
64	Loder Creek (east arm)	Salt spring effluorescent crust.	H,T,B	Q	
66	Doughboy Hollow Creek	Surface encrustation on low terrace.	H	T,B	G,I,K
67	Abbey Green Creek	Surface encrustation on sands.	H,T	Q	
127	Spurwater Creek	Surface encrustation on stream banks.	H,G,B	Q	F
129	Coalhole Creek	Surface encrustation on banks.	H		
		Efflorescences in sandstone joints.	H		F
		Crystallaria in brown earth.	C,Q	F	

Table 7 (cont)

135	Swamp	Surface encrustation ob banks.	H	T,B	
	Creek	Precipitate from spoil heap.	H, Q	F	T,D
		Nodules and joint plane infills from lower B horiz. of podzolic.	H, D	Q, F	I, K
171	Rixs Creek	Joint plane infills and macrocutans in subsolum of brown podzolic.	C, Q		F, M
		Tubules in lower B horizon of brown podzolic.	Q	F	C
		Carbonate lenses in sandstone.	D		Q
180	Drayton	Salt encrustation on casing of artesian bore.	H, G	B, T	Ch,K, M
308	Vere	Soluble salts in pallid zone of deep weathering profile.	H		D

Mineral Abbreviations

B	Bloedite
C	Calcite
Ch	Chlorite
D	Dolomite
F	Feldspar
G	Gypsum
H	Halite
I	Illite
I-M	Interstratified Illite and Montmorillonite
K	Kaolinite
M	Montmorillonite
Q	Quartz
T	Thenardite

Halite is the dominant mineral in salt encrustations (Table 7) and occurs in drainage lines and salt springs in the WI2 and GM provinces. It is also prominent in planar void infills resulting from contemporary wetting and drying of the subsola in soils near salt-affected areas; halite crystals also coat ped faces in the lower B horizon of these soils. Invariably there is a secondary diffuse layer (halite) around the root zone but the older concretionary, tubular and macro-cutanic pedological structures do not contain halite. Thus redistribution of halite into the unsaturated zone appears to be comparatively recent phenomenon.

The sulphate minerals thenardite and bloedite are subordinate to halite in the WI2 and GM provinces, and gypsum was found only in salt efflorescences in the GM province.

In contrast to their abundance in precipitates in the saturated zone, carbonate minerals are not important constituents of salt efflorescences owing to the lower CO_2 partial pressures in the unsaturated zone which promote carbonate precipitation before the groundwaters reach the surface; this results in an enrichment of Na^+, Cl^-, and SO_4^{2-} in groundwaters in the unsaturated zone: the abundance of concretionary carbonates in the soils of the Central Lowlands (Fig. 2) supports this argument.

Two main categories of salt efflorescences are present in the upper Hunter River valley area. The first and most spectacular of these comprises salt crusts up to several centimetres thick which are formed by evaporative concentration of stream waters, springs, and seepages in the GM and WI2 provinces of the Central Lowlands; of these, the highest frequency of salt efflorescences occurs in the Wollombi Brook valley between Broke and Singleton. The Mulbring Silstone in particular is responsible for a large number of salt scalds and salt-affected streams. Salinisation of soils, streams and groundwaters in the Central Lowlands is closely related to rock type, and the intensity of halite salting is greatest in provinces where groundwaters have the strongest connate-marine signature. Some point sources of natural salt contamination existed before European settlement in the Central Lowlands or were contemporaneous with it, as evidenced by early geographic names with salinity connotations - such as Saltwater Creek.

Forest clearing has undoubtedly exacerbated degradation of the land by promoting salting under conditions of increased runoff , erosion and rising water tables in the Central Lowlands.

The second category of salt efflorescences in the upper Hunter River valley area appears to be controlled in part by geological and geomorphological features. The efflorescences consist of small-scale salt scalds extending downstream from ephemeral springs along the nick point separating the upper and low pediments on the northeastern and southern sides of the Hunter River valley. Salt crusts in these areas comprise patchy impure films, 1 mm to 2 mm thick, which drape tunnelled dispersive clays. Most springs at the head of the salt scalds on the northeastern side of the Hunter River valley - between Bowmans Creek and the headwaters of Bettys Creek - are roughly coincident with the Hunter Thrust Fault and probably represent saline waters upwelled from the underlying Wittingham Coal Measures. However, similar springs on the western footslopes of Mount Surprise, and in the hills above Muscle and Grasstree Creeks occur in Carboniferous rocks at least three kilometres from the Hunter Thrust Fault. Most salt scalds at the change of slope on the southern side of the valley between Alcheringa and Bulga seem to emanate from intermittent saline springs at the contact between the Wollombi and Wittingham Coal Measures. In August 1982 one of these springs was still flowing out of the base of the Watts Sandstone (lowest member of the Wollombi Coal Measures) above Appletree Creek. Other salt scalds in this area appear to be related to springs and seepages at the contact between the basal fanglomerate of the Narrabeen Group and the underlying Wollombi Coal Measures.

The physical controls on this second category of salting in the upper Hunter River valley area are unresolved, nor is the chemical composition of the precipatates known; however, many of the southern salt efflorescences seem to have a close link with saline springs from the Denman Formation, others appear to be related to flushing of secondary salts from porous coarse-grained rocks. The connection between the Hunter Thrust Fault and the ephemeral springs and salt scalds on the northeastern side of the valley is tenuous because there are too many exceptions involving examples of salting away from the fault zone. An alternative explanation is that the salt efflorescences may represent the positions of maximum fluctation of the capillary fringe induced by a combined contrast in soil and rock

permeability, coincident with the change in slope of the landsurface. A decrease in soil permeability arises from the onlap of open colluvium in the subsola of the fan soils against the older podzolic soils of the lower pediment where more advanced pedogenesis has resulted in a higher degree of secondary porefilling in the subsola. This is also an area where permeability changes would be expected in the underlying fractured rock since it marks the transition zone between a horizontal maximum principal stress direction in the rocks of the central valley section and a vertical principal stress direction in the rocks of the elevated areas.

Minor elements

Analyses for B, Cu, Mn, Zn, Mo, Co, P, Fe, and Al for 100 upper Hunter River valley groundwaters (Appendix 2) show that group mean concentrations of Cu, Mn, Zn, Mo, Co, and Fe are not significantly different from zero, but the variances of Mn, Zn and Fe concentrations are high because of anomalous high counts in outliers of groundwaters of the Permian fractured rocks; Cu, Mo, and Co concentrations are uniformly low throughout the eight hydrochemical provinces. Means and 95 -percent confidence intervals for the significant trace elements B, P, and Al are shown for each province in Figure 14. Within the Permian fractured rocks there is a trend for these elements to be minimized in the WO province and maximized in the GM province. More specifically, mean concentrations of B, P, and Al are significantly higher in the GM province than in any other province, but there is no significant difference between mean concentrations in the WO and WI provinces.

Boron content in Permian coals and interseam beds has been used as a palaeo-environmental indicator by Swaine (1962, 1971), and his results are reproduced in part in Figure 14 for comparison with dissolved B in the upper Hunter River valley groundwaters. Swaine (1962) regarded seawater as the primary source of B in the Permian sediments, and concluded that the Greta Coal Measures were marine-influenced, the Tomago Coal Measures (Wittingham correlatives) were influenced by brackish or intermittent marine conditions and the Newcastle Coal Measures (Wollombi correlatives) were freshwater deposits. In a subsequent study of Bowen Basin coals Swaine (1971) stipulated that differences in boron content only become significant if marine transgression occurred during the very early stages

of coalification which allowed uptake of B by organic matter; this is consistent with conclusions drawn from the sulphur isotope study of Smith & Batts (1974). The trend established by Swaine (1962) for the Permian coals is reflected in the B concentrations of their groundwaters (Fig. 14). The most likely source of B in the CARB-TRIAS province groundwaters is from dissolution of minerals such as tourmaline; in the HFP province groundwaters B probably represents a composite derived from all the other provinces.

Phosphorus levels in groundwaters are generally considered to be high when their concentration exceeds about 0.2 ppm; Figure 14 shows that most of the upper Hunter River valley groundwaters fall into this category. A significant proportion of phosphorus in groundwaters of the Permian Coals probably represents initial fixation of organic collophanes in the peat swamps, but the trend of increasing P with increasing degree of marine influence (Fig. 14) suggests a second source involving dissolution of phosphate minerals formed in marine muds of estuaries and embayments. The comparatively high P concentrations (0.4 ppm) in the TRIAS province may be partly derived from phosphatic nodules in the Narrabeen Group described by Mayne & others (1974) whereas the source of P in the CARB province is more likely to be dissolution of primary phosphate minerals of the apatite group. A proportion of the phosphorus content in the HFP province groundwaters may be derived from modern applications of phosphate fertilizers in the irrigation areas.

Aluminium concentrations (Fig. 14) probably comprise a substantial proportion of particulate gibbsite or alumino-silicates because samples were filtered only to +0.45 μm; Hem (197C) describes Al determinations from samples inflated by gibbsite crystals of 0.10 μm diameter which easily pass through the standard laboratory filters. Al solubility is highest in acid waters and Hem (1970) quotes Al concentrations of several hundred ppm in waters of pH less than 4. Therefore the Permian acid peat swamps would have been an important sink for Al which could have attained quite high concentrations as alumina gels. Al concentrations in groundwater of the Permian fractured rocks are roughly proportional to the abundance of the alumino-carbonate mineral, dawsonite, in the aquifers.

Baseflow in the upper Hunter River valley area

The groundwater sampling program was undertaken during August 1982, near the end of a prolonged drought; the previous significant rainfall to recharge the groundwater store occurred in March 1981. The sampling program therefore presented a unique opportunity for investigating baseflow chemistry and identifying the main sources of groundwater salinity; there was no rainfall during the period of sampling.

At the time of sampling very few minor streams in the upper Hunter River valley area were flowing and baseflow samples for these streams - comprising bed underflow waters - were taken from depths ranging up to 2 m below the base of the stream bed. A piezometer of perforated PVC casing was jetted into the sands of the steam bed and then pumped intermittently until the EC of the pumped water had attained a constant value (±10%) over at least two consecutive pumping cycles. In most cases the requirement of constant salinity in bed underflow water over the final two pumping cycles necessitated an average of five cycles of alternating drawdown and recovery spread over a couple of days; for this reason, most variations in baseflow chemistry covered a timespan of more than one day. The constraint on suitability of sites for grab samples in flowing streams was that the lateral variation in EC across the stream should not exceed 10%.

Initially attempts were made to measure longitudinal variations in baseflow chemistry in every stream contained within, and draining into, the Denman-Singleton-Muswellbrook Triangle, particularly across geological and structural boundaries; however in some minor streams this objective was hindered by the following factors:

- generally no bed underflow water was intercepted within 2 m of the base of clay-bottomed streams (e.g. Farrells Creek);
- the requirement of constant salinity over at least two pumping cycles could not be attained within reasonable time (e.g., Whites Creek);
- disturbance to natural drainage by engineering works and

restricted acces (e.g., Mount Arthur, Howick, and Saltwater Creek areas).

Baseflow sampling was prematurely terminated by rains at the end of August 1982. Longitudinal variations in concentrations of the major ions in baseflow of the upper Hunter River and its tributaries are shown in Figures 15 to 20 and sample locations in Plate 2.

In flowing streams the locus for each ionic species between sampling points is controlled to some extent by ionic composition estimated from intervening EC measurements; however, there is no similar control in the bed underflow waters. The frequency of grab samples in the flowing streams was lowest along those sections where variation in EC measurements was small, and highest where large fluctuations were recorded. Changes in composition in response to mixing between two streams - schematically represented in Figures 15 to 20 - were calculated by proportion from known initial and thoroughly mixed concentration values, and estimated stream discharges; the loci of ion concentrations at, and immediately below, stream junctions represent the average value across the main stream, which is not necessarily the same as the concentration at the centre-line. Where the baseflow chemistry of the tributary stream was not greatly different from that of the main steam, the average concentration across the main stream after mixing was approximately equal to the centre-line concentration locus (e.g., Goulburn River-Wybong Creek). However, where stream salinities were highly different (e.g. Wybong Creek-Big Flat Creek), EC traversing showed that the saline tributary plume was not thoroughly dispersed into the main stream's waters for 1 to 2 km downstream from their confluence. In such cases, the schematic loci of ion concentrations were quite different from actual concentrations along the centre-line of the main stream.

Salinity variations in the major streams of the upper Hunter River valley during August 1982 are shown in Figures 15a to d (measurements taken in previous years over a range of flow conditions are documented by Garman, 1980.) The Hunter River is the only stream in the valley where variations in the chemistry of its waters could not be solely attributed to groundwater influences because its flow was regulated by the addition of waters from Glenbawn Dam. From Rouchel to upstream of Denman there was a

small but steady increase in salinity, Cl^- and HCO_3^- increased at a faster rate than the other ions (Fig 15a). There are no major tributaries in this section of the river so the increase in dissolved salts represented the combined effects of the groundwater inflows and returns from irrigation waters. A significant saline inflow was recorded near Denman, and further downstream inflow of the Goulburn River resulted in a sustained increase in Na^+, Cl^-, and HCO_3^- and a temporary decrease in SO_4^{2-} concentrations (Fig. 15a). (The Hunter-Goulburn River junction also defines the boundary between the HFP1 and HFP2 hydrochemical provinces). Salinity of the Hunter River changed very little between the Goulburn River and Bayswater Creek confluences, showing that any groundwater inflows from the Permian rocks to the north were largely diluted by fresher groundwaters from the Triassic escarpment to the south. A pronounced increase in total dissolved salts occurred between the Bayswater Creek confluence and Lemington; groundwater inflow in this section of the Hunter River was exclusively from the WI2 hydrochemical province, but its effect was diminished by the inflow of fresher surface waters from Glennies Creek and Wollombi Brook. Apart from a minor increase in salinity below the Loders Creek confluence, the Hunter River waters showed a progressive dilution in the large meanders around Singleton - owing most probably to interchange between the river and groundwaters stored in the alluvium, perhaps induced by heavy well-pumping at that time. The low salinity of these waters is surprising since a large part of the meander belt is underlain by the Mulbring Siltstone, a unit associated with many salt-affected areas elsewhere in the upper Hunter River valley.

Salinity variation in baseflow of the Wollombi Brook (Fig. 15b), a major southern tributary of the Hunter River, showed that rates of increase in Na^+ and Cl^- were lowest in baseflow waters in the section traversing the Triassic rocks and then increased progressively through the Wollombi and Wittingham Coal Measures, the highest rates of uptake of Na^+ and Cl^- coinciding with a levelling-off in HCO_3^- concentrations in the Wittingham Coal Measures just upstream from the Hunter River. Baseflow chemistry of Wollombi Brook therefore appears to be strongly controlled by lithology.

Glennies Creek, a major stream draining a large catchment in the northeast of the study area, showed that uptake of Na^+, Cl^-, and SO_4^{2-} (Fig. 15c) was considerably increased as the stream flowed across the Hunter

Thrust Fault (which separates Carboniferous rocks in its headwaters from Permian rocks in its lower reaches). The Cl^- locus within 2 km either side of the fault zone was accurately located by intensive EC traversing. Significantly, the Cl^- concentrations were found to increase several kilometres upstream from the Hunter Thrust Fault, indicating the extent of atmospheric recycling of Cl^- in the Glennies Creek valley; conversely, significant increases in SO_4^{2-} were detected in Glennies Creek only downstream of the Hunter Thrust Fault.

The lower reaches of the Goulburn River showed very little variation in dissolved salts (Fig. 15d), apart from a sustained step increase of Cl^- and Na^+ and, to a lesser extent, Ca^{2+} and Mg^{2+} at its confluence with the Wybong Creek. Garman (1980) traced chemical variations in the Goulburn River from its headwaters in the Tertiary basalts to its junction with the Hunter River. He equated the progressive decline in HCO_3^-/Cl^- and $(Ca^{2+} + Mg^{2+})/Na^+$ ratios in baseflow waters with distance from silicate sources in weathered basalts, and attributed the marked increase in Cl^- concentrations in the lower reaches of the Goulburn River to inflow from the Wybong Creek.

The baseflow chemistry of the major tributary streams in the western part of the study area is shown in Figures 16a to c. The headwaters of Wybong Creek to the north of the study area drain Tertiary basalts where silicate-weathering provides an abundant supply of HCO_3^- to baseflow waters; however, in the section studied (Fig. 16a) the Wybong Creek drains rocks only of the Narrabeen Group. Steady increases in EC values were first detected about 0.5 km upsteam from the confluence with Big Flat Creek but the highest salinities were measured at the junction of the two streams where the introduction of highly saline bed underflow waters from Big Flat Creek was greatest; however, this saline plume did not become thoroughly mixed within the Wybong Creek waters until about 2 km further downstream.

Martindale Creek drains the Wollombi Coal Measures for much of its course, but its tributaries drain the Narrabeen Group rocks. Its moderate rate of increase in baseflow salinity (Fig. 16b) was similar to that of the other north-flowing streams emanating from the Triassic escarpment, but it was the only stream in which HCO_3^- was not the dominant anion; this probably reflected seepage from the irrigation waters because pumping of shallow groundwaters from alluvial terraces was far greater in the Martindale Creek

valley than in any other valley to the east incised into the Triassic rocks.

Baseflow of Sandy Creek (Fig. 16c) was characterised by high Cl^- and HCO_3^- and low SO_4^{2-} concentrations in common with most other streams draining fractured rocks of the WI1 hydrochemical province (sample stations 81, 91 and 96 are bed-underflow samples, but lack confirmatory EC measurements between sampling points). Infiltration of Spring Creek waters caused a substantial decrease in bed underflow salinity, though the dilution effect was negated within a few kilometres downstream by the introduction of saline groundwaters from the Wittingham Coal Measures. In August 1982 surface flow in Sandy Creek commenced from seepages and outwash from bed-load gravels about 1 km upstream from station 235 (Fig. 16c). (It was not possible to obtain samples downstream from station 235 owing to impedance of the natural flow regime by holding ponds.).

Of the most prominent two streams draining the Muswellbrook Anticline, Saddlers Creek on the the western limb showed marked increases in Na^+ and Cl^- (Fig. 17a; Pl.2) and a concurrent decrease in SO_4^{2-} as it crossed from the Maitland Group rocks to flow over the Wittingham Coal Measures. The eastern limb of the Muswellbrook Anticline is drained by Bayswater Creek (Fig. 17b); the nature of the baseflow chemistry in its upper reaches in the Maitland Group rocks is unknown because its waters are impounded in the Elecom fly-ash dam and Lake Liddell. From Lake Liddell to station 105 baseflow characteritics of Bayswater Creek were obscured by artificial discharges and diversion associated with coal washery and mining activities; however, downstream from this point Bayswater Creek was relatively undisturbed, and under low-flow conditions its baseflow waters probably approached equilibrium with groundwaters of the Wittingham Coal Measures by the time it reached the Hunter River. The fundamental difference between baseflow chemistry in the lower reaches of Saddlers Creek and Bayswater Creek during August 1982 was that the former was characterised by WI1 hydrochemical province signature (low SO_4^{2-}/Cl^- ratios) whereas the latter exhibited high SO_4^{2-}/Cl^- ratios typical of WI2 province groundwaters.

Most streams in the northeastern part of the study area show changes in baseflow chemistry as they flow from Carboniferous rocks to the Permian

sediments of the central lowlands. Unlike most other south-flowing streams in the CARB provinces, Bowmans Creek showed a small but steady decrease in dissolved salts as it approached the Hunter Thrust Fault (Fig. 18a). EC measurements between stations 163 and 132 decreased linearly and continuously throughout this section of the stream indicating that the decline in baseflow salinity was induced by groundwater dilution rather than tributary inflows. A marked increase in the concentrations of all ions occurred where Bowmans Creek traversed the Hunter Thrust Fault and intercepted groundwaters from a small faulted block of Maitland Group sediments, an area whose landsurface was dotted with severe salt scalds. Downstream from station 126 saline waters discharging at a rate of about 30 L/sec from Foybrook Mine constituted the bulk of surface flow in Bowmans Creek and caused an abrupt change in the baseflow chemistry of the stream: (high SO_4^{2-} and Cl^- concentrations at station 126 are characteristic of groundwaters of the GM and lower WI2 (Vane Subgroup) provinces). Between Foybrook Mine (station 126) and the Swamp Creek confluence baseflow salinity dropped sharply, mainly owing to dilution by alluvial groundwaters, although a small part of the decrease in HCO_3^- and SO_4^{2-} concentrations was caused by the precipitation of carbonate and sulphate minerals on the banks and low terraces of Bowmans Creek. Further downstream mixing and equilibration of the Swamp Creek saline waters with shallow groundwaters of the alluvium resulted in a steady decrease in baseflow salinity in Bowmans Creek to its junction with the Hunter River.

The rates of increase of the various ions in baseflow of Swamp Creek (Fig. 18b) between stations 139 and 140 conformed with stream baseflow waters in equilibrium with groundwaters of the WI2 province -being characterized by approximately equal rates of enrichment of Cl^-, Na^+ and SO_4^{2-}, and constant or slowly declining HCO_3^- concentrations. Between stations 140 and 135 the channel of Swamp Creek has been diverted around the open-cut Swamp Creek Mine. Saline seepages from clay overburden dumps adjacent to the lower section of the diversion channel resulted in sharply increased concentrations of Cl^-, Na^+, SO_4^{2-}, and Mg^{2+} in baseflow waters. Continually increasing EC values to a maximum of 12500 µS/cm(~7500 mg/L TDS) were recorded in baseflow waters in the section through the non-vegetated overburden dumps. At station 135 immediately downstream from these dumps, the banks and bed-load sediments of Swamp Creek were thickly coated with a precipitate of halite, thenardite, and bloedite, which partly

explains the sudden drop in SO_4^{2-} concentrations (Fig. 18b). Downstream from here to its confluence with Bowmans Creek, Swamp Creek drains rural land; analyses to station 133 recorded a steadily decreasing baseflow salinity caused by groundwater mixing and dilution, even though its channel was coated with salt encrustations for most of this distance. Below station 133 the introduction of highly saline WI2 province groundwaters resulted in a significant increase in Cl^- concentrations.

In the headwaters of Muscle Creek (Fig. 18c) HCO_3^- was the dominant anion in baseflow traversing Carboniferous rocks above the Hunter Thrust Fault. Downstream through the Maitland Group rocks rates of uptake of Cl^- and SO_4^{2-} rose while HCO_3^- concentrations diminished slightly. Between stations 206 and 205 Muscle Creek crosses volcanics and marine sediments of the Dalwood Group; baseflow chemistry through the Dalwood Group rocks was characterised by increases in rates of enrichment of all ions except Cl^- which tapered off slightly. Below station 205 Muscle Creek re-enters Maitland Group rocks, but it was not practical to continue hydrochemical tracing because of disturbance by urban development. Variations in ion concentrations in Muscle Creek baseflow indicate that subtle differences are discernable in the groundwater chemistry of the pre-Wittingham Coal Measures Permian rocks, which suggests that some definition of the hydrochemical system is lost by combining these units together as a single province. A more satisfactory partitioning of the GM province would have separated the marine provinces (upper-Maitland Group and lower-Dalwood Group from the intervening Greta Coal Measures, but partitioning of data would have resulted in a gross imbalance in group sizes, and an excessive number of hybrids. The important difference hydrochemically between the Maitland and Dalwood Groups is that submarine volcanics are abundant in the latter, and groundwaters of the Dalwood Group would therefore be expected to contain products of silicate mineral dissolution in addition to the background salts associated with a marine depositional environment.

Variations in concentrations of dissolved ions in Stringybark Creek are shown in Figure 18d; this stream was sampled in June 1983, ten months after the end of the drought. In addition to a baseflow component, the samples are comprised of an unknown proportion of interflow waters, but even in this flow regime, lithology clearly influences the stream water chemistry - as shown by the rates of increase of Cl^-, Na^+, and SO_4^{2-} as the

stream flows from Carboniferous to Permian rocks. Station 321 is a repeated sample of station 124 taken during the previous August; a comparison of ionic ratios distinctly shows the addition of dissolved CO_2 in the interflow waters.

Previous examples have depicted the common trend of increased rates of Cl^- and SO_4^{2-} enrichment as streams cross the Hunter Thrust Fault from the Carboniferous rocks of the southern New England Fold Belt to the Hunter River floodplain entrenched in the Permian rocks of the valley floor. The baseflows of streams within the CARB province therefore appear to be characterised by gradually increasing solute concentrations dominated by relatively uniform increments of HCO_3^- and cations released by silicate weathering. However, this is not the case in the eastern part of the CARB province; rather, baseflow compositions seem to be more highly influenced by atmospheric recycling of salts within a 10-20 km radius of the boundary of the Permian source area. The intensity of redistributed airborne salts in the eastern CARB province varies inversely with distance from the Hunter Thrust Fault, as shown by the variation in HCO_3^-/Cl^- ratios of baseflow waters in the Goorangoola-Glennies Creek valley (Table 7a).

TABLE 7A. CHANGE IN MEAN $HCO_3^-:Cl^-$ RATIOS IN BASEFLOW OF GOORANGOOLA-GLENNIES CREEK VALLEY

Location	Trunk stream	Mean $HCO_3^-:Cl^-$ (concentrations in meq/L)	Mean distance from Hunter Thrust Fault (km)
Native Dog Creek	Goorangoola Creek	0.8	13
Campbells Creek	Goorangoola Creek	0.65	8
Dawleys Creek	Goorangoola Creek	0.5	2
Brandys-Sawyers Creek	Glennies Creek	0.4	2

Goorangoola Creek is entrenched into Carboniferous rocks in a meridional valley bounded by the Bullock and Razorback Ridges (Pl.2). The ascendancy of the solution of locally redistributed salts over silicate

mineral dissolution as the dominant process controlling baseflow chemistry of Goorangoola Creek is clearly shown (Fig. 18e) by the downstream decline in HCO_3^-/Cl^- ratios. This trend was overprinted by mixing with waters from Campbells Creek downstream from station 157; and by subsurface recharge through gravel aquifers of fresher waters impounded by levees built around a former cut-off meander upsteam from station 152 (see Pl.2).

The baseflow chemistry of two highly saline streams draining Permian rocks in the eastern and southeastern parts of the study area are shown in Figures 19a and b. In Main Creek (Fig. 19a) baseflow salinity increased sharply about midway between stations 165 and 174 where the stream intersects massive conglomerate overlying the Bayswater coal seam. (Two kilometres further west this conglomerate coincides with what appeared to be a major source of salts in Bettys Creek.) Rapid declines in Na^+ and Cl^- concentrations occurred in the Main Creek baseflow downstream from the conglomerate where its waters mixed with shallow alluvial groundwaters. It was not possible to decide if the conglomerate represented a considerable secondary salt store that was diffusing salts into the stream, or whether the impermeable nature of the conglomerate underbed induced stagnation of perched waters with slowly increasing solute concentration by capillary zone losses.

Variations in baseflow salinity of Loder Creek (Fig.19b) are a direct consequence of differences in structure and fracture permeability in the Permian rocks of the Wollombi Brook valley. The headwaters of Loder Creek drain coals and interseam sediments of the Jerrys Plain Subgroup, upper Wittingham Coal Measures (see Table 1), and large amounts of Na^+ and Cl^- were taken into solution in its bed-underflow waters. The Mount Thorley Monocline (Pl.1) which is defined by a local steepening of dip from angles of less than 10° to over 40°, appears to restrict lateral transmission of groundwaters from the Wittingham Coal Measures through to the underlying Mulbring Siltstone of the Maitland Group; certain up-gradient salt springs in the Wittingham Coal Measures may well be generated by back-up and overspill of groundwaters in response to this impediment. At depth this permeability restriction results in conditions approaching groundwater stagnation, and produces some of the most saline waters in the upper Hunter River valley. A secondary consequence of this impedance to groundwater throughflow is that groundwaters have much longer residence time in the

aquifers and are thus able to equilibrate with a greater diversity of the less-soluble minerals in the coal seams. On crossing the Mount Thorley Monocline the baseflow of Loder Creek showed a progressive decline in salinity despite inflows from several highly saline tributaries draining the Mulbring Siltstone. However, from station 61 to its confluence with the Hunter River, the stream flows close to the axis of the Loder Dome and its baseflow was diluted by the considerable storage of fresher groundwaters in sets of tensile fractures with enhanced permeability. There was also a noticeable progressive increase in stream discharge along the Loder Dome.

The effect on the baseflow chemistry of upwelling groundwaters from a structural discontinuity is shown in two streams in the northwest of the study area (Figs 20a and b). A vertical upward flow of saline groundwaters with a strong WI2 province signature along the trace of a diagonal fault transcurrent to the Mount Ogilvie Fault is intercepted by Spring Creek (Fig. 20a) and Big Flat Creek (Fig. 20b). Baseflow salinity in Spring Creek did not decline rapidly in response to groundwater dilution because the decay loci were reinforced by an additional pulse of saline groundwaters from the Denman Formation (top of the Wittingham Coal Measures - see Table 1) near station 86. The permeability of the Triassic rocks underlying the lower section of Big Flat Creek was not high enough to admit inflows of diluting groundwaters sufficient to equilibrate the baseflow with the TRIAS groundwaters. In this respect, Big Flat Creek was the only stream measured in the study area where baseflow chemistry was completely dissimilar to the groundwaters of the rocks through which it flowed.

In summary, the variations in baseflow chemistry of most rivers and tributaries in the study area indicate that the Permian rocks were the major source of salt loads in the upper Hunter River valley streams during August 1982; the addition of salts from saline groundwaters and baseflow traversing Permian hydrochemical provinces resulted in an increase in total soluble salts in the Hunter River from an initial concentration of 285 mg/L at Rouchel to 825 mg/L at Singleton, but ephemeral concentrations of almost 1000 mg/L were recorded locally; salinities would have been very much higher if diluting waters had not been regularly released from the Glenbawn Dam, just north of the study area. Although baseflow measurements were taken when the drainage system was under severe drought conditions, salt

loads carried by streams in the first flush after the rains would undoubtedly have attained higher values due to re-dissolution of efflorescent crusts in the stream channels. The variation in longitudinal concentrations of the conservative ions in Figures 15 to 20 shows that there is considerable interaction between groundwaters and baseflow in the upper Hunter River valley streams, which testifies to the robustness of the system in dispersing saline pulses generated both artifically and naturally. There has been considerable speculation on the effect of coal mining and related activities on water quality of the streams in the region. In this survey two instances of accelerated enrichment of solutes in baseflow due to mining were detected in the Bowmans Creek catchment; however, without pre-mining baseflow measurements for comparison, it is not possible to assess objectively the quantity of solutes that could be attributed directly to mining since groundwaters in these areas are known to have high background salinities. The greatest uptake of salts by the streams was from natural sources: lithological differences and structural discontinuities in the Permian rocks.

CHEMICAL EQUILIBRIA

Data preparation

Not all sample analyses in Appendix 1 are complete enough to use in equilibria interpretations; especially so with soluble SiO_2 and K^+, although K^+ concentrations of samples were often estimated by the mean K^+ value of the particular hydrochemical province. Owing to the nearly uniform distribution of K^+ in the study area (Fig. 4) this procedure introduced only minor errors in the total chemical balance. Also some samples were rejected on the basis of an unacceptable ionic balance according to the constraint:

$$\left| \frac{\Sigma[\text{cations}] - \Sigma[\text{anions}]}{\Sigma[\text{cations}] + \Sigma[\text{anions}]} \right| > 0.10,$$

where ion concentrations are in milli-equivalents per litre (meq/L).

This screening yielded a data set of 491 samples distributed amongst the hydrochemical provinces as follows: CARB, 33; TRIAS, 17; WO, 87; HFP1, 31; HFP2, 77; WI1, 69; WI2, 100; and GM, 77.

Analytical concentrations were converted to molalities and the ionic strength (I) was obtained by the equation:

$$I = \tfrac{1}{2}\Sigma m_i z_i^2 \quad \ldots\ldots\ldots\ldots\ldots\ldots\ldots (1),$$

where m_i is the molal concentration, and z_i the valence of each ionic species.

Activity coefficients, Ψ_i, for each ionic species were obtained from the Debye-Huckel equation (Garrels & Christ, 1965):

$$-\log\Psi_i = \frac{Az_i^2 (I)^{\frac{1}{2}}}{1+a_i B (I)^{\frac{1}{2}}},$$

where A and B are characteristics of H_2O, and a_i is the effective diameter of the ion in solution.

Various refinements of the Debye-Huckel equations are available (Stumm & Morgan, 1970), but as the ionic strength of these ground-waters average about 10^{-2}M, the errors involved in using the unmodified Debye-Huckel equation are negligible. Carbon dioxide pressure (P_{CO2}), CO_3^{2-} and OH^- concentrations were then calculated by:

$$P_{CO2} = \frac{(HCO_3^-).\ \Psi HCO_3^-.\ (H^+)}{K_{CO2}} \quad .....(2),$$

$$(CO_3^{2-}) = \frac{K_{HCO_3^-}.\ K_{CO_2}.\ P_{CO_2}}{CO_3^{2-}.\ (H^+)^2} \quad .....(3),$$

$$(OH^-) = \frac{K_{H_2O}}{\Psi OH^-.\ (H^+)} \quad .....(4),$$

where K_{CO_2} and $K_{HCO_3^-}$ are the dissociation constants of the CO_2-H_2O system; $K_{H^2\ O}$ the dissociation constant of H_2O; and (HCO_3^-) the total dissolved CO_2. ( ) are used to denote molal concentrations, and the activity of H^+ is taken as 1.0.

These values were then substituted back into equation (1) and the calculations reiterated to a constant ionic strength. At the same time electroneutrality of the system

was corrected by distributing the error amongst all the species in proportion to their contribution to the electroneutrality equation:

$$2(Ca^{2+}) + 2(Mg^{2+}) + (Na^{+}) + (K^{+}) + (H^{+}) = 2(CO^{2-}_{3}) + 2(SO^{2-}_{4}) + (HCO^{-}_{3}) + (Cl^{-}) + (OH^{-}) \quad \ldots\ldots\ldots\ldots (5).$$

All subsequent calculations were made from these 'filtered' data sets of molality and activity coefficients.

Disequilibrium indices

The potential for a mineral to crystallise from solution can be expressed in terms of a Disequilibrium Index: defined as the ratio of the ionic product of reactants to the thermodynamic solubility product of a given mineral (Paces, 1972). This can be explained most readily by the example of dolomite - $CaMg(CO_3)_2$:

at equilibrium,

$$CaMg(CO_3)_2 = Ca^{2+} + Mg^{2+} + 2CO^{2-}_{3}$$

and

$$K_{sp(dolomite)} = [(Ca^{2+}).\ \Psi Ca^{2+}] \ .\ [(Mg^{2+}).\ \Psi Mg^{2+}] \ .\ [(CO^{2-}_{3}).\ \Psi CO^{2-}_{3}]^2$$

where $K_{sp(dolomite)}$ is the solubility product of dolomite at 25°C and 1 atmosphere pressure.

The Disequilibrium Index (Q) is then given by:

$$Q = \log_{10}\left| \frac{(Ca^{2+}).\ \Psi Ca^{2+}.\ (Mg^{2+}).\ \Psi Mg^{2+}.\ [(CO^{2-}_{3}).\Psi\ CO^{2-}_{3}]^2}{K_{sp(dolomite)}} \right|$$

..... (6)

where values for the numerator are obtained from the water analysis, and $K_{sp(dolomite)}$ is obtained from published thermodynamic data.

When the analytical values equal the actual solubility product of the mineral in equation 6, Q equals zero and equilibrium is established. Positive values of Q indicate supersaturation, while negative values indicate undersaturation with respect to a particular mineral. Precipitation of authigenic minerals is theoretically only possible in supersaturated groundwaters; conversely, mineral dissolution is a distinct possibility in undersaturated waters. In mixed salt systems values of Q ranging from -0.5 to +0.5 are generally taken to represent a state of equilibrium because of the uncertainties in the analytical values, and variations of K_{sp} in the presence of other ionic species.

A large number of minerals can be screened in this way using computer programs such as WATEQ (Truesdell & Jones, 1974) or modifications. However in this study only those minerals known or suspected to occur authigenically in significant quantities in the upper Hunter River valley have been compared with the water samples. (Congruent solubility products of minerals used for equilibria calculation are given in Table 8).

Simple carbonate minerals

Figure 21 shows the frequency distribution of Disequilibrium Indices for the total sample space using calcite ($CaCO_3$), magnesite ($MgCO_3$), and natron ($Na_2CO_3.10H_2O$). Calcite and magnesite have very similar distributions, and their Q-values indicate that a large proportion of the water samples are in an equilibrium or supersaturated state with them; in some examples the calculated ion products were up to 100 times greater than that required for equilibrium. On the other hand, Q values for natron averaged around -8.0 thus indicating that simple sodium carbonates would not be expected in upper Hunter River valley aquifers.

A breakdown of the Q-values for calcite and magnesite (Fig. 22)

showed that in all but the TRIAS and WO provinces, 81-97 percent of samples exhibited saturation with respect to calcite; the percentages were only slightly lower for magnesite. Even so, approximately 50 percent of the WO samples and 30 percent of the TRIAS samples were similarly saturated. Disequilibrium Indices were not calculated for siderite ($FeCO_3$) since Fe was detected only in 8 of the 100 samples analysed for minor elements. It is therefore highly unlikely that precipitation of siderite can occur in the contemporary hydrogeochemical system.

TABLE 8. CONGRUENT SOLUBILITY PRODUCTS (K°) OF MINERALS

$CaSO_4.2H_2O$	Gypsum	2.399×10^{-5}
$CaCO_3$	Calcite	4.467×10^{-9}
$CaMg_3(CO_3)_4$	Huntite	1.076×10^{-30}
$CaMg(CO_3)_2$	Dolomite	1.0×10^{-17}
$Mg(OH)_2$	Brucite	7.079×10^{-12}
$MgCO_3$	Magnesite	1.0×10^{-8}
$Mg_4(CO_3)_3(OH)_2$	Hydromagnesite	1.259×10^{-35}
$MgSi_3O_6(OH)_2$	Sepiolite	1.0×10^{-24}
NaCl	Halite	3.819×10^{1}
$Na_2CO_3.10H_2O$	Natron	4.89×10^{-2}
Na_2SO_4	Thenardite	6.62×10^{-1}
$Na_2Mg(SO_4)_2.4H_2O$	Bloedite	4.169×10^{-3}
$NaAlCO_3(OH)_2$	Dawsonite	4.115×10^{-7}
SiO_2	Amorphous silica	1.995×10^{-3}
$Al(OH)_3$	Gibbsite	9.120×10^{7}
$Al_2Si_2O_5(OH)_4$	Kaolinite	4.677×10^{6}
$Na_{0.33}Al_{2.33}Si_{3.67}O_{10}(OH)_2$	Beidellite	1.122×10^{19}
$CaAl_2Si_2O_8$	Anorthite	5.012×10^{24}
$KAlSi_3O_8$	Microcline	2.188×10^{1}
$Na_2Ca(SO_4)_2$	Glauberite	1.998×10^{0}
SiO_2	Chalcedony	2.999×10^{-4}

Complex carbonate minerals

Complex carbonate species may be represented (Fig. 23) by minerals such as hydromagnesite - $Mg_4(CO_3)_3(OH)_2$, huntite - $CaMg_3(CO_3)_4$, dolomite - $CaMg(CO_3)_2$, and dawsonite - $NaAlCO_3(OH)_2$; the complex iron carbonate mineral ankerite - $Ca(Fe,Mg)(CO_3)_2$, was not compared to the water analyses because of the inhibiting Fe concentrations mentioned earlier. These complex carbonates show a high proportion of saturation and supersaturation, although the distribution of Q-values is more widely

dispersed than for calcite or magnesite. Hydromagnesite and huntite in particular show a polymodal distribution - Disequilibrium Indices range from +6 to < - 12.5. Increasing the proportion of Mg^{2+} or OH^- in the mineral formula apparently reduces the possibility of complex carbonates being in equilibrium with the groundwaters.

Partitioning the Disequilibrium Indices into hydrochemical provinces (Fig. 24) shows that the distribution of Q-values for dolomite is very similar to that of calcite and magnesite. For hydromagnesite, WI1, WI2, and GM are the only provinces to show appreciable proportions of saturated samples, while huntite-saturation is more widespread (38-68% of samples) over the HFP2, WI1, WI2, and GM provinces. Significantly, the solubility products (K_{sp}) of these complex carbonates are much lower than those for the simple carbonates; therefore, in theory, they should take priority in sequential precipitation from the Ca^{2+}-Mg^{2+}-CO_3^{2-}-OH^- system.

The remaining complex carbonate mineral dawsonite (Fig. 23), is comparatively abundant in the Permo-Triassic rocks of the upper Hunter River valley despite its otherwise very limited global distribution. Only 93 samples were available for calculation of Disequilibrium Indices, but this is sufficient to show that the ionic products are well above the values of saturation with respect to dawsonite. The relatively high concentrations of Na^+(10^{-2}M), compared to approximately 10^{-5}M for both Al^{3+} and CO_3^{2-} is partly responsible for the large Q-values. The formation of dawsonite is unusual because it represents a combination reaction between alumino-silicate weathering, simple salt formation, and CO_2 pressure; presumably by the reaction of dissolved CO_2 with gibbsite:

$$Al(OH)_3 + HCO_3^- + Na^+ = NaAlCO_3(OH)_2 + H_2O.$$

High soluble-SiO_2 concentrations would probably favour the formation of kaolinite from gibbsite (as discussed later), so dawsonite-formation may be largely dependant on a highly specific leaching environment involving removal of SiO_2 while allowing access of CO_2 and Na^+.

All hydrochemical provinces are represented in the dawsonite distribution (Fig. 23), although only one sample from each of the CARB and TRIAS provinces is included. The GM and WI2 provinces contain the highest Q-

values, but since all samples were supersaturated with respect to dawsonite, little significance can be attached to this observation.

Simple sodium minerals

Since sodium chloride is frequently associated with saline groundwaters and salt efflorescences in the upper Hunter River valley a comparison was made (Fig. 25) between halite (NaCl), mirabilite ($Na_2SO_4.10H_2O$), and natron ($Na_2CO_3.10H_2O$); (various other sodium sulphates and carbonates could have been used, but the minerals chosen represent the least-soluble forms). The large negative Q-values (extreme undersaturation) indicate that none of these sodium salts could have formed within the contemporary groundwater system; concentrations in the order of 10^6 to 10^8 times the observed values would have been required to achieve saturation; however, the presence of halite and thenardite (the anhydrous form of mirabilite) in surface evaporite encrustations (Table 7) indicates the magnitude of evaporative processes in concentrating these highly soluble salts.

Sulphate minerals

Of the sulphate minerals (Fig. 26), gypsum ($CaSO_4.2H_2O$) was the most abundant and least undersaturated; mirabilite, bloedite, and glauberite showed increasing undersaturation over greater ranges of Disequilibrium Indices. Only about 5% of the samples, entirely within the WI2 and GM provinces, exhibited gypsum equilibrium; however, the high proportion of Q-values between -0.5 and -1.5 in these provinces indicates that gypsum should be significant in the early products of evaporative concentration. As gypsum is unlikely to form in high-bicarbonate waters (because of the preference for Ca^{2+} to combine with HCO_3^-); it would not be commonly expected to form authigenic minerals in the alkaline groundwaters of the upper Hunter River valley.

Bloedite ($(Na_2Mg(SO_4)_2).4H_2O$) was identified in a number of evaporites (Table 7) and is considered to form by substitution of Mg^{2+} in the thenardite or mirabilite crystal structure. On the other hand glauberite ($Na_2Ca(SO_4)_2$) was not detected in this survey, despite its

former abundance in the Mulbring Siltstone - as discussed previously. The very low Q-values for glauberite indicate that it is extremely unlikely to form under present conditions, even as an evaporite, as it requires very low temperatures to become a stable phase. Both bloedite and glauberite have similar multi-modal distributions (Fig. 27), which is well illustrated by glauberite for each hydrochemical province; the GM and WI2 provinces have considerably higher Q-values owing to their higher SO_4^{2-} status, but even so there is considerable variation within a number of the provinces.

The secondary (less undersaturated) mode in the mirabilite distribution (Fig. 26) is composed almost entirely of samples from the GM province where 92% of samples had Disequilibrium Indices greater than -5.5.

Silica minerals

Amorphous silica (SiO_2) and sepiolite ($MgSi_3O_6(OH)_2$) were chosen to represent a large range of possible silicates; sepiolite because Mg^{2+} is the most likely cation to form a silicate in the presence of low aluminium concentrations. Although more insoluble minerals such as chrysotile ($Mg_3Si_2O_5(OH)_2.5H_2O$) or talc ($Mg_3Si_4O_{10}(OH)_2.10H_2O$) would normally form in preference to sepiolite in this groundwater environment they have not been identified in the upper Hunter River valley aquifers. Likewise, chalcedony has been widely identified in the study area although amorphous SiO_2 is generally considered to be the most probable low-temperature silica form despite its higher solubility.

Amorphous silica and chalcedony have very narrow ranges of Q-values (Fig. 28); chalcedony is displaced noticeably into the saturated zone - about 80 percent of the samples are saturated - distributions in the individual provinces (Fig. 29) are remarkably consistent. For amorphous silica relatively little increase in SiO_2 concentration of the groundwaters would be required for equilibrium to exist. Hydrochemical provinces showing equilibrium with respect to amorphous silica are HFP2 ($-0.5<Q<+0.5$ for 30% of samples), WI1 (20%), WO(20%), and HFP1 (13%). In the contemporary leaching environment of the upper Hunter River valley, aqueous SiO_2 is derived from dissolution of silicate minerals, and hence the more aggressive the percolating groundwaters, in terms of dissolved CO_2-induced acidity, the more SiO_2 would be expected in solution. A comparison of SiO_2

concentrations and CO_2 pressure (Fig. 30) does not show a well-defined trend, although the components are significantly positively correlated (r = 0.37).

In spite of having a much smaller K_{sp}-value than aqueous SiO_2, sepiolite does not exhibit a high degree of sample saturation. The OH moiety of sepiolite apparently results in a reduction and variation of Q-values similar to the simple and complex carbonates. The WI1, WI2, WO, and HFP2 provinces have 12-13% saturated samples whereas the TRIAS and HFP1 groups have none.

The role of carbon dioxide

The examples discussed indicate that the carbonate systems are the most important in the upper Hunter River valley groundwaters. Sources of dissolved CO_2 include influx of atmospheric CO_2 with recharge rainwater, oxidation of coal, and dissolution of carbonate minerals.

Computed CO_2-pressures (Fig. 31) average around 10^{-2} atmos compared with $10^{-3.5}$ for standard atmospheric pressure. Even allowing for possible losses of dissolved CO_2 during sample collection, this represents an active medium for silicate weathering - as discussed later.

The fact that ionic products often exceed the solubility product of various carbonate minerals by several orders of magnitude indicates that other factors influence the initiation of precipitation reactions. In particular the ionic strength of a solution can have a marked effect on the equilibrium constant of mineral systems (Block and Waters, 1968; Jurinak, 1984). Dolomite and calcite were observed in a number of surface salt encrustations, which accords well with the stability diagram for Ca and Mg carbonates at various CO_2 pressures presented by Garrels and Christ (1965): magnesite and hydromagnesite are stable phases only at CO_2 pressures less than 10^{-6} atmospheres, and Ca/Mg ratios of less than 10^{-3} - neither condition is commonly satisfied in the upper Hunter River valley groundwaters. When these groundwaters are exposed to the atmosphere there is a loss of dissolved CO_2 accompanied, less significantly, by a rise in pH which can be calculated by rearranging the electroneutrality equation 5 as follows:

$$2(Ca^{2+}) + 2(Mg^{2+}) + (Na^{+}) + (K^{+}) - 2(SO_4^{2-}) - (Cl^{-}) = 2(CO_3^{2-}) + (HCO_3^{-}) + (OH^{-}) + (H^{+}) \quad \ldots\ldots\ldots\ldots\ldots\ldots\ldots\ldots (7)$$

The right-hand side of the equation can be expressed in terms of (H^+) - as in equations (3) and (4) - together with

$$(HCO_3^{-}) = \frac{K_{CO_2} P_{CO_2}}{HCO_3^{-}.(H^{+})}$$

The left-hand side of equation 7 and activity coefficients for CO_3^{2-}, HCO_3^{-}, and OH^{-} are obtained as described previously and the equation is solved for H^{+}. Iteration is used to achieve the final values at a prespecified level of accuracy.

Mean analytical values were taken for each hydrochemical province and new pH values were calculated assuming equilibration with atmospheric CO_2. Marked changes were observed (Fig. 32): the pH of TRIAS and WO province samples increased by about 2.7 units while samples from the remaining provinces averaged an increase of about 1.6 units. These changes, together with the new values of CO_3^{2-}, HCO_3^{-}, and OH^{-} alter the Disequilibrium Indices to larger values, thus increasing the tendency to supersaturation and precipitation of pH-dependant minerals. This is clearly demonstrated for calcite (Figs. 33 a and b) and sepiolite (Figs. 33c and d) in the WO and GM provinces which were specifically selected on the basis of the clusters shown in Figure 32.

A further consequence of carbonate precipitation from discharging groundwater is that Na^{+}, Cl^{-}, and SO_4^{2-} concentrations will increase accordingly. Evaluation of the mixing effects with the atmosphere and surface waters is not within the scope of the present study, but it is apparent that stream-water quality may be strongly dependant on the type of equilibrium reactions described above.

Aluminosilicates

Garrels & McKenzie (1967) have proposed a weathering model

(consistent with many groundwater compositions) that involves the attack of minerals such as feldspars (high silica and cation contents) by CO_2-enriched water, which leaves a gibbsite residue; however, unless the dissolved silica is removed rapidly, kaolinite becomes the stable solid phase at the expense of gibbsite. Early stages of weathering are thus characterised by water compositions consistent with kaolinite and very low soluble Al concentrations. As weathering of the primary minerals continues, silica and cation concentrations, and pH increase until montmorillonite forms. It is therefore likely that compositions of deeper groundwaters, or those in long contact with primary mineral grains, move away from the gibbsite-kaolinite boundary towards kaolinite-montmorillonite equilibrium.

This proposed weathering sequence contrasts with that of Jackson & Sherman (1953), and later supported by the results of Rai & Lindsay (1975); however, the two models are compatible under Garrels & McKenzies' (1967) assumption that the weathering products (silica and cations) accumulated in situ whereas Rai & Lindsay (1975) assumed that the weathering products were rapidly removed by leaching. Undoubtedly both situations occur in natural groundwaters with aquifer permeability, effective porosity and position along flow lines having a large influence on the movement of weathering products and hence the tendency for either gibbsite or montmorillonite to become the stable mineral forms.

In applying thermodynamic principles to chemical weathering, a decision must be made as to whether congruent or incongruent dissolution will be considered. Rai & Lindsay (1975) considered congruent dissolution in which the starting-point mineral dissociated into its individual components under the influence of H^+; for example,

$$NaAlSi_3O_8 + 4H^+ + 4H_2O = Na^+ + Al^{3+} + 3H_4SiO_4$$
(low albite)

Garrels & McKenzie (1967), Stumm & Morgan (1970), among others report such weathering in incongruent terms; such as,

$$NaAlSi_3O_8 + 4\tfrac{1}{2}H_2O + H^+ = \tfrac{1}{2}Al_2Si_2O_5(OH)_4 + 2H_4SiO_4 + Na^+$$
(low albite) (kaolinite)

Again, both approaches may be correct depending on the hydrodynamic environment, but since rapid removal of weathering products is not likely and Al^{3+} concentrations are not unduly high (2ppm), the incongruent relationship appears to be the more appropriate model for the upper Hunter River Valley groundwaters; Figure 34 illustrates this weathering sequence assuming calcic plagioclase anorthite ($CaAl_2Si_2O_8$) as a starting point mineral. The solubility products used are those of Stumm and Morgan (1970) who point out that the boundary conditions can vary markedly with the molecular formulae chosen for the solid constituents. This is particularly so for some of the plagioclase feldspars in which isomorphous substitution within the crystal lattice is more common in the intermediate compositions than the pure end-members.

Assuming the anticlockwise weathering sequence described previously, it can be seen that a number of upper Hunter River valley groundwater samples have very low soluble SiO_2 concentrations and hence are located in the gibbsite stability field, where their distribution within that field is an artefact due to analytical detection limits. The only hydrochemical provinces not represented in the gibbsite stability field are HFP1 and HFP2; most samples are from the WI2 and GM provinces. Only two samples appear to come under the control of anorthite, once again representing the WI2 and GM provinces.

Most samples lie within the kaolinite stability field with a strong tendency to congregate towards the kaolinite-montmorillonite boundary, as predicted for a model incorporating the accumulation of weathering products. In fact, 151 of the 493 samples are located within the montmorillonite field which also includes 55 percent of the HFP2 samples. The TRIAS province has no montmorillonite representatives, while 15-30 percent of samples in the remaining provinces meet the equilibrium requirements. In general this distribution conforms with the geomorphological environment: the TRIAS province occupies an elevated position in which rainfall infiltration is enhanced in the open colluvial soils, and soluble silica is likely to be removed fairly rapidly in interflow and groundwaters under the prevailing hydraulic gradients. Conversely, HFP2 groundwaters represent a sink towards which weathering products from the surrounding uplands are directed.

In high-Ca^{2+} environments, it has been suggested (Stumm and Morgan, 1970) that calcite control of CO_2 pressure may exert considerable control on the weathering 'aggressiveness' of groundwaters. Since the carbonate system has been demonstrated to be a major feature of these groundwaters, the tendency for calcite to form has been compared with the tendency for Ca-montmorillonite to be a stable phase; as shown in Figure 35 where the vertical axis represents the kaolinite-Ca-montmorillonite boundary derived from:

$$\underset{\text{(Ca-montmorillonite)}}{3Ca_{0.33}Al_{4.67}Si_{7.33}O_{20}(OH)_4} + 2H^+ + 3H_2O = \underset{\text{(kaolinite)}}{7Al_2Si_2O_5(OH)_4}$$

$$+ 8H_4 + SiO_4 + Ca^{2+}$$

$$\left(\log K = \log \frac{(Ca^{2+})}{(H^+)^2} + 8 \log (H_4SiO_4) = -15.4\right)$$

where ( ) represents active concentration.

Calcite saturation occurs concurrently with a wide range of alumino-silicate stability conditions (Fig. 35), and in conjunction with gibbsite (Zone A), kaolinite (Zone B) and Ca-montmorillonite (Zone C); any causal inter-relationship is therefore rather tenuous. This is not surprising since silicate minerals are not the only source of Ca^{2+} in the upper Hunter

River valley groundwaters. Prior marine transgressions, dissolution of carbonate minerals, and the continual influence of cyclic salt all represent past and present alternative sources of Ca^{2+}.

Figure 36 shows a similar type of analysis to that used in Figure 34, except that it traces the weathering of sodic plagioclase (albite) to Na-montmorillonite. It demonstrates the major difficulties associated with obtaining meaningful results with stability diagrams, that is, the need to ascertain detailed mineralogy of the aquifers and the solubility constants for these minerals. Two sets of mineral boundaries have been plotted in Figure 36, one from Stumm & Morgan (1970), the other from the free energy of formation (ΔG_f^o) data collated by Rai & Lindsay (1975). In the former, a large proportion of the water samples plot in the albite stability field, a few in the Na-montmorillonite field, and the remainder largely in the kaolinite field. With Rai and Lindsay's data, virtually all of the samples plot in the kaolinite field, with the montmorillonite boundary displaced well into the zone where amorphous silica precipitation would be expected. Both sets of boundaries use the same mineral formulae, but there are obviously considerable differences in the incongruent dissolution solubility constants. Unless this information is known for specific localities, the results must be regarded only as an indication of the likely operative water-mineral equilibria.

The equivalent plots for K-feldspar dissolution are shown in Figure 37 together with boundaries calculated from data provided by Garrels & Christ (1965) and Rai & Lindsay (1975). Again, there are considerable differences in the stability field boundaries, but in this case the general result is not affected greatly. Apart from those samples having very low soluble SiO_2, virtually all the remaining samples lie within the kaolinite stability field.

In summary, apart from the difficulties of boundary conditions described above, it would seem that the bulk of upper Hunter River valley groundwaters examined have compositions compatible with kaolinite formation. This places them about mid-way through the chemical weathering cycle regardless of whether accumulating or leaching conditions are prevalent. There is a tendency for the groundwaters to congregate towards the kaolinite-montmorillonite boundary, but it is regrettable that free energy of formation and solubility constants for montmorillonites of various compositions are so poorly established, even for the pure end-members. However, the analytical approach demonstrated still remains valid, and the groundwater-aluminosilicate equilibria relationships in the upper Hunter River valley, or in any other groundwater system for that matter, could only be refined with publication of further mineral solubility constants.

STATISTICAL ANALYSIS

(a) Variation between hydrochemical provinces

Canonical variates

Contrasts in groundwater chemistry between the eight hydrochemical provinces were analysed by the method of canonical variates (Rao, 1952).

Canonical variates analysis discriminates between (a priori) group means by generating linear functions of the variables for which the ratio of the between-groups mean square to the within-groups mean square is maximised subject to the within-groups mean square being set to unity. The eigenvalues (λ_i) are extracted from the characteristic determinant:

$$|BW^{-1} - I| = 0$$

where

$$B = \frac{1}{k-1} H \quad \text{and} \quad W = \frac{1}{n-k} E$$

H = between-groups sums of squares and cross-products matrix;

E = within-groups sums of squares and cross-products matrix;

I = identity matrix;

k = number of groups;

n = total sample size.

The dimensions of λ_i are reduced according to min (p, k-1), where p = number of variables.

The corresponding eigenvectors ($\mathbf{c}_i$) are derived from

$$(BW^{-1} - I)(WC) = 0$$

subject to the constraints - $\mathbf{C}_i\ WC_i = 1$ for unit variance;

and $\mathbf{C}'_i\ WC_j = C_i'\ BC_j = 0$ - so that the canonical vectors are uncorrelated for all i = j.

The first canonical vector, C_1, is the direction of maximum variation between group means, $\mathbf{C}_2$ is the direction of the maximum of the remaining variation, and so on for the third and subsequent vectors. The proportion of the total variance accounted for by the j largest canonical variates is given by the ratio:

$$\sum_{i=1}^{j} \lambda i \Big/ \sum_{i=1}^{\min(p,\,k-1)} \lambda i$$

The canonical variate scores of the ith group mean are given by:

$$Y_{il} = \mathbf{C}_1'\ (\mathbf{X}_i - \mathbf{G}),\ \ldots\ ,\ Y_{ir} = \mathbf{C}_r'\ (\mathbf{X}_i - \mathbf{G})$$

where $\mathbf{X}_i$ is the mean vector of the ith group,

and **G** is the vector of grand means.

Censoring and transformation of data

Only six variables were used in the canonical variates analysis, viz. HCO_3^-, Cl^-, SO_4^{2-}, Ca^{2+}, Mg^{2+}, and Na^+. The K^+ and SiO_2 measurements were omitted because of the large number of missing values, and because of significant rounding errors associated with detection limits of these ions in the laboratory. Measurements of pH were omitted because it was considered that the true natural variation of this parameter was too sensitive to sampling errors. Electrical conductivity, or the regression estimate of total soluble salts, was omitted because it largely depends on the six major ions, and is therefore redundant.

The raw data was $\log_{10}$- transformed, partly to attempt to satisfy the necessary condition for canonical variates analysis of homogeneity of the covariance matrices of each group, but more importantly, to approach multinormality. If data are multinormally distributed, the canonical variates analysis transforms the within-groups' ellipsoids of variation to spheres in the space defined by the canonical axes. Therefore, a two-dimensional graphical plot of the positions and inter-group distances of the canonical variate means may be greatly enhanced by delineation of confidence circles about the mean scores. It will be subsequently shown in the principal components analyses that the $\log_{10}$- transformation is indeed appropriate for the upper Hunter River valley groundwater data.

Results

The first four canonical roots and vectors are shown in Table 9.

Table 9. CANONICAL ROOTS AND VECTORS FOR UPPER HUNTER HYDROCHEMICAL PROVINCES

($\log_{10}$ transformed data; n = 670, p = 6, k = 8)

	Canonical vectors (loadings)			
Variable	1	2	3	4
HCO_3^-	0.31	0.98	4.28	1.07
Cl^-	-0.24	-2.34	0.52	3.90
SO^{2-}	-0.87	0.91	0.06	1.38
Ca^{2+}	-0.50	2.18	-1.15	-3.00
Mg^{2+}	0.73	0.40	-0.51	-0.33
Na^+	-1.89	-0.69	-1.38	-4.73
Canonical root	1.60	0.77	0.19	0.07
% variance	60.3	28.9	7.2	2.6

As the canonical variate scores are adjusted for the grand mean, a positive/negative loading on a variable will generate a positive/negative contribution to a canonical variate score if the deviate of the group mean

relative to the grand mean is positive. However, the magnitude of the contribution depends on both the deviate and the loading.

Interpretation of the canonical vectors (i)

The magnitude and signs of the loadings for the first canonical variate, Y_1, show that this vector primarily separates the groups according to Na^+ (strong negative) and SO_4^{2-} (intermediate negative) against Mg^{2+} (intermediate positive). Since SO_4^{2-} has the greatest between group variance, its contribution to Y_1 scores is somewhat greater than the unstandardised loadings would indicate; similarly, the contribution of Mg^{2+} loadings on Y_1 scores is diminished because Mg^{2+} has the lowest variance of these three elements. In systems where a concept of growth is valid, the first canonical variate is generally a 'sizing' vector (Blackith & Reyment, 1971). In the present study, Y_1 is not an absolute discriminator of size because its loadings are of mixed signs, yet ranking of group means along Y_1 is identical to a 'size' ranking by mean total (log-transformed) soluble salts. High positive scores are attained by groups where waters are low in Na^+ and SO_4^{2-}; in the study area such waters are generally of low salinity status. Conversely, waters high in Na^+ and SO_4^{2-} produce high negative scores, and these two elements are always prominent in the high salinity groundwaters of the upper Hunter River valley area. Y_1 is therefore analagous to a sizing vector because it orders groups by salinity status, but the between-groups separations along Y_1 are not proportional to arithmetic differences between mean total soluble salts of the provinces. Rather, separations are distorted according to the degree of relict marine influences indicated by Na^+ and SO_4^{2-} (and Cl^-) concentrations versus the relative influence of the contemporary continental leaching regime on the chemistry of the waters; the continental signature is indicated by Mg^{2+} (and HCO_3^-) concentrations which are linked to silicate and carbonate mineral dissolution.

The second canonical variate, Y_2, separates the provinces according to hydrochemical facies and is not connected in any way to salinity. Na^+-Cl^--type waters with negative scores are contrasted against Ca^{2+}-SO_4^{2-} and Ca^{2+}-HCO_3^--type waters with a minor contribution from Mg^{2+} associated with the latter facies. Again, standardised SO_4^{2-} loadings make a greater contribution to Y_2 scores than does HCO_3^-.

Figure 38 shows the separation of group means along the first and second canonical variates which together account for 89% of the total sample variance. The ($+Y_1$, $+Y_2$) quadrant contains the plots of the group means with the best quality groundwaters of the upper Hunter River valley area; these waters are characterised by low salinities - bicarbonate to chloride ratios greater than 1 and sodium adsorption ratios less than 3. Mean scores of the HFP1 and HFP2 provinces plot well within this field, while the CARB province plots marginal to the Y_1 axis owing mainly to an increased proportion of Cl^- over HCO_3^- in areas proximal to the Hunter Thrust Fault.

The ($+Y_1$, $-Y_2$) quadrant contains the means of the WO, WI1, and TRIAS provinces groups. The high positive Y_1 score for the TRIAS province is a consequence of its low salinity status, and the high negative Y_2 score is generated by low Ca^{2+}, SO_4^{2-}, and HCO_3^- concentration relative to Cl^- and Na^+. The WO group mean has a lower Y_1 score primarily because of increased concentrations of Ca^{2+} and HCO_3^-. The WI1 province plots close to the Y_2 axis because of its higher salinity, and its Y_2 score is not greatly different from that of the WO province group since its increased Cl^- concentrations are compensated for by concurrent increases in Ca^{2+} and HCO_3^- concentrations.

The GM and WI2 group means which are widely separated from the other six provinces along Y_1, have the highest salinities, and therefore have high negative Y_1 scores. Furthermore, Y_1 divides the four Permian fractured-rock provinces into two clusters: the GM and WI2 group means are separated on the basis of their strong relict marine signature; whereas the WI1, WO provinces are clustered with the 'continental' groundwater provinces. The GM province is contrasted with the WI2 province along Y_2, reflecting the sub-dominance of SO_4^{2-} in the anions of the GM province.

Loadings for the third and fourth canonical variates, Y_3 and Y_4, have the unusual property of polarising anions (positive loadings) against cations (negative loadings). Together, Y_3 and Y_4 account for almost 10% of the total variation, and therefore order the groups in a non-random manner. Our interpretation of these vectors is that Y_3 separates groups according

to the intensity of silicate and carbonate mineral dissolution, and Y_4 discriminates rates of mineral dissolution under a continental leaching regime against rates of molecular diffusion from the matrix of certain marine sedimentary rocks. Thus Y_3 and Y_4 are process-response vectors. Separation of groups along Y_5 and Y_6 does not seem to be of any consequence.

A plot of group means relative to Y_2 and Y_3 is shown in Figure 39. Whilst these two variates account for only just over one third of the total variation, they are nevertheless the most meaningful for understanding this system since they indicate the relationship between hydrochemical processes and facies variations. In fact, Blackith & Reyment (1971) quote many similar cases in morphometric applications of canonical variates analysis where physically important contrasts between groups have been attained, even with statistically insignificant vectors.

In Figure 39, the distances between the TRIAS, WO and WI1, and WI2 group means mainly reflect their variation in Y_3 scores. The rays linking these provinces are schematic only, the unbroken lines representing direction of groundwater flow, and the broken lines indicating hydrochemical processes which are important in the genesis of these waters. Groundwaters originating by recharge in fractured rocks of the Triassic escarpment in the southern and western sections of the study area flow through the Wollombi Coal Measures on the lower hillslopes, and the proportion of these waters which is not intercepted en route then flows through the Wittingham Coal Measures on the Hunter River valley floor and ultimately discharges into the floodplain alluvium. The mode of transmission varies from base flow in steams to interflow, shallow lateral throughflow, and deep circulation.

It has been shown previously that the topographic settings of the fractured-rock provinces dictate the hydraulic gradients, therefore mean groundwater velocities are highest in the TRIAS province, next highest in the WO province and lowest in the WI1 and WI2 provinces. Under conditions of rapid throughflow of recharge waters initially low in H_2CO_3, hydrolysis of silicate minerals is retarded by the combined effects of low concentrations of H^+ ions and rapid groundwater velocites. Under slower flow regimes and continuing addition of vertical recharge waters enriched

in H_2CO_3, incongruent dissolution of silicates induces HCO_3^- concentrations in proportion to the valences of the cations of the silicate minerals; the intensity of this process would be reflected in increasing Y_3 scores. Therefore Y_3 (Fig. 39) separates incipient silicate dissolution in the TRIAS province from incongruent silicate dissolution in the other provinces in which groundwater flow rates are lower. The contrast depends highly on differences in groundwater velocities, and probably also on vegetation and soil characteristics. For carbonate minerals, the TRIAS-WO-WI1-WI2 groundwater flow path represents the progression from undersaturated to supersaturated conditions; that is, the high negative Y_3 score of the TRIAS province represents an active medium where carbonate minerals are being dissolved, whereas Y_3 scores closer to zero represent conditions where waters are in equilibrium with respect to carbonates, or areas where carbonates are being precipitated.

The separation of these groups along Y_2 reflects facies variations; in terms of processes, the broken rays in the direction of Y_2 (Fig. 39) probably represent dispersion of aerosols through the groundwater system, thus these small distances can be regarded as Na^+ and Cl^- background. In this context, aerosols are composed of locally redistributed salts in addition to a steady-state component of solutes in maritime rainfall.

The major proportion of groundwater leaving the upper Hunter River valley is of HFP2 composition, which at any instant in time can be considered as a mixture of the other seven groups. The large separation along Y_2 between the WI1, WI2 provinces and the HFP2 province (Fig. 39) is far greater than the distances representing dispersion of background salts from the TRIAS and WO provinces; it indicates molecular diffusion of dominantly Na^+ and Cl^- from connate marine salts of the Wittingham Coal Measures. This input of Na^+-Cl^--type water is strongly diluted by waters of the HFP1 province (Fig. 39).

The contribution from the CARB province is approximately equally composed of the products of silicate and carbonate mineral dissolution (Y_3) and dispersion of background salts (Y_2). The trend of local redistribution of salts to be maximised in the eastern part of the CARB province has been described, but it is also pertinent to note that the CARB province occupies the high country in the northeast of the study area (Pl. 2) and therefore

probably receives higher rates of marine aerosols in rainfall. The GM province has a higher Y_2 score than the HFP2 province, primarily because of its higher SO_4^{2-}/Cl^- ratios. The magnitude of the Y_2 separation between these two provinces represents the algebraic sum of chloride (negative) and sulphate (positive) diffusion; the sense of direction indicates that sulphate diffusion dominates over chloride. The GM group also contributes products of carbonate mineral dissolution to the HFP2 province groundwaters from solution of carbonates in joints by acids released by sulphide oxidation, a mechanism which incidently explains the buffering of pH in this system.

Distances between groups

The complete linkage dendrogram based on $\log_{10}$-transformed data of the eight hydrochemical provinces is shown in Figure 40. The similarity measure is Mahalanobis's Generalized Distance. The provinces essentially form four clusters: TRIAS, CARB-HFP2-HFP1, WO-WI1, and GM-WI2.

Further partitioning of data

The eight hydrochemical provinces were divided into twenty-five subgroups (Table 10) and re-analysed by the method of canonical variates. The provinces were partitioned in such a way that the effects of geographic variation and differences in mode of transmission of the groundwaters could be assessed. An exception was the CARB province where the split was done to test differences between the two major geological units alone, given that a division based on the well established geographic variation in the CARB province would have contributed no new information. Again, the six variables were $\log_{10}$-transformed.

TABLE 10. SUBDIVISION OF UPPER HUNTER RIVER VALLEY HYDROCHEMICAL PROVINCES FOR CANONICAL VARIATES ANALYSIS.

Subgroup	Parent group	Description of subgroup	No. of samples in subgroup

1	)	Baseflow, Wollombi Coal Measures	20
2	)	Wells and bores; Bulga to	17
	)	Alcheringa	
3	) WO	Wells and bores; Broke valley north	25
	)	to Bulga	
4	)	Wells and bores, western Wollombi Coal	31
	)	Measures, Martindale valley to northern	
	)	boundary of study area	
5	)	Surface samples, wells on lateral	17
	)	drainage from Carboniferous rocks, and	
	)	wells in direct hydraulic continuity	
	)	with the Hunter River (<100 m from	
	)	bank)	
	)		
6	)	Wells on lateral drainage from Wollombi	21
	)	Coal Measures.	
	) HFPI		
7	)	Wells on lateral drainage from	29
	)	Wittingham Coal Measures.	
	)		
8	)	Wells with lateral drainage from	19
	)	Maitland Group	
9	)	Surface samples, Hunter River	17
	)		
10	)	Wells on lateral drainage from Maitland	44
	)	Group	
	)		
11	) HFP2	Wells on lateral drainage from Wollombi	21
	)	and Wittingham Coal Measures	
	)		
12	)	Wells and bores, Lemington, on lateral	23
	)	drainage from Wittingham Coal Measures	
13	)	Baseflow, lower Wittingham Coal	26

	)	Measures; Broke valley	
	)		
14	) WI2	Baseflow, lower Wittingham Coal	39
	)	Measures; Foybrook-Falbrook	
	)		
15	)	Bores in lower Wittingham Coal Measures	34
16	)	Baseflow, lower Wittingham Coal	19
	)	Measures; central area	
17	)	Baseflow and wells, Branxton Formation	46
	)	and Greta Coal Measures	
	) GM		
18	)	Baseflow and wells, Mulbring Siltstone	39
	)		
19	)	Bores in Maitland Group and Greta Coal	41
	)	Measures	
20	)	Baseflow, upper Wittingham Coal	32
	)	Measures	
	)		
21	) WI1	Wells, upper Wittingham Coal Measures	36
	)		
22	)	Bores, upper Wittingham Coal Measures	22
23	TRIAS	Baseflow, wells, and springs,	19
		Narrabeen Group	
24	)	Baseflow and wells, Gilmore Group	16
	) CARB		
25	)	Baseflow, Wallaringa Formation	17

Results

The first four canonical roots and vectors are shown in Table 11.

TABLE 11. CANONICAL ROOTS AND VECTORS FOR UPPER HUNTER RIVER VALLEY HYDROCHEMICAL SUBGROUPS

($\log_{10}$ transformed data, n = 670, p = 6, k = 25)

	Canonical vectors (loadings)			
Variable	1	2	3	4
HCO_3^-	0.24	0.61	-4.77	-1.08
Cl^-	0.82	-1.98	-0.33	-7.46
SO^{2-}	0.72	1.17	-0.01	-0.11
Ca^{2+}	-0.15	2.66	0.58	-0.20
Mg^{2+}	-0.77	0.06	1.03	2.61
Na^+	1.76	-0.82	1.42	6.21
Canonical root %	1.96	1.29	0.53	0.18
Variance	46.5	30.6	12.6	4.4

Interpretation of the canonical vectors (ii)

The physical interpretation of separations between subgroups by these four new vectors is essentially the same as for the initial canonical variates analysis run on the eight groups. Likewise, Y_1 is a discriminator of size (TSS), except that signs of the loadings are reversed, and the weighting on Cl^- is increased at the expense of SO_4^{2-}; the latent discriminatory power of Y_1 in marine versus continental influences is preserved. Similarly, Y_2 differentiates groups according to hydrochemical facies except that positive scores are more highly identified with Ca^{2+}-SO_4^{2-} than Ca^{2+}-HCO_3^- waters. Again, Y_3 and Y_4 (Table 11) are 'process'

vectors which contrast groups according to the intensity of silicate and carbonate mineral dissolution, and diffusion of connate marine salts. However, in contrast to the initial canonical variates analysis, signs are reversed, loadings on Mg^{2+} are increased at the expense of Ca^{2+}, and the components linked with diffusion and flushing of connate salts are almost exclusively identified with Cl^-; the effect of SO_4^{2-} deviations on Y_3 and Y_4 scores are negated by low weights on SO_4^{2-} in both vectors.

Separation of the 25 subgroup means along the Y_1 and Y_2 vectors is shown in Fig. 41. Subgroup means of the HFP1, HFP2, and CARB provinces plot in the ($-Y_1$, $+Y_2$) quadrant which is characterized by low TSS - Ca^{2+} is the dominant cation and SO_4^{2-} and/or HCO_3^- the dominant anion(s). The Y_1 scores of the HFP1 subgroups (Fig. 41) show a gradual increase in salinity - from surface samples and wells receiving lateral drainage from Carboniferous rocks, to wells underlain by the Wollombi Coal Measures, to wells underlain by the Wittingham Coal Measures and Maitland Group. Y_2, a strong positive discriminator of SO_4^{2-}, separates those subgroups of the HFP1 and HFP2 provinces which comprise wells underlain by the Maitland Group rocks; this contrast implies significant groundwater mixing in certain areas of the floodplain alluvium, a feature that will be later explored by principal components analysis.

Ninety-five-percent confidence circles of the CARB subgroups 24-25 (Fig. 41) intersect both clusters of HFP1 and HFP2 subgroups, showing that groundwaters of the floodplain retain a strong Carboniferous province signature throughout the study area. The CARB-HFP2 link obtained in both sets of canonical variates analyses shows that a high proportion of wells of the HFP2 subgroups above Singleton are in direct hydraulic continuity with the Hunter River because underlying lithological variations cause negligible difference in Y_1 scores for the means of the HFP2 subgroups distal to Maitland Group rocks.

In the ($-Y_1$, $-Y_2$) quadrant (Fig. 41), which is characterised by waters of low salinity (Na^+ is the dominant cation and Cl^- the dominant anion), the 95% confidence circle of the TRIAS group (23) intersects confidence circles of the southern WO subgroups 2-3 of subsurface samples, and the WO subgroup 1 of baseflow samples (which reflects the source of these streams in Triassic rocks). Y_1 and Y_2 separate the WO subgroup 4

from the TRIAS-southern WO cluster, principally because of significantly increased proportions of Ca^{2+}, SO_4^{2-} and HCO_3^- in the WO 4 subgroup. There are two explanations for this contrast: groundwater velocities are much lower in the western Wollombi Coal Measures and thereby permit a greater intensity of silicate dissolution which completely overprints the TRIAS signature, or the increased Ca^{2+} and HCO_3^- concentrations are weathering products from either Tertiary basalts to the northwest or underlying dolerite intrusives. A concomitant substantial increase in mean Mg^{2+} concentration in WO subgroup 4 favours the hypothesis of silicate mineral dissolution from basic rocks.

The WI1 subgroups are separated by Y_1 and Y_2 vectors into end-members - wells (subgroup 21) and bores (subgroup 22) - and intermediate baseflow (subgroup 20). The distances between subgroup means indicate that, at the time of sampling, streams draining the WI1 province were intercepting roughly equal proportions of shallow and deeply-circulating groundwaters.

Means of the GM subgroups 17-19 have positive Y_1 scores because of their high salinity, and positive Y_2 scores - (their anionic composition is such that $(SO_4^{2-} + HCO_3^-) > Cl^-$); these subgroups also have the highest Ca^{2+} concentrations. Subgroup 19 (bores in the GM group) is enriched in HCO_3^- which, in these deeper waters, may be due in part to oxidation of coal by sulphate. Subgroups 17 and 18 (baseflow in the Mulbring Siltstone and Branxton Formation-Greta Coal Measures respectively) have lower Y_2 scores because of increased mean $Na^+:Ca^{2+}$ and $Cl^-:(HCO_3^- + SO_4^{2-})$ ratios; this reflects active flushing of diffused connate marine salts in the oxidation zone.

The WI2 subgroups 13-16 are high-salinity groundwaters with Na^+ the dominant cation and Cl^- the dominant anion. The increased concentration of all ions, although with relatively minor changes in ionic proportions, in subgroup 13 separates this group from the other WI2 subgroups along Y_1 and Y_2 and suggests conditions of groundwater stagnation. The most likely concentration mechanism is increased residence time in the aquifer owing to impedance of groundwater throughflow by the Mt. Thorley Monocline. The least saline baseflow waters draining the Lower Wittingham Coal Measures were found in the northern part of the valley (subgroup 14). Y_1 and Y_2

scores for the central area (subgroup 16) are intermediate between subgroups 14 (north) and 13 (south) baseflow scores, thus indicating a southward trend of increasing Y_1 and decreasing Y_2 scores for the WI2 subgroups which reflects a sympathetic increasing Na^+-Cl^- concentration gradient; in addition to structural controls related to the Hunter Thrust Fault, this may represent a transition across a palaeogeographic boundary. During the Late Permian marine transgressions the Wittingham Coal Measures closest to the Hunter Thrust would have had a greater thickness of sediments saturated by the freshwater lens extending from the landmass of the New England Fold Belt.

Distances between subgroups

In the complete-linkage dendrogram of the 25 subgroups (Fig. 42), with Mahalanobis's D^2 as the similarity measure, clustering shows that the original relationships between the eight hydrochemical groups have been largely preserved with one exception - the TRIAS group is linked with the southern WO subgroups 2-3 and the WI1 subgroups 20 and 22. This gives essentially three main clusters: HFP1-HFP2-CARB, with some WO and WI1 hybrids; WO-WI1-TRIAS; and GM-WI2.

Comparison of the canonical variates analyses

Results from the two canonical variates analyses are consistent. Angles between the two sets of canonical vectors are -27°(Y_1), 13°(Y_2),-10°(Y_3), and -33°(Y_4). Grouping in the first analysis was based solely on geological provenance whereas the finer partitioning of data in the second analysis additionally incorporated geographic variation and, where possible, differences in mode of transmission (baseflow, and shallow and deep groundwaters). The fact that the integrity of the geological groups is maintained through both analyses testifies to the resilience of the data and shows that geological provenance is the single most important factor in influencing groundwater chemistry in the upper Hunter River valley.

(b)Variation within hydrochemical provinces

Principal components

Principal components analysis (pca) is a long-established technique for investigating within-group dependence structures of multivariate observations. The p dimensions of correlated variables required for adequate description of the hydrochemical system are reduced by rigidly rotating the coordinate axes of the original observation space to the directions of maximum variation of the dispersion of sample points and generating q<p uncorrelated components as linear functions of the original variables.

The eigenvalues, λ_i, are extracted from the determinantal equation:

$$|S - \lambda I| = 0$$

where S = covariance matrix of observations, and I is the identity matrix.

The corresponding eigenvectors, $\mathbf{a}_i$, are derived from

$$(S-\lambda I)\ \mathbf{a}_i = \mathbf{0}$$

subject to the constraints $\mathbf{a}'_i\ \mathbf{a}_j = \mathbf{0}$ for orthogonality,

and $\mathbf{a}'_i\ \mathbf{a}_i = 1$ for uniqueness of the eigenvectors.

The constraint for uniqueness also determines the property

$$\text{Var}\ (Y_i) = \lambda_i$$

where $Yi = a_{1i}X_1 + \ldots\ldots\ldots + a_{pi}X_p$ is the ith principal component of the p-variate observation matrix X.

The first principal component Y_1, associated with the dominant eigenvalue of S, explains the maximum proportion of the sample variance; the second principal component Y_2, associated with the second largest

eigenvalue of S accounts for the maximum of the remaining variance, and so on, for the third and subsequent principal components corresponding to successively smaller eigenvalues. The proportion of the total variance accounted for by the first j principal components is given by the ratio

$$\sum_{i=1}^{j} \lambda i / tr(S) \quad ; \quad 1 \leq j \leq p$$

The principal component scores of the ith individual are

$$Y_{i1} = \mathbf{a}'_1 (\mathbf{X}_i - \mathbf{G}), \ldots\ldots\ldots, Y_{ip} = \mathbf{a}'_p (\mathbf{X}_i - \mathbf{G})$$

Where X_i is the observation vector for the ith individual, and **G** is the vector of sample means.

In cases where the variables exhibit significant inequality of variance, the eigenvalues and eigenvectors are extracted from the sample correlation matrix R, and the principal component scores of the ith individual are then given by:

$$Y_{i1} = \mathbf{a}'_1 \mathbf{z}_i, \ldots\ldots\ldots\ldots, Y_{ip} = \mathbf{a}'_p \mathbf{z}_i$$

where $\mathbf{z}_i$ is the vector of standardized observations whose elements $z_{ij} = \dfrac{x_{ij} - g_j}{s_j}$ are the "standard scores" of the original variables.

Methodology

As in the canonical variates analyses only the six major ions HCO_3^-, Cl^-, SO_4^{2-}, Ca^{2+}, Mg^{2+}, and Na^+ were used in the principal components analyses. Likewise, variables were $\log_{10}$-transformed to stabilize variances, and two sets of principal components were extracted from each hydrochemical province - one from the S matrices and the other from the R matrices. Finally, the pooled data were subjected to two principal component analyses; eigenvalues and eigenvectors were extracted from the S

and R matrices of $\log_{10}$-transformed observations.

Results

The first three principal components from S and R matrices are shown in Table 12.

TABLE 12. PRINCIPAL COMPONENTS EXTRACTED FROM COVARIANCE AND CORRELATION MATRICES OF UPPER HUNTER RIVER VALLEY HYDROCHEMICAL PROVINCES

(log_{10}-transformed data).

	CARB province					
	Loadings (S matrix)			Loadings (R matrix)		
	1	2	3	1	2	3
HCO_3^-	-0.17	0.26	0.24	-0.44	-0.13	0.28
Cl^-	-0.28	0.46	-0.48	-0.44	-0.04	-0.43
SO_4^{2-}	-0.86	-0.52	0.02	-0.23	0.95	0.19
Ca^{2+}	-0.21	0.35	0.52	-0.42	-0.18	0.48
Mg^{2+}	-0.27	0.49	0.32	-0.46	-0.19	0.20
Na^+	-0.20	0.30	-0.58	-0.41	0.05	-0.66
Eigenvalue	16.38	6.68	1.23	4.33	0.82	0.60
% Variance	66.2	27.0	5.0	72.2	13.7	10.0
	TRIAS province					
HCO_3^-	-0.49	0.02	-0.61	-0.42	-0.36	-0.49
Cl^-	-0.33	0.32	0.38	-0.46	0.26	0.27
SO_4^{2-}	0.44	0.84	-0.32	0.11	0.78	-0.61
Ca^{2+}	-0.46	0.10	-0.42	-0.43	-0.25	-0.46
Mg^{2+}	-0.43	0.33	0.34	-0.47	0.16	0.19
Na^+	-0.25	0.29	0.30	-0.45	0.33	0.24
Eigenvalue	22.50	12.92	2.81	4.08	1.31	0.42
% Variance	57.2	32.9	7.2	68.0	21.8	7.0
	WO province					
HCO_3^-	-0.25	0.32	0.53	-0.37	0.43	0.59
Cl^-	-0.40	0.29	-0.45	-0.46	0.05	-0.46
SO_4^{2-}	-0.60	-0.79	0.02	-0.24	-0.89	0.16
Ca^{2+}	-0.36	0.19	0.53	-0.43	-0.06	0.44
Mg^{2+}	-0.41	0.27	0.03	-0.47	0.02	-0.04
Na^+	-0.35	0.27	-0.47	-0.44	0.13	-0.47

Eigenvalue	80.40	33.75	7.03	4.17	0.88	0.46
% Variance	62.4	26.2	5.5	69.5	14.7	7.7
			HFP1 province			
HCO_3^-	-0.12	0.11	0.01	-0.39	-0.22	0.24
Cl^-	-0.44	0.55	0.24	-0.48	-0.19	0.09
SO_4^{2-}	-0.76	-0.61	-0.20	-0.34	0.45	-0.78
Ca^{2+}	-0.27	0.11	0.45	-0.43	0.32	0.10
Mg^{2+}	-0.23	0.12	0.49	-0.44	0.31	0.46
Na^+	-0.28	0.54	-0.68	-0.35	-0.72	-0.34
Eigenvalue	28.21	11.11	4.43	3.43	0.95	0.63
% Variance	60.2	23.7	9.5	57.2	15.8	10.5
			HFP2 province			
HCO_3^-	-0.18	0.18	-0.03	-0.45	0.02	0.09
Cl^-	-0.25	0.41	-0.53	-0.45	-0.33	-0.24
SO_4^{2-}	-0.77	-0.63	-0.02	-0.16	0.88	-0.39
Ca^{2+}	-0.24	0.19	0.23	-0.42	0.24	0.52
Mg^{2+}	-0.45	0.56	0.54	-0.45	-0.04	0.39
Na^+	-0.22	0.23	-0.62	-0.43	-0.23	-0.60
Eigenvalue	37.09	25.05	6.39	3.48	1.00	0.77
% Variance	50.6	34.2	8.7	57.9	16.7	12.8
			WI1 province			
HCO_3^-	-0.30	0.28	-0.29	-0.41	0.43	-0.05
Cl^-	-0.47	0.24	-0.04	-0.49	0.09	-0.06
SO_4^{2-}	-0.52	-0.84	-0.11	-0.25	-0.59	-0.75
Ca^{2+}	-0.23	0.04	0.66	-0.34	-0.54	0.52
Mg^{2+}	-0.40	0.23	0.52	-0.45	-0.15	0.34
Na^+	-0.45	0.31	-0.45	-0.46	0.38	-0.22
Eigenvalue	88.72	38.05	14.51	3.76	0.98	0.76
% Variance	58.9	25.3	9.6	62.6	16.3	12.7

WI2 province

HCO_3^-	-0.18	-0.17	-0.42	-0.38	0.51	0.45
Cl^-	-0.44	-0.22	-0.22	-0.49	0.06	0.01
SO_4^{2-}	-0.42	-0.52	0.58	-0.40	-0.09	-0.81
Ca^{2+}	-0.21	0.25	0.57	-0.27	-0.77	0.30
Mg^{2+}	-0.65	0.67	-0.12	-0.41	-0.25	0.23
Na^+	-0.37	0.38	-0.32	-0.48	0.27	-0.06
Eigenvalue	129.89	25.58	16.63	3.85	0.98	0.54
% Variance	68.9	13.6	8.8	64.2	16.4	9.0

GM province

HCO_3^-	-0.12	-0.43	0.54	-0.22	0.91	0.27
Cl^-	-0.44	-0.41	-0.01	-0.46	0.01	-0.27
SO_4^{2-}	-0.57	0.54	-0.34	-0.43	-0.27	-0.07
Ca^{2+}	-0.24	0.44	0.63	-0.34	-0.31	0.77
Mg^{2+}	-0.45	0.01	0.28	-0.49	-0.02	0.12
Na^+	-0.45	-0.42	-0.32	-0.45	0.05	-0.48
Eigenvalue	78.78	11.81	9.76	3.90	0.90	0.74
% Variance	72.1	10.8	8.9	65.0	15.0	12.4

POOLED

HCO_3^-	-0.19	0.27	-0.04	-0.37	0.43	0.56
Cl^-	-0.43	0.38	0.23	-0.46	0.23	-0.21
SO_4^{2-}	-0.65	-0.74	0.10	-0.37	-0.39	-0.59
Ca^{2+}	-0.24	0.01	-0.65	-0.37	-0.65	0.42
Mg^{2+}	-0.38	0.31	-0.53	-0.43	-0.14	0.19
Na^+	-0.41	0.36	0.48	-0.44	0.41	-0.29
Eigenvalue	1029.14	201.66	100.40	4.17	0.69	0.56
% Variance	72.7	14.2	7.1	69.5	11.5	9.3

Interpretation of the principal components

(i) **Principal components from within groups covariance matrices.** In every case except the TRIAS group (Table 12) the coefficients of the first principal components from the S matrix, $Y_1(S)$, are all negative, and coefficients of the second and subsequent principal components ($Y_2(S)$,...) are of mixed signs. Both conditions are necessary and sufficient to conclude that $Y_1(S)$ is a sizing vector corresponding to concentration (TSS) which explains from a minimum of half the variance in the HFP2 group ranging up to 72% of the variance in the GM group; that is, the second and higher principal components are increasingly less important for explaining differences between individuals in groups with higher background salinities.

The second principal components $Y_2(S)$ explain about a quarter of the variations in the CARB, WO, HFP1, HFP2, and WI1 groups with negative loadings on SO_4^{2-} and positive loadings for the remaining ions. $Y_2(S)$ therefore compares the species of highest variance (SO_4^{2-}) with other ions in the hydrochemical provinces having low to intermediate salinity, apart from in the TRIAS group, where $Y_1(S)$ and $Y_2(S)$ can be readily interchanged (Table 12) - an indication that in this small sample space the variation due to SO_4^{2-} is greater than the variation in total soluble salts.

In the most saline two hydrochemical provinces, WI2 and GM, the vector identified with size, $Y_1(S)$, accounts for about 70% of the total variance, whereas $Y_2(S)$ only explains 14% in the WI2 group and 11% in the GM group. In the WI2 group $Y_2(S)$ is polarized between divalent ions with positive loadings and univalent ions with similar negative loadings; nevertheless, in both groups the second principal components are still strongly identifed with SO_4^{2-}, which in both cases is the most highly correlated variable with $Y_2(S)$, not only because its loadings are dominant or co-dominant, but also because the SO^{2-}_4 deviations from the mean are highest in these groups. It seems that in higher salinity waters, $Y_2(S)$ not only maintains the discriminatory power of SO_4^{2-}, but also incorporates information on sulphate associations; a trend that may well be related to the propensity of SO_4^{2-} to form ion pairs and complexes in concentrated salt solutions.

As an exercise in data reduction, the first two principal components successfully explain 80-90% of the variance within each group; however, apart from demonstrating the importance of both salinity and SO_4^{2-} concentrations, they do not elucidate hydrochemical processes in the study area. Y_3, although explaining only 5% of variation within the eight hydrochemical provinces, is perhaps the most interesting of the $Y_i(S)$ vectors, as illustrated in Table 13 - the provinces are arranged in the order: boundary (regional recharge), intermediate (regional transmission-discharge), and mixing (regional sink) zones. The associated physical relationships between the various sources of ions and the dominant processes that affect their movement throughout the landscape are shown in Figure 46.

TABLE 13. COMPARISION OF CHEMICAL FACIES FROM SIGNIFICANT $Y_3(S)$ LOADINGS FOR UPPER HUNTER RIVER VALLEY HYDROCHEMICAL PROVINCES.

Regional hydrological zone	Hydrochemical province	Chemical facies: Significant 'continental' loadings	Chemical facies: Significant 'marine' loadings
Boundary zone (recharge)	CARB	Ca^{2+} - Mg^{2+} - HCO_3^-	Na^+ - Cl^-
	TRIAS	Ca^{2+} - HCO_3^- - SO_4^{2-}	Na^+ - Mg^{2+} - Cl^-
	WO	Ca^{2+} - HCO_3^-	Na^+ - Cl^-
Intermediate zone (tranmission-discharge)	WI1	Ca^{2+} - Mg^{2+}	Na^+ - HCO_3^-
	WI2	Ca^{2+} - SO_4^{2-}	Na^+ - HCO_3^- - Cl^-
	GM	Ca^{2+} - Mg^{2+} - HCO_3^-	Na^+ - SO_4^{2-}
Mixing zone (sink)	HFP1	Ca^{2+} - Mg^{2+} - Cl^-	Na^+ - SO_4^{2-}
	HFP2	Ca^{2+} - Mg^{2+}	Na^+ - Cl^-

In the CARB and WO boundary provinces $Y_3(S)$ compares Na^+-Cl^- waters with Ca^{2+}-(Mg^{2+})-HCO_3^- waters and indicates a clear genetic distinction between 'marine' and 'continental' influences (parentheses indicate subordinate ion). Since these provinces have never been transgressed by marine waters, the 'marine-related' constituents must represent combined dispersion of oceanic aerosols and locally redistributed Na^+ and Cl^- in rainfall, although in the WO group a minor proportion of these salts are derived from upwards transmission of connate marine salts from the underlying marine units in the Wittingham Coal Measures. The 'continental-related' constituents reflect the key role of dissolved CO_2 in infiltrating rainfall and its interaction with soils and fractured rocks to release cations and soluble SiO_2 (not included as a variable in principal component analyses); the important processes are dissolution of alumino-silicate and carbonate minerals, oxidation of carbonaceous materials, and ion exchange.

In the TRIAS group $Y_3(S)$ contrasts 'marine' and 'continental' signatures in waters; there is an additional emphasis on mobility of the ions, and signs of the loadings are reversed. The convervative ions Na^+ and Cl^- tend to move most rapidly through the system whereas the divalent ions Ca^{2+}, Mg^{2+}, and SO_4^{2-} are more inclined to form ionic complexes and minerals which greatly reduce their rate of movement. Of the divalent ions, Ca^{2+} is most likely to be removed from groundwaters by ion exchange, and SO_4^{2-} is susceptible to adsorption, particularly by silica and alumina gels which are generally abundant in waters in contact with oxidised coals; thus, in the absence of vermiculite traps, Mg^{2+} is the most mobile divalent ion in the upper Hunter River valley groundwaters. HCO^-_3 ions are intermediate in the sense that, although they are not involved in ion-exchange reactions, they are prominent in carbonate and silicate dissolution/precipitation reactions.

Hence, within the boundary hydrochemical provinces, $Y_3(S)$ primarily contrasts individuals according to the dominance of the Ca^{2+}-HCO_3^- or Na^+ - Cl^- facies, while Mg^{2+} alternates between them depending on the importance of the ion-mobility factors. The processes operative within these hydrochemical provinces are solely governed by the reaction and transmission of dissolved CO_2 and aerosols in infiltrated rainfall. Solute transport is dominated by convection and dispersion and there are no connate marine salts in the boundary provinces; however, the intermediate provinces WI1, WI2 and GM are somewhat more complicated systems because they have their own inherent characteristics which tend to overprint the background partitioning of elements from rainfall infiltration; in certain areas they are modified by antecedent chemical signatures of groundwaters transmitted laterally from adjacent provinces.

In the WI1 and WI2 groups (Table 13), HCO_3^- loadings in $Y_3(S)$ are no longer associated with the divalent cations, but are linked to Na^+ loadings in the 'marine' facies waters. The Na^+-HCO_3^- association represents leaching and diffusion of connate marine salts, a process which is much slower than the convection and dispersion of elements in rainfall. To appreciate the significance of the Na^+-HCO_3^- link, it is necessary to review the post-Permian chemical evolution of the upper Hunter River valley groundwaters. At the cessation of the final transgressive phase represented by the Denman Formation, interstitial waters of the Wittingham

Coal Measures and underlying sediments would have had a dominantly Na^+-Cl^- composition. Even though the near-surface palaeohydrologic regime during progradation of the overlying Wollombi Coal Measures and Triassic sediments was characterized by leaching under a continental freshwater environment, large-scale 'piston-flushing' of connate marine waters from the underlying Permian sediments would have been only possible if the appropriate groundwater-seawater pressure differentials existed. At the time it is quite likely that a large proportion of interstitial marine fluid in the deep sediments was expelled as burial compaction caused a reduction in porosity; however, a considerable time lag probably occurred before matrix diffusion became a prominent factor in the chemical makeup of these waters. Translocation of connate fluids from marine-influenced coal seams into adjacent coarse-grained sediments would have continued throughout the duration of rank advance of the coals. The major change in the hydrochemical regime of the upper Hunter River Valley was the maximisation of the groundwater-seawater potential difference as a result of Tertiary uplift and incision of drainage systems. Groundwater inflows from the Carboniferous and Triassic highland, and downwards percolation from the formerly extensive basalt caps would have been enriched in Ca^{2+}, Mg^{2+}, aqueous SiO_2, and HCO_3^- from silicate mineral dissolution. In addition, igneous activity would have mobilised connate marine fluids in rocks of the WI1 province; cation exchange of Ca^{2+} for Na^+ in the sodium-saturated Permian sediments would have removed much of the available Ca^{2+} from solution in the infiltrating groundwaters leaving Na^+ as the dominant cation. Initial groundwater outflows from the valley would have been dominantly Na^+-Cl^- -rich because of the mobility of these ions, but with continued flushing Na^+-HCO_3^--type waters would have become increasingly important in the effluent groundwaters.

One way of representing the evolutionary path of groundwaters from marine regression to equilibrium under a continental leaching hydrologic regime is by the sequence

$$Na^+ - Cl^- \rightarrow Na^+ - HCO_3^- \rightarrow Ca^{2+} - HCO_3^-.$$

$Y_3(S)$ scores indicate that pore waters in the Wittingham Coal Measures have attained the second stage of this evolutionary sequence. Waters in the WI1 group are more advanced in the sequence than those of the WI2 group, as

shown by their association with relict Na^+-Cl^--type waters, which reflects the lengthy exposure of the WI1 province to flushing by meteoric waters as well as heating and mobilisation of connate marine waters in a significant proportion of the WI1 province by the action of igneous intrusions.

Divalent ions in the 'continental' facies of the WI1 and WI2 provinces (Table 13) represent silicate and carbonate mineral dissolution or precipitaiton. The SO_4^{2-} association in the WI2 group is identified with the contemporary strong continental signature of oxidation of sulphides.

In the GM group the process of diffusion of connate marine salts is most important and it accounts for the maximum variation within this province, after elimination of the variation due to total soluble salts; that is, $Y_3(S)$ in the WI1 and WI2 groups is interchanged with $Y_2(S)$ in the GM group, and the near-equal loadings for Cl^- and HCO_3^- show that the GM groundwaters are the least advanced of any group in the marine-to-continental hydrochemical sequence. $Y_3(S)$ in the GM group represents a secondary dimension for comparing individuals according to 'marine' versus 'continental' influences: the 'marine' facies describes the Na^+-SO_4^{2-} residue in the diffusion of connate marine salts after the variation in Cl^- concentrations along flow lines has been accounted for by $Y_2(S)$; the continental facies favours contemporary precipitation of carbonate minerals, (as in the WI1 province) with the dominant continental process of oxidation of sulphides having been described by $Y_2(S)$. The polarisation of ions in $Y_3(S)$ in the GM group (Table 13) is repeated in the fourth principal components in the other Permian fractured-rock provinces.

Finally, $Y_3(S)$ loadings in the HFP1 and HFP2 groups cannot be readily separated into marine and continental facies because the provinces cannot be considered as discrete systems in which only two genetically dissimilar hydrochemical processes are dominant. In fact, outputs from all processes which have been described by $Y_3(S)$ in the fractured-rock provinces (Table 13) can be expected to be inherited to varying degrees in the regional groundwater sinks of the floodplain. In general terms, $Y_3(S)$ is a 'mixing' vector which weighs the proportion of Carboniferous and Triassic waters represented by the positively correlated loadings in the HFP1 and HFP2 groups against accession of saline groundwaters from the Permian fractured rocks (represented by negatively correlated loadings).

The ion associations indicate that the HFP1 Province is sensitive to inflow of sulphate groundwaters from the GM Province whereas in the HFP2 Province input of chloride waters from the Wittingham Coal Measures is more important; the locations of these inflows will be identified later by R-mode principal components. The interesting feature in the $Y_3(S)$ loadings for the floodplain provinces is the redundancy of the HCO_3^- variable in either system, which indicates that variations in HCO_3^- concentrations throughout the floodplain are statistically of minor importance compared to the HCO_3^- variations in groundwaters of the fractured-rock aquifers.

(ii) **Principal components from pooled covariance matrix.** Table 14 shows the linear correlation coefficients of the principal components extracted from the pooled S matrix ($Y_i(S_p)$ with $\log_{10-}$ transformed variables.

TABLE 14. CORRELATIONS OF PRINCIPAL COMPONENTS FROM POOLED COVARIANCE MATRIX OF UPPER HUNTER RIVER VALLEY HYDROCHEMICAL PROVINCES

($\log_{10-}$ transformed data).

	Principal Component		
Variable	Y_1	Y_2	Y_3
HCO_3^-	-0.64	0.41	-0.04
Cl^-	-0.90	0.36	0.15
SO_4^{2-}	-0.89	-0.45	0.05
Ca^{2+}	-0.70	0.02	-0.60
Mg^{2+}	-0.83	0.30	-0.37
Na^+	-0.88	0.34	0.32

Nearly 73% of the variance, in the upper Hunter River Valley groundwaters is explained by total soluble salts - as shown in Table 14 by the high negative correlations of $Y_1(S_p)$ with all $\log_{10-}$ transformed variables.

In common with the within-groups results, $Y_2(S_p)$ compares negatively correlated SO_4^{2-} with the other variables apart from Ca^{2+} which is redundant because of its near-zero loading (see Table 12).

Similarly, $Y_3(S_p)$ contrasts individuals according to hydrochemical facies; the marine end-member is represented by Na^+-Cl^- (positive loadings) and the continental end-members Ca^{2+} and Mg^{2+} (negative loadings). However, the important chemical evolutionary trend in the groundwaters of the Permian fractured rocks described by the within-groups pca doesn't figure in the pooled data. Environmental impact statements make extensive use of the sodium absorption ratio (SAR) to compare upper Hunter groundwaters. It is therefore of interest to note that ranking of individuals by $Y_3(Sp)$ scores is approximately the same as ranking them by SAR values, since

$$Y_3(Sp) = \log \left| \frac{Na^{0.48}}{Ca^{0.65}\, Mg^{0.53}} \right| + \log \left| \frac{Cl^{0.2}\, SO_4^{0.1}}{HCO_3^{0.04}} \right|$$

Neglecting the smaller term on the right-hand containing the anions

$$Y_3 \sim \tfrac{1}{2} \log \left| \frac{(Na)}{CaMg} \right|$$

$$= \tfrac{1}{2} (\log Na - (\log Ca + \log Mg))$$

$$\text{but } \log (SAR) = \log \left| \frac{(Na)}{\tfrac{1}{2}(Ca + Mg)} \right|$$

$$= \log Na - \tfrac{1}{2} \log (Ca + Mg) - \tfrac{1}{2} \log \tfrac{1}{2}$$

$$\sim \tfrac{1}{2} (2 \log Na - \log (Ca + Mg)) \text{ omitting the additive constant.}$$

(iii) **Principal components from within groups correlation matrices.** In any system where a concept of 'growth' is valid a principal components analysis will invariably generate a first principal component that is highly identified with 'size', especially for log-transformed data (Blackith & Reyment, 1971). In this study, the 'size' dimension is a

measure both of groundwater salinity, which may be related to the abundance of total soluble minerals in a particular hydrochemical province, and the residence time of the groundwaters in aquifers. However Y_1 generally does not give much insight into chemical processes.

In a six-variable system, the second and third principal components must be relied on to carry out this task, and the most informative polarization of vectors utilises cation-anion associations (hydrochemical facies) so that trends shown by samples along flow lines within and between facies may be linked to chemical processes. The comparison of individuals by facies should preferably begin with Y_2 since it explains the maximum proportion of variance after total soluble salts. In a sense the second principal components derived from the S matrices do not succeed in this regard because the comparison of individuals is in terms of species (SO_4^{2-} versus the rest) rather than facies, an indication that the sample space is weighted too heavily by the unduly high variance of SO_4^{2-}. To overcome this problem the variables were standardized by the transformation

$$z_{ij} = \frac{x_{ij} - g_j}{s_j}$$

which equates variances of each observation to unity. The principal components extracted from R, the covariance matrices of these standardised variables, is shown in Table 12.

The effect of changing from S to R matrices is to decrease the proportion of total variation explained by the first principal components by about 5% in the groups of highest ionic strength (WI2 and GM), and to increase it by a similar amount in each of the other groups. This trend is reversed in $Y_2(R)$; the average increase in the WI2 and GM groups is 4%, while the proportion in all other groups drops by an average of 12%. The amount of total variation explained by $Y_3(R)$ is increased by an average of 5% above $Y_3(S)$ uniformly across all groups.

The $Y_1(R)$ coefficients (Table 12) show that the first principal

components from the within-group R matrices are all vectors of size, again with minor exception of the TRIAS group which no longer shows an interchange of the Y_1 and Y_2 vectors, as was the case for components extracted from the S matrix. However $Y_1(R)$ still orders individuals in the TRIAS Province primarily on ionic strength, as shown by the almost-equal loadings on HCO_3^-, Cl^-, Ca^{2+}, Mg^{2+} and Na^+, which are four times the SO_4^{2-} weighting and of opposite sign.

In the CARB group $Y_2(R)$ is positively correlated with SO_4^{2-} and negatively correlated with Ca^{2+}, Mg^{2+}, and HCO_3^-; Na^+ and Cl^- are redundant variables because of their near-zero loadings. In the TRIAS group the comparison of individuals by $Y_2(R)$ is based on Ca^{2+}-HCO_3^- (negative loadings) primarily against Na^+ - SO_4^{2-} and secondarily against Na^+ - Mg^{2+} - Cl^- (positive loadings). In the WO group $Y_2(R)$ is essentially a speciation vector which compares negatively correlated SO_4^{2-} against positively correlated HCO_3^-. $Y_2(R)$ compares individuals of the floodplain provinces according to the facies relationships Na^+ - HCO_3^- - Cl^- with Ca^{2+} - Mg^{2+} - SO_4^{2-} (HFP1) and Na^+-Cl^- with Ca^{2+} - SO_4^{2-} (HFP2). In the WI1 group $Y_2(R)$ is negatively identified with Ca^{2+} and SO_4^{2-} whereas Na^+ and HCO_3^- have significant positive correlations.

The essential difference in Y_2 scores from the S to R matrices in the provinces of low to intermediate ionic strength is that the standardisation has, in most cases, introduced an ion association with SO_4^{2-}, or at the very least, has polarised the second principal components by species (i.e. the high variance of SO_4^{2-} is no longer the dominant factor in $Y_2(R)$ as it was in the S-matrix mode analyses).

However, in the higher salinity groups the usefulness of $Y_2(R)$ in elucidating hydrochemical processes is not greatly increased by the change from S to R-mode. In the WI2 province, Na^+-HCO_3^- waters are compared with the divalent cations; ordering of individuals by $Y_2(R)$ in the WI2 province is somewhat similar to that of $Y_3(S)$, but with a 180° rotation. In the GM province, HCO_3^- is positively correlated with $Y_2(R)$, and Ca^{2+} and SO_4^{2-} are negatively correlated.

The polarisation of significant $Y_3(R)$ loadings is shown in Table 15. Note that $Y_3(R)$ explains an average of 10% of total within-group variances,

twice that accounted for by the third principal components extracted from the covariance matrices.

TABLE 15. COMPARISON OF CHEMICAL FACIES FROM SIGNIFICANT $Y_3(R)$ LOADINGS FOR UPPER HUNTER RIVER VALLEY HYDROCHEMICAL PROVINCES.

Position	Province	Chemical facies	
		Significant 'continental' loadings	Significant 'marine' loadings
Boundary	CARB	Ca^{2+} - Mg^{2+} - HCO_3^- - SO_4^{2-}	Na^+ - Cl^-
	TRIAS	Ca^{2+} - HCO_3^- - SO_4^{2-}	Na^+ - Mg^{2+} - Cl^-
	WO	Ca^{2+} - HCO_3^- - SO_4^{2-}	Na^+ - Cl^-
Inter-mediate	WI1	Ca^{2+} - Mg^{2+}	Na^+ - SO_4^{2-}
	WI2	Ca^{2+} - Mg^{2+} - HCO_3^-	SO_4^{2-}
	GM	Ca^{2+} - HCO_3^-	Na^+ - Cl^-
Sink	HFP1	Mg^{2+} - HCO_3^-	Na^+ - SO_4^{2-}
	HFP2	Ca^{2+} - Mg^{2+}	Na^+ - SO_4^{2-} - Cl^-

In the CARB, TRIAS, and WO boundary provinces, $Y_2(R)$ contrasts individuals on the basis of 'marine' (Na^+-Cl^-) versus 'continental' (Ca^{2+}-HCO_3^--SO_4^{2-} influences; again, the linkage with Mg^{2+} depends upon whether ion mobility is important within the system. The only difference between $Y_3(R)$ and $Y_3(S)$ scores is that SO_4^{2-} makes a much larger contribution to the 'continental' component of the $Y_3(R)$ scores. A similar interpretation of the physical meaning of the R-mode facies is involved here, namely that the Na^+-Cl^- type represents the process of rapid convection and dispersion of conservative ions in aerosols, and the Ca^{2+}-HCO_3^- facies reflects slower silicate and carbonate mineral dissolution. The incorporation of SO_4^{2-} into the latter facies represents dissemination of this ion from the continental sulphate store.

In the WI1, WI2, and GM groups the marine-to-continental evolutionary trend of flushing of interstitial marine fluids, ion-exchange and diffusion of connate marine salts, previously described by $Y_3(S)$, is now explained by $Y_2(R)$ which also discriminates sulphide oxidation as the most important continental-type process in these rocks. $Y_3(R)$ contrasts individuals on the basis that the carbonate dissolution/ precipitation reaction represents the 'continental' process responsible for the largest independent variation in the system after that resulting from sulphide oxidation is taken out, and the 'marine' Na^+-SO_4^{2-}-Cl^- association describes the role of sulphate as a residual in diffusion of connate marine salts. The low weighting of SO_4^{2-} in $Y_3(R)$ for the GM province implies that sulphate concentration gradients due to molecular diffusion are insignificant when compared to variations in SO_4^{2-} concentrations generated around zones of sulphide oxidation.

The third principal components in the floodplain groups are 'mixing' vectors whose interpretation is now much more straight-forward in the light of the above $Y_3(R)$ results for the boundary and intermediate provinces. In the HFP1 and HFP2 provinces, the Ca^{2+}-Mg^{2+}-(HCO_3^-) association is inherited from the 'continental' processes of silicate and carbonate mineral dissolution, predominantly from the CARB province. The contrasting Na^+-SO_4^{2-}-(Cl^-) 'marine' association is identified with the component of saline groundwater inflows from adjacent Permian rocks and is attributable to diffusion of connate marine salts. The molecular diffusion process is assumed to be independent of the much more rapid process of sulphide oxidation whose effects were described by $Y_2(R)$. In terms of relative mobilities of chloride and sulphate ions in solution, early-stage diffused groundwaters would be enriched in Cl^- and later-stage waters would exhibit SO_4^{2-}/Cl^- ratios somewhat in excess of the baseline oceanic level of 0.1 (in meq/L). Hence the Na^+-SO_4^{2-} facies groundwaters from the Permian rocks contiguous with the HFP1 province represent later stage waters than the Na^+-SO_4^{2-}-Cl^- association in rocks draining into the HFP2 province. Therefore $Y_3(R)$ implies that the rocks adjacent to the HFP1 province are more highly leached than those further down the valley peripheral to the HFP2 province. The difference in the contribution of HCO_3^- loadings between the two HFP groups indicates the diminishing influence of the Carboniferous source area with increasing distance downstream. This trend in no way

contradicts the close measure of similarity observed between the HFP2 and CARB group means by canonical variates analysis because $Y_3(R)$ is simply an independent measure of the third-most important factor after the dominating effects of size (TSS) and 'rapid' thermodynamics have been separated out.

(iv) **Principal components from pooled correlation matrix**

Correlations between $\log_{10}$- transformed variables and the first three principal components extracted from the pooled correlation matrix are shown in Table 16.

TABLE 16. CORRELATIONS OF PRINCIPAL COMPONENT SCORES FROM POOLED CORRELATION MATRIX OF UPPER HUNTER RIVER VALLEY HYDROCHEMICAL PROVINCES

(Log_{10}- transformed data).

	Principal Component		
Variable	Y_1	Y_2	Y_3
HCO_3^-	-0.76	0.36	0.42
Cl^-	-0.93	0.19	-0.16
SO_4^{2-}	-0.76	-0.32	-0.44
Ca^{2+}	-0.75	-0.54	0.32
Mg^{2+}	-0.88	-0.12	0.14
Na^+	-0.90	0.34	-0.21

The dimension identified with total soluble salts ($Y_1(R_p)$ takes up almost 70% of the total variance. $Y_2(R_p)$ and $Y_3(R_p)$, which explain 12% and 9% of the variation respectively, are independent measures of the strength of relict 'marine' versus 'continental' hydrogeologic influences on the groundwater composition of individuals; that is, $Y_2(R_p)$ and $Y_3(R_p)$ scores show how far removed individuals are from equilibrium with a fresh water leaching environment.

In $Y_2(R_p)$, the negatively correlated ion association Ca^{2+}-Mg^{2+}-SO_4^{2-} dominantly represents sulphide oxidation in high-salinity waters, while in low-salinity waters it is identified with silicate and carbonate mineral

dissolution. The contrasting Na^+-HCO_3^--Cl^- facies is linked with matrix diffusion of intermediate-stage marine interstitial fluids and connate salts in high-salinity groundwaters, and dispersion of aerosols in low-salinity waters.

In $Y_3(R_p)$, the comparison is Ca^{2+}-Mg^{2+}-HCO_3^- (the signature of silicate and carbonate mineral dissolution precipitation reactions and the role of dissolved CO_2 in infiltrated meteoric waters) against the Na^+-SO_4^{2-}-Cl^- facies which again is identified with diffusion of later stage connate marine waters and salts. The essential difference between the representations of marine-facies waters in the second and third principal components is that $Y_2(R_p)$ depends on the interaction of meteoric and connate waters and includes cation exchange; $Y_3(R_p)$ is an independent measure of the sulphate residual in connate waters induced by the difference in mobility between chloride and sulphate ions in solution.

Consistency of principal components analyses

TABLE 17. ANGLES BETWEEN CORRESPONDING SETS OF PRINCIPAL COMPONENTS DERIVED FROM S AND R MATRICES OF SIX LOG$_{10}$-TRANSFORMED VARIABLES, UPPER HUNTER RIVER VALLEY GROUNDWATERS.

	$Y_1(S) \wedge Y_1(R)$	$Y_2(S) \wedge Y_2(R)$	$Y_3(S) \wedge Y_3(R)$
CARB	46°	-46°	13°
TRIAS	24°	32°	21°
WO	23°	28°	11°
HFP1	33°	-44°	48°
HFP2	44°	-46°	34°
WI1	18°	45°	44°
WI2	19°	-59°	-60°
GM	11°	-46°	32°
POOLED	21°	54°	-50°
Mean abs. differences	27°	44°	35°

Table 17 shows that corresponding angles between the three sets of vectors are significantly different, with the largest variations occurring in the second and third principal components. This is almost entirely due to the high SO_4^{2-} variance.

In the S-mode first principal components, SO_4^{2-} has either the dominant loadings, or is co-dominant with Cl^-. When deviations from the mean are included in $Y_1(S_p)$ scores, it is evident that SO_4^{2-} is the most important single contributor to the ordering of individuals by size (TSS). However, when variables are standardised, the relative contribution of SO_4^{2-} is no greater than the other variables in the $Y_1(R)$ and $Y_1(R_p)$ scores.

The dominance of SO_4^{2-} carries through to the second principal component in all the S-mode analyses, and since $Y_2(S)$ and $Y_2(S_p)$ are essentially speciation vectors, there is no clear distinction between the various sulphate-producing processes. The S-mode second principal components seem rather to have a closer association with the activity of sulphate in solution. Conversely, $Y_2(R)$ and $Y_2(R_p)$ also have prominent SO_4^{2-} loadings, but these vectors additionally include ion associations which may be related to hydrochemical processes. In this case the dominant influence of SO_4^{2-} loadings in R-mode second principal components of the Permian fractured-rock provinces is a consequence of sulphide oxidation.

The comparison of individuals by their S and R-mode Y_3 scores is similar in the sense that they are discriminated primarily by the relative influences of relict 'marine' versus 'continental' influences. However, since so much of the SO_4^{2-} variance has been taken up in the first two S-mode components, it does not often figure prominently in the third vector. In contrast, $Y_3(R)$ and $Y_3(R_p)$ are not constrained in this manner, so substantial SO_4^{2-} loadings are present in most of the R-mode third principal components. This accounts for the dissimilarity in $Y_3(S)$ and $Y_3(R)$. Again, hydrochemical processes independent of those derived from Y_2 may be inferred from ion associations in $Y_3(R)$ and $Y_3(R_p)$.

In all future discussion of principal components, the $Y_i(Rp)$ form will be used. The R-mode analysis is preferred since cause-and-effect relationships are more readily identified from the second and third components. The pooled correlation matrix is used because of the difficulties in translating from one within-group observation space to another, and also for the philosophical reason that the only discrete hydrochemical provinces in the study area are the TRIAS and CARB groups; in all others the proportion of groundwater which is not derived from within-

group infiltration will bear an antecedent signature of the upgradient province. However, even the CARB and TRIAS groups cannot be considered as truly independent since cyclic salts deflated from the lower-lying provinces are re-deposited in their border areas.

Clustering by principal components

Plots of Y_1 and Y_2 scores from the pooled correlation matrix are shown in Figure 43. For clarity of presentation the plots have been divided into hydrochemical provinces (Figs. 43(a)-43(g), however, when all points are superimposed onto the one plot, an approximate elliptical scatter of data is attained - a favourable indication that the $\log_{10}$-transformed variables are close to being multinormally distributed (Blackith & Reyment, 1971).

Figures 43a to 43g depict groups of individuals from hydrogeological catchments. Separation of clusters permits visual assessment of the similarity between groundwater catchments within the same hydrochemical province, and as such does not warrant a detailed description here. Aspects which should be borne in mind are that the spread of within-catchment Y_1 scores primarily reflects residence time; and variations along Y_2 show the relative strength of modern 'continental' processes with negative scores versus relict and contemporary 'marine' influences with positive scores. For example, Y_2 scores of baseflow and subsurface samples from Wollombi Brook, Martindale Creek, Doyles Creek, and Milbrodale Brook, catchments in the WO group (Fig. 43b) show a dominant 'marine' influence, but the positive Y_1 scores indicate that it is of low salinity - a combination which, together with the geomorphic settings of these valleys, has previously been highly identified with the relatively rapid process of dispersion of aerosols in rainfall. These four streams have a substantial TRIAS input, as shown by their proximity to the TRIAS mean (Y_1, Y_2) score, and they are in fact the streams of greatest length in the south of the area. The other streams draining the southern escarpment are much shorter, and their catchments have smaller reliefs; they form the cluster of Hayes Creek, Appletree Creek, and Wambo Creek (Fig. 43b), which is almost equally influenced by 'marine' (rapid transmission of univalent ions) and 'continental' (slower dissolution/precipitation reactions involving the divalent ions) processes, a consequence of lower hydraulic gradients

dictated by subdued relief. These two major clusters may in turn be compared with catchments incised into the western escarpment, namely Spring Creek, Big Flat Creek, and Sandy Creek-Coal Creek (Fig. 43b); this cluster is dominated by slow, 'continental' processes, mainly silicate mineral dissolution. In this regard it is interesting to note the similarity of scores of Spring Creek waters with the corresponding scores of bore and well waters from the Fordwich Sill, a major dolerite intrusion in the Wollombi valley. An association between mineral dissolution in basic rocks and groundwaters of the western Wollombi Coal Measures was inferred in the canonical variates analysis; pca has independently identified a more specific link with the Spring Creek valley.

In summary, the plots of principal component scores (Figs. 43a-g) basically partition data into four fields, each one associated with a particular hydrochemical process and a central mixing zone (Fig. 43h). Points in the $(+Y_1+Y_2)$ quadrant distant from the origin are primarily identified with the steady state dispersion of aerosols. Compared with other hydrochemical processes in the upper Hunter River valley area, dispersion of aerosols is rapid and is important in the TRIAS and WO provinces. The $(+Y_1,-Y_2)$ quadrant is closely identified with silicate and carbonate mineral dissolution/precipitation, which in turn depends on groundwater velocity and supply of CO_2-charged meteoric waters. Carbonate mineral dissolution/precipitation is comparatively rapid, though not as fast as dispersion of aerosols, but reactions involving aluminosilicates are much slower. The CARB group is prominent here, and because of the importance of the Hunter River in the floodplain provinces, the HFP1 and HFP2 provinces are similarly included. The $(-Y_1,+Y_2)$ quadrant is dominated by the process of diffusion of connate salts from the WI2 province (Molecular diffusion is the slowest known process in hydrochemistry). Oxidation of sulphides is the most important factor in the $(-Y_1,-Y_2)$ quadrant which contains most samples from the GM group.

The mixing zone centred about the mean (Y_1,Y_2) score at the origin is of most interest for management of groundwater quality in the upper Hunter River valley. In this field all four of the major processes are represented to varying degrees, and the nature of their interaction is the subject of the next section.

Interpretation of non-reactive groundwater mixing by principal components

Some inferences can be made on the likelihood of significant groundwater mixing between subgroups of hydrochemical provinces by contrasting distances between canonical variate means (cf. Fig. 41), but it must be remembered that canonical variates analysis is a technique for discriminating group means only, since distances between individuals are not invariant under the canonical variates transformation. However, distance relationships between individuals are preserved in principal component scores from the pooled dispersion matrix, in this case the covariance matrix of standardised variates.

Figs 44 a-d show condensed plots of (Y_1, Y_2) scores from certain clusters of individuals in the central groundwater mixing zone (Fig. 43h). To avoid cluttering the diagrams with all the data points, the results are represented by elliptical envelopes which contain 95% of (Y_1, Y_2) scores for a particular hydrochemical province (Figs. 44 a-d); the group mean scores are the centres of the ellipses which are constructed so that the ratio of their semi-major to semi-minor axes is equal to the ratio of eigenvalues $(\lambda_1/\lambda_2)^{\frac{1}{2}}$ of the pooled correlation matrix.

Locations of significant groundwater mixing in the study area may be identified by the proximity of individuals to their own group mean score as compared to their closeness to other group mean scores. In effect, Y_1, and Y_2 are now serving as linear discriminant functions for hydrodynamic mixing.

Undoubtedly groundwater mixing is of most consequence in the Hunter River floodplain alluvium. In Figure 44a the HFP1 ellipse has been partitioned into five segments, of which four represent likely mixing zones between groundwaters of the alluvium and the adjacent Permian fractured-rock provinces on the basis of distances between individuals and group means; the remainder contains the samples which are hydraulically connected to the Hunter River and whose scores are closely identified with the source areas of the CARB-TRIAS province. Significant inflows of GM-type waters are evident from the Hilliers Creek valley and from the Aberdeen and Hunter Thrust Faults. The Bayswater Seam subcrop coincides with the zone of inflow of WI1 waters where it intersects the river below Ramrod Creek (Fig.

44a); in these areas the trace of the Bayswater Seam defines the WI1-WI2 boundary (Pl. 2). The WO province signature is prominent in the distal wells of the 'K' traverse drilled by Williamson (1958) above Denman (see Plate 2).

In the HFP2 group (Fig. 44 b) the cluster of wells at Neotsfield on the eastern edge of the study area plot within the GM mixing zone, which suggests that the syncline between the Belford Dome and Sedgefield Anticline is a permeability barrier that induces upward leakage of groundwaters from the Maitland Group rocks into the floodplain alluvium.

Inflows of WI2 type groundwaters occur in five wells on the southern side of the Hunter River at Alcheringa. The distribution of principal component scores of these wells (Fig. 44b) shows that the intensity of the WI2 signature decreases away from the confluence with Saddlers Creek, indicating that the most likely source of the WI2-type groundwater input is the Saddlers Creek valley, with the groundwaters probably upwelling along fractures parallel to an anticlinal axis that is collinear with Saddlers Creek; however, the mixing zone might also be related to the triple junction of the Mt Coricudgy Anticline, Mt Ogilvie Fault, and Saddlers Creek Anticline. This mixing zone is one of the few in the entire floodplain that transects the Hunter River; everywhere else the river appears to be a true dividing streamline for groundwater flow. The Hunter River traverses the coal seams of the Malabar and Mount Ogilvie Formations of the Wittingham Coal Measures at Jerrys Plains, and the principal component scores of the HFP2 wells in this region indicate accession of WI2-type groundwaters (Fig. 44b). However, downstream from Jerrys Plains to Neotsfield, aquifer storage and replenishment of low-salinity waters from tributary streams such as Wollombi Brook and Glennies Creek are sufficient to generate (Y_1, Y_2) scores which plot within the CARB-TRIAS background field.

High-Cl^- groundwater inputs from the WI1 province seem to emanate mostly from the Denman Formation at the top of the Wittingham Coal Measures. In the HFP2 province a baseflow sample (number 263, bed underflow water) in Appletree Creek at its junction with the Hunter River plots in this field; the source was probably a spring flowing from the

Denman Formation nearly 1 km upstream. There are many such saline springs along the contact between the Wollombi and Wittingham Coal Measures on the southern footslope of the valley between Alcheringa and Wambo Creek. During drought conditions in August-September 1982, most springs had ceased to flow, but numerous small-scale salt scalds testified to their activity in wetter times.

Principal component scores of samples at the confluence of Martindale Creek and the Hunter River form two discrete clusters (Fig. 44 b). Surface samples and well waters which are in hydraulic continuity with the Hunter River show a strong WO-type input, thus reflecting the influx of Goulburn River waters. Wells closer to Martindale Creek plot near the TRIAS province mean indicating that there may be substantial piping of Triassic groundwaters along a lineament of the Mt Rombo spur.

In the WO province (Fig. 44 c), inflows of WI2-type ground waters occur in wells adjacent to Sandy Creek, and in a meridional band in the Dalswinton area. Apparently the alluvium of Sandy Creek intercepts saline waters from the Mt Ogilvie Fault zone and transmits them downstream by bed underflow and these waters may be dispersed radially where intercepted by the cones of depression of pumping wells. However, the WO-WI2 mixing zone at Dalswinton cannot readily be explained and must be related to an unknown geological structure, probably associated with the Mt Ogilvie Fault.

Some bores and deeper wells of the WO group in localised groundwater discharge zones in the south and west of the study area intercept waters which have a significant WI1 signature (Fig. 44c). At the scale of this investigation it is not possible to be more specific on the origin of these waters; however, it is likely that most of the dissolved salts are contributed by upwards flow from the Denman Formation.

Non-reactive groundwater mixing zones of the WI1 province are shown in Figure 44d. Similar zones are unlikely to be detected for the WI2 and GM groups because of the inherently high salinities of these groups which overprint the discriminatory power of $Y_1(R_p)$. The only detected zone of mixing between GM and WI1 province ground waters occurs in wells of the Dart Brook valley adjacent to Maitland Group rocks. Waters with a WI2 signature occur in the lower Spring Creek and Sandy Creek valleys and seem

to emanate from the saline groundwaters of the Mt Ogilvie cross fault. Other WI1-WI2 mixing zones are indicated in areas of vertical upwards flow in the Wollombi valley and may in part be 'overspill' induced by structural impedance of the lateral transmission of groundwaters by the Mt Thorley Monocline.

Perhaps the most significant of the WI1-WI2-type groundwater mixing zones is the western limb of the Muswellbrook Anticline, in particular the Saddlers Creek valley (Fig 44d). This result accords well with the HFP2-WI2 groundwater mixing zone across the Hunter River at Alcheringa, and adds credibility to the hypothesis of a likely major geological dislocation as the plane of transmission of upwelling WI2 groundwaters.

The principal components of hydrochemical trends and equilibria

Figure 45a and 45b show the ($Y_2(R_p)$, $Y_3(R_p)$) scores of individuals whose waters have simultaneously reached or exceeded saturation with respect to gypsum, amorphous silica, and chalcedony, and all three of the complex carbonates (dolomite, huntite, and hydromagnesite) considered earlier in the equilibrium calculations. The domains shown in Figure 45c are envelopes which enclose at least 80% of (Y_2, Y_3) scores for a particular hydrochemical subgroup, but they may also contain points from other subgroups. Since the second and third principal components together account for only 21% of total variance, the (Y_2, Y_3) plots are not particularly well suited for use as a clustering technique. As explained previously $Y_2(R_p)$ and $Y_3(R_p)$ compare individuals by hydrochemical facies and are thus explicitly independent of total soluble salts, however, there is an indirect size dependence in their interpretation. In the high-salinity groundwaters of the Permian fractured-rock provinces $+Y_2(R_p)$ is identified with the evolution of diffused connate 'marine' fluids, whereas in lower salinity groundwaters of the TRIAS, WO, and CARB provinces groups it is a measure of the rapid dispersion of the univalent ions in aerosols transmitted by infiltrated rainwaters; the $-Y_2(R_p)$ 'continental' association describes sulphide oxidation in high salinity waters and is linked with slower dispersion of the divalent ions, particularly SO_4^{2-}, in low-salinity waters. $Y_3(R_p)$ polarises the HCO_3^--Ca^{2+}-(Mg^{2+}) 'continental' association of silicate and carbonate mineral dissolution/precipitation

reactions against the SO_4^{2-}-Na^+-(Cl^-) 'marine' association, a secondary measure of diffusion of connate salts based on the sulphate residual.

The ($+Y_2$,$+Y_3$) quadrant essentially partitions the sample space into four hydrochemical facies, each of which is associated with distinct mineral equilibria fields, some of which are shown in Figs 45a and 45b. This quadrant is primarily identified with maturation of groundwaters with significant diffused connate marine salts, and is secondarily linked with silicate and carbonate mineral dissolution/precipitation; from the proportion of its area saturated and supersaturated with respect to silica and the complex carbonates, it is evident that precipitation dominates. The west limb of the Muswellbrook Anticline has the greatest proportion of samples in this quadrant, indicating that both of the above hydrochemical processes are the most important factors in this subgroup. The ($+Y_2$,$-Y_3$) quadrant is most highly identified with the 'marine' Na^+-(Cl^-) ion association, and points distal to the origin bear the signature of diffusion of immature connate marine waters and saturation with respect to the complex carbonates. This quadrant contains the largest proportion of WI2 samples, in particular those from the Wollombi Brook valley. Points which plot in the ($-Y_2$, $+Y_3$) quadrant represent areas where the 'continental' processes of silicate and carbonate mineral dissolution/precipitation and/or sulphide oxidation are dominant. The key major elements are Ca^{2+} and (Mg^{2+}); most of the HFP1 and HFP2 samples are located here. A minor proportion of samples in this quadrant have attained silica saturation, but it is clearly evident that mineral dissolution rather than precipitation dominates. The ($-Y_2$, $-Y_3$) quadrant segregates the high-sulphate waters of the GM and WI2 provinces, and contains the gypsum saturation field.

The relationship between groundwater facies, mineral equilibria, and hydrochemical trends will now be considered using principal components. Ideally, hydrochemical trends are best traced by sequential sampling in the same aquifer along groundwater flow lines; however, such arrangements of sampling points were not available in the study area, the nearest alternative being the baseflow measurements, some of which are plotted in Figure 45a and 45b.

The headwaters of Martindale Creek, Spring Creek, Doyles Creek, and Wollombi Brook drain the TRIAS province and then flow through the WO province. Within these provinces the loci of the four streams (equated here with groundwater flow lines) generally show the same trend of continuous increases in Cl^- and HCO_3^- concentrations in roughly the same proportions; if this process were to be continued uninterrupted, the waters would ultimately reach the silica and complex carbonate saturation fields in the $(+Y_2,+Y_3)$ quadrant. However, in the Wollombi Brook samples, (Fig. 45b) the TRIAS-WO trend is reversed upon interception of solutes from the Wittingham Coal Measures, and the concurrent increases in Cl^-, Na^+, and SO_4^{2-} and decline in HCO_3^- rotate the locus back towards the $-Y_3$ axis which is a measure of the diffusion of connate marine salts. In Spring Creek (Fig. 45b), the locus is rotated 90° across the Mt Ogilvie cross fault, and the trend is then towards the WI1 province domain associated with diffusion of juvenile connate waters.

Glennies Creek, Muscle Creek, and Bowmans Creek baseflow samples show the same trend of decreasing Y_2 and Y_3 scores towards the gypsum saturation field as Cl^- increasingly dominates over HCO_3^-, and SO_4^{2-} concentrations progressively increase with distance away from the CARB province in the Permian fractured-rock provinces of the Central Lowlands. The trend towards gypsum saturation in Bowmans Creek (Fig. 45a) is perturbed at station 126 by an input of Na^+-Cl^- waters which rotates the locus towards the WI2 domain; however, on subsequent mixing with local groundwaters further downstream the locus reverts back towards gypsum saturation. Since water quality of the Hunter River is of critical importance in the region, its locus is included in Figure 45a, but it is acknowledged that the points defining its locus cannot be directly related with groundwater flow lines in the adjacent Permian rocks because of the regulated flow component in the river. Above Denman the Hunter River locus shows a similar trend to the TRIAS-WO province baseflow loci. There is a marked facies change at Denman which reverses the locus towards the direction of the CARB-Permian province streams. Inflow and mixing of Goulburn River waters results in a compensating facies change back towards the value of its original position above Denman, but displaced further along Y_2 towards the silica, and complex carbonates saturation fields. From the Goulburn River confluence to Jerrys Plains the Hunter River locus again reverts to the CARB-Permian province trend reflecting accession of

groundwater seepages from the Wittingham Coal Measures. There is a minor facies change between Jerrys Plains and the Bayswater Creek-Singleton section of the river where the lower Y_3 scores mainly result from disproportionate decreases in HCO_3^- concentrations.

Sandy Creek and Saddlers Creek (Fig. 45a) both drain the WI1 province. Unlike the trends shown by the TRIAS-WO and CARB-Permian province streams, sequential WI1 baseflow samples show far greater variation along Y_2 and Y_3. This indicates the importance of the process of diffusion of connate juvenile waters of Na^+-HCO_3^- facies in groundwaters of the WI1 province. In contrast, the trend of the loci of WI2 groundwater flowlines, represented here by baseflow in Loder Creek (Fig. 45a), is dominated by the process of diffusion of immature connate 'marine' waters, which accounts for the trend towards the Na^+-(Cl^-) facies of the ($+Y_2$,$-Y_3$) quadrant. The solutions are not concentrated enough to reach halite saturation, but the domain represented by stations 54, 57 and 55 (Fig. 45 a) is supersaturated with respect to the complex carbonates ($Q_{huntite}$>2.5, $Q_{hydromagnesite}$>2, $Q_{dolomite}$>3). On intersecting the Maitland Group rocks, the Loder Creek baseflow locus is rotated towards gypsum saturation. Baseflow in other streams draining the Loder Dome, such as Nine Mile Creek and the east arm of Loder Creek, show the same trend (Fig. 45a).

In summary, the facies changes shown by (Y_2, Y_3) scores of baseflow samples are probably a reasonable approximation to hydrochemical trends along groundwater flow lines in the provinces drained by these streams. Flow lines emanating from the Triassic escarpment show increased sensitivity to 'continental' Y_3 processes of silicate and carbonate mineral dissolution reactions as groundwater velocities decline through the Wollombi Coal Measures. Conversely, flow lines in the Wittingham Coal Measures show progressively decreasing Y_3 scores in the WI2 group, and progressively increasing Y_2 scores in the WI1 province - a consequence of the maturity of diffused connate marine salts solutions and the fact that carbonate precipitation dominates over carbonate dissolution within these provinces. Flow lines in the GM province converge towards gypsum saturation by concurrent decreases in Y_2 and Y_3 scores. It is interesting to note that facies changes interpreted from (Y_2, Y_3) plots (Fig 45c) are generally much more pronounced than those obtained by visual inspection of baseflow longitudinal profiles (cf. Wollombi Brook Figs. 15b and 45b), or

even by the use of conventional trilinear diagrams since the method associated with the latter loses two degrees of freedom by using ionic proportions.

SYNTHESIS

From a combination of graphical techniques, chemical equilibrium models, and multivariate statistical methods, it has been possible to discriminate the various hydrochemical processes which exert the greatest influence on groundwater chemistry in the upper Hunter River valley. Based on geological differences the system is partitioned into eight provinces, each with a unique hydrochemical signature.

The fractured rocks of the southern New England Fold Belt constitute the CARB province, characterised by groundwaters of low to moderate salinity (mean TSS = 790 mg/L) which grade from Ca^{2+}-Mg^{2+}-HCO_3^- facies to Na^+-Cl^- facies towards the Hunter Thrust Fault, thus reflecting the increase down flow lines of solution of locally redistributed cyclic salts over silicate mineral dissolution.

The TRIAS province comprises the scarp-forming fractured rocks of the Triassic Narrabeen Group in the south and west of the study area, and their associated groundwaters. These groundwaters are of low to moderate salinity (mean TSS = 600 mg/L), dominated by Na^+-(Mg^{2+})-Cl^-, and generally have low HCO_3^- concentrations, a consequence of rapid groundwater throughflow and mostly shallow soil cover depleted in organic matter so that the major source of dissolved CO_2 in recharge waters is atmospheric.

The Permian fractured rocks forming the Central Lowlands and footslopes have been divided into four provinces namely, WO, WI1, WI2, and GM1. The WO province is composed of groundwaters of the Wollombi Coal Measures which occupy the footslopes below the Triassic escarpment. WO-type groundwaters are moderately saline (mean TSS = 1070 mg/L) dominated by Na^+, Mg^{2+}, Cl^-, HCO_3^-. The hydrochemical processes which have most influence on these groundwater compositions are oxidation of coal seams and silicate mineral dissolution in the abundant tuffaceous interseam beds. The fundamental difference between the Wollombi Coal Measures and the underlying Permian rocks is that the latter were periodically submerged by oceanic waters at varying stages of diagenesis; to this day the solute inputs from these marine transgressions maintain a profound influence on the groundwater chemistry of the Permian fractured rocks of the Central Lowlands.

Groundwaters of the Wittingham Coal Measures are divided into those of the intruded rocks of the Jerrys Plains Subgroup in the west which form the WI1 province, and waters of the non-intruded rocks of the WI2 province in the eastern and south-eastern parts of the study area. WI1 groundwaters are of moderate to high salinity (mean TSS = 2300 mg/L), whereas waters of the WI2 province are the most saline in the Hunter River valley (mean TSS = 5700 mg/L). Hydrochemical facies grade from Na^+, Cl^-, HCO_3^- in the WI1 province to Na^+-Cl^- in the WI2 province, and mean SO_4^{2-} concentrations are over ten times higher in the WI2-type groundwaters. The lower average salinities and different chemical composition of the WI1-type groundwaters are a consequence of both a longer period of flushing by meteoric waters and prior thermal mobilisation of connate marine fluids peripheral to the Tertiary intrusives.

The GM province consists of groundwaters of the Maitland Group, Greta Coal Measures, and Dalwood Group, and therefore incorporates the largest proportion of marine sedimentary rocks in the study area, as reflected in the chemistry of its waters; they are dominantly Na^+, Mg^{2+}-Cl^-, SO_4^{2-} facies and are highly saline (mean TSS = 4300 mg/L). The strong marine signature is perpetuated through the upper seams of the Greta Coal Measures because these beds were saturated by oceanic waters while they were still actively growing peats.

The largest groundwater storage in the upper Hunter River valley is in the buried sands and gravels of the floodplains. These sediments are by far the most permeable aquifers, and their water quality is of critical importance to irrigation activities. During drought conditions in August 1982, there was considerable withdrawal of groundwaters from wells in the floodplain; this pumping induced surface recharge in areas peripheral to the Hunter River but resulted in deteriorations in water quality in some outlying areas which were not in direct hydraulic continuity with the bed underflow waters of the river. The floodplain is divided into the HFP1 and HFP2 provinces; the boundary between the two is the Hunter-Goulburn River confluence which marks a distinct break in mean grainsize, sorting, and provenance of the aquifers, separating the coarse-grained lithic sediments derived from the Carboniferous rocks in the HFP1 province from the fine-grained dominantly quartzose sands eroded from the Triassic rocks in the HFP2 province. In terms of hydrochemical facies, the HFP1 and HFP2

provinces are similar, with Mg^{2+} dominant over Na^{+} in HFP1 type groundwaters grading to Na^{+} dominant over Mg^{2+} in HFP2 groundwaters; HCO_3^- and Cl^-, in that order, are the most abundant anions in both groups. However, increased contact time with the Permian rocks results in an increase in mean TSS from 650 mg/L in the HFP1 province to 840 mg/L in the HFP2 province.

Over the total sample space of 673 individuals, HCO_3^-, Ca^{2+}, and aqueous SiO_2 concentrations approach log-normal distributions and can therefore be considered as the products of many small interdependent causes in a statistically homogeneous system characterised by dissolution/precipitation reactions and ion exchange under a continental leaching environment. In contrast, log_{10}- transformed SO_4^{2-}, Na^{+}, Mg^{2+}, and Cl^- concentrations approach bimodal distributions and it is no coincidence that these four elements together constitute over 97% of dissolved ions in ocean water. As a simplistic overview, the low concentration modes of the SO_4^{2-}, Na^{+}, Mg^{2+}, and Cl^- distributions can be considered with HCO_3^-, Ca^{2+}, and SiO_2 as representing the dissemination of 'elements' from the continental solute store, whilst the high concentration modes of the former four elements are a legacy of the Permian marine transgressions.

The strength of modern continental processes against relict marine influences is indicated by the pattern of solute behaviour within the hydrochemical provinces. The highest rates of HCO_3^- enrichment relative to Cl^- are attained in the CARB and TRIAS provinces, a consequence of carbonate and silicate mineral dissolution by aggressive waters in the recharge zones. Similar high rates of HCO_3^- accretion occur in the WO and WI1 provinces which partly reflect active leaching in the higher parts of the valley floor, although the groundwaters probably also contain a component resulting from solution of silicates in the dolerite intrusions. The effects of an additional source of HCO_3^- from oxidation of coals by sulphates in the reducing zones of the WI2 and GM provinces is more than offset by the increased potential for carbonate mineral precipitation, and therefore significantly lower rates of HCO_3^- enrichment occur in these provinces. The HFP provinces also record low rates of HCO_3^- enrichment relative to Cl^- - an expression of the conservative behaviour of Cl^- compared to HCO_3^- along flow lines converging towards the groundwater sinks of the floodplain - and it is also likely that some HCO_3^- losses occur from

degassing as the semi-confined aquifers of the Permian fractured rocks discharge into the phreatic aquifers of the floodplain.

The behaviour of aqueous SiO_2 relative to Cl^- shows that the Permian fractured-rock provinces separate into the WO, and WI1 groups with the dominant continental influence of silicate mineral dissolution resulting in linearly increasing SiO_2 concentrations along flow lines; in contrast the WI2, GM groups with strong relict marine influences are characterised by decreasing silica solubilities along flow lines as Cl^- concentrations increase by molecular diffusion. In particular, the Muswellbrook-Denman-Jerrys Plains triangle is segregated on the basis of high SiO_2:Cl^- ratios, and this area probably represents a zone of maximum intrusive activity. The same clustering of the Permian fractured-rock provinces is attained by trends in the SO_4^{2-}:Cl^- ratios. The WO and WI1 provinces have a significantly lower rate of SO_4^{2-} enrichment down flow lines than the WI2 and GM provinces. In this case, trends within the WO and WI1 provinces mostly reflect the systematics of SO_4^{2-} derived from the continental sulphate store, and represent processes ranging from infiltration of aerosols in contemporary rainfall to dissemination of terrigenous sulphates accumulated in the WO and WI1 peat swamps; however, there was also an input of oceanic sulphate during the brief marine transgression represented by the Denman Formation, particularly in the southern part of the study area. The strong marine signature in the WI2 and GM provinces is represented by the high rates of SO_4^{2-} accretion along flow lines, the combination of molecular diffusion of primary SO_4^{2-} in connate marine salts, and oxidation of sulphides. No acid waters associated with pyrite oxidation were detected during the survey because in the undisturbed environment the change in pH induced by acids released from the oxidation reaction is buffered by HCO_3^- which may be concurrently produced by dissolution of authigenic carbonates. However, in spoil heaps this buffering mechanism will not operate if the critical fluid transmission rate lies between the pyrite oxidation and carbonate dissolution reaction rates.

Calculations of Disequilibrium Indices for minerals which have precipitated under past and present groundwater regimes in the upper Hunter River valley permit broad comparisons to be made between palaeohydrochemical environments and the present one. Saturation and supersaturation with respect to the simple carbonate minerals calcite and

magnesite is the norm in groundwaters of the floodplain and fractured rocks of the Central Lowlands; however, the validity of equilibrium models for those parts of the alluvial system which are in direct hydraulic continuity with the Hunter River is questionable because of the comparatively high groundwater velocities, perhaps groundwater-mineral relationships in the alluvial aquifers would be more suitably analysed by rate kinetics. The abundance of calcite precipitates in the contemporary hydrochemical system is manifested in the ubiquitous calcite joint and cleat linings in the Permian coals and interseam beds; its former presence is recorded by the calcite cements and older planar void infills in these rocks. Magnesite is slightly more soluble than calcite but has not been reported in the study area - the available CO_3^{2-} after precipitation of complex carbonates is apparently all consumed by calcite. In contrast to the high potential for calcite precipitation in the groundwaters of the Central Lowlands, it and other Ca - Mg minerals would be dissolved in contact with most waters in the TRIAS and WO provinces in the southern and western recharge zones, but not by waters of the CARB province in the northern recharge zone.

The former abundance of siderite in groundwaters of the upper Hunter River valley is indicated by its presence as a cement and replacement mineral throughout the Permian rocks, particularly in the terrigenous sequences. However, on chemical considerations siderite must be classified as a product of a palaeohydrochemical regime since there is simply not enough dissolved Fe^{2+} in the present groundwaters of the study area for siderite precipitation to be significant on a regional scale. Corroborating petrographic evidence indicates that siderite formed during early diagenesis. Solubility of Fe^{2+} and Al^{3+} is greatly increased in acid waters, hence the Permian peat swamps would have been important zones of accumulation for these elements. Both Fe^{2+} and Al^{3+} have subsequently been lost to the system in oxy-hydroxides, but Al^{3+} has also been consumed by precipitation of the rare complex carbonate mineral, dawsonite. Disequilibrium Indices show the contemporary hydrochemical system in the upper Hunter River valley is conducive to precipitation of dawsonite, and its petrologically determined range as an authigenic mineral spanning the period from early diagenesis to the present implies that the palaeohydrochemical environment was also characterised by alkaline waters rich in Na^+ and Al^{3+}. However, the mechanism responsible for the concurrent removal of SiO_2 from solution in order to prohibit kaolinite

precipitation is not fully understood.

Although halite, thenardite, and bloedite commonly occur in salt efflorescences throughout the WI2 and GM provinces, the groundwaters in these provinces are grossly undersaturated with respect to these minerals. Similarly, glauberite would be dissolved by all of the groundwater samples in this data set, and it is therefore not surprising that primary glauberite is never observed in the Permian rocks. On the other hand, glauberite pseudomorphs composed of calcite, dolomite, and dawsonite could have formed at any diagenetic stage because groundwaters of the Permian marine sequences are supersaturated with respect to these minerals, and presumably have always been so. The gypsum pseudomorphs are more time-specific since there are no waters in this data set capable of precipitating gypsum; however, there are several samples in the GM province which are in equilibrium with gypsum.

The very narrow range of Disequilibrium Indices for chalcedony and amorphous silica shows indirectly that the solubilities of these minerals control silica concentrations in the upper Hunter River valley groundwaters.

Models based on incongruent dissolution of K-feldspar and Ca-plagioclase allocate many of the region's groundwaters to the kaolinite stability field, a result which is consistent with the observed abundance of kaolinite as an authigenic mineral in the Permian coals and other fractured-rock aquifers. Evidently silica and cations leached from the fractured rocks of the valley accumulate in the groundwater sinks around the low permeability margins of the HFP2 province because this area has the largest proportion of waters in equilibrium with Ca-montmorillonite. However, in the model for incongruent dissolution of Na-plagioclase, sample points are generally evenly dispersed about the albite-kaolinite boundary, which suggests that albite would not be dissolved by about half of the groundwater samples in this data set, particularly the sodium-rich waters of the WI2 and GM provinces. Stability diagrams are only useful in describing the genesis of waters if dissolution of a particular mineral and its weathering products represents a substantive source of the ions forming the axes of the diagram. In this regard we consider that, in terms of aluminosilicate groundwater equilibrium, the maturity of the upper Hunter

River valley groundwaters, is best explained by the K-feldspar and Ca-plagioclase stability diagrams since silicate dissolution represents an important source of both K^+ and Ca^{2+} in this system. Conversely, dissolution of sodic plagioclase is only an important process for Na^+ enrichment in those samples which comprise the low-concentration mode of the distribution of Na^+ in this system; samples in the high-concentration mode are highly identified with diffusion of connate marine salts.

The interaction between modern continental hydrochemical processes and marine connate salts in the upper Hunter River valley fractured-rock aquifers is a recurring theme throughout this study; the interaction of these processes is illustrated in Fig 46. This concept is introduced on a regional scale by comparing the distributions of the 'continental elements' - K^+, Ca^{2+}, SiO_2, and HCO_3^- - against distributions of the four major 'elements' comprising the bulk of dissolved solids in ocean waters - Cl^-, Na^+, SO_4^{2-}, and Mg^{2+}. On a province-wide scale, composition diagrams of solute behaviour identify the WI2, GM and, to a lesser extent, WI1 provinces as systems which can be approximated by simple linear mixing models between meteoric and oceanic waters. At the other end of the spectrum the floodplain provinces can be considered as mixing systems between Hunter River surface waters and groundwaters of the fractured-rock provinces. Salt efflorescences are the surface expressions of the strong association between inherent marine solutes and the provinces comprising the Wittingham Coal Measures and the older Permian rocks in the Central Lowlands; in particular, the Mulbring Siltstone of the GM province is the unit which is most highly identified with surface salting - the Wollombi Brook valley appears to be the worst salt-affected area in the upper Hunter River valley. The subsurface expressions of the link between marine solutes and the older Permian fractured-rock provinces is represented by the accretion of Na^+, Cl^-, and SO_4^{2-} along groundwater flow lines, and is equated in this report with sequential baseflow measurements along certain streams during the drought conditions in August 1982.

Inferences about the relative strength of continental and relict marine influences on the chemistry of the upper Hunter River valley groundwaters is put onto a quantitative footing by the use of multivariate statistical methods. The two techniques used in this study are related in the following way: the principal components measure several independent

directions of evolutionary change in the upper Hunter River valley groundwaters, whereas the canonical variates shown how far the evolutionary processes have progressed up to the present time. Thus, after the variation due to size effects is removed, $Y_2(R_p)$ compares the strongest 'marine' influence of diffusion and maturation of connate waters against the strongest 'continental' process of sulphide oxidation; separation of group means along the second canonical vector indicates that diffusion of Na^+-Cl^--type groundwaters is the dominant 'marine' signature in the Wittingham Coal Measures, and sulphide oxidation is co-dominant with diffusion of connate marine salts in the GM province. $Y_3(R_p)$ compares the next most prominent 'continental' process of silicate and carbonate mineral dissolution/precipitation reactions against a secondary measure of diffusion of connate marine salts based on the relative mobilities of SO_4^{2-} and Cl^- ions. Likewise, the third canonical variate contrasts group means according to the intensity of silicate and carbonate mineral dissolution/precipitation reactions, and also emphasises the importance of ion mobility effects.

The hypothesis that geological provenance is the dominant control in the chemistry of the upper Hunter River valley groundwaters has been tested by regrouping the data into smaller subsets which incorporate geographic variation and differences in the mode of transmission, and then subjecting the subgroups to a second canonical variates analysis. The integrity of the grouping by geological provenance is maintained through the second canonical variates analysis, thus showing that geology is the dominant control in the chemistry of the upper Hunter River valley groundwaters. On the scale of individuals, groundwater mixing zones are identified by the discrimination of hybrids according to their first and second principal component scores. In this survey several important mixing zones have been identified, but there may well be others undetected in areas of limited data coverage. In the floodplain provinces, significant inputs of GM-type groundwaters emanate from the Aberdeen and Hunter Thrust Faults, the Hilliers Creek Valley, and the Neotsfield area to the east of Singleton. Inputs of WI2-type groundwaters occur at Jerrys Plains and Alcheringa; the latter mixing zone is of special significance because the source is sufficiently strong to overprint the role of the Hunter River as a dividing streamline for groundwater flow. Perhaps the strongest source of WI2-type groundwaters is upwelling along the Mt Ogilvie Fault. The input of these

waters into the TRIAS and WO systems is reflected by saline pulses in baseflow chemistry of Big Flat Creek and Spring Creek, and their dispersion through the local groundwaters is shown by the shift in principal component scores of bores and wells in the lower sections of the valleys drained by these streams.

DISCUSSION

There is no doubt that the sources of saline groundwaters in the upper Hunter River valley are the GM, WI2, and, to a lesser extent, WI1 provinces. Within these provinces the fine-grained marine sediments comprising the Mulbring Siltstone, Bulga Formation, and Denman Formation represent the strongest primary sources of marine solutes; however, there is a trend for the salinities of groundwaters disseminated from these units to be maximised towards the south of the study area in the Wollombi Brook valley.

There also appears to be a trend of increasing soluble salts with age of these units, reflecting a higher degree of leaching by meteoric waters in units nearer to the landsurface. From the spatial variation in salinity it might be inferred that the Wollombi Brook valley to the south is a younger geomorphic surface than the main Hunter-Goulburn River valleys, but it might also be an expression of distance from Permian shorelines. From sulphur isotope studies (Smith and Batts, 1974) and trace element analyses (Swaine, 1962), previous workers have established that the upper seams of the Greta Coal Measures and the Vane Subgroup were enriched in marine solutes by direct contact between transgressing marine waters and the growing peats. Accretion of marine solutes in buried coals would have occurred at a slow rate by downwards diffusion, the depth of penetration of the solute front being dependent upon the duration of the marine transgression, depth of ponding, and rate of sedimentation on the seafloor.

The fact that Permian marine solutes are still diffusing out of rocks in the study area requires some explanation. Firstly, the opportunity for convective and dispersive flushing of connate marine fluids has existed only since Tertiary uplift created the appropriate difference between the high potential of the uplifted Upper Hunter Dome Belt and the

low potential eastwards towards the coast. In the intervening period, the Permian rocks were at or below mean sea level, and it is quite feasible that brines may have accumulated at depth during this period. The groundwater flux out of the upper Hunter River valley system in the early stages after uplift would have been composed of Na^+-Cl^--SO_4^{2-}-rich waters of far higher salinity than modern groundwater outflows. In particular, early drainage waters from the Mulbring Siltstone would have transported solutes derived from glauberite and halite dissolution, neither of which exists as a primary mineral today, and Na^+, Cl^-, and SO_4^{2-} concentrations exceeding those of sea-water may well have been attained along flow lines of deep circulation. The present brittle fracture system in the Permo-Triassic rocks developed in response to uplift and erosional unloading, and resulted in enhanced fracture permeability in the coals relative to the interseam beds. In the contemporary Permian fractured-rock system, groundwater flow lines are strongly refracted about the coal-sediment interfaces, and most groundwaters are preferentially transmitted along the paths of least hydraulic resistance, (viz. the conduits formed by an interconnected network of cleats and bedding plane separations in the coal seams). Geochemical studies in the Wollombi Brook valley indicate that there has been translocation of salts from the coal seams into the reservoir rocks of the adjacent coarse-grained sediments. The convective component of this process would have been exhausted long before Tertiary uplift, and represents lateral expulsion of interstitial fluids from the coals due to consolidation and decreasing porosity with rank advance, the greatest decrease in porosity occuring during early coalification. Porosity of the bituminous coals in the upper Hunter River valley now averages around one-tenth of that of the original peats.

Molecular diffusion is therefore the only hydrochemical process which is sufficiently slow to explain the persistence, from Tertiary uplift to the present, of marine solutes in the active leaching regime of the upper Hunter River valley groundwaters. The Wollombi Brook valley geochemical studies show that the current status of the system, in that area at least, is described by molecular diffusion of solutes from the coal matrix towards the cleats and bedding-plane partings. In areas of unimpeded groundwater drainage to the north of the valley, particularly in the WI1 province, it may well be that solutes are being diffused from the interseam sediments towards the highly permeable coal fractures, but this

process could only be established by detailed geochemical analyses. In the Mulbring Siltstone, molecular diffusion drives the marine solutes from the rock matrix towards tension fractures. The rate of diffusion depends on the concentration gradient between the rock matrix and the fracture, hence, if solute transport along fracture planes is impeded by factors such as structural boundaries or mineral precipitates on fracture faces, the rate of flux of solutes is considerably retarded. Both factors are operative in the WI2 and GM provinces in the Wollombi Brook valley. From principal components analyses it has been possible to discriminate the dimension associated with molecular diffusion of connate marine salts; for similar positions along flow lines in groundwater discharge zones, WI1-type groundwaters are only at the juvenile stage, and WI2 and GM-type waters have not advanced past the immature stage of the evolutionary sequence Na^+-$Cl^- \rightarrow Na^+$-$HCO_3^- \rightarrow Ca^{2+}$-$HCO_3^-$, despite active circulation of groundwaters in this system since Tertiary uplift. Therefore, in planning for future development in the upper Hunter River valley, it should be recognised that high background salinities in groundwaters of the Central Lowlands are natural phenomena which will persist for the foreseeable future.

ACKNOWLEDGEMENTS

This study was a joint research project between BMR Division of Continental Geology and CSIRO Division of Water and Land Resources. We wish to acknowledge the useful collaboration and support received from our colleagues in the following organizations:

Centre for Resource and Environmental Studies, Australian National University;

CSIRO Division of Mineral Chemistry;

Hydrogeology and Research Sections, NSW Water Resources Commission;

Environmental Geology Section, NSW Geological Survey;

Hunter Valley Conservation Trust.

At the commencement of the project we sought access in writing to twenty existing and proposed collieries in the upper Hunter River valley for groundwater sampling. These requests were refused for seven sites, and nine companies did not reply. To the four companies which granted us access to groundwater sampling points we are most grateful for their valuable contribution to the project. These companies are:

Buchanan Borehole Collieries Pty. Ltd.;
Drayton Coal Pty. Ltd.;
Muswellbrook Coal Co. Pty. Ltd;
Costain Australia Ltd. (Ravensworth No. 2 Open-cut Colliery)..pl70

REFERENCES

AUSTRALIAN GROUNDWATER CONSULTANTS, 1982 - Preliminary report on effects of coal mining on the groundwater resources of the Upper Hunter valley.

BLACKITH, R.E., & REYMENT, R.A., 1971 - MULTIVARIATE MORPHOMETRICS. Academic Press, London.

BLOCK, J. & WALTERS, O.B., 1968 - The $CaSO_4$-Na_2SO_4-NaCl-H_2O system at 25° to 100°C. Journal of chemical and Engineering Data. 13, 336-44.

BRANAGAN, D., HERBET, C., & LANGFORD-SMITH, T., 1975 - AN OUTLINE OF THE GEOLOGY AND GEOMORPHOLOGY OF THE SYDNEY BASIN. Science Press, Sydney.

BRITTEN, R.A., 1975 - Singleton-Muswellbrook district. In Knight, C.L. (Editor) - Economic geology of Australia and Papua New Guinea 2, Coal. Australasian Institute of Mining and Metallurgy Monograph 6, 191-205.

BUNNY, M.R., 1967 - Geology and coal resources of the Liddell State coal mine holding, Hunter Valley, New South Wales. Geological Survey of New South Wales, Records 12(2), 81-123.

CONYBEARE, C.E.B., & CROOK, K.A.W., 1968 - Manual of sedimentary structures. Bureau of Mineral Resources, Australia, Bulletin 102.

CROFT & ASSOCIATES, 1979 - Saxonvale coal mine, environmental impact statement.

CROFT & ASSOCIATES, 1981 - Mt Thorley coal mine, environmental impact statement.

DAVID, T.W.E., TAYLOR, T.G., WOOLNOUGH, W.G., & FOXALL, H.G., 1905 - Occurrence of the pseudomorph glendonite in New South Wales. Geological Survey of New South Wales, Record 8, 161-79.

EUGSTER, H.P., & JONES, B.F., 1979 - Behaviour of major solutes during closed-basin brine evolution. American Journal of Science, 279, 609-31.

GALLOWAY, R.W., 1971 - Pre-basalt, sub-basalt and post-basalt surfaces of the Hunter Valley, New South Wales. In Jennings, J.N., & Mabbutt, J.A. (Editors) - Land form studies from Australia and New Guinea. Australian National University Press, Canberra.

GARMAN, D.E.J., 1980 - The Hunter River Valley, water quality present and future. In Hunter environment symposium, Department of Geography, University of Newcastle, NSW, Proceedings.

GARMAN, D.E.J., 1982 - Future water quality in the Hunter River. Proceedings of the 52nd. ANZAAS Conference, Macquarie University, Sydney.

GARRELS, R.M., & CHRIST, C.L., 1965 - SOLUTIONS, MINERALS AND EQUILIBRIA. Harper, New York.

GARRELS, R.M., & MacKENZIE, F.T., 1967 - Origin of the chemical compositions of some springs and lakes. In Equilibrium concepts in natural water systems, Advances in Chemistry Series 67, American Chemical Society.

GATES, G.W., & KALF, F.R., 1983 - The effects of coal mining on the water quality in the Upper Hunter Valley, New South Wales. International Conference on Groundwater and Man., Sydney, Proceedings.

GRIFFIN, R.J., 1960 - The groundwater resources of the Wollombi Brook catchment area. Department of Mines, New South Wales Technical Report 8.

HEM, J.D., 1970 - Study and interpretation of the chemical characteristics of natural water. United States Geological Survey, Water-Supply Paper 1473.

HERBET, C., & HELBY, R., 1980 - A guide to the Sydney Basin. Geological Survey of New South Wales, Bulletin 26.

JACKSON, M.L., & SHERMAN, G.D., 1953 - Chemical weathering of minerals in soils. Advances in Agronomy, 5, 219-318.

JURINAK, J.J., 1984 - Salt affected soils: thermodynamic aspects of the soil solution. In Shainberg & Shalhevet (Editors) - SOIL SALINITY UNDER IRRIGATION. Springer Verlag, Berlin.

KEMEZYS, M., & TAYLOR, G.H., 1964 - Occurrence and distribution of minerals in some Australian coals. Journal of the Institute of Fuel, 37, 389-97.

KEMPER, E., & SCHMITZ, H.H., 1975 - Stellate nodules from the Upper Deer Bay Formation (Valanginian) of arctic Canada. Geological Survey of Canada, Paper 75-1C, 109-19.

LOUGHNAN, F.C., 1966 - Analcite in the Newcastle Coal Measure sediments of the Sydney Basin, Australia. The American Mineralogist, 51, 486-94.

LOUGHNAN, F.C., & SEE, G.T., 1976 - Dawsonite in the Greta Coal Measures at Muswellbrook, New South Wales. The American Mineralogists, 52, 1216-9.

LOUGHNAN, F.C., & GOLDBERY, R., 1972 - Problems with the genesis of dawsonite in the Sydney Basin. NSW Geological Society of Australia, Specialists Group Meeting, Canberra 1972, Abstracts, D29-D32.

MAYNE, S.J., NICHOLAS, E., BIGG-WITHER, A.L., RASIDI, J.S., & RAINE, M.J., 1974 - Geology of the Sydney Basin - a review. Bureau of Mineral Resources, Australia, Bulletin 149.

PACES, T., 1972 - Chemical characteristics and equlibration in natural water-felsic rock-CO_2 system. Geochimica et Cosmochimica Acta, 36, 217-40.

PRICE, N.J., 1966 - FAULT AND JOINT DEVELOPMENT IN BRITTLE AND SEMI BRITTLE ROCK. Pergamon, Oxford.

RAI, D., & LINDSAY, W.L., 1975 - The thermodynamic model for predicting the formation, stability and weathering of common soil minerals. Soil Science Society of America, Proceedings, 39, 991-6.

RASMUS, P.L., ROSE, D.M., & ROSE, G., 1969 - Singleton 1:250 000 Geological Series (First Edition). NSW Department of Mines, Sydney. (SI56-1).

RAO, C. RADHAKRISHNA, 1952 - ADVANCED STATISTICAL METHODS IN BIOMETRIC RESEARCH. Wiley, New York.

ROBIE, R.A., HEMINGWAY, B.S., & FISHER, J.R., 1978 - Thermodynamic properties of minerals and related substances at 298.15 K and 1 bar (10^5 pascals) pressure and at higher temperatures. United States Geological Survey, Bulletin 1452.

SINCLAIR, KNIGHT & PARTNERS P.L., 1981 - Mt Arthur North coal project, environmental impact statement.

SINCLAIR, KNIGHT & PARTNERS P.L., 1983 - Black Hill coal mine environmental assessment.

SINCLAIR, KNIGHT & PARTNERS P.L., 1982 - Mt Arthur South coal project, environmental impact statement.

SMITH, J.W., & BATTS, B.D., 1974 - The distribution and isotopic composition of sulphur in coals. Geochimica et Cosmochimica Acta, 38, 121-33.

STORY, R., GALLOWAY, R.W., VAN de GRAAFF, R.H.M., & TWEEDIE, A.D., 1963 - general report of the Hunter Valley. CSIRO, Land Research series 8.

STUMM, W., & MORGAN, J.L., 1970 - AQUATIC CHEMISTRY. Wiley - Interscience, New York.

SWAINE, D.J., 1962 - Boron in New South Wales Permian coals. Australian Journal of Science, 25, 265-6.

SWAINE, D.J., 1971 - Boron in coals of the Bowen Basin as an environmental indicator. Proceedings of the 2nd Bowen Basin Symposium, October 1970, Geological Survey of Queensland, Report 62, 41-8.

TRUESDELL, A.H., & JONES, B.F., 1974 - WATEQ, a computer program for calculating chemical equilibria on natural waters. United States Geological Survey Journal of Research, 2, 233-48.

WELLMAN, P., & McDOUGALL, I., 1974 - Potassium-argon ages on the Cainozoic volcanic rocks of New South Wales. Journal of the Geological Society of Australia, 21 (3), 247-72.

WILLIAMSON, W.H., 1958 - Groundwater resources of the Upper Hunter Valley. NSW Government Printer, Sydney.

APPENDIX 2. TRACE ELEMENTS IN UPPER HUNTER VALLEY GROUNDWATERS (ppm)

Site	B	Cu	Mn	Zn	Mo	Co	P	Fe	Al
CARB									
131	.07	.01		.01			.06		.60
161	.18	.01					.28		.49
TRIAS									
2	.02	.01					.35		.72
229	.02	.01	.02				.44		.72
231	.02	.01	.04				.50		.74
288				.09			.15		.38
WO									
6	.05	.01					.14		.18
45	.03	.01	2.61				.14	.12	.20
46	.01	.01					.06		.26
50	.03	.01	.34		.01		.02		.17
82	.02	.01					.38		.79
83	.03	.01					.07		.28
87	.03	.01					.17		.51
89	.03	.01	.10	.61	.02		.03		.38
102	.02	.01					.05		.25
261	.08	.01	.86				.47	.19	.60
265	.11		.01				.43		.30
298	.06			.04			.18		.11

299	.06			.02	.02		.21	.10	.11
307	.09	.01	.05				.26		.29
HFP1									
280	.04			.07			.28		.66
HFP2									
17	.03	.01					.17		.53
20	.03	.01					.11		.68
23	.02	.02	.22	.08			.04		.51
25	.06	.01	.90				.09		.43
270	.09		.01				.52		.87
28	.03	.01					.25		.64
111	.03	.01	.01			.01	.07		.49
291	.03						.27		.43
WI1									
95	.06	.01		.02		.01	.24		.81
97	.05	.01		.01			.07		.55
145	.03	.01					.19		.50
217	.05		1.31				.34		.29
239	.18		.02	.54			.63		.33
253	.05						.20		.27
284	.08	.25	.01				.37		.79
37	.04	.01	.27				.06		.26
WI2									

30			.01				.09		.65
32	.04	.01					.18	.14	.64
33	.04	.01						.75	.44
34	.06	.01	.05	.04			.77		.91
35	.13	.03	.10	.07			.74		.89
40	.06	.01					.59		1.00
42	.09	.01					.92		1.25
48	.07		.09			.01	.47		.40
54	.08	.01	.01		.04		.75		.64
58	.05						.48		.29
104	.07	.01		.01	.09	.01	.46		.64
105	.21	.01					.44		.67
107	.07	.01	.08			.01	.96		.67
108	.04	.01				.01	.07		.92
112	.05	.01					.17		.89
115	.04	.01					.17		.77
116	.05	.01	.12	.03		.01	.29		1.01
117	.01	.01		.02			.08		.48
118	.05	.01				.01	.16		.93
119	.01		.01	.05			.03	.43	.08
125	.12	.01					.26		.64
133	.02	.01	.01				.25		.69
135	.08		.29	.01			.53		1.02
136	.05		4.89				.15	.01	1.14
138	.10	.01			.02		.54		.49
139	.05	.01	.12				.16		.52
141	.08				.02		.57		.61
142	.03	.01					.46		.85
147	.10						.60		.97

179	.04	.01	.57				.52		.90
200	.14		.09				.45		.59
227	.13	.01	.52				.91		1.47
232	.08		.01				1.00		.51
255	.05	.06	.50				.34		.37
GM									
62	.19	.01	.11	.08			1.38		1.60
64	.21	.02	.20	.01			1.61		1.66
66	.30	.02	21.72	.01		.01	.33	.02	1.25
67	.36	.01	.13	.01			1.22		1.26
69	.04			.02	.01		.48		.31
124	.08	.01		.01			.23		1.00
127	.06	.01	.04	.01			.47		1.59
182	.29	.01	.16	.01			.46		1.68
183	.18	.01	.07	.04			1.03		1.48
184	.11	.01	.22	.02			1.03		1.69
185	.08	.01	.04				.31		.52
186	.15	.01	.22	.04			1.08		1.60
187	.19	.02	.71	.01	.01		1.35		1.87
193	.22	.02	.80				.70		1.21
194	.06	.01	.03	1.81			.35		.39
195	.18	.01	.26	.05	.01		1.22		1.54
199	.15	.02	.39				1.55		1.91
206	.07	.01	.32				.52		1.02
207	.03		.19				.21		.48
208	.07		.03	.04			.47		1.03
209	.10				.02		.24		.99
212	.07	.01	.29	.16			.91		1.60

213	.49		.02	.06	.28	1.02
214	.06	.01	.01		.43	1.49
228	.52		.01	.07	.30	1.02
236	.14			.03	.71	1.34
289	.09	.01	.04		.23	.67

Blank space represents no element detected.

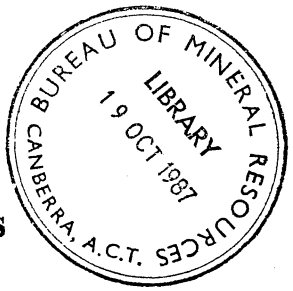

AGE	GEOLOGICAL UNIT AND MEDIAN THICKNESS (m)*			LITHOLOGY
QUATERNARY	ALLUVIUM		12 (MU) 14 (SI) 13 (MA) 8 (BR)	*Heterogeneous clays, silts, sands and gravels*
TERTIARY			100 (WY)	*Olivine basalts* *Dolerite sills, lacoliths, necks*
EARLY TRIASSIC	NARRABEEN GROUP		200 (WY) 350 (BR) 400 (MA)	*Interbedded shales and sandstones on basal fanglomerate*
LATE PERMIAN	SINGLETON SUPERGROUP	Wollombi Coal Measures	280 (WA) 230 (BR) 340 (DC) 290 (MA) 230 (WY)	*Coal measure sequence with numerous tuff, conglomerate, arenite and claystone interseam beds*
		Wittingham Coal Measures: Jerrys Plains Subgroup	410 (WY) 640 (WA) 340 (BR)	*Coal measure sequence with 12 major named seams and numerous splits. Fluvial conglomerate, sandstone and claystone interseam beds of irregular thickness terminating in marine laminites (Denman Formation)*
		Wittingham Coal Measures: Archerfield Sandstone	10 (MA) 15 (DC)	*Massive coarse sandstone*
		Wittingham Coal Measures: Vane Subgroup	80 (WY) 200 (WA) 150 (BR) 250 (DA)	*Coal measure sequence with 7 major named seams. Fluvial sandstone and siltstone interbeds terminating in marine laminated siltstone (Bulga Formation)*
		Wittingham Coal Measures: Saltwater Creek Formation	20 (WY) 40 (BR) 30 (WA) 50 (MU)	*Massive sandstone with basal silty phases*
	MAITLAND GROUP	Mulbring Siltstone	250 (SI) 300 (LI) 140 (MA)	*Fossiliferous and pyritic shale, siltstone and fine sandstone*
		Muree Sandstone	60 (SI)	*Pebbly and tillitic sandstone*
EARLY PERMIAN		Branxton Formation	220 (MA) 300 (DC) 330 (DA) 500 (SI) 520 (LI)	*Tillitic sandstone, siltstone and conglomerate*
	GRETA COAL MEASURES	Rowan Formation	110 (LI) 140 (MU)	*Sandstone, siltstone, shale and mudstone with intercalated coal seams*
		Skeletar Formation	20 (LI) 80 (MU)	*Rhyolite, chert and tuffaceous claystone*
	DALWOOD GROUP	Farley Formation	150 (SI)	*Micaceous sandy siltstone, mudstone, shale, minor limestone*
		Rutherford Formation	400 (SI)	*Conglomeratic sandstone with erratics, mudstone, marl*
		Allandale Formation / Lochinvar Formation	> 800 (SI)	*Andesitic tuff, breccia, basalt; major shale and conglomerate*
CARBONIFEROUS	KUTTUNG GROUP	Undifferentiated		*Acid and crystal tuff, conglomerate (includes glacigene sediments of Seaham Formation)*
		Gilmore Volcanics		*Interbedded tuffs and sandstones*
		Wallaringa Formation		*Conglomeratic acid tuffs on basal conglomerate*

19 156-1 60

*Location key: WY Wybong, BR Broke, DC Doyles Creek, SI Singleton, LI Liddell, MU Muswellbrook, WA Wambo–Bulga, DA Dartbrook–Aberdeen

Record 1987/23

TABLE 1. Stratigraphic units in the upper Hunter River valley.

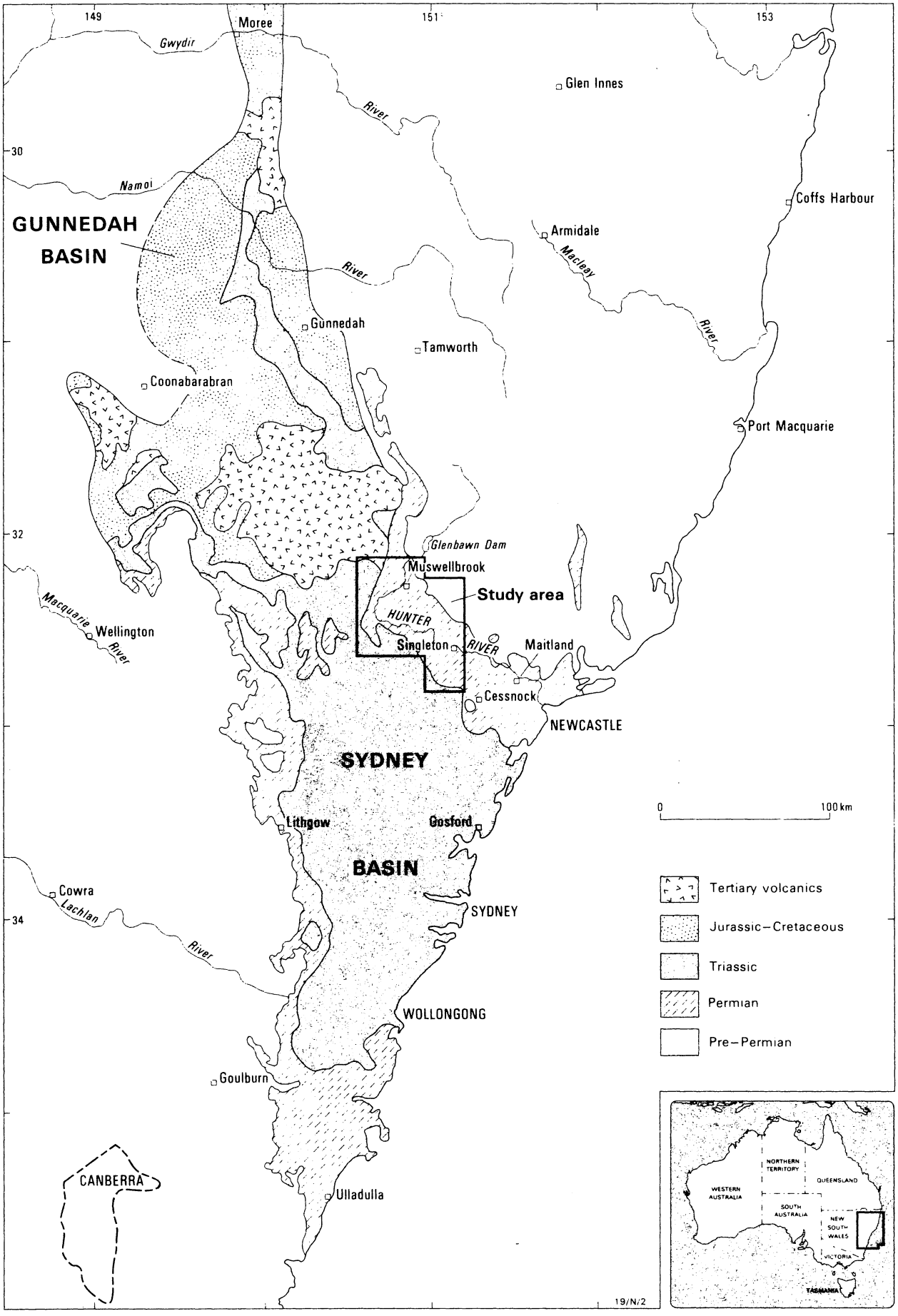

Record 1987/23

FIG 1. Locality map and generalised surface geology

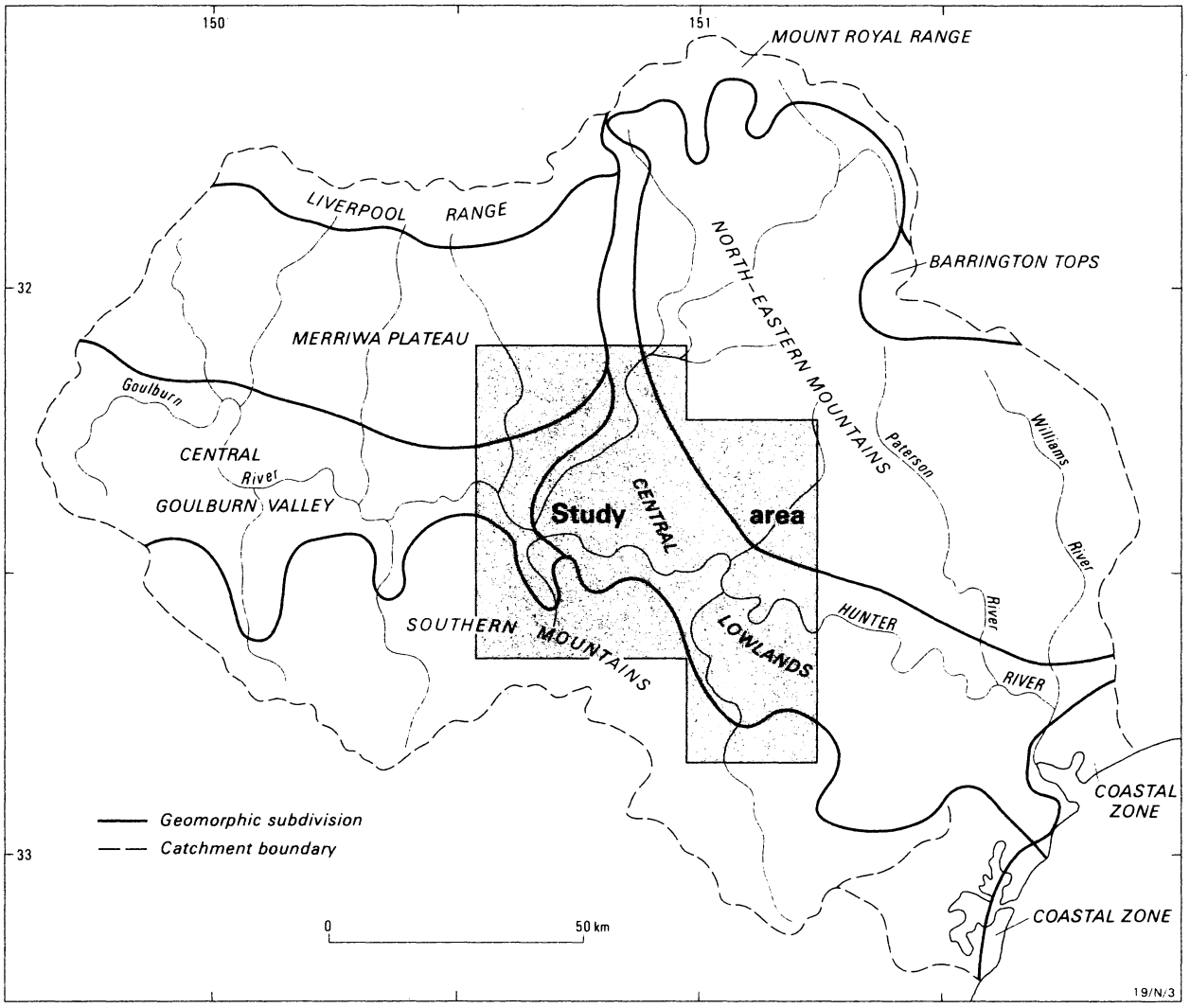

Record 1987/23

FIG 2. Geomorphic subdivisions, Hunter River valley catchment (after Story et al, 1963)

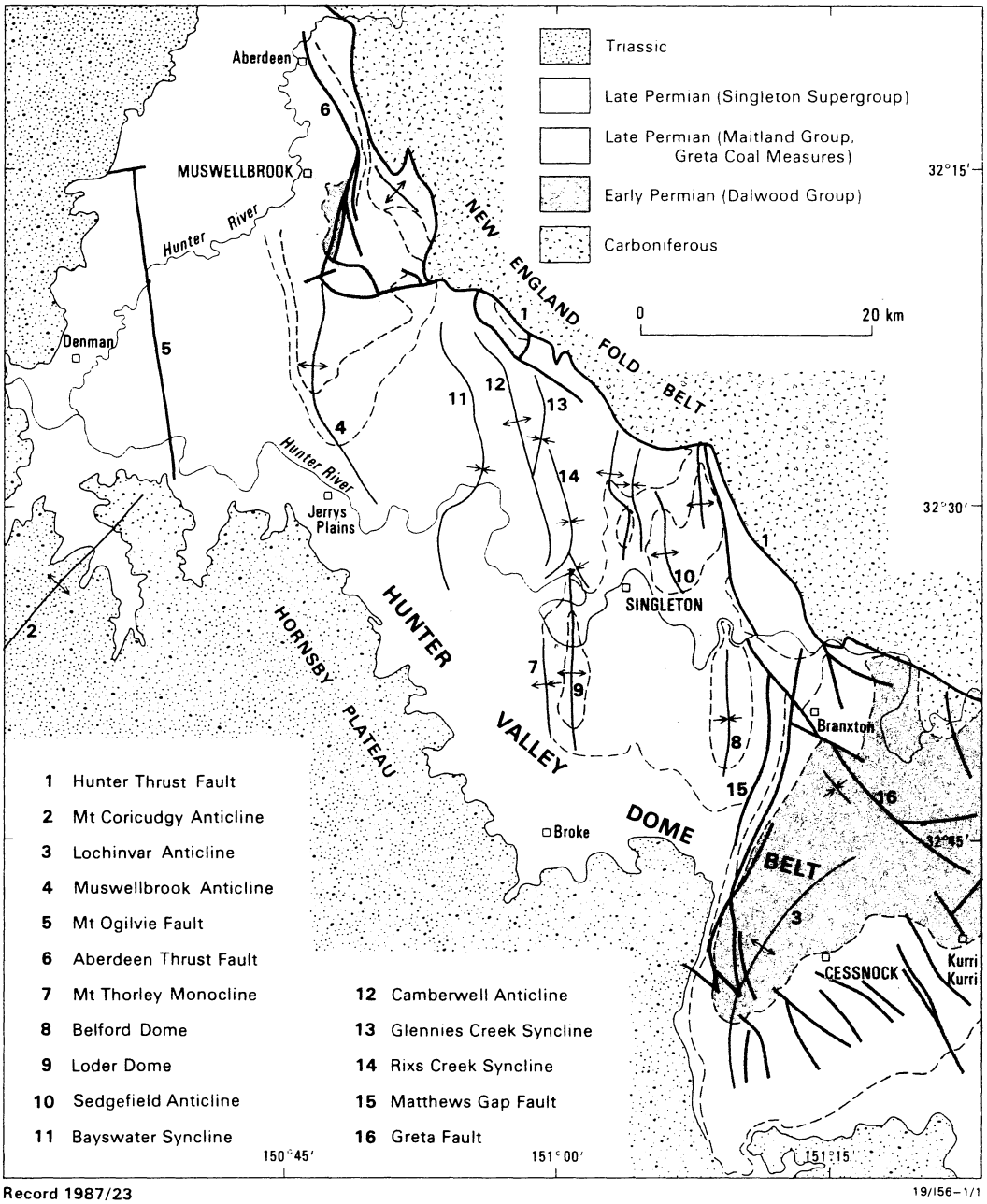

Record 1987/23

19/156-1/1

FIG 3. Generalised geology and major structures, Hunter Valley Dome Belt

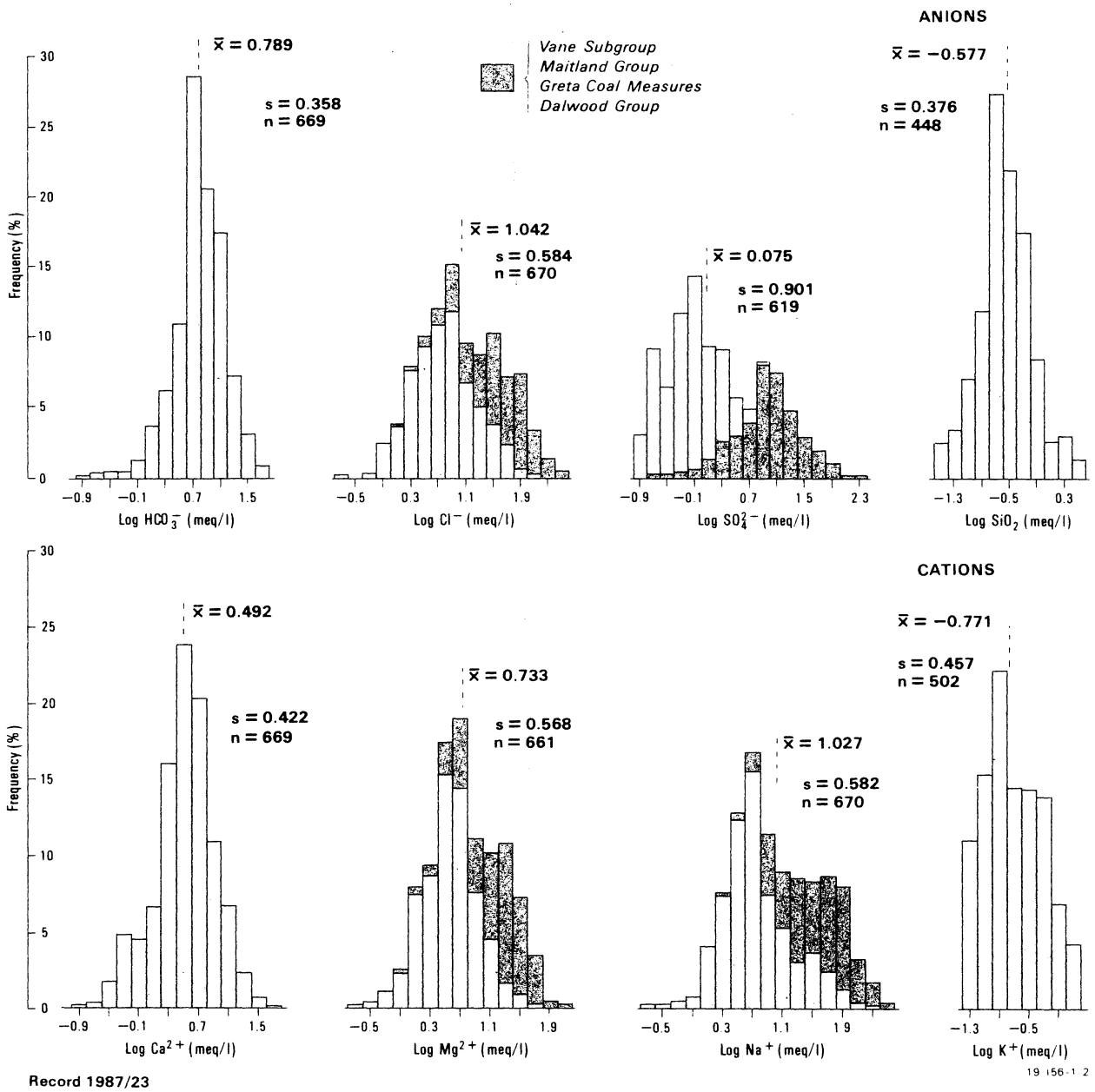

FIG 4. Frequency distribution of anion and cation concentrations in upper Hunter River valley groundwaters

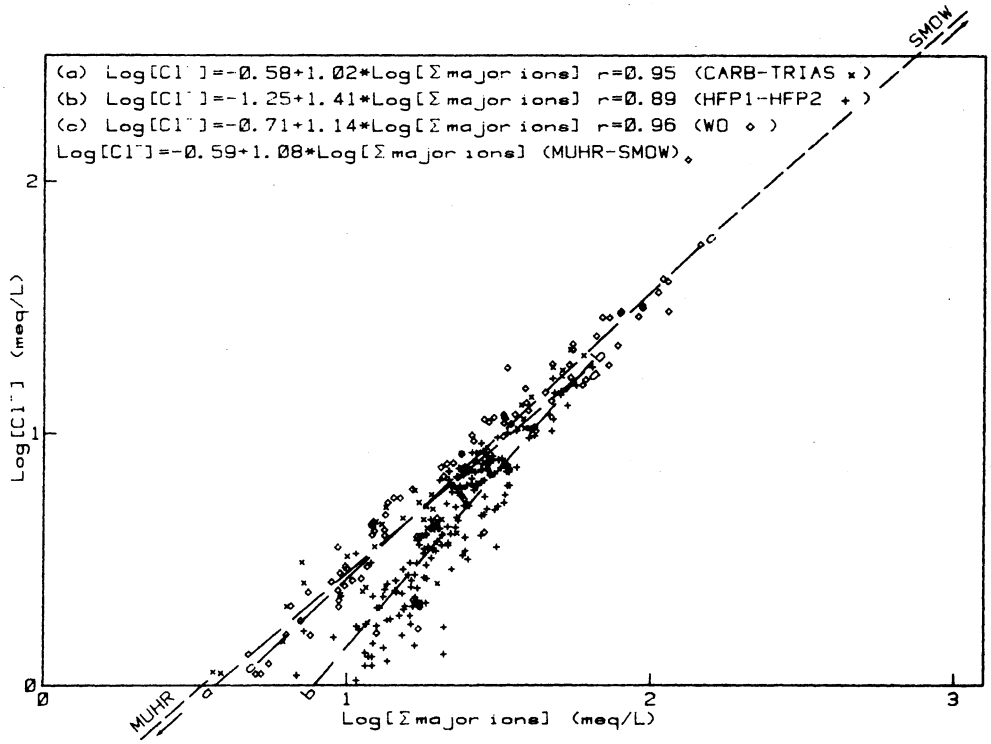

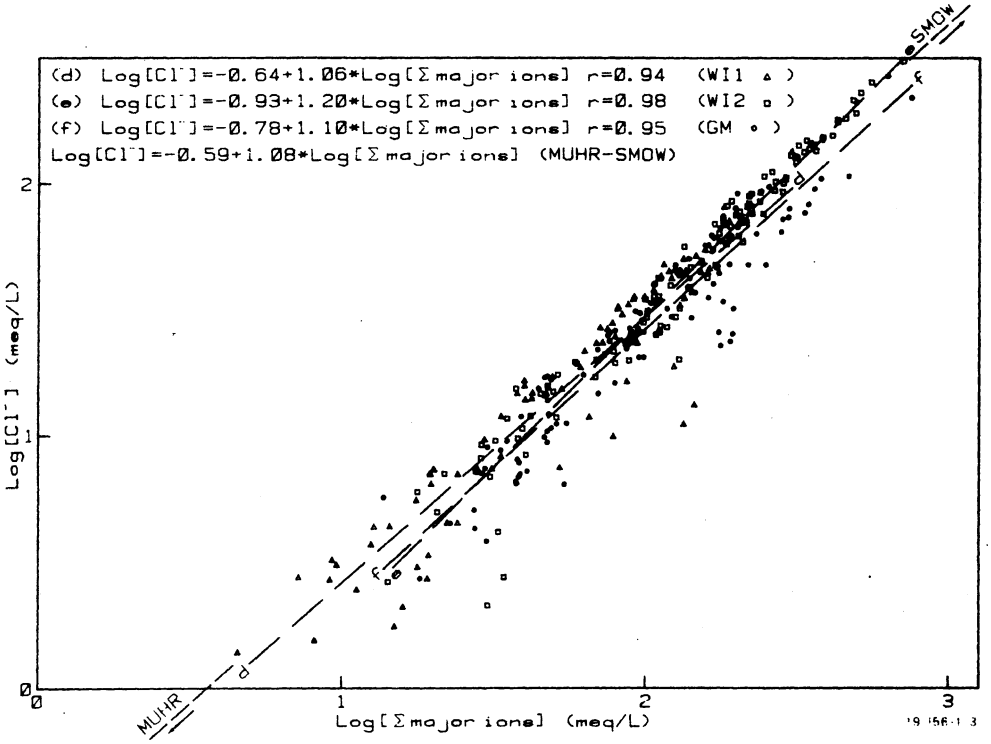

FIG 5a) Composition diagrams of chloride concentrations versus 5b) total ions by hydrochemical province

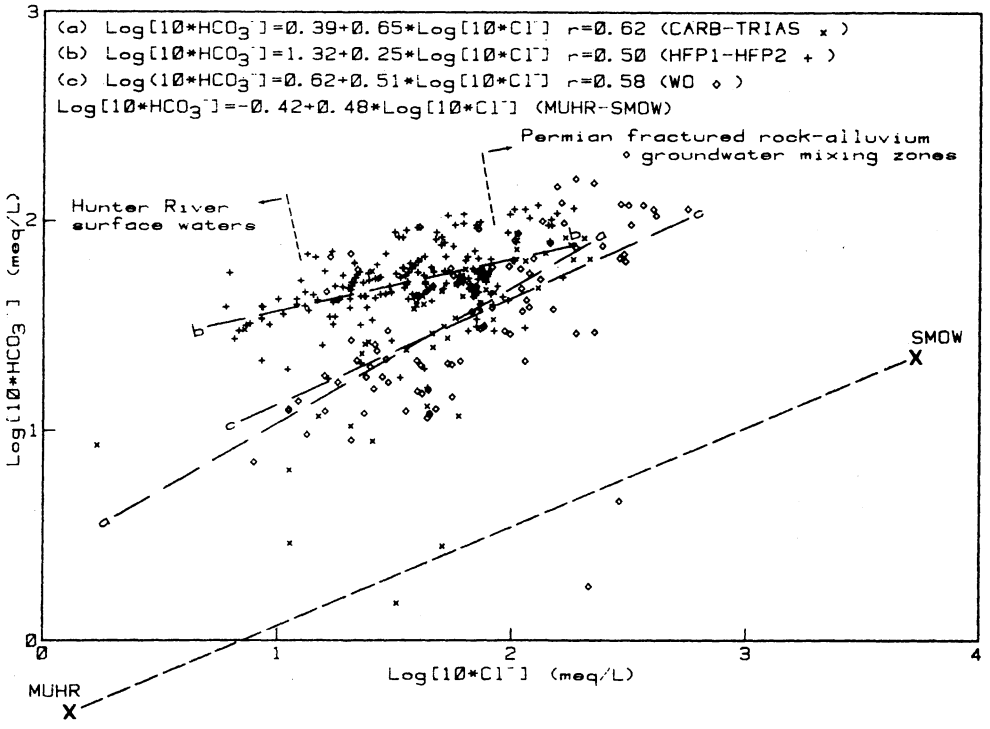

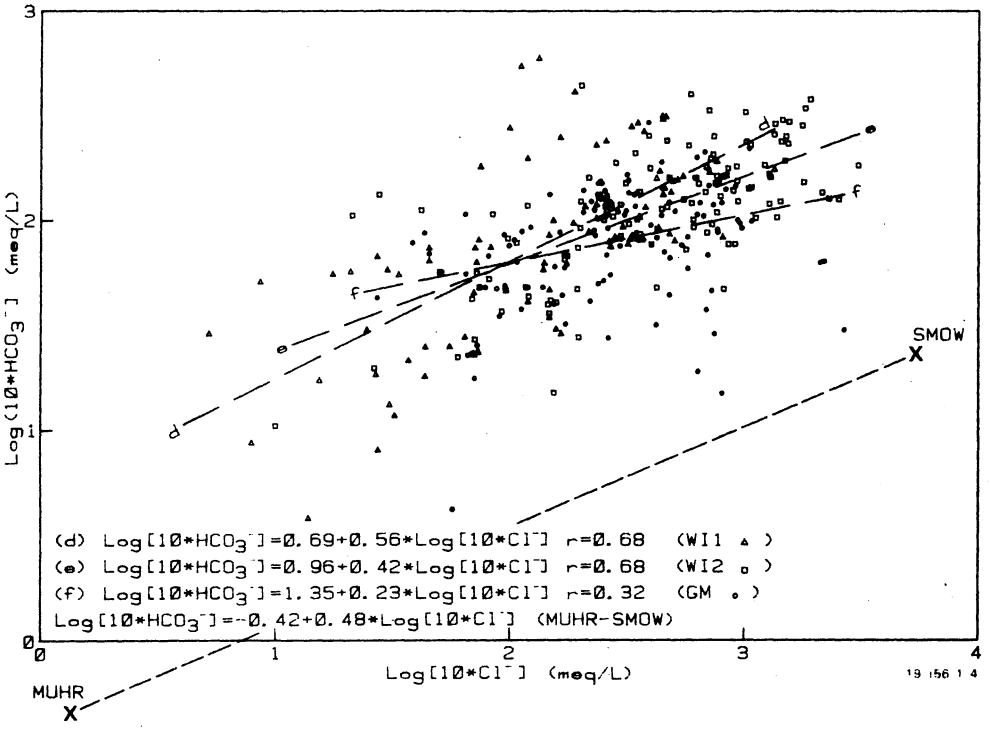

Record 1987/23

FIG 6a) Composition diagrams of bicarbonate versus chloride

6b) concentration by hydrochemical province

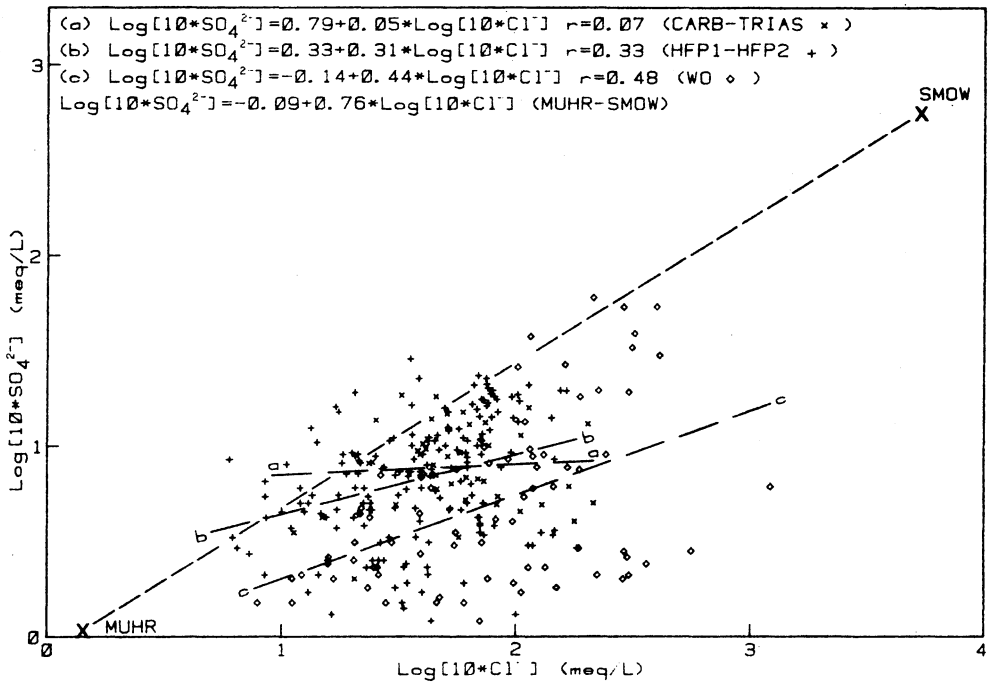

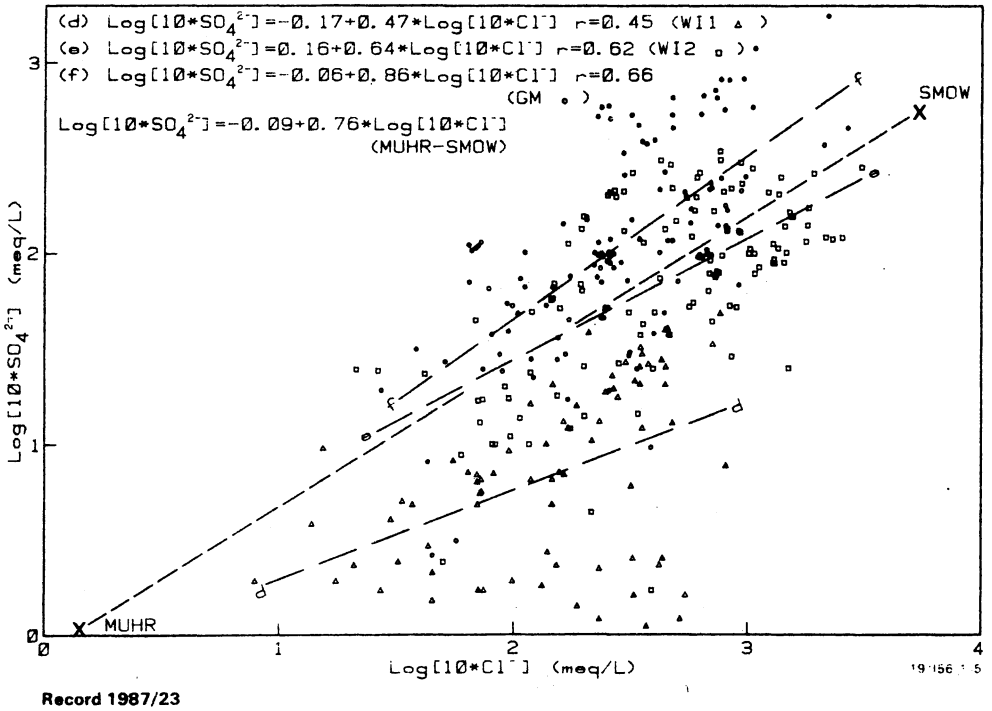

Record 1987/23

FIG 7a) Composition diagrams of sulphate versus chloride

7b) concentrations by hydrochemical province

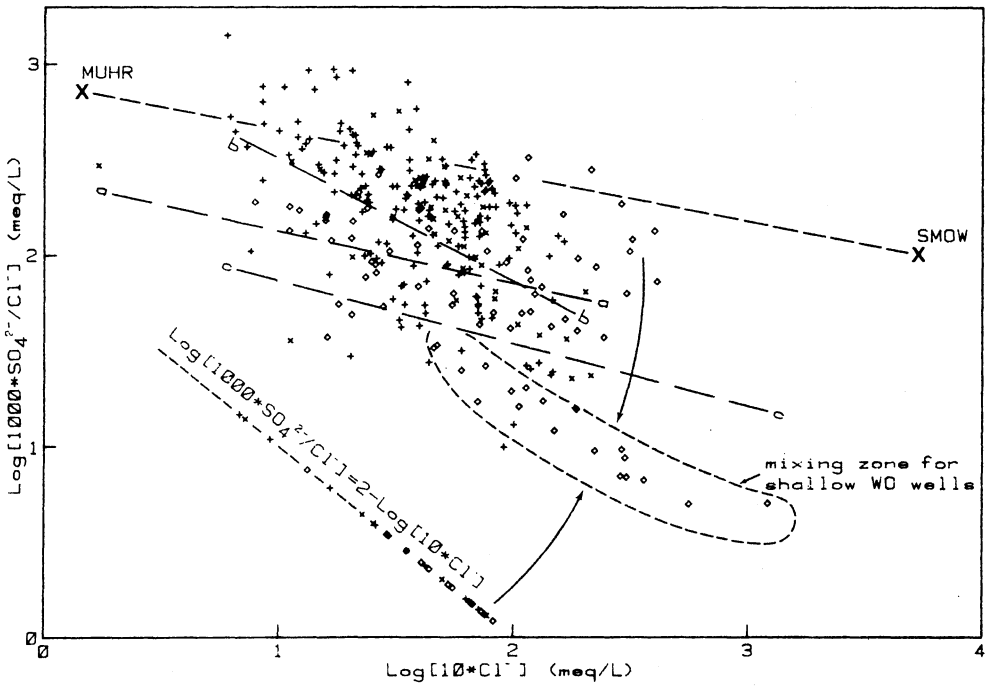

(a) $Log[1000*SO_4^{2-}/Cl^-]=2.40-0.28*Log[10*Cl^-]$ r=-0.16 (CARB-TRIAS x)

(b) $Log[1000*SO_4^{2-}/Cl^-]=3.15-0.64*Log[10*Cl^-]$ r=-0.39 (HFP1-HFP2 +)

(c) $Log[1000*SO_4^{2-}/Cl^-]=2.19-0.33*Log[10*Cl^-]$ r=-0.22 (WO ◇)

$Log[1000*SO_4^{2-}/Cl^-]=2.91-0.24*Log[10*Cl^-]$ (MUHR-SMOW)

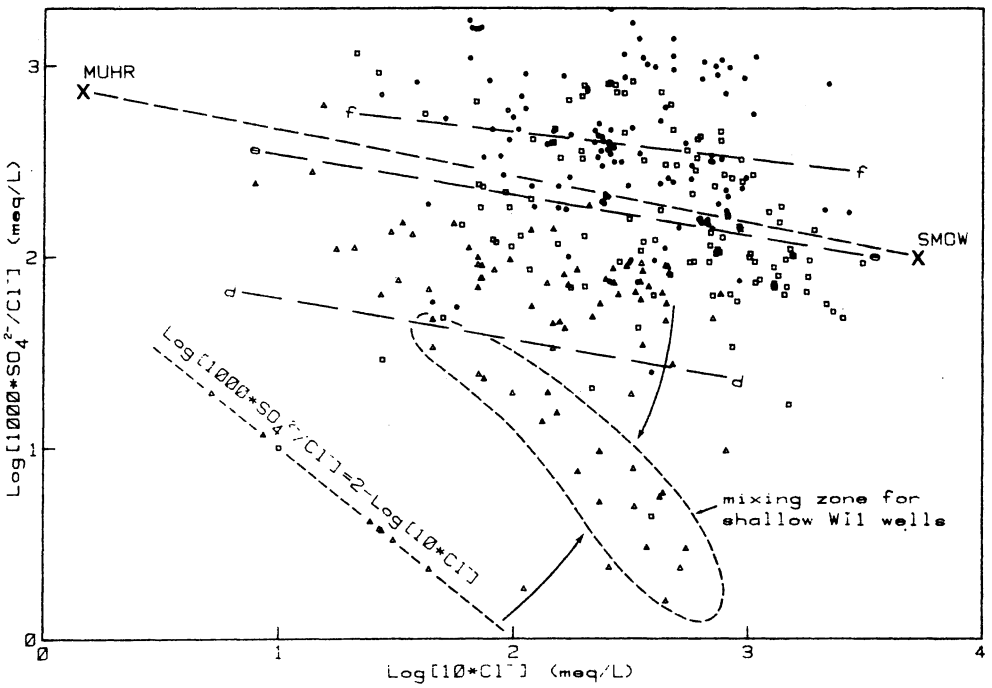

(d) $Log[1000*SO_4^{2-}/Cl^-]=2.00-0.22*Log[10*Cl^-]$ r=-0.19 (WI1 △)

(e) $Log(1000*SO_4^{2-}/Cl^-]=2.75-0.21*Log[10*Cl^-]$ r=-0.25 (WI2 □)

(f) $Log[1000*SO_4^{2-}/Cl^-]=2.94-0.14*Log[10*Cl^-]$ r=-0.14 (GM ◇)

$Log[1000*SO_4^{2-}/Cl^-]=2.91-0.24*Log[10*Cl^-]$ (MUHR-SMOW)

19 156 ' 6

FIG 7c) Composition diagrams of normalized sulphate versus chloride

7d) concentrations by hydrochemical province

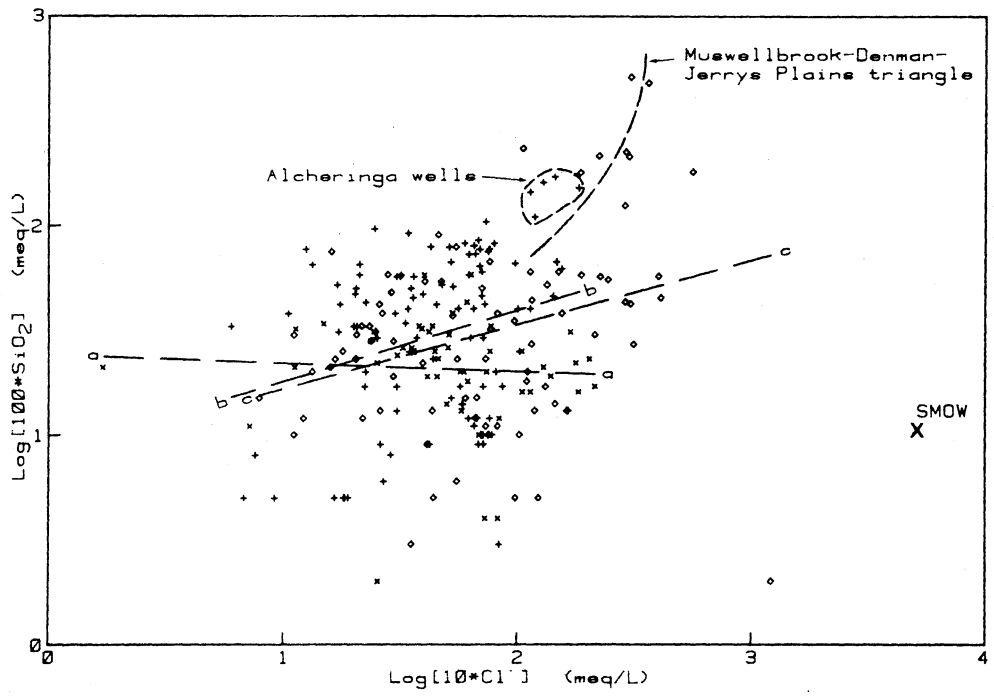

(a) $Log[100*SiO_2] = 1.38 - 0.04 * Log[10*Cl^-]$ r=-0.06 (CARB-TRIAS x)
(b) $Log[100*SiO_2] = 0.92 + 0.34 * Log[10*Cl^-]$ r=0.27 (HFP1-HFP2 +)
(c) $Log[100*SiO_2] = 0.91 + 0.31 * Log[10*Cl^-]$ r=0.31 (WO ◇)

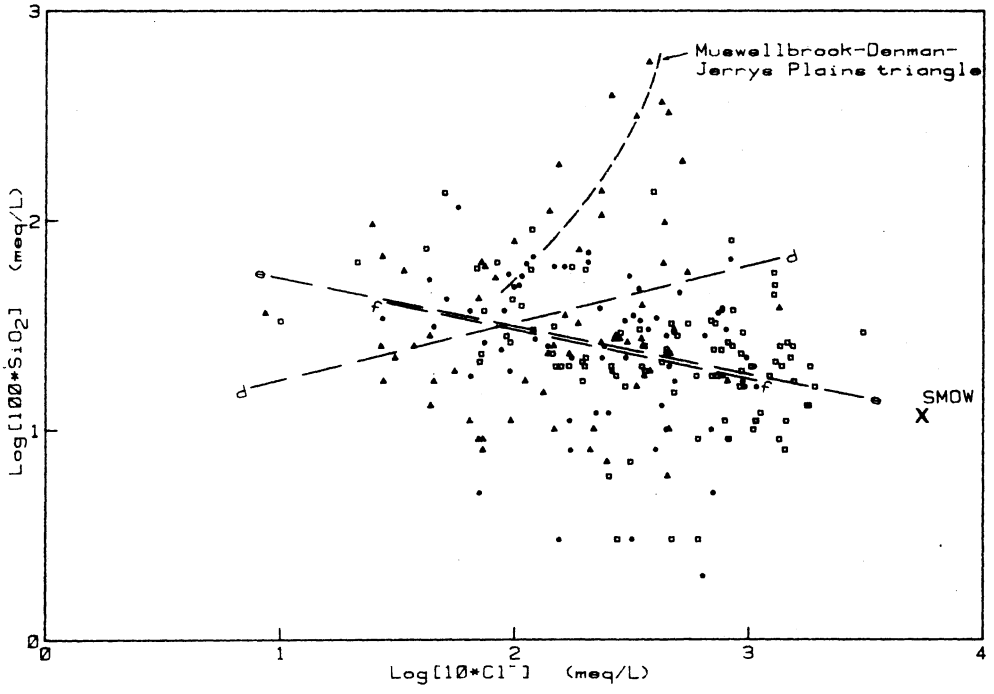

(d) $Log[100*SiO_2] = 0.97 + 0.27 * Log[10*Cl^-]$ r=0.23 (WI1 △)
(e) $Log[100*SiO_2] = 1.95 - 0.23 * Log[10*Cl^-]$ r=-0.37 (WI2 □)
(f) $Log[100*SiO_2] = 1.95 - 0.24 * Log[10*Cl^-]$ r=-0.27 (GM ○)

19 156 1 7

Record 1987/23

FIG 8a) Composition diagrams of silica versus chloride

8b) concentrations by hydrochemical province

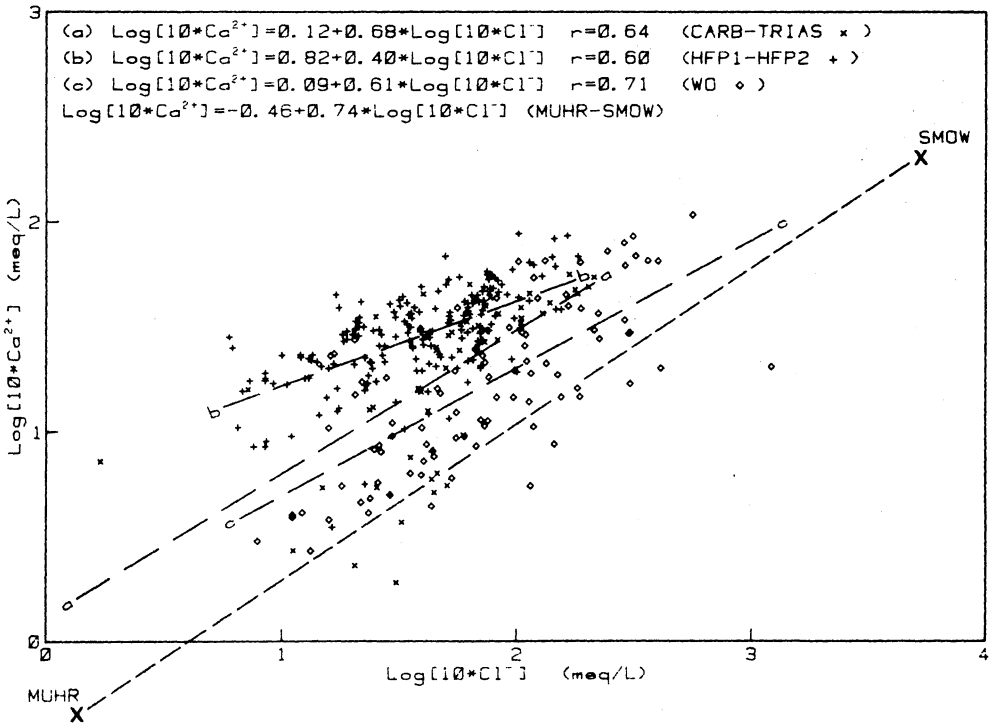

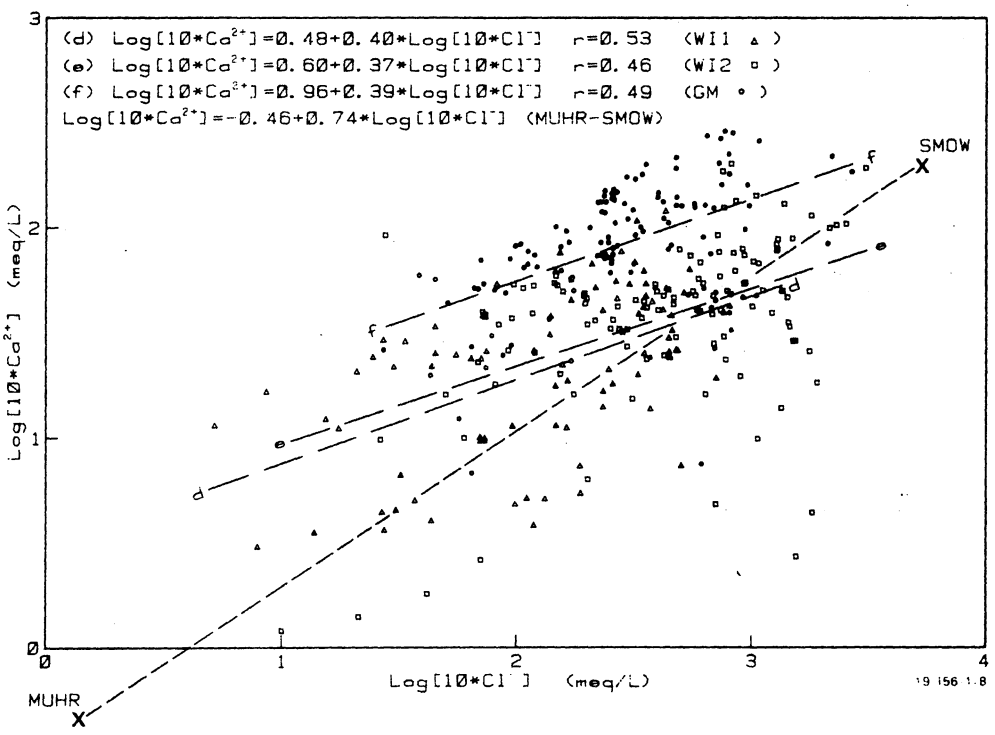

Record 1987/23

FIG 9a) Composition diagrams of calcium versus chloride concentrations

9b) by hydrochemical province

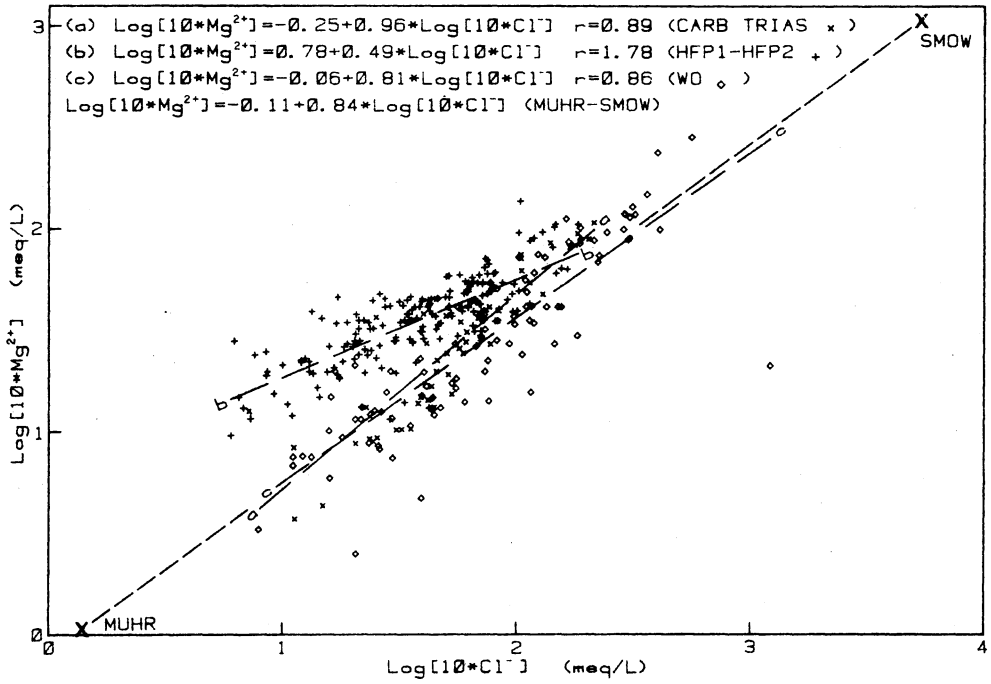

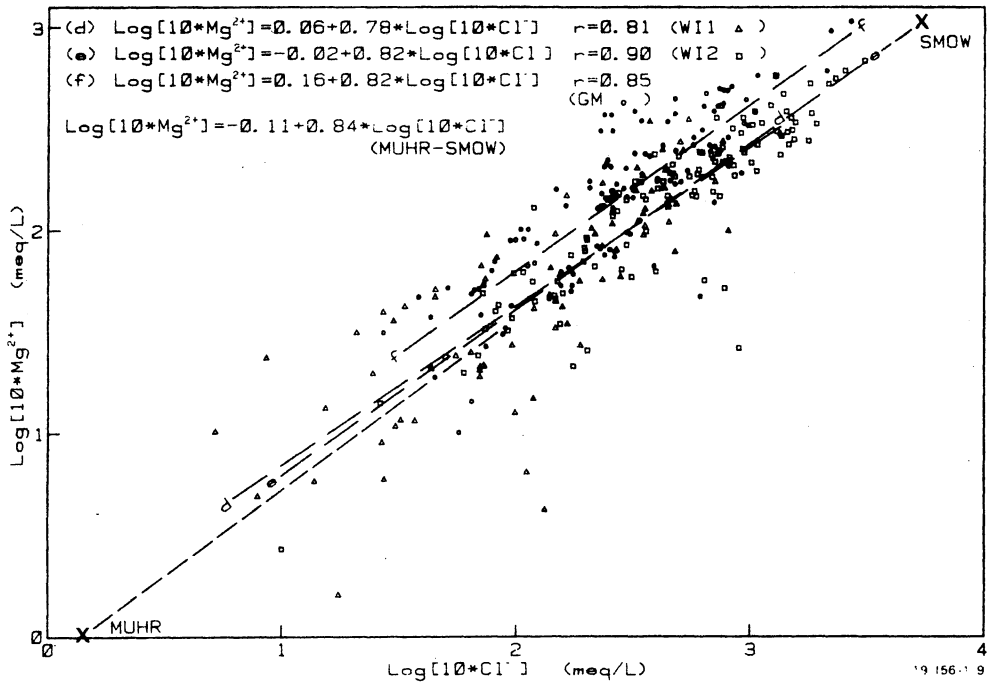

Record 1987/23

FIG 10a) Composition diagrams of magnesium versus chloride concentrations
10b) by hydrochemical province

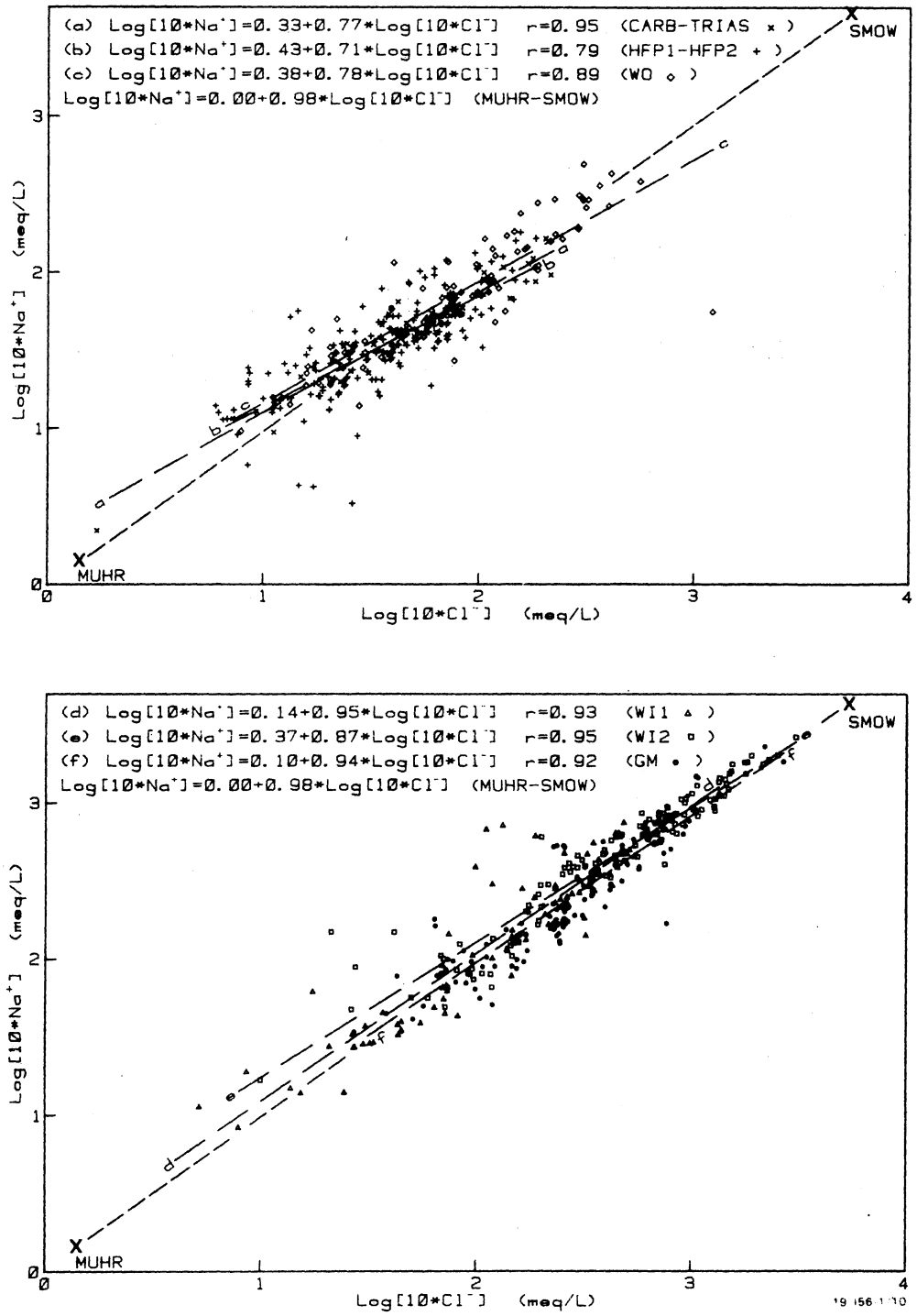

FIG 11a) Composition diagrams of sodium versus chloride concentrations
11b) by hydrochemical province

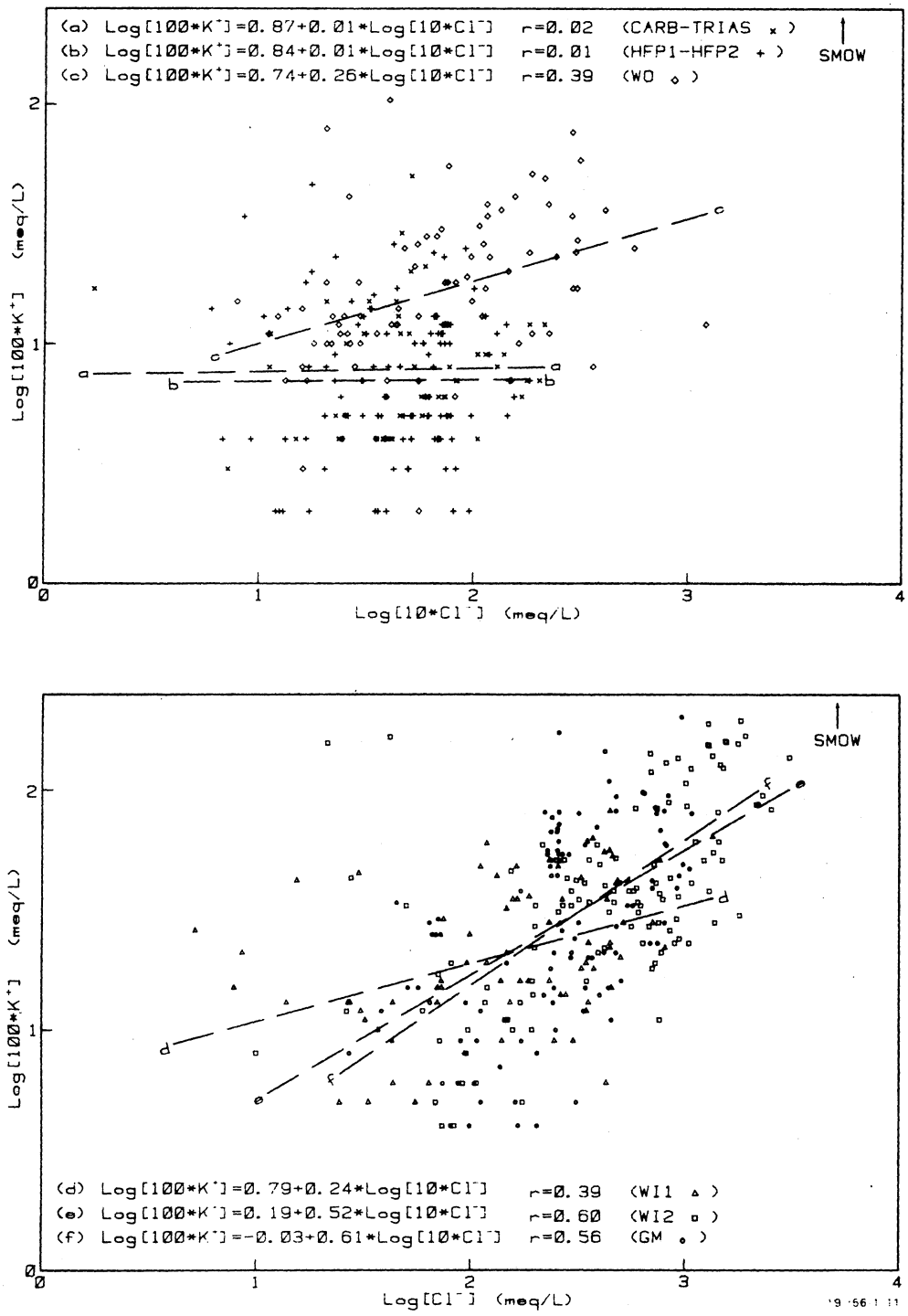

Record 1987/23

FIG 12a) Composition diagrams of potassium versus chloride
12b) concentrations by hydrochemical province

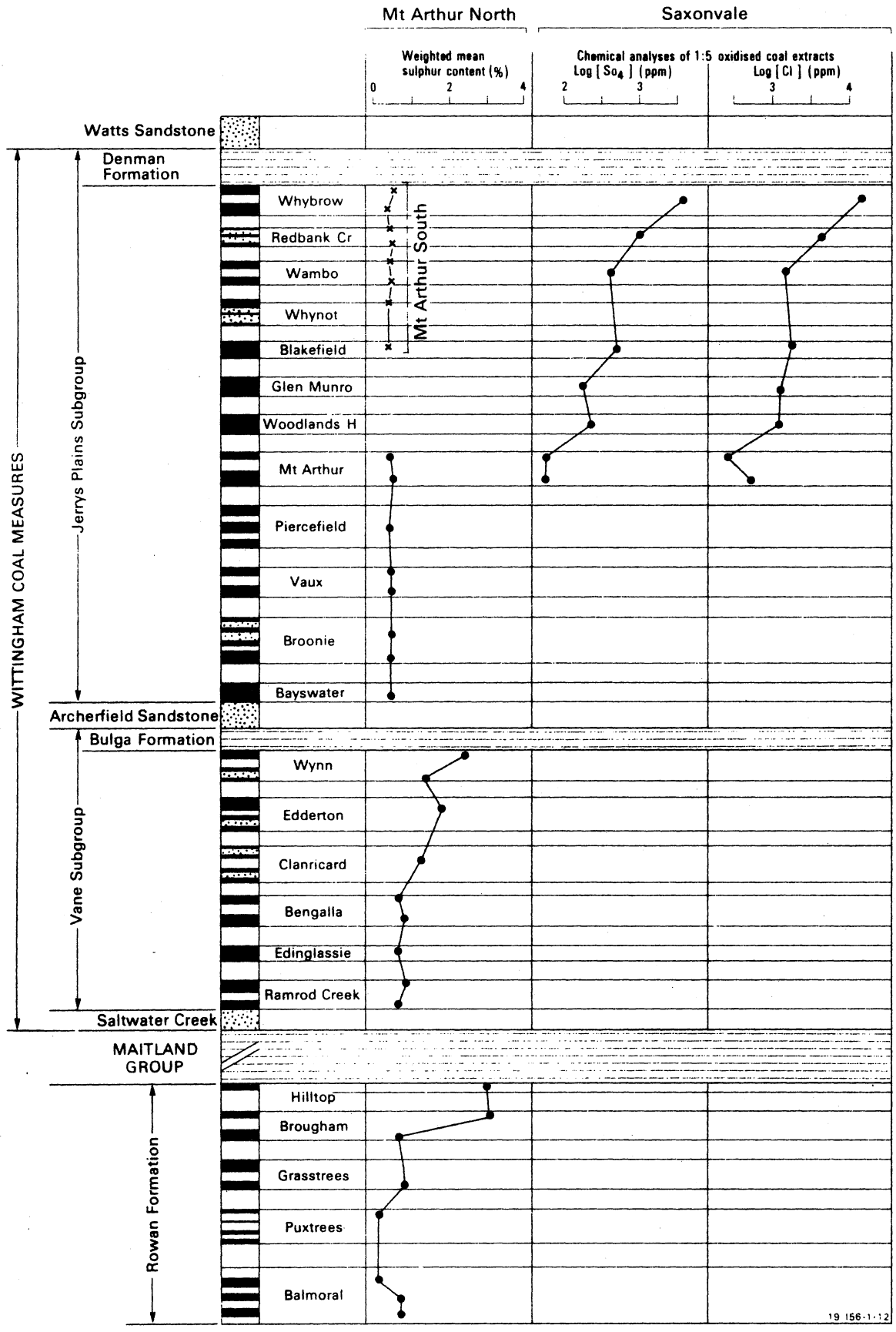

Record 1987/23

FIG 13. Variations in sulphur, sulphate and chloride contents of coal seams from the Wittingham and Greta Coal Measures

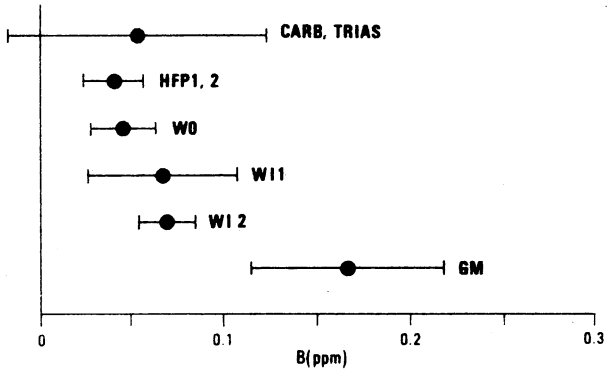

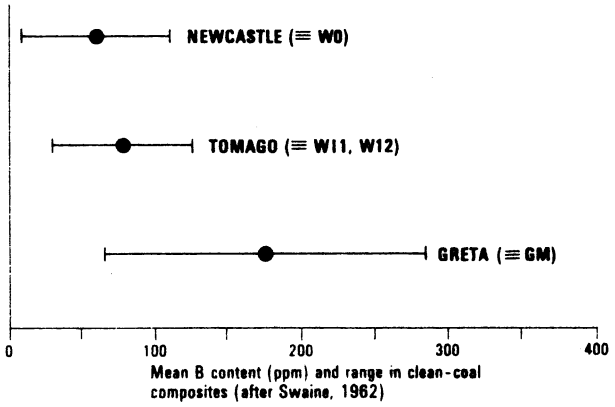

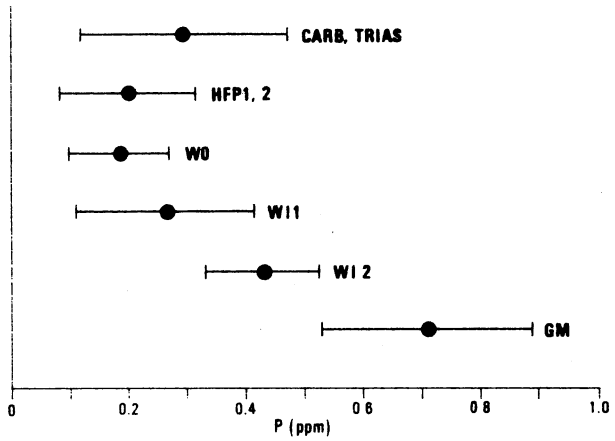

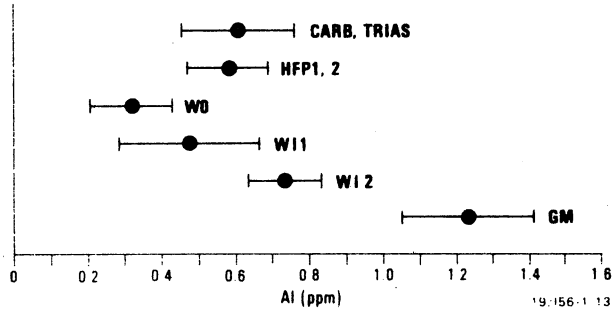

Record 1987/23

FIG 14. Means and ninety-five per cent confidence intervals for B, P and Al concentrations by hydrochemical province

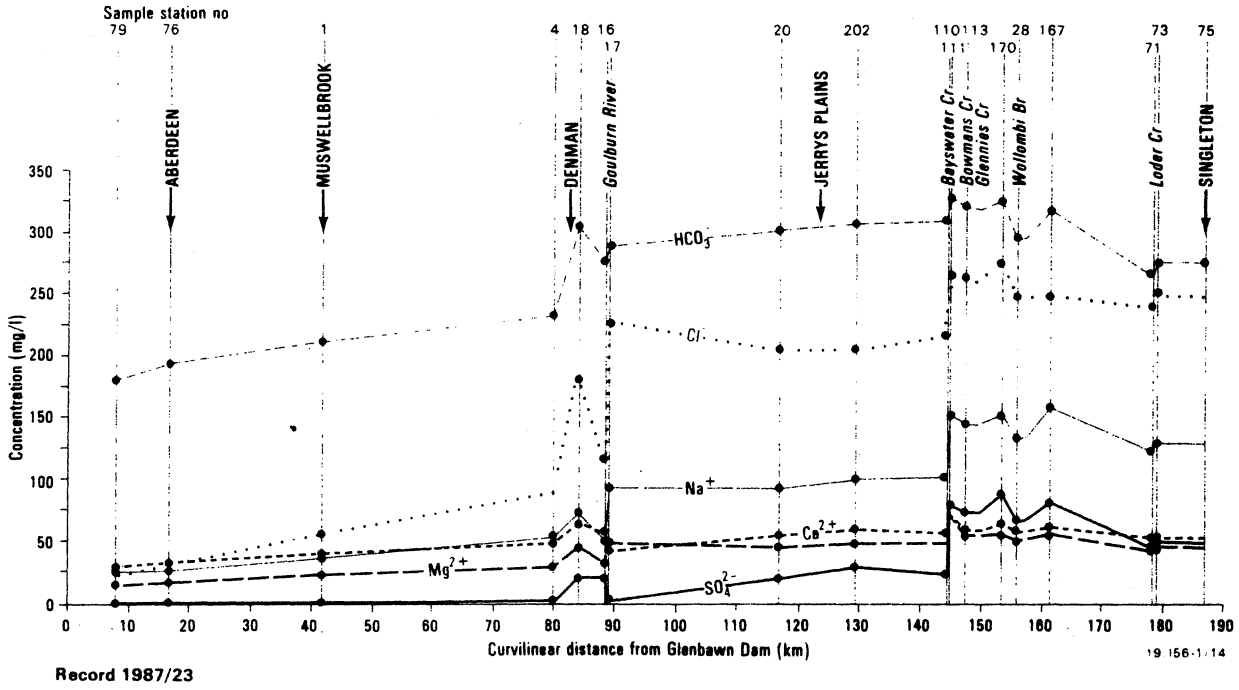

Record 1987/23

FIG 15a Longitudinal variations in concentrations of major ions, Hunter River; August 1982

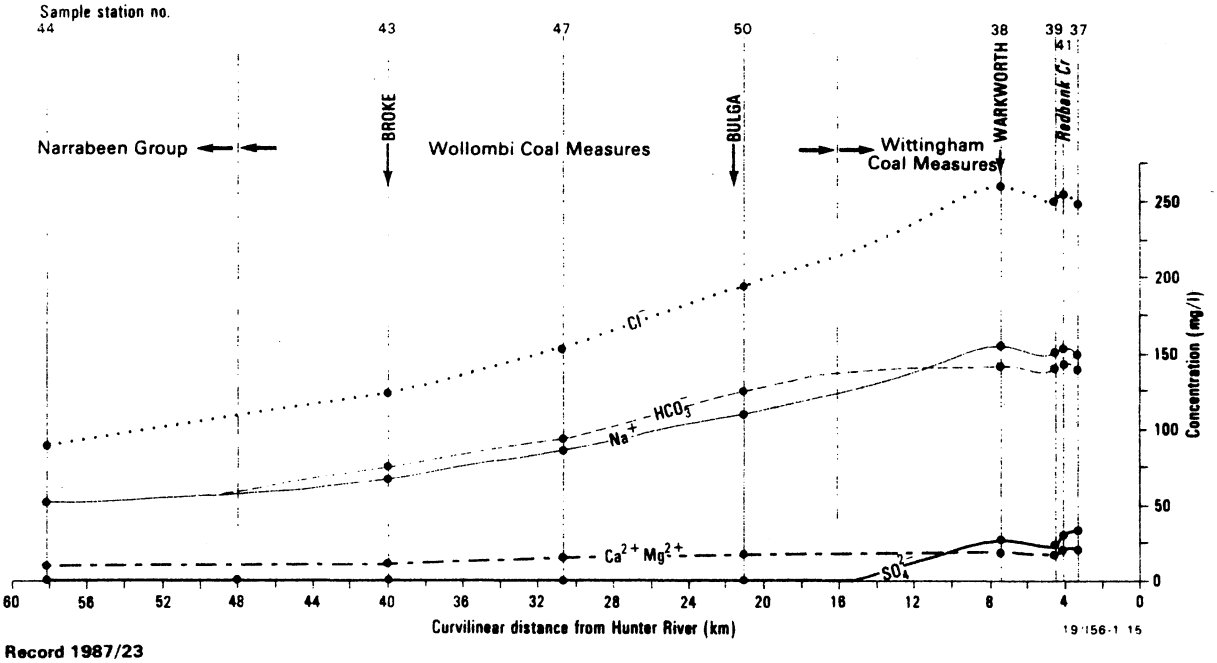

FIG 15b Longitudinal variations in concentrations of major ions, Wollombi Brook; 5, 6/8/82

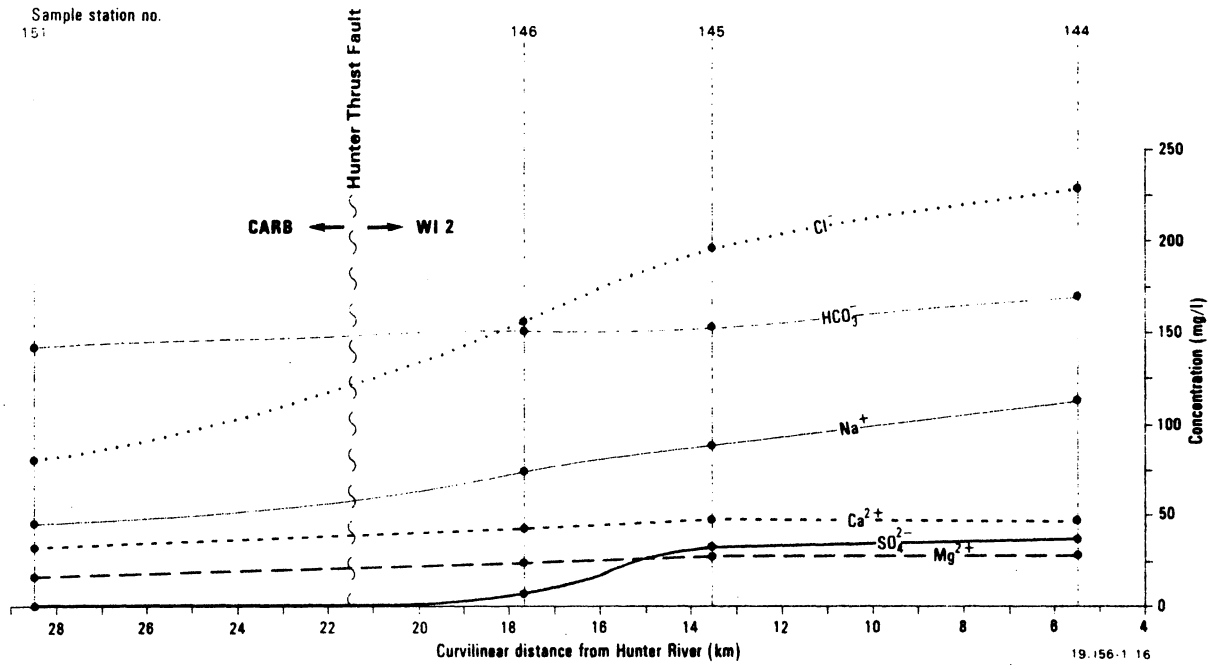

FIG 15c Longitudinal variations in concentrations of major ions, Glennies Creek; 16/8/82

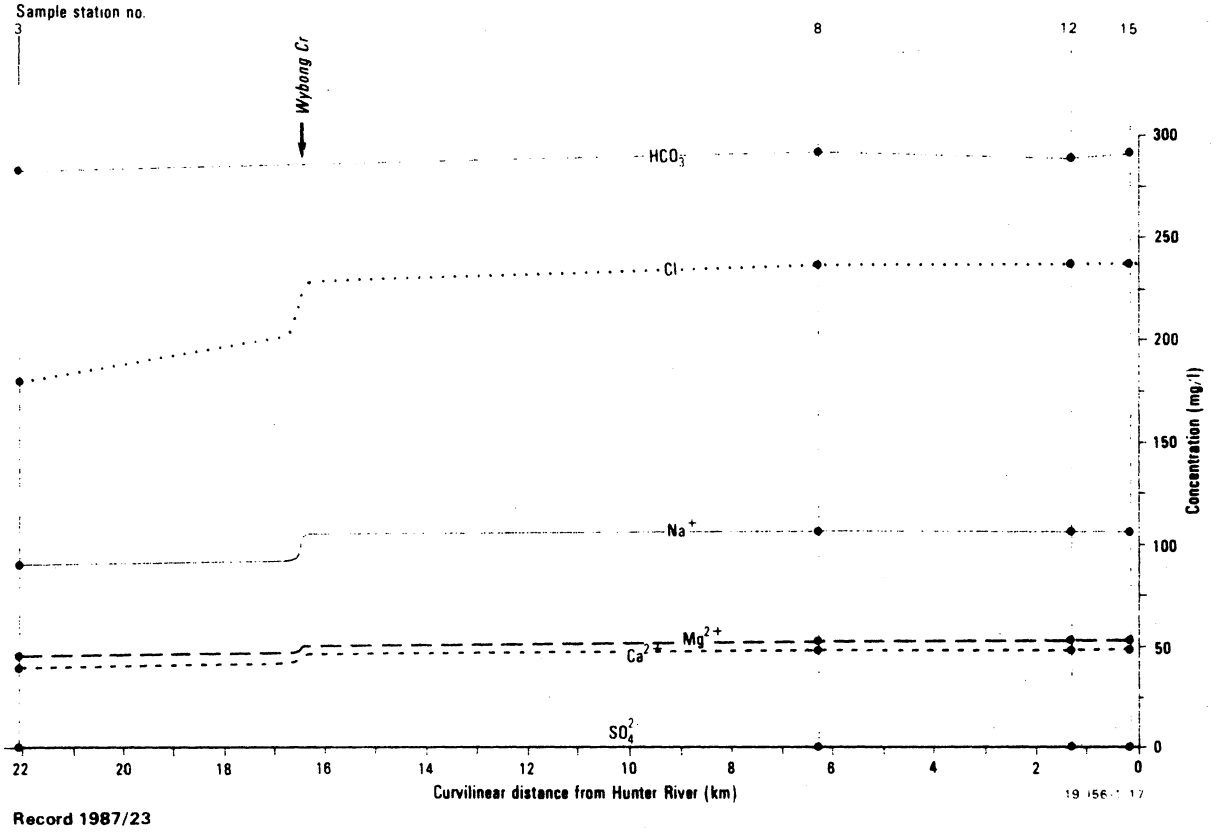

FIG 15d Longitudinal variations in concentrations of major ions, Goulburn River; 3, 4/8/82

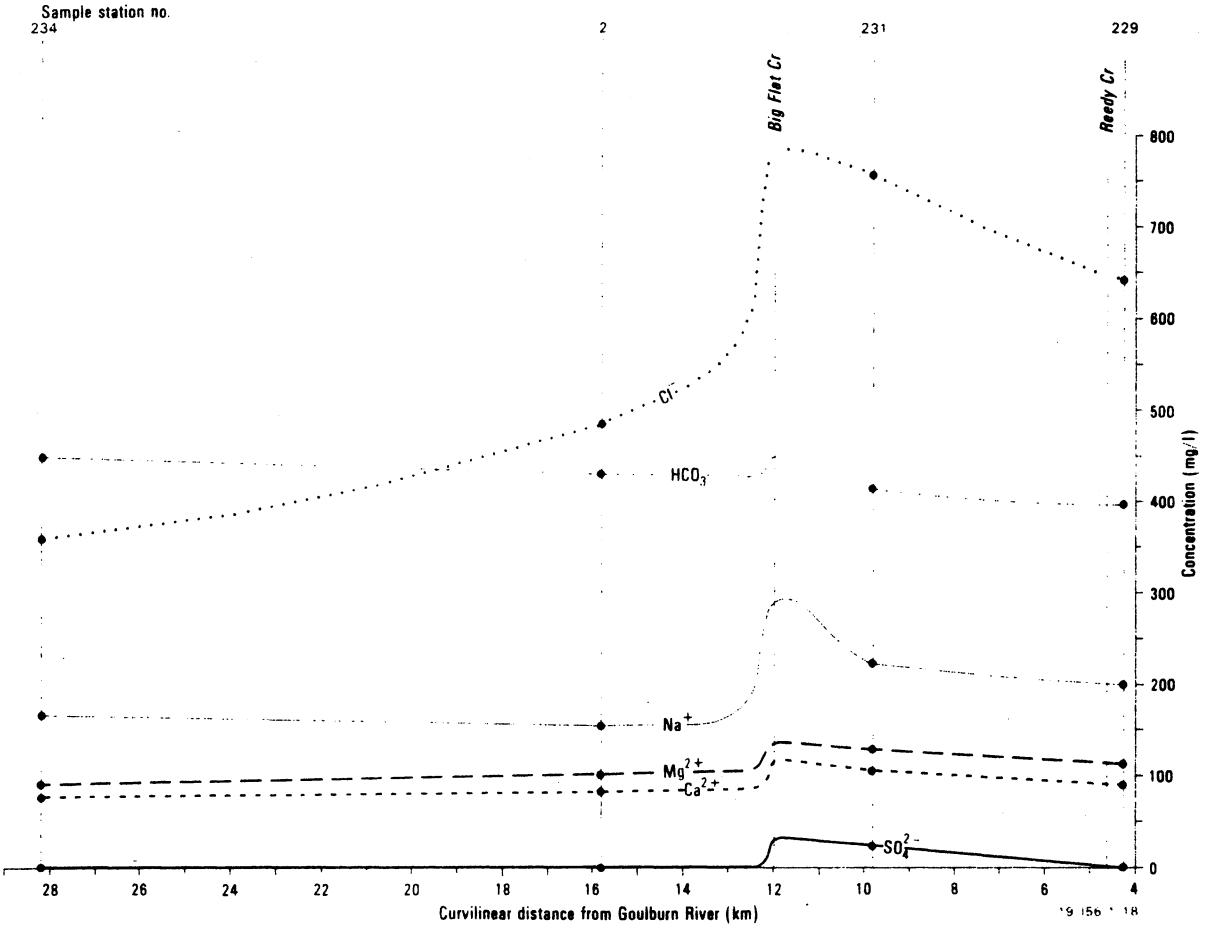

FIG 16a Longitudinal variations in concentrations of major ions, Wybong Creek; August 1982

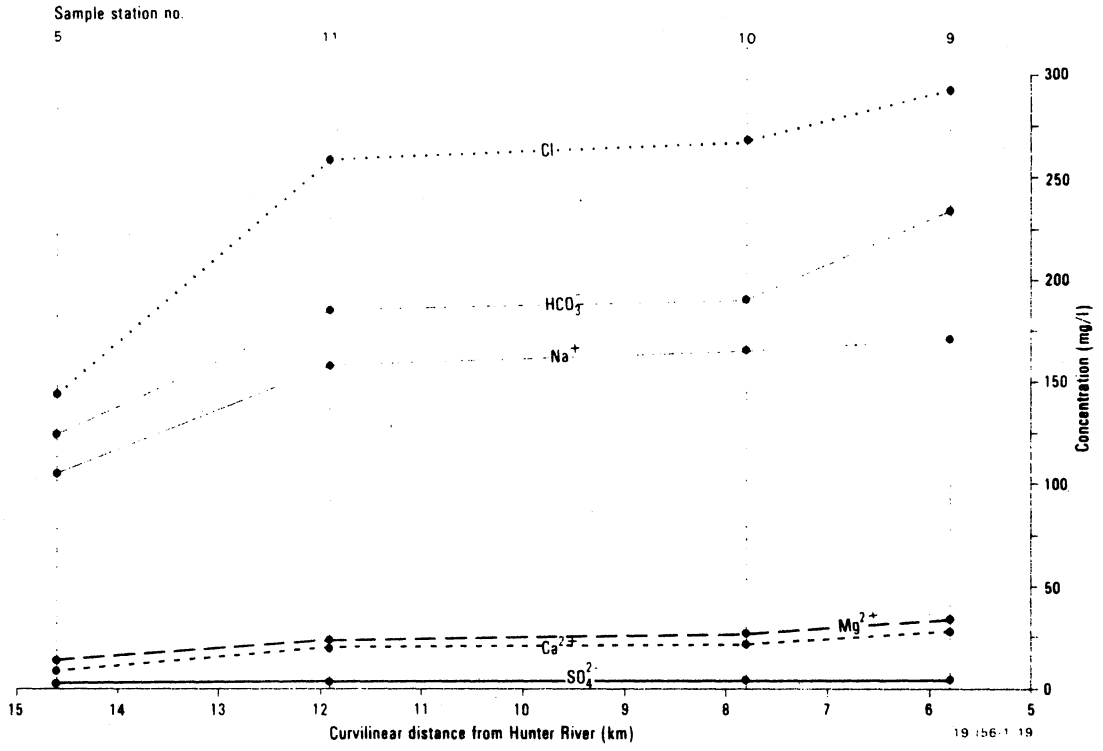

Record 1987/23

FIG 16b Longitudinal variations in concentrations of major ions, Martindale Creek; 4/8/82

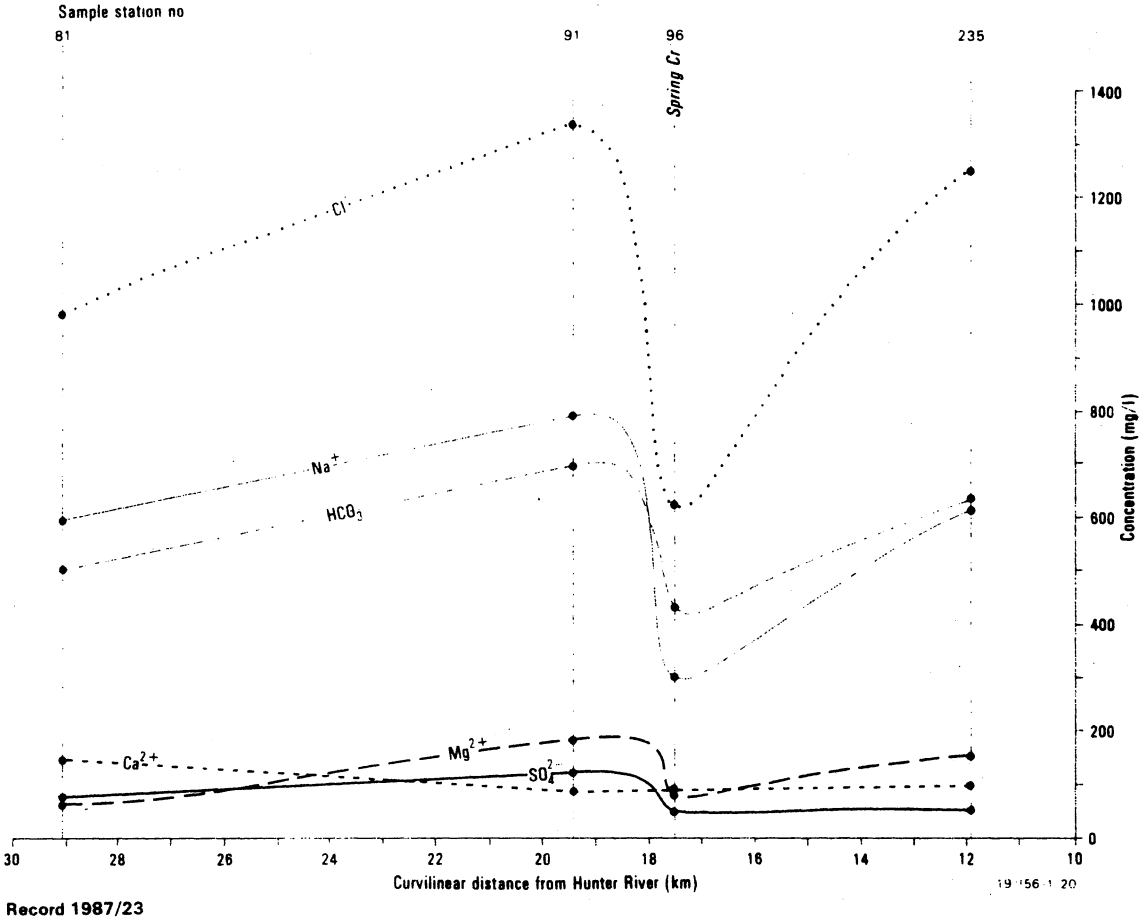

FIG 16c Longitudinal variations in concentrations of major ions, Sandy Creek; August 1982

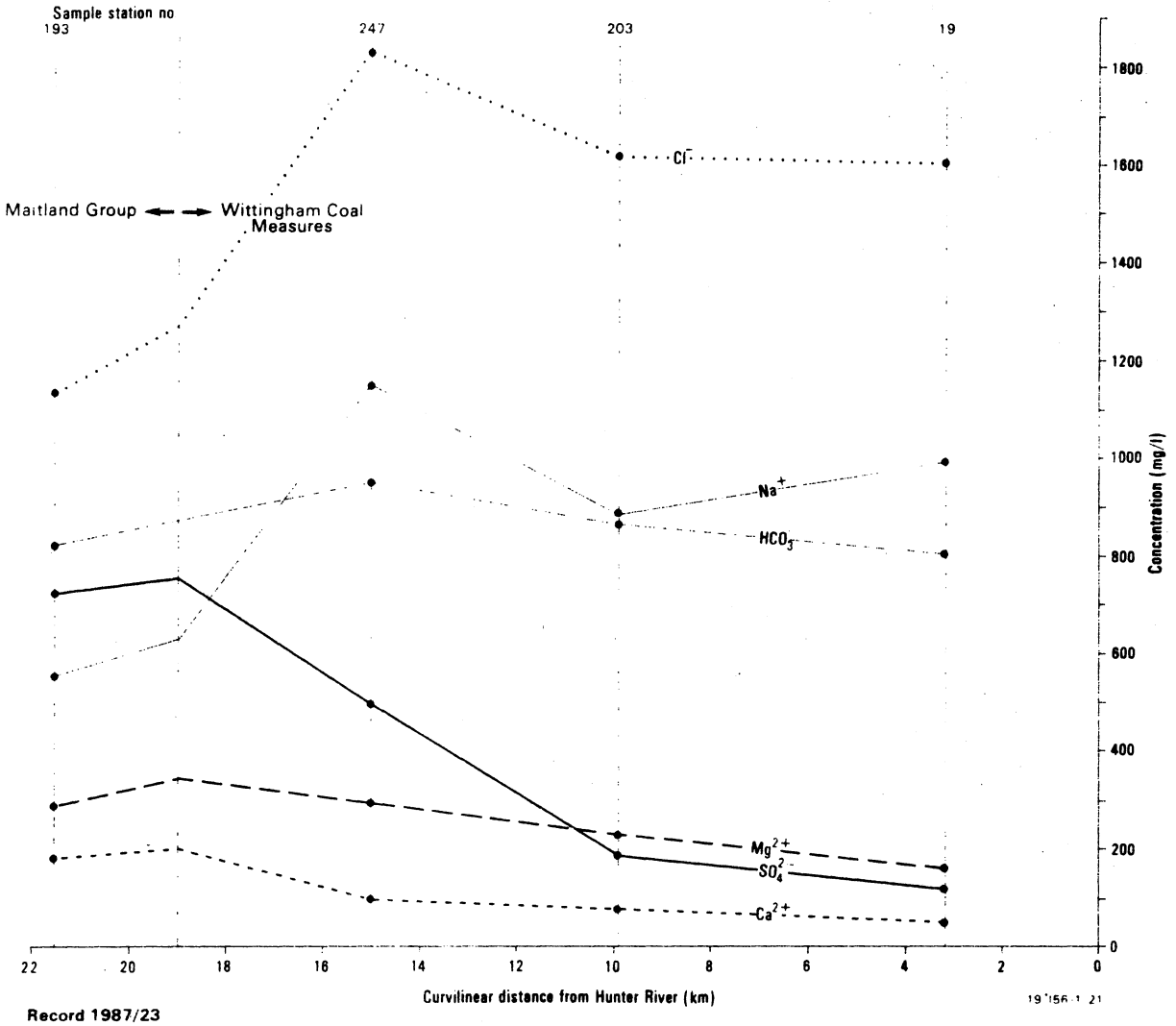

FIG 17a Longitudinal variations in concentrations of major ions, Saddlers Creek; 13-18/8/82

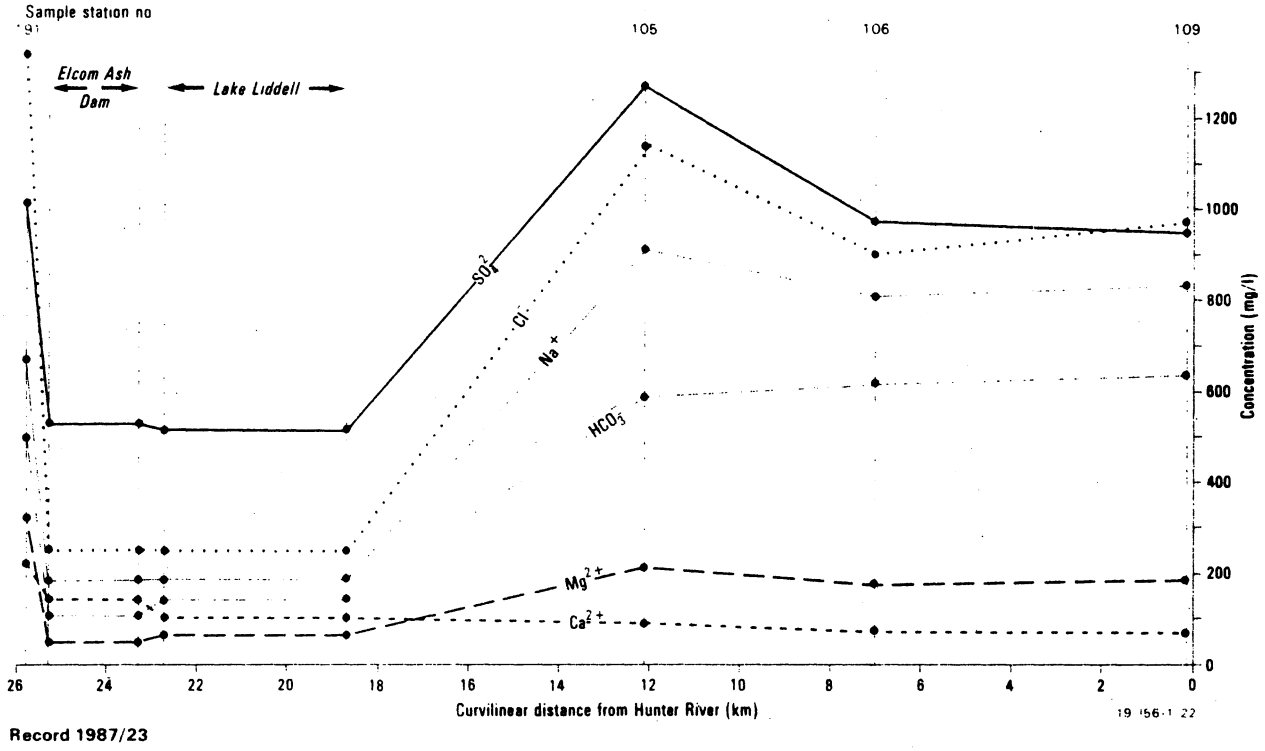

FIG 17b Longitudinal variations in concentrations of major ions, Baywater Creek; 13-18/8/82

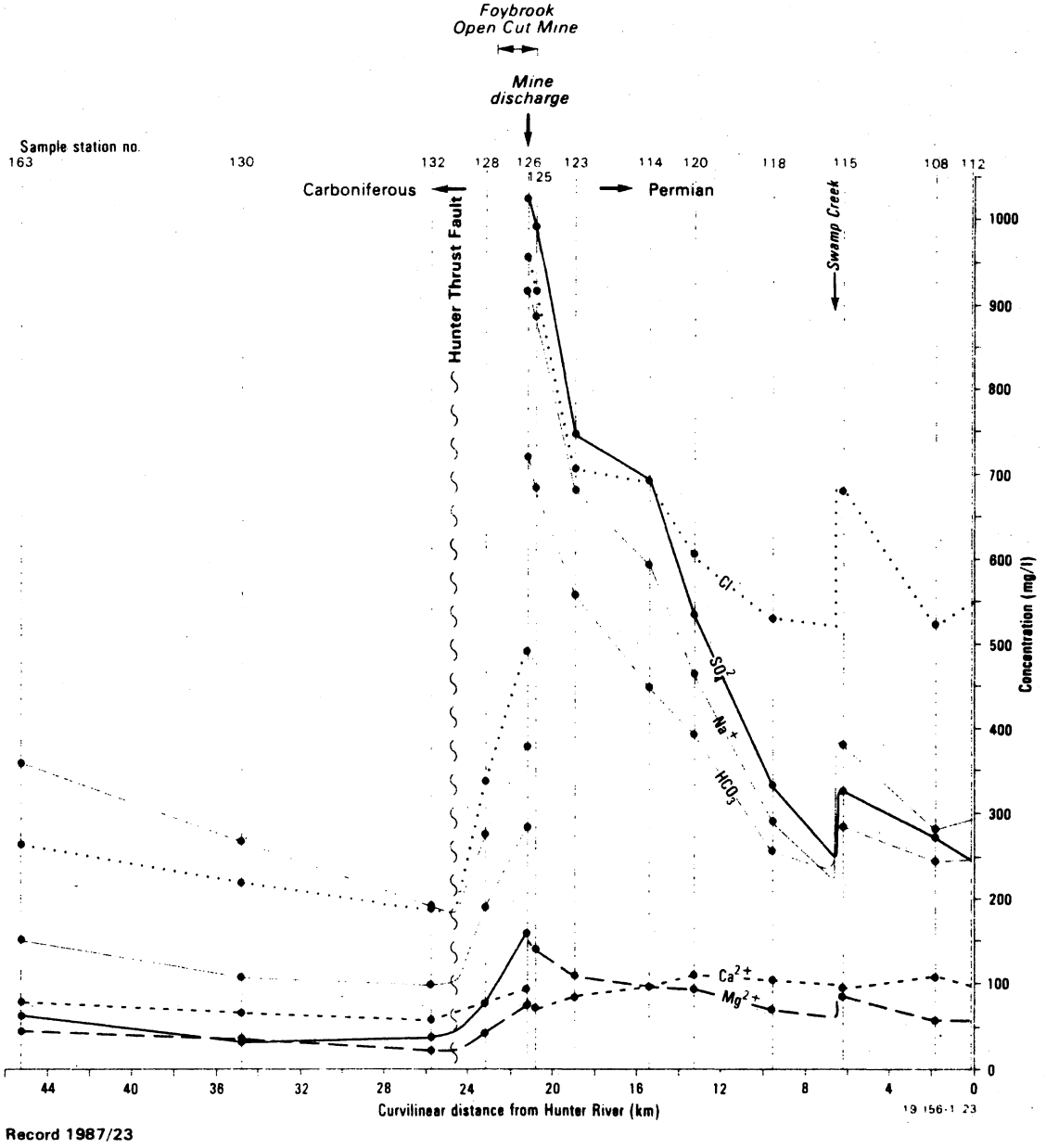

FIG 18a Longitudinal variations in concentrations of major ions, Bowmans Creek; 13, 14/8/82

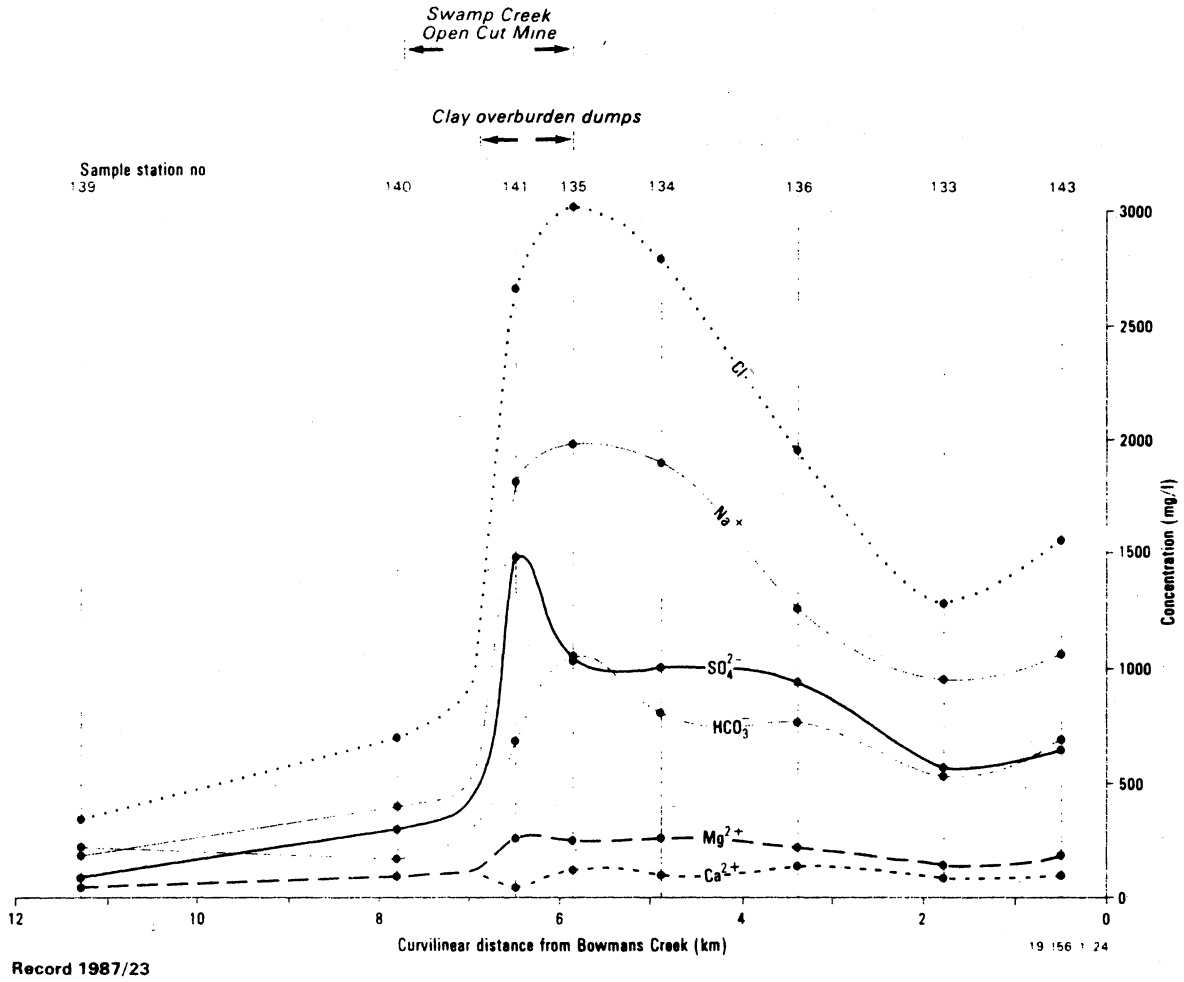

Record 1987/23

FIG 18b Longitudinal variations in concentrations of major ions, Swamp Creek; 15/8/82

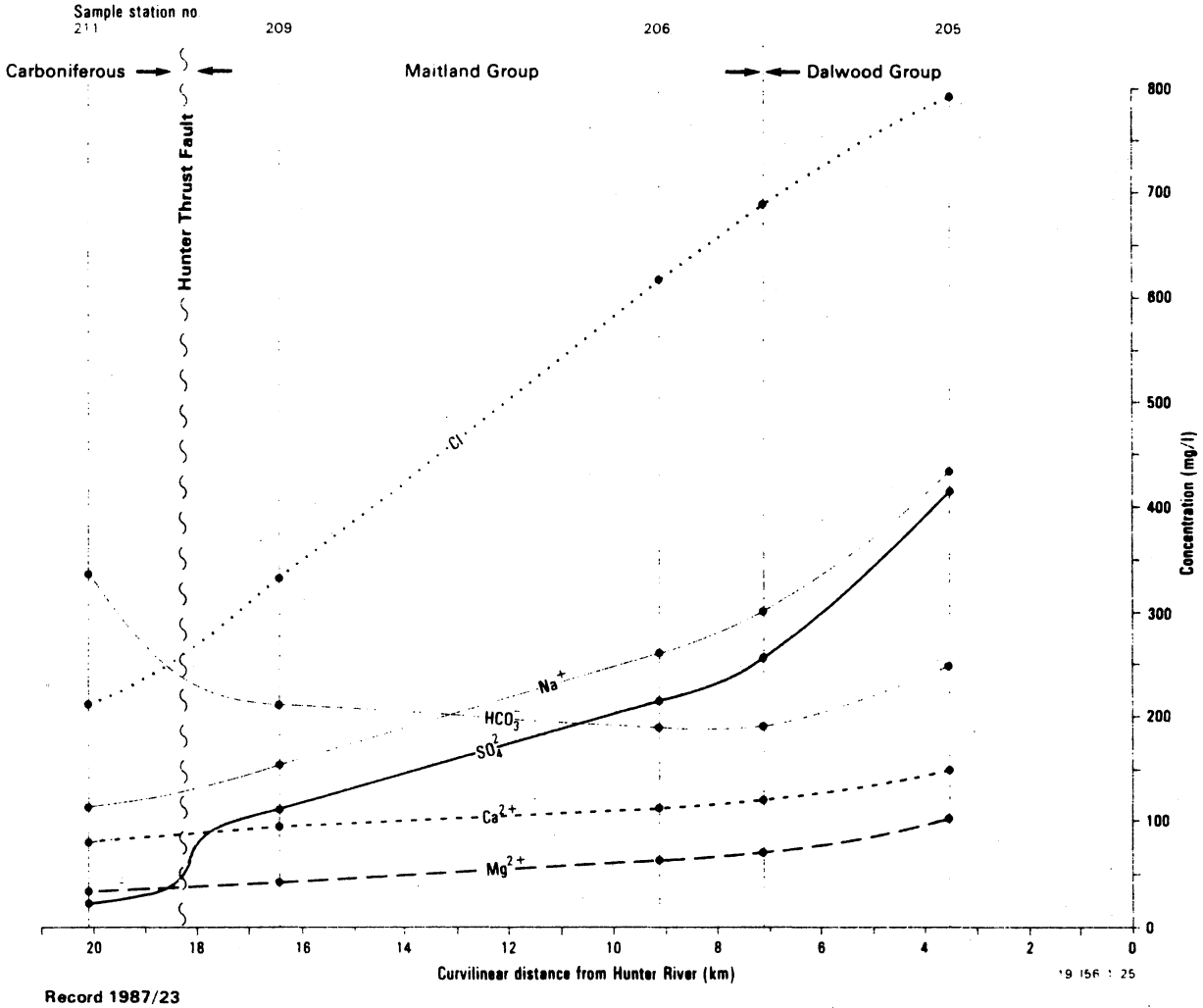

FIG 18c Longitudinal variations in concentrations of major ions, Muscle Creek; 20/8/82

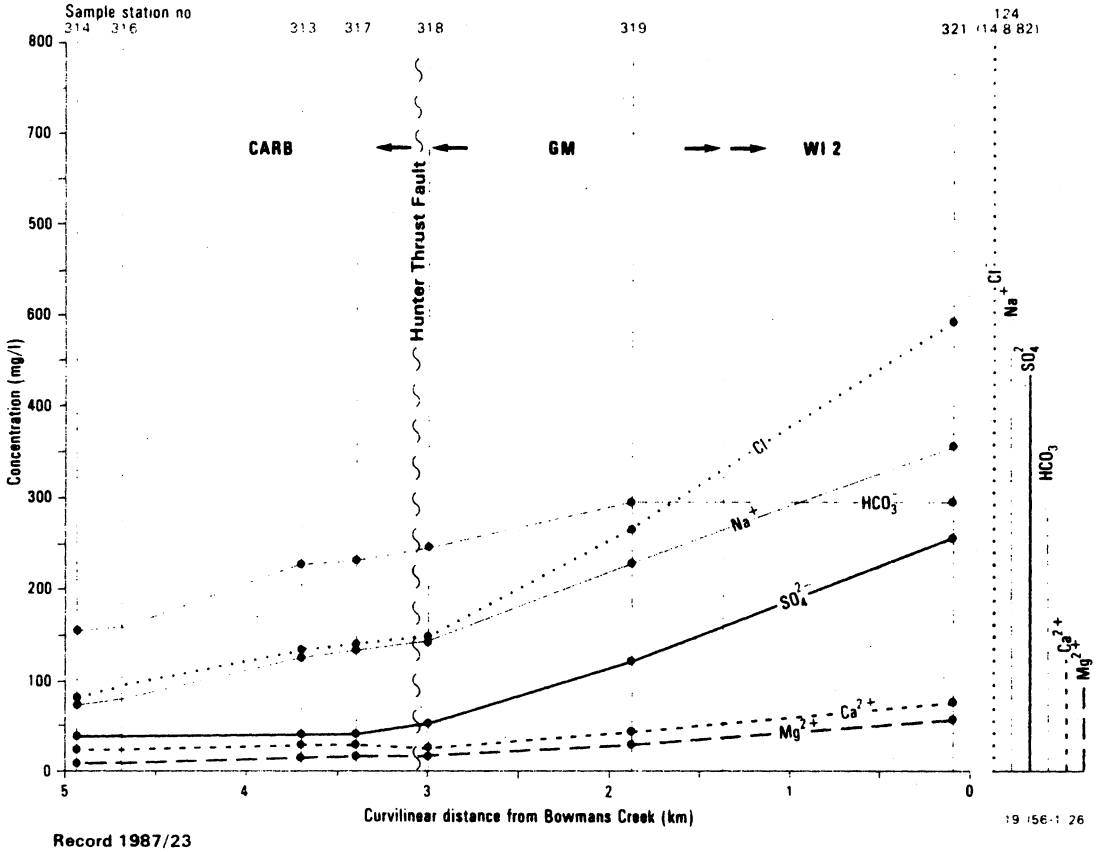

FIG 18d Longitudinal variation in concentrations of major ions, Stringybark Creek; 20/6/83

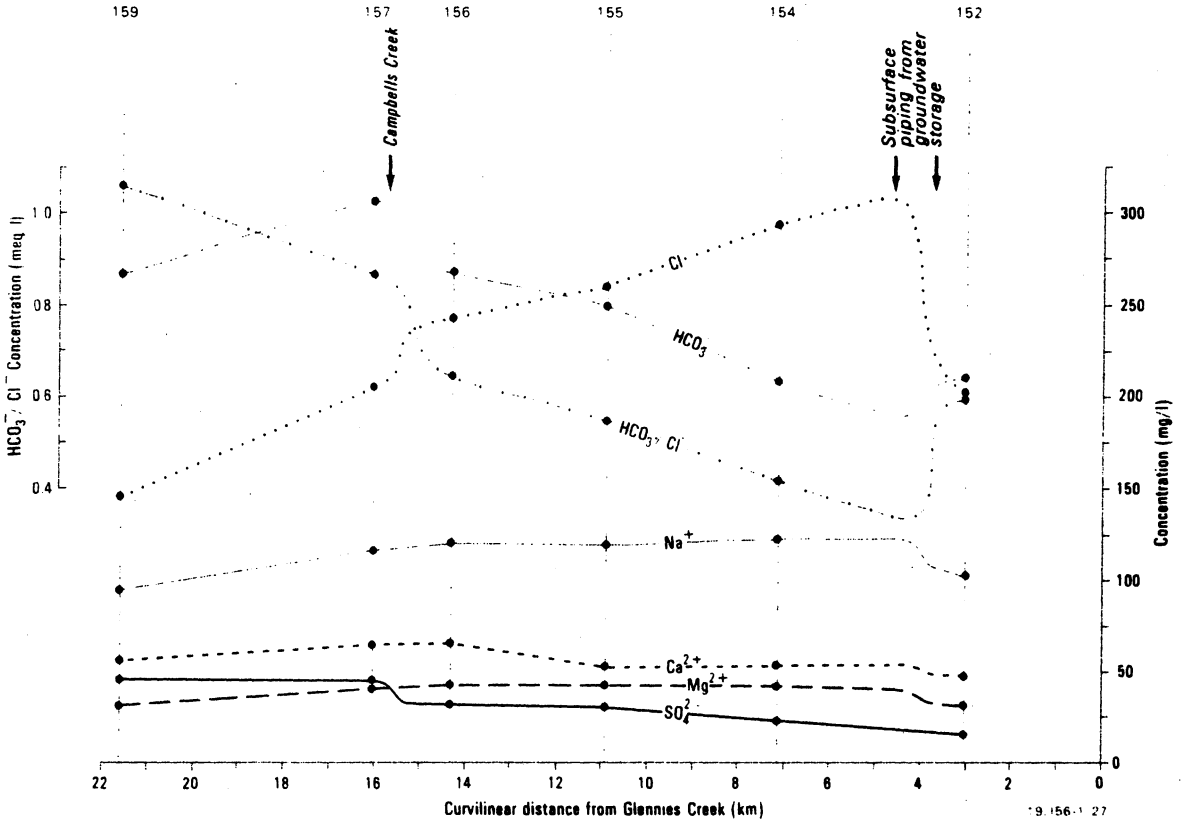

FIG 18e Longitudinal variations in concentrations of major ions and decline in HCO_3^-/Cl^- ratio, Goorangoola Creek; 16/8/82

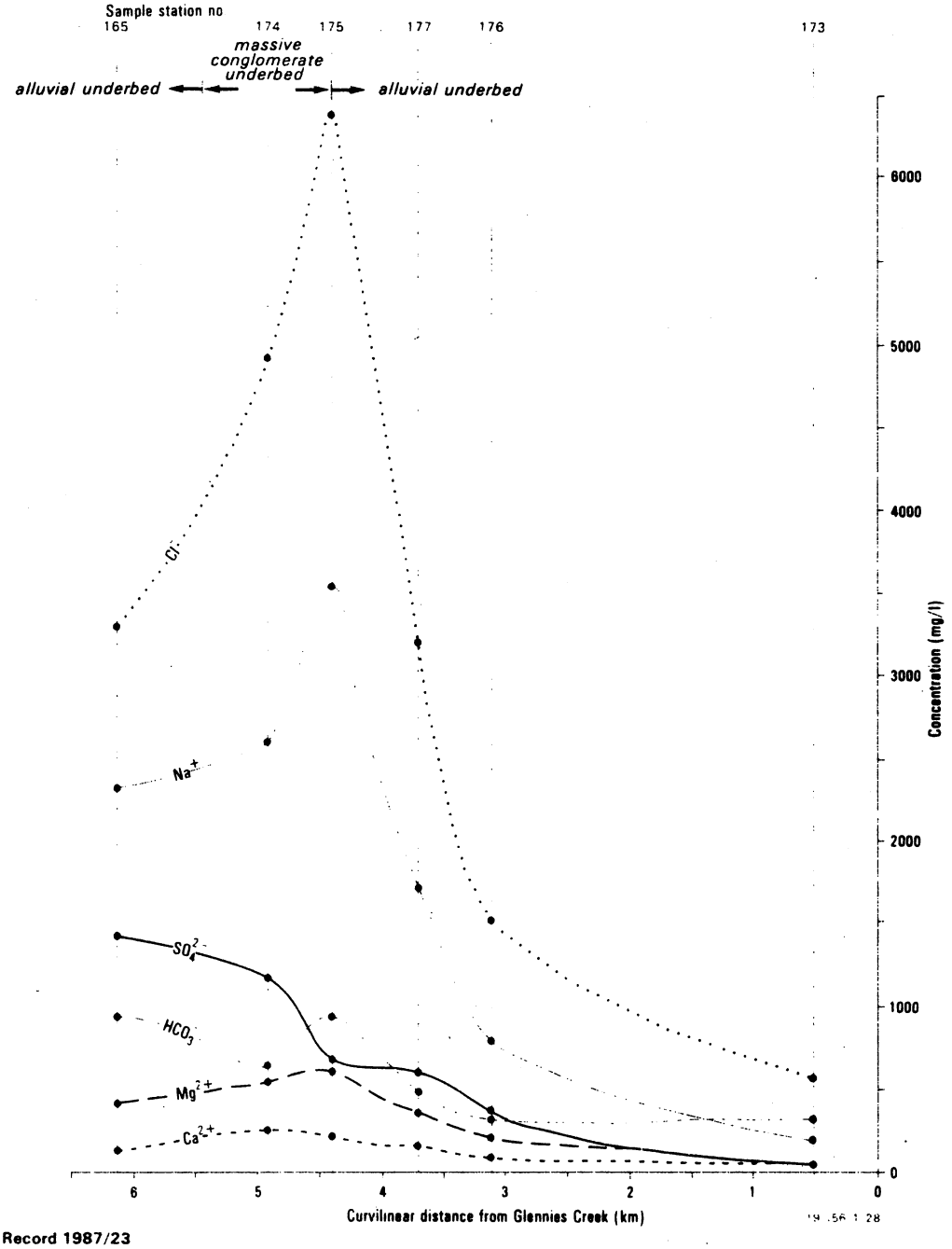

Record 1987/23

FIG 19a Longitudinal variations in concentrations of major ions, Main Creek; 17/8/82

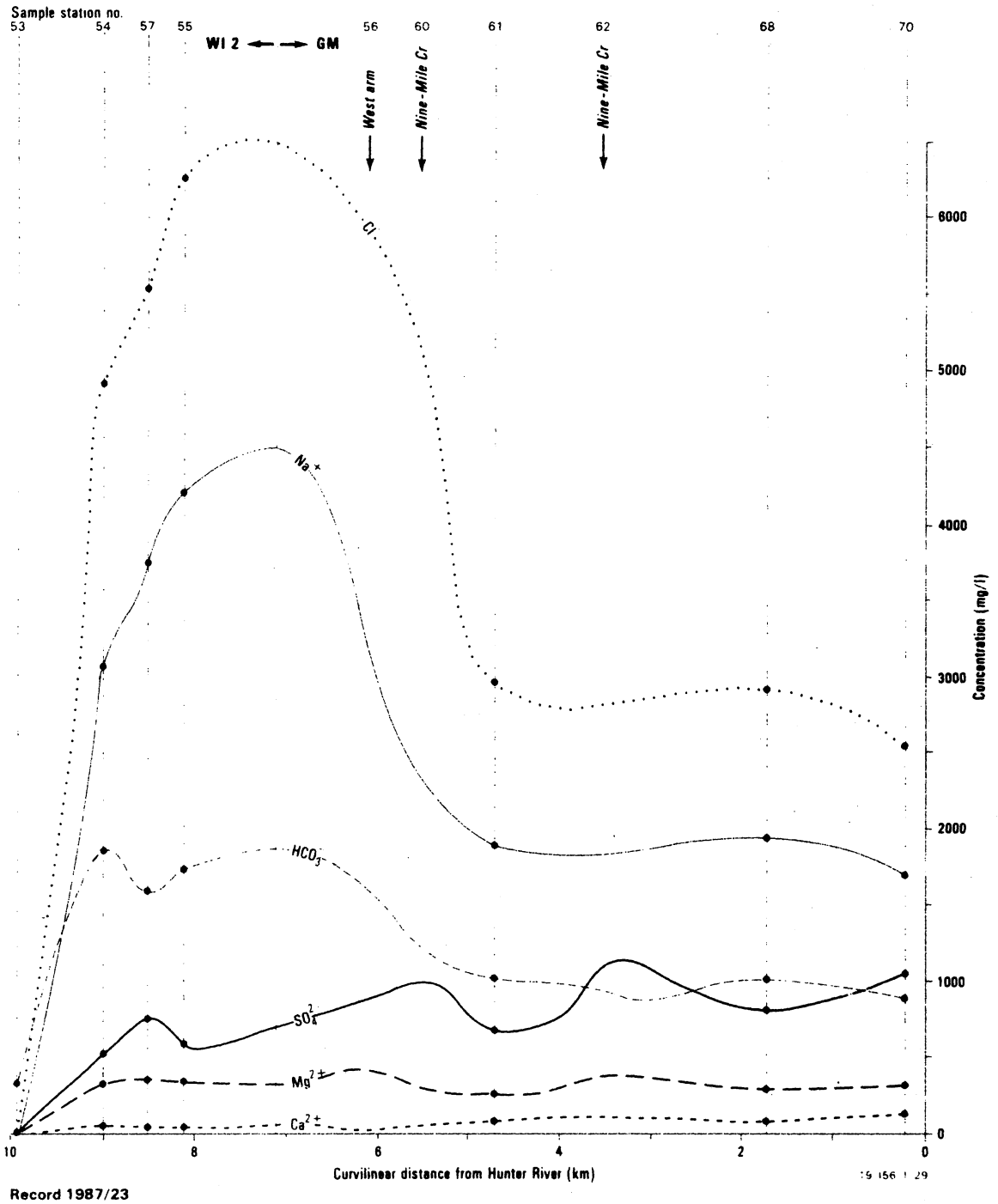

FIG 19b Longitudinal variations in concentrations of major ions, Loder Creek; 9, 10/8/82

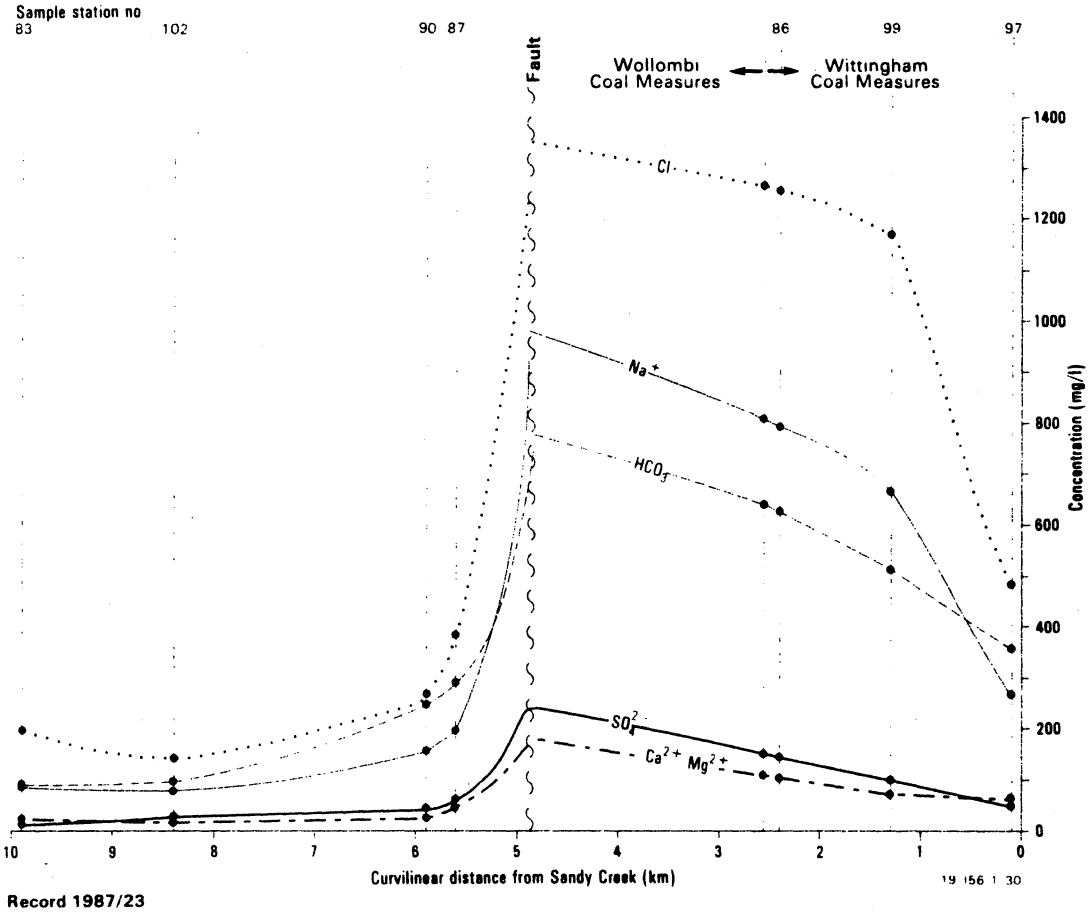

FIG 20a Longitudinal variations in concentrations of major ions, Spring Creek; 11-12/8/82

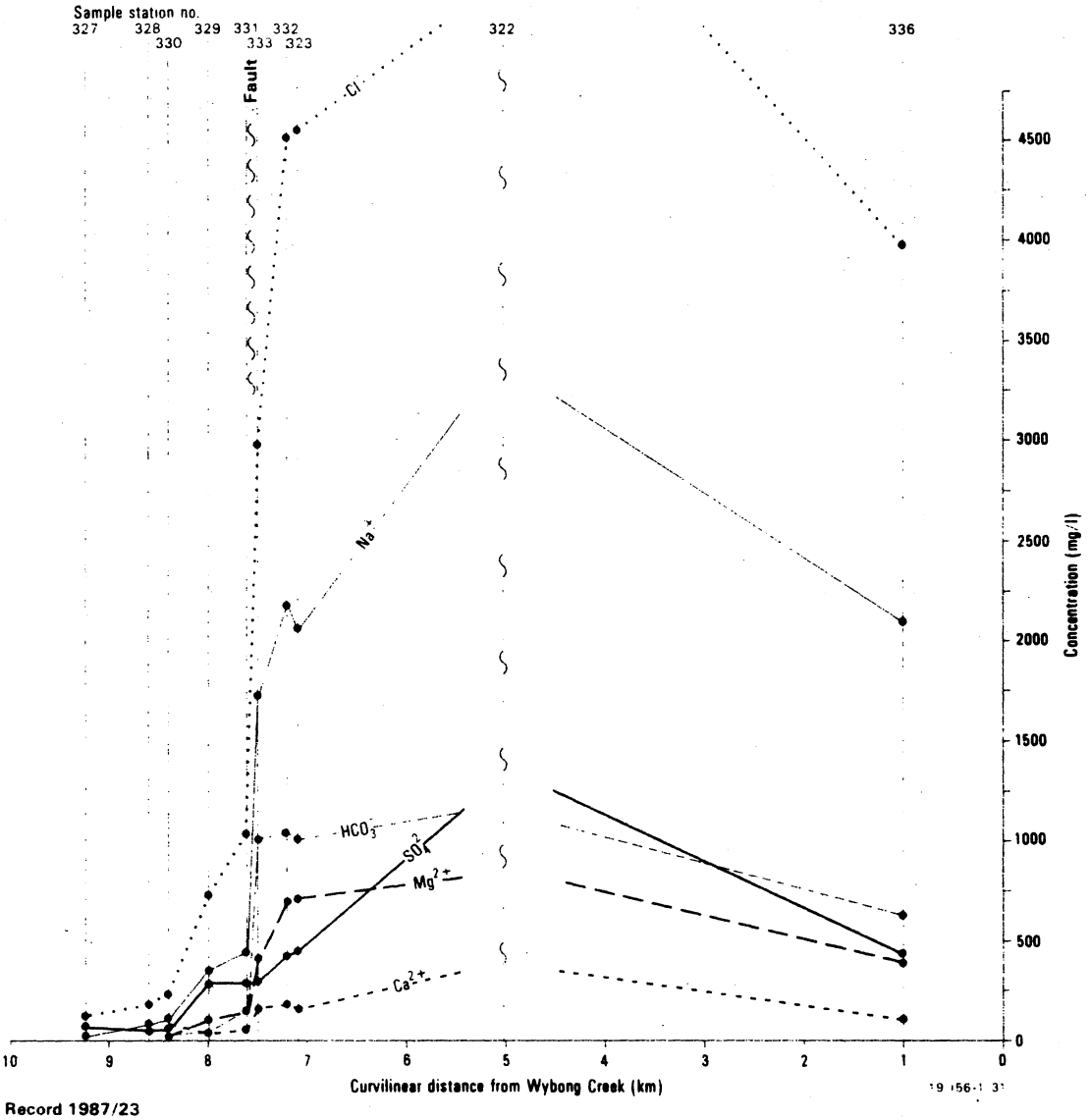

FIG 20b Longitudinal variations in concentrations of major ions, Big Flat Creek; 29/6/83

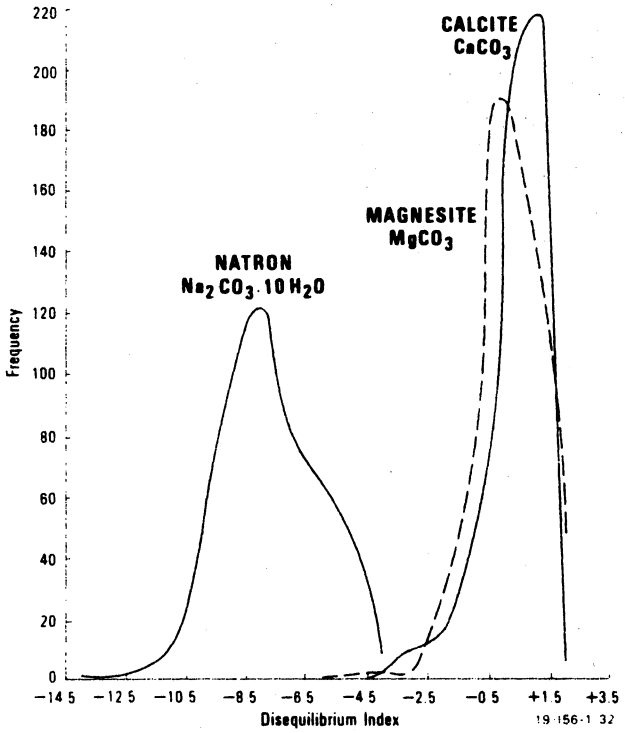

Record 1987/23

FIG 21. Distribution of Disequilibrium Indices for the simple carbonate minerals calcite, magnesite and natron in Upper Hunter groundwaters

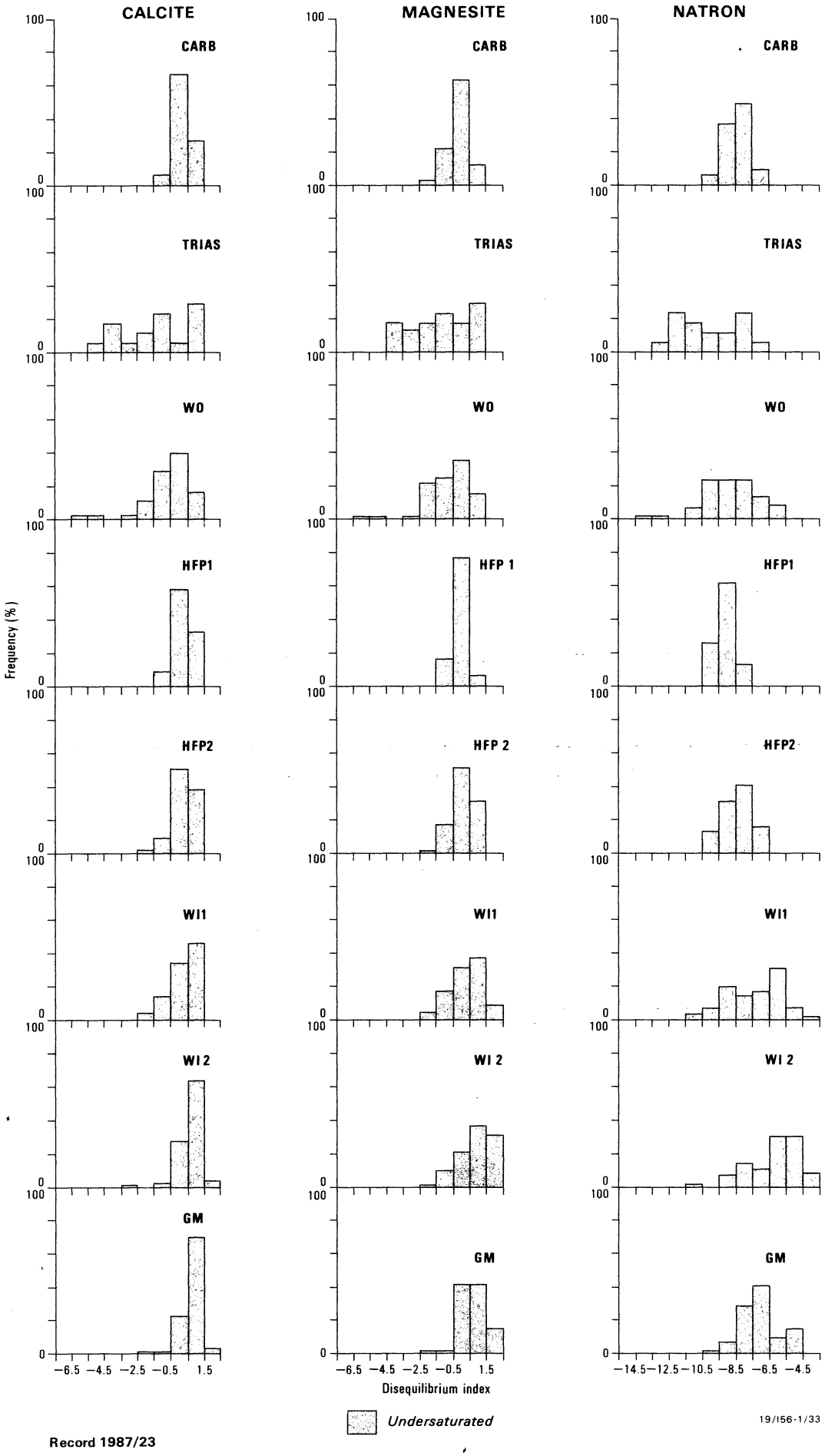

Record 1987/23

FIG 22 Distribution of calcite, magnesite and natron Disequilibrium Indices by hydrochemical province

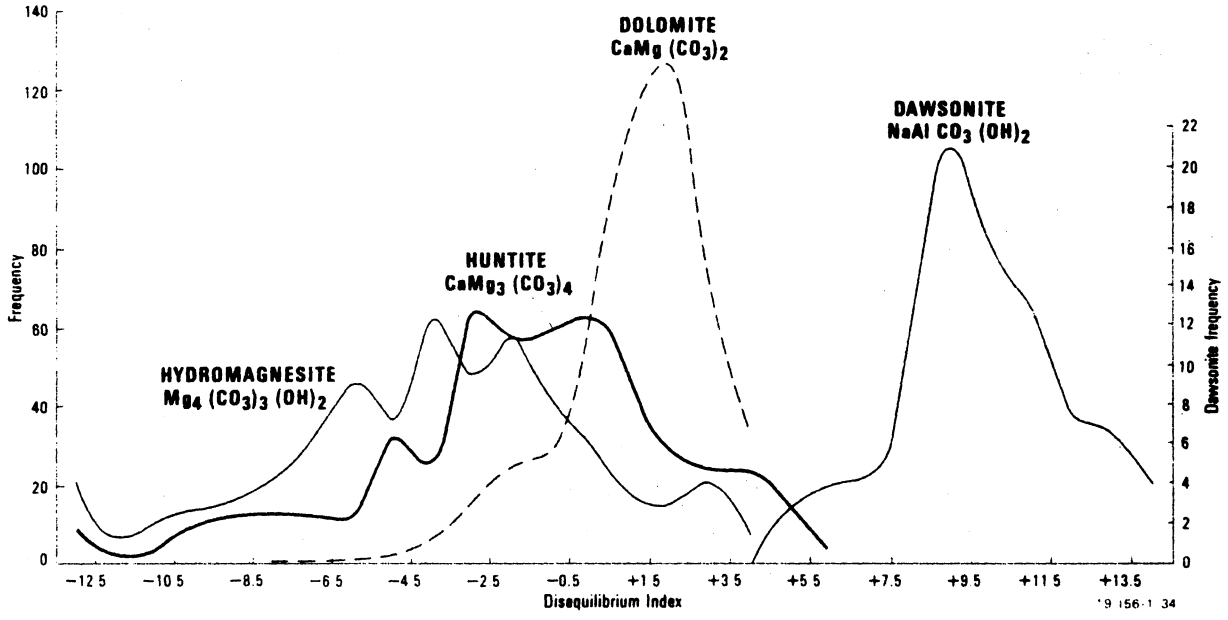

Record 1987/23

FIG 23. Distribution of Disequilibrium Indices for the complex carbonate minerals dawsonite, dolomite, huntite and hydromagnesite in upper Hunter Valley groundwaters.

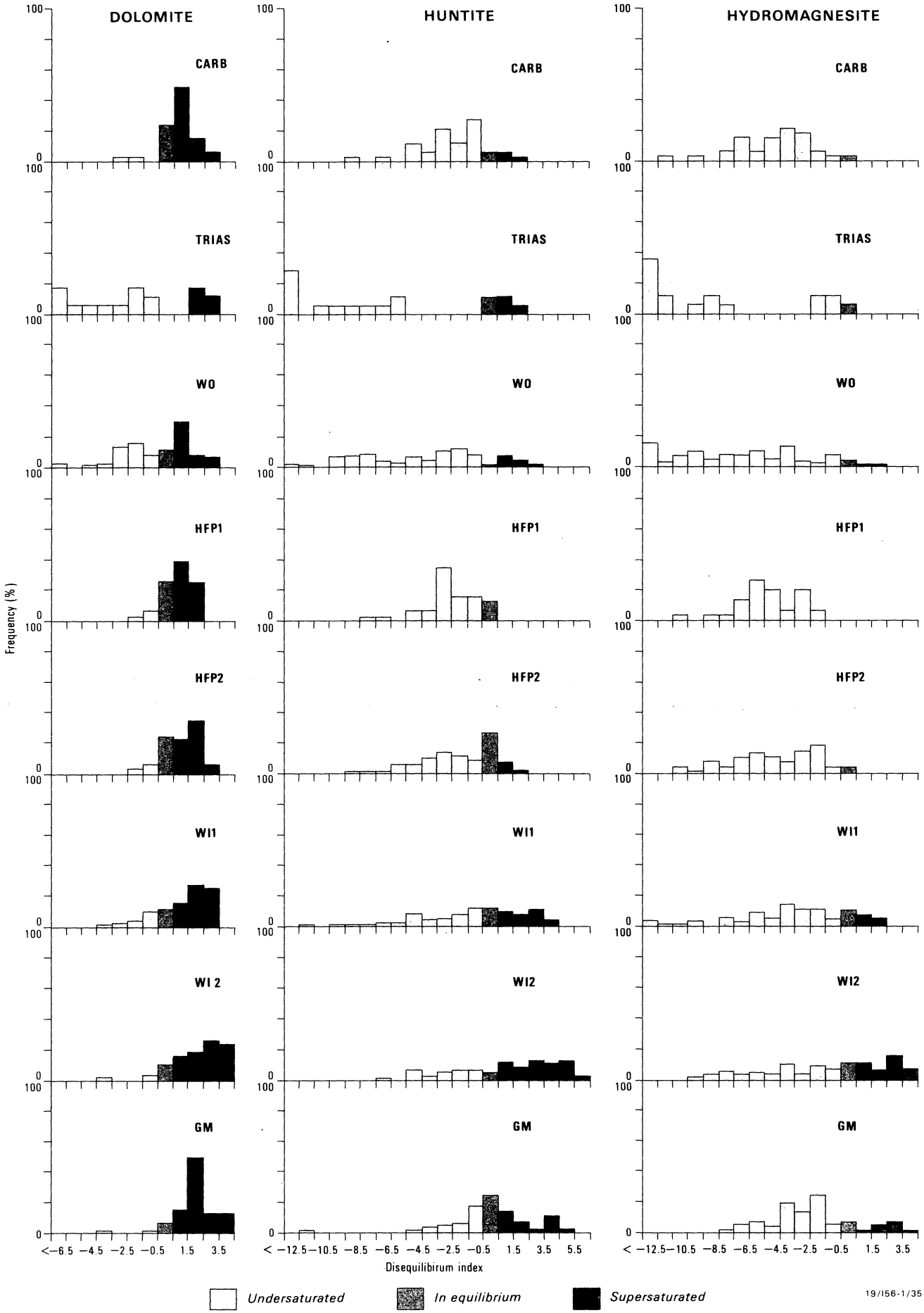

Record 1987/23

FIG 24. Distribution of dolomite, huntite and hydromagnesite Disequilibrium Indices by hydrochemical province

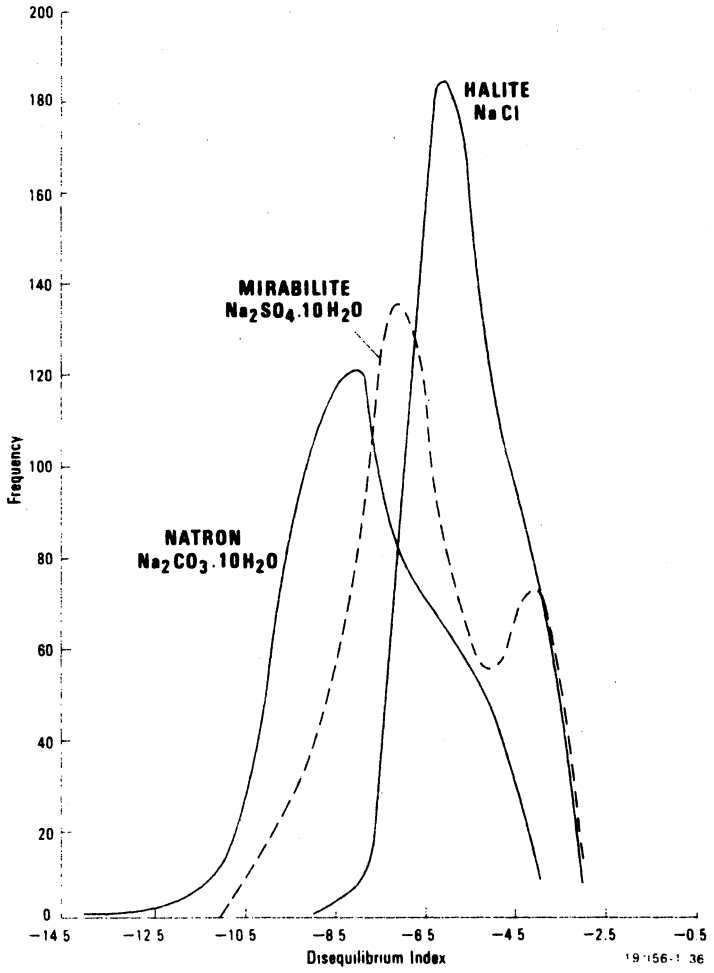

Record 1987/23

FIG 25. Distribution of Disequilibrium Indices for the simple sodium minerals halite, mirabilite and natron in Upper Hunter Valley groundwaters

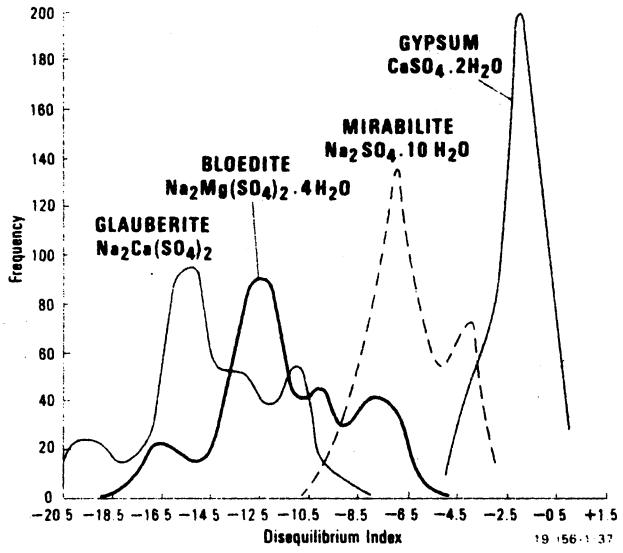

Record 1987/23

FIG 26. Distribution of Disequilibrium Indices for the sulphate minerals gypsum, mirabilite, bloedite and glauberite in upper Hunter Valley groundwaters

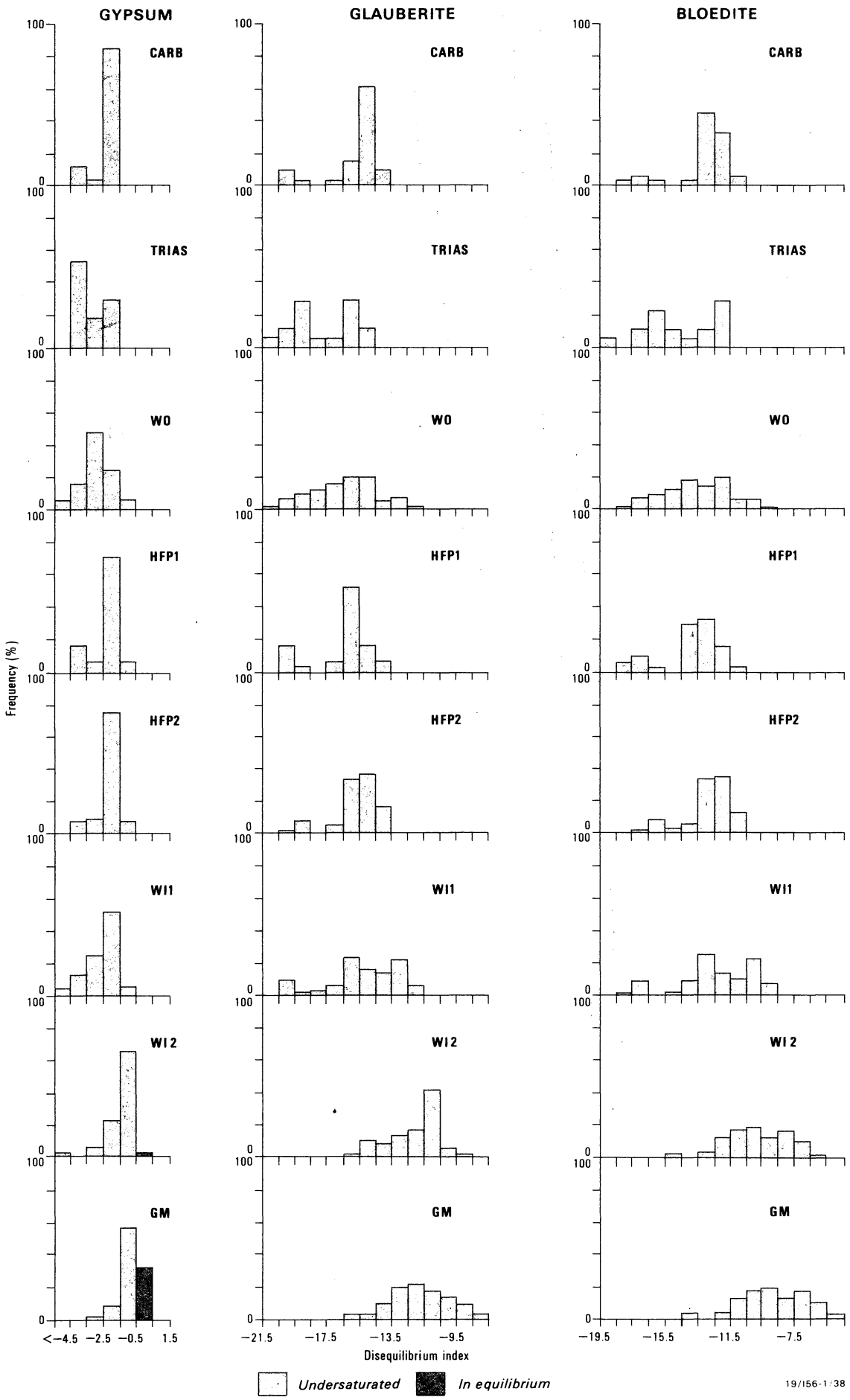

Record 1987/23

FIG 27 Distribution of gypsum, glauberite and bloedite Disquilibrium Indices by hydrochemical province

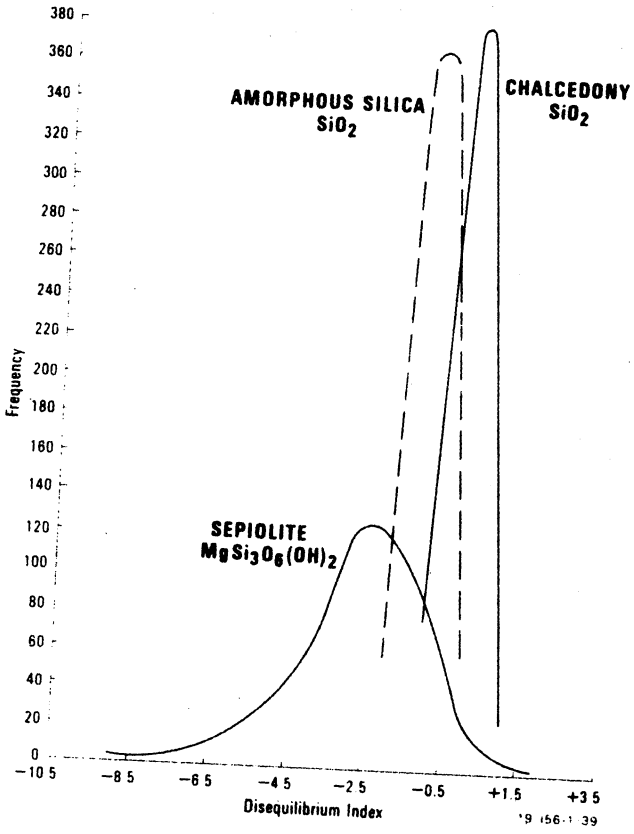

Record 1987/23

FIG 28. Distribution of Disequilibrium Indices for chalcedony, amorphous silica and sepiolite

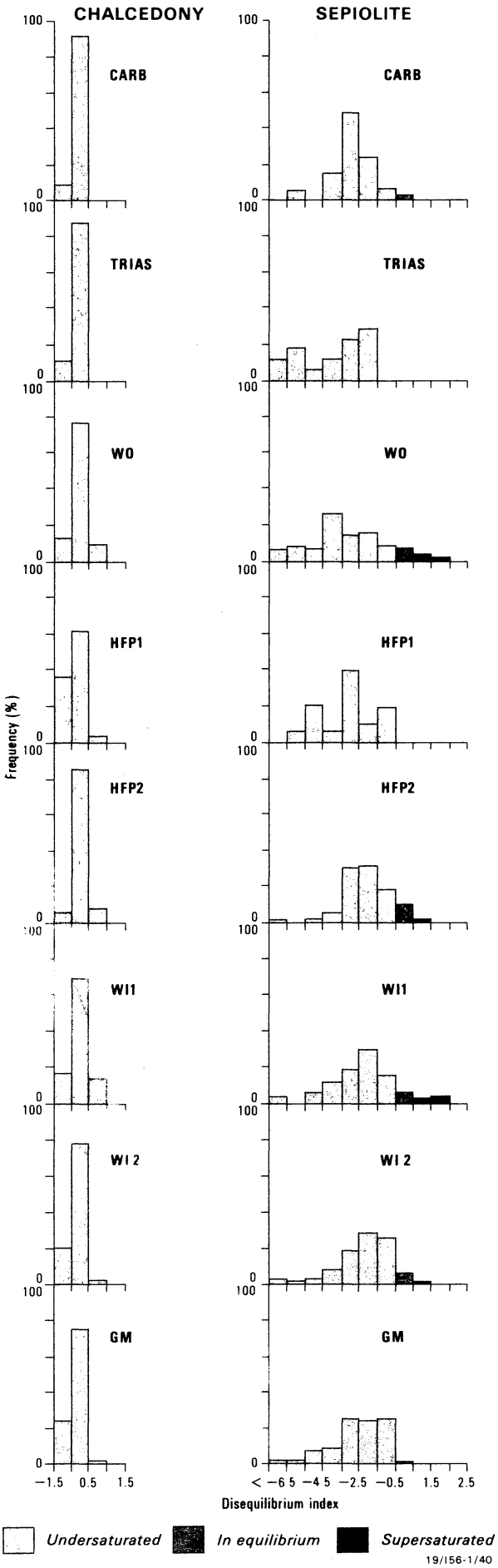

Record 1987/23

FIG 29. Distribution of chalcedony and sepiolite Disequilibrium Indices by hydrochemical province

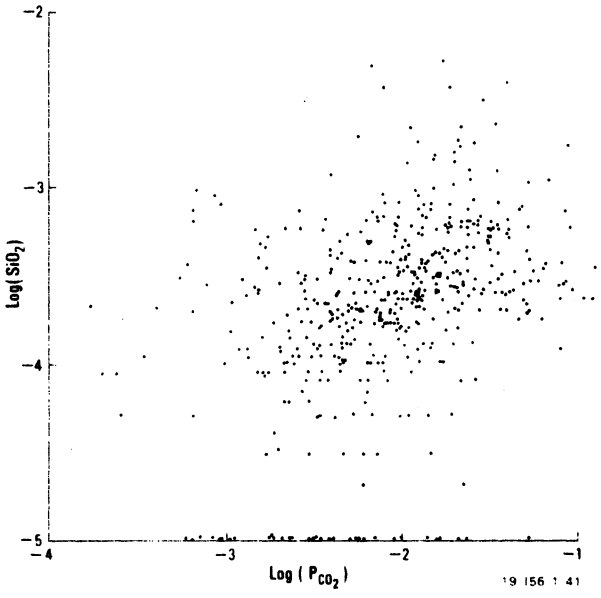

Record 1987/23

FIG 30. Relationship between soluble silica and the groundwater carbon dioxide partial pressure, upper Hunter Valley

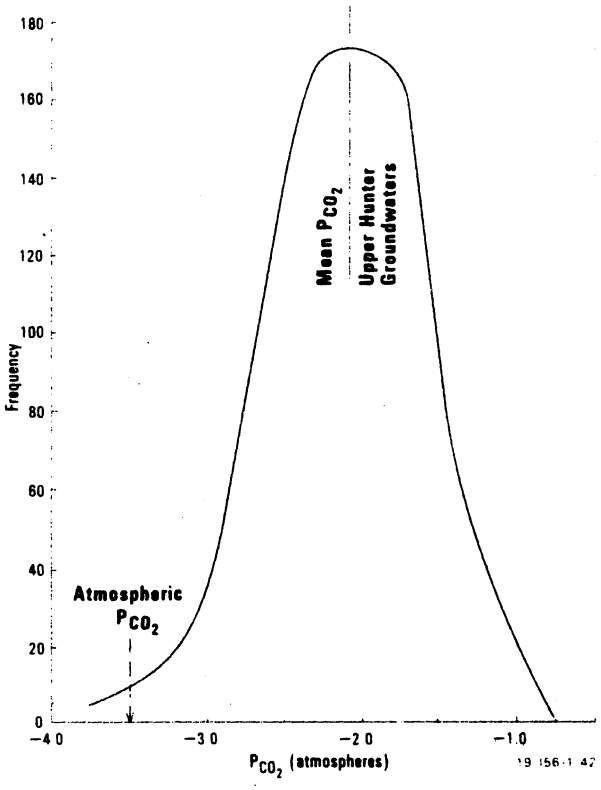

Record 1987/23

FIG 31. Distribution of carbon dioxide partial pressures in upper Hunter Valley groundwaters

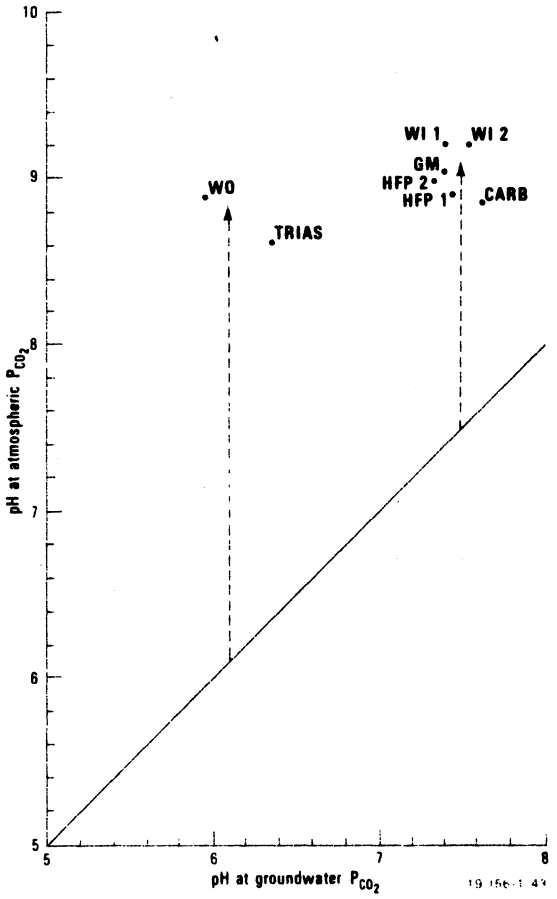

Record 1987/23

FIG 32. The effect on groundwater pH upon reaching equilibrium with atmospheric carbon dioxide

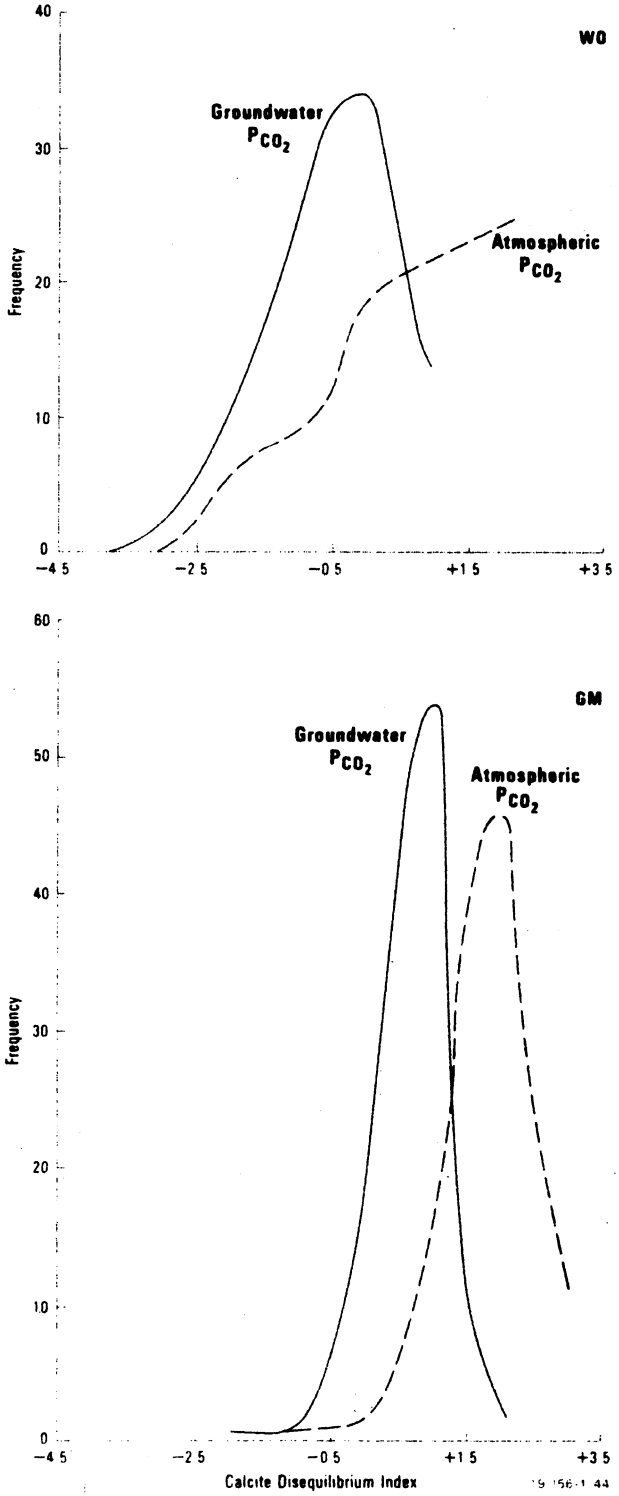

Record 1987/23

FIG 33a) The effect on calcite Disequilibrium Index values for WO and 33b) GM groundwaters upon reaching equilibrium with atmospheric carbon dioxide

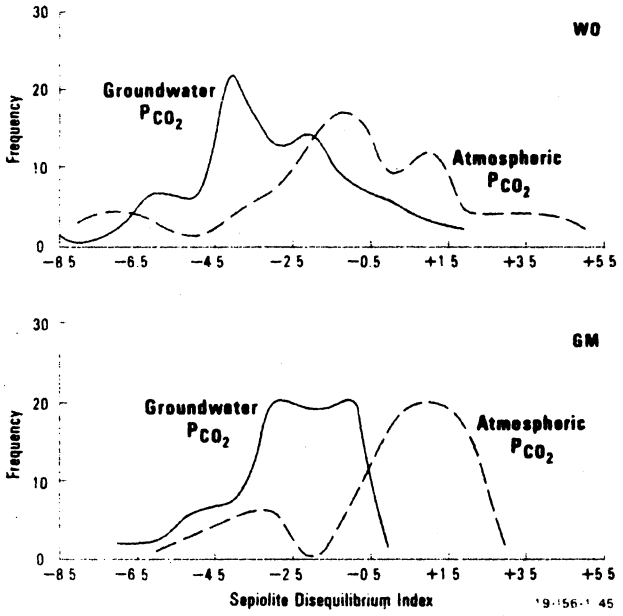

Record 1987/23

FIG 33c) The effect of sepiolite Disequilibrium Index values for WO
33b) and GM groundwaters upon reaching equilibrium with atmospheric carbon dioxide

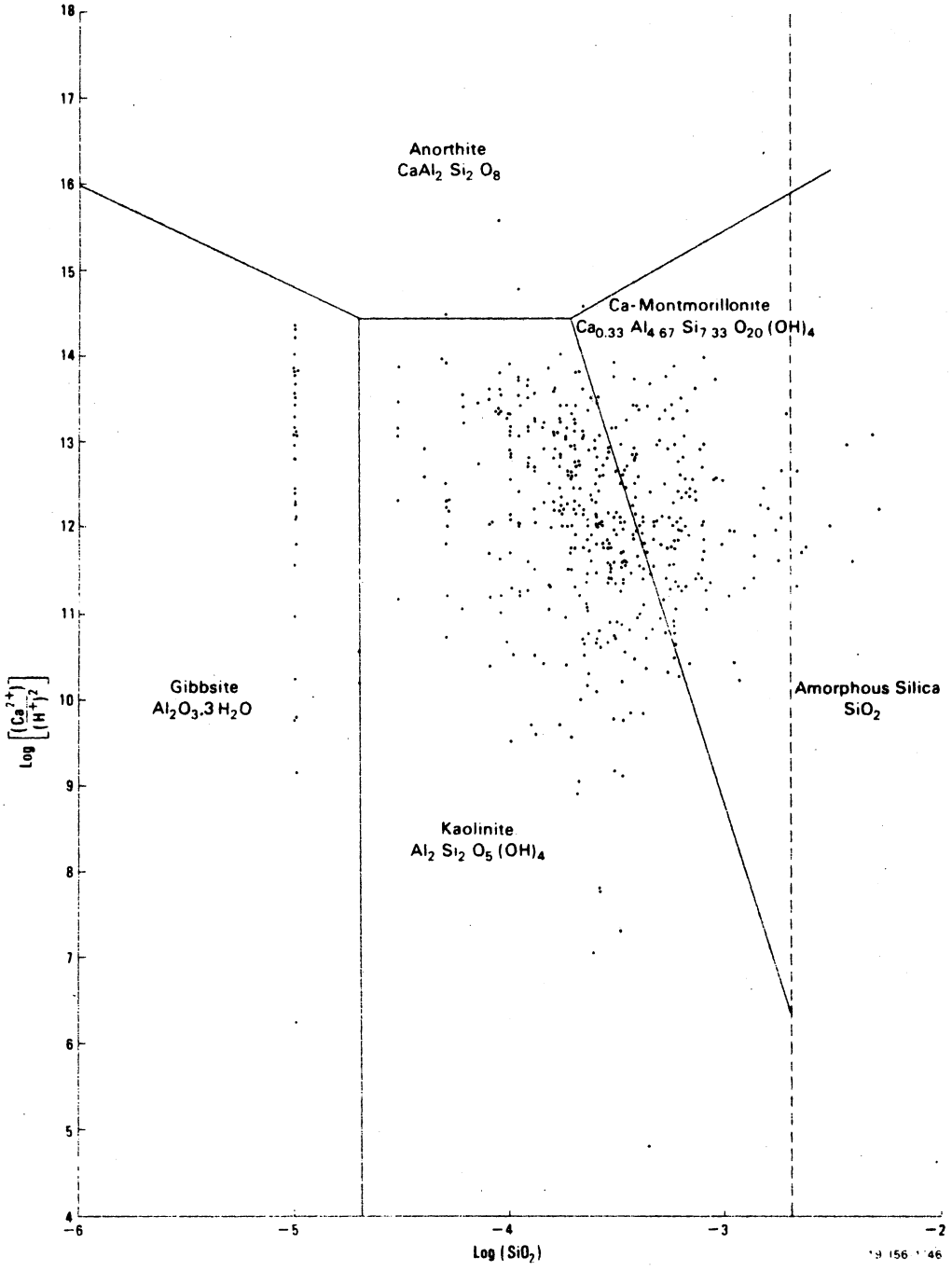

Record 1987/23

FIG 34. Stability fields of some minerals in the Ca-Al-Si-H_2O system at 25°C as a function of Ca^{2+}, H^+ and soluble SiO_2. Points are from the upper Hunter Valley groundwaters and boundaries are from thermodynamic data of Stumm and Morgan (1970).

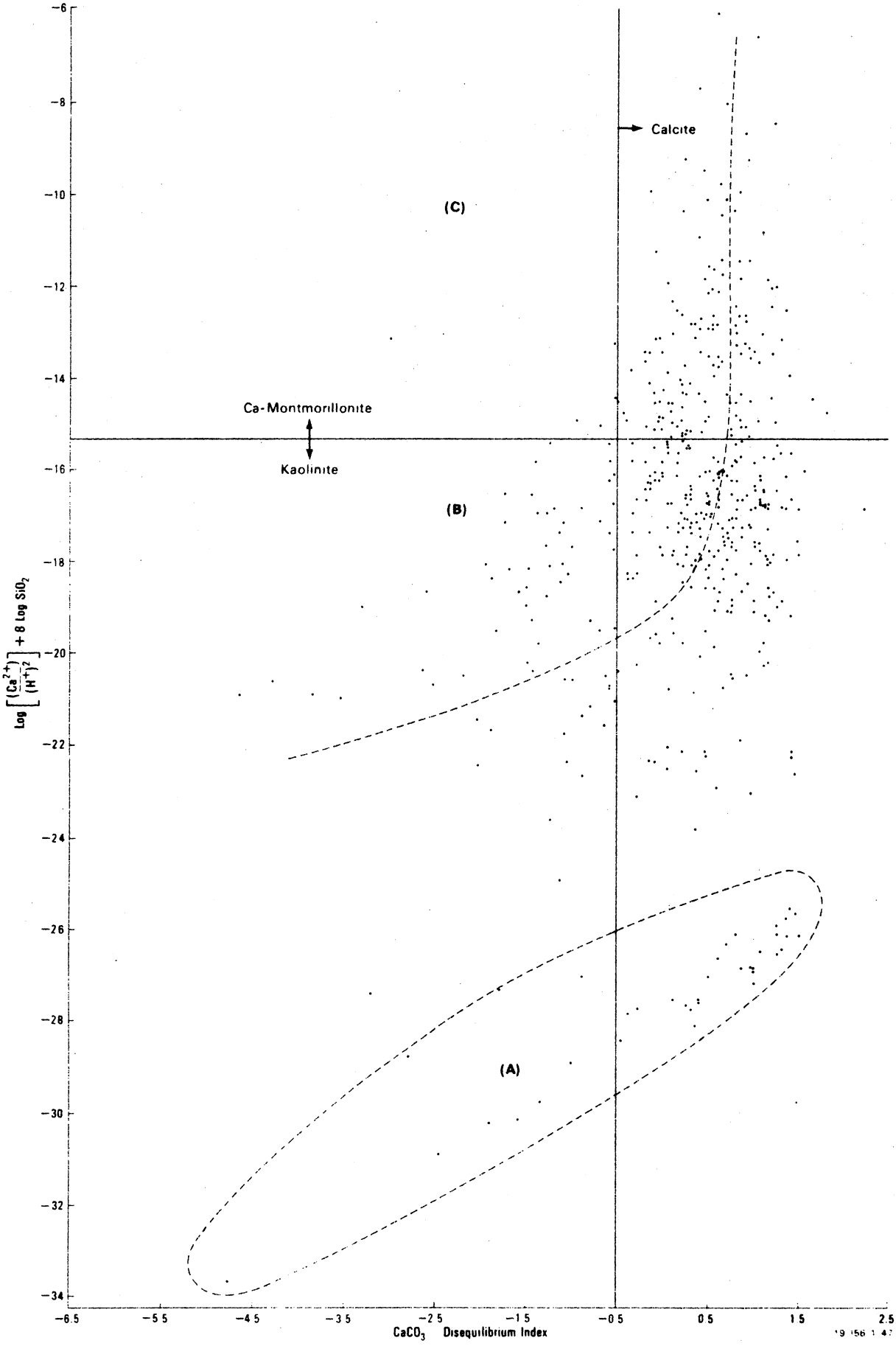

Record 1987/23

FIG 35. The relationship between the calcite Disequilibrium Index and the tendency for Ca-montmorillonite to form a stable phase in the upper Hunter Valley groundwaters.

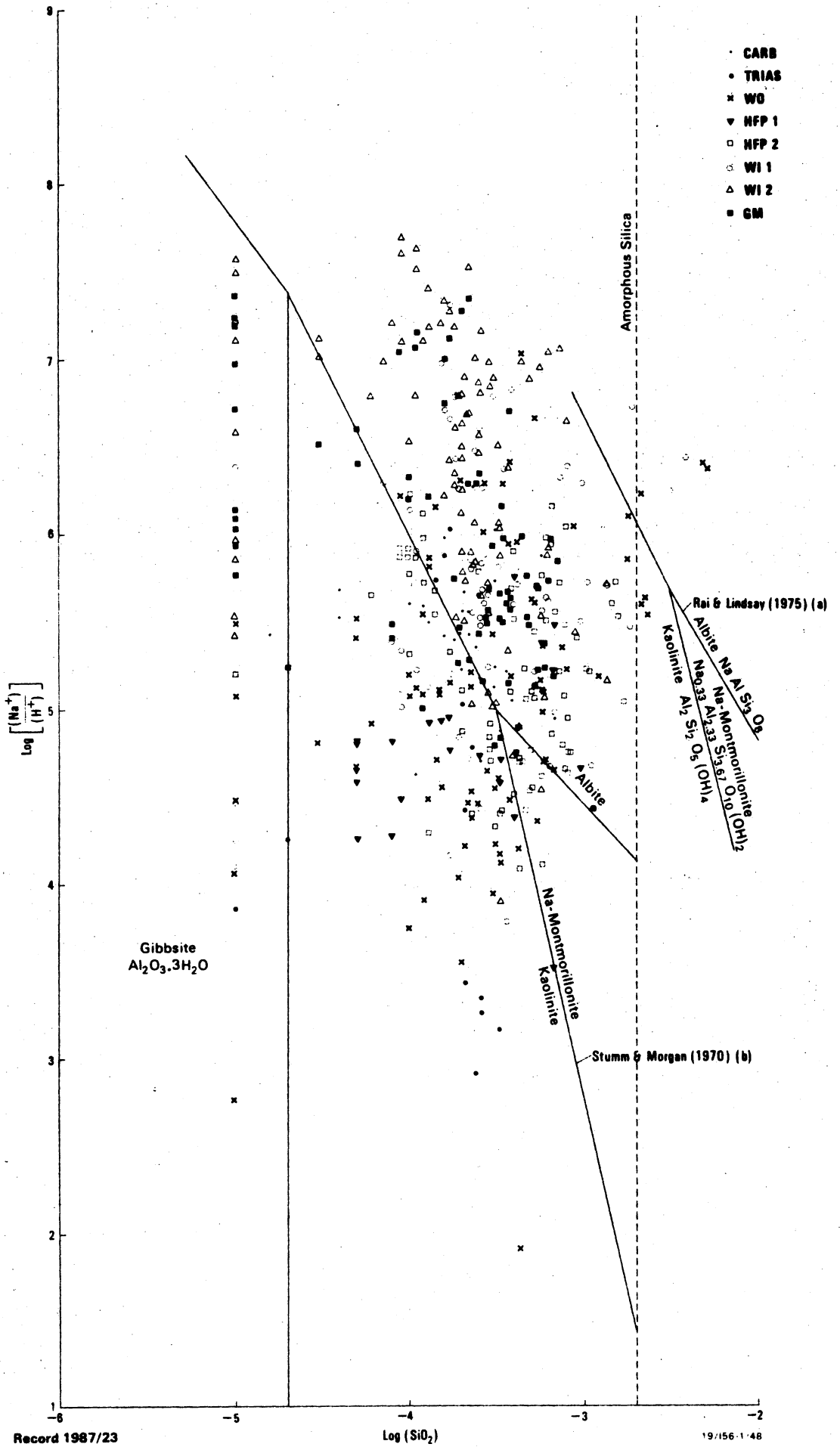

Record 1987/23

19/156-1-48

FIG 36. Stability fields of some minerals in the Na-Al-Si-H_2O system at 25°C as a function of Na^+, H^+ and soluble SiO_2. Points are from the upper Hunter Valley groundwaters and boundaries (a) from thermodynamic data of Rai and Lindsay (1975) and (b) Stumm and Morgan (1970)

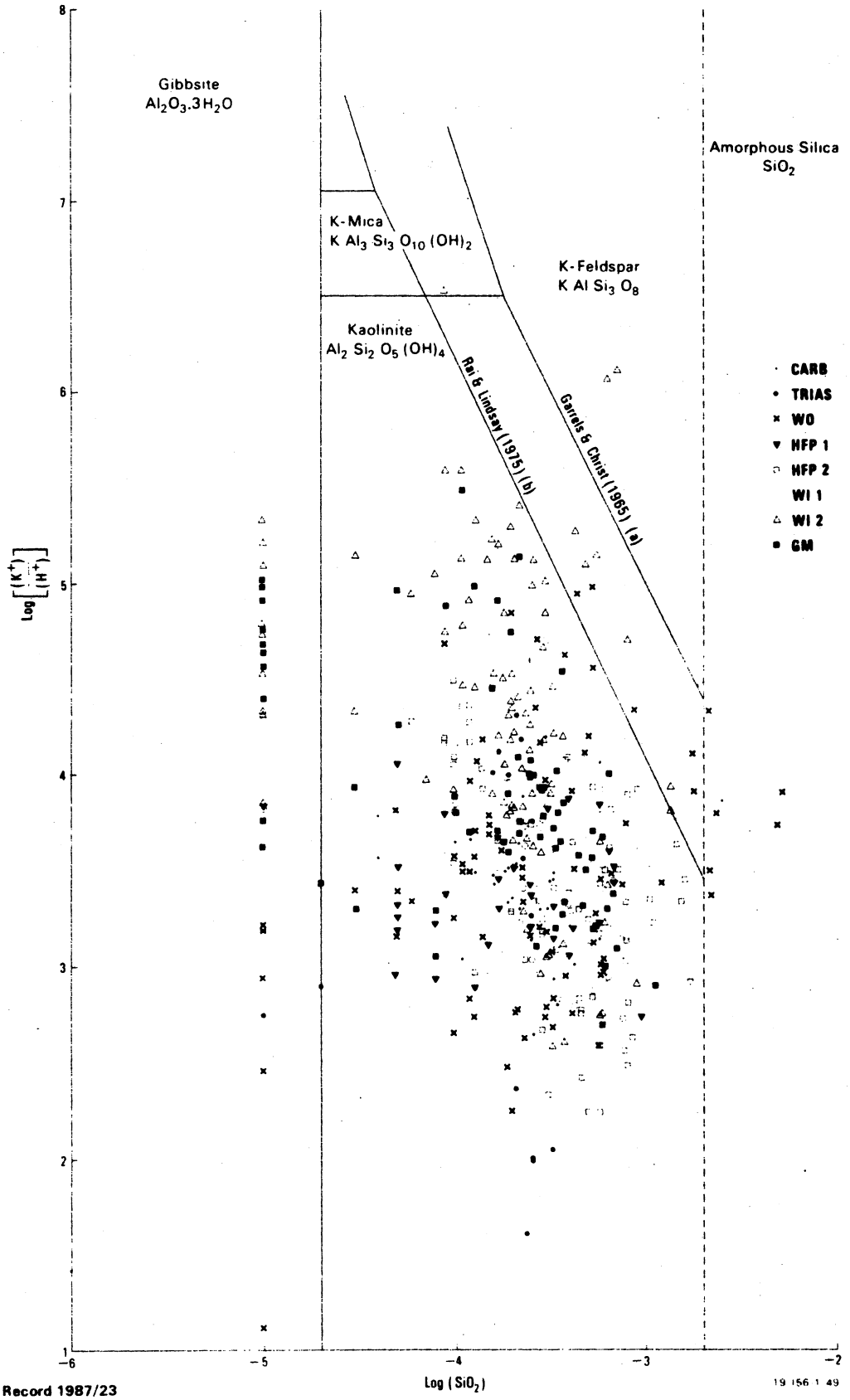

Record 1987/23

FIG 37. Stability fields of some minerals in the K-Al-Si-H_2O system at 25°C as a function of K^+, H^+ and soluble SiO_2. Points are from upper Hunter Valley groundwaters and boundaries (a) from thermodynamic data of Garrels and Christ (1965) and (b) from Rai and Lindsay (1975).

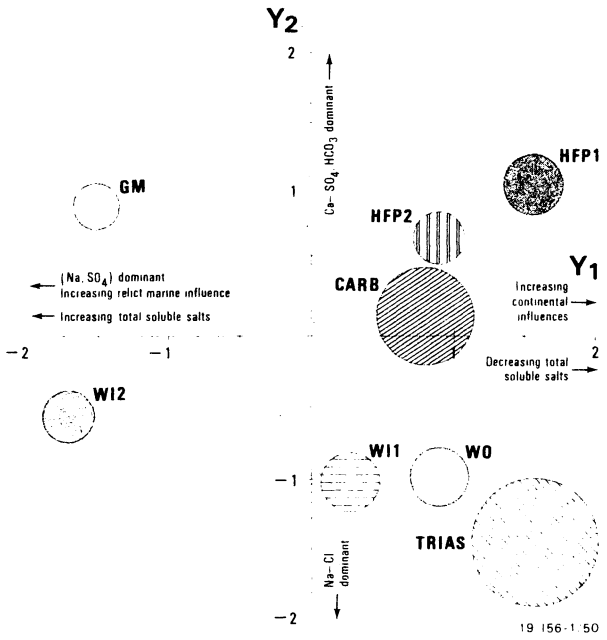

Record 1987/23

FIG 38. Canonical variate plot showing salinity and facies variations of upper Hunter Valley groundwaters. Based on six $\log_{10}$- transformed variables. Ninety-five per cent confidence circles shown

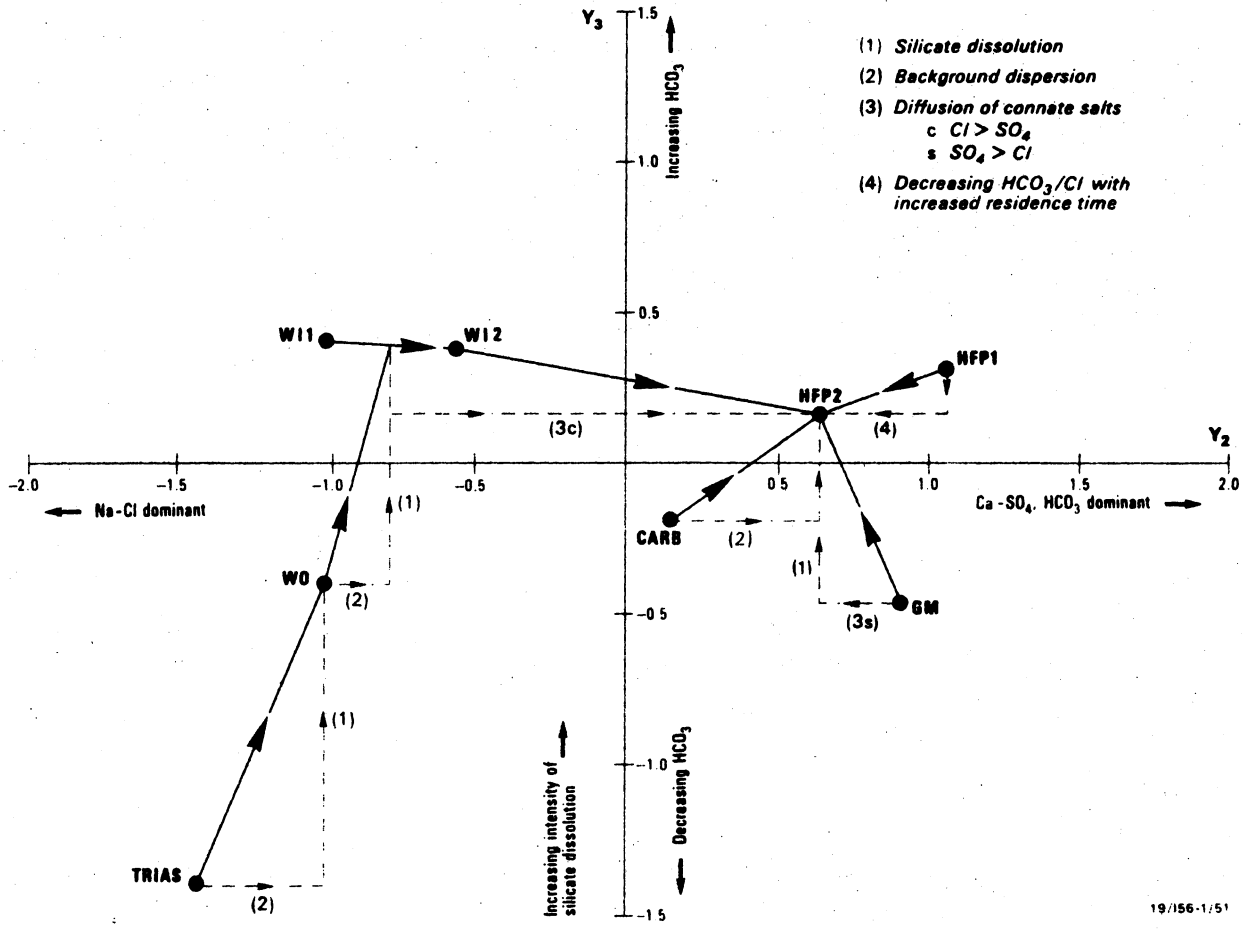

Record 1987/23

FIG 39. Canonical variate plot showing facies and silicate dissolution variations of upper Hunter Valley groundwaters. Based on 6 $\log_{10}$- transformed variables. Ninety-five per cent confidence circles shown

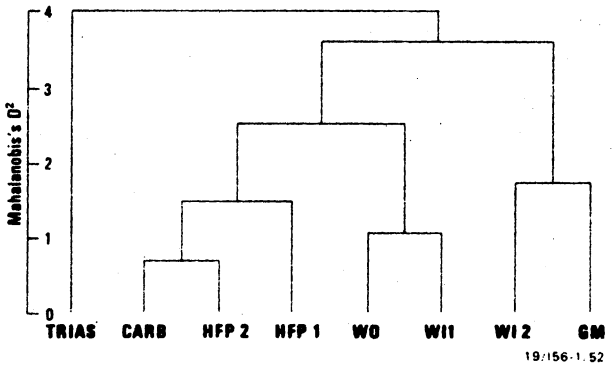

Record 1987/23

FIG 40. Complete linkage dendrogram of upper Hunter Valley hydrochemical provinces based on 6 $\log_{10}$- tranformed variables

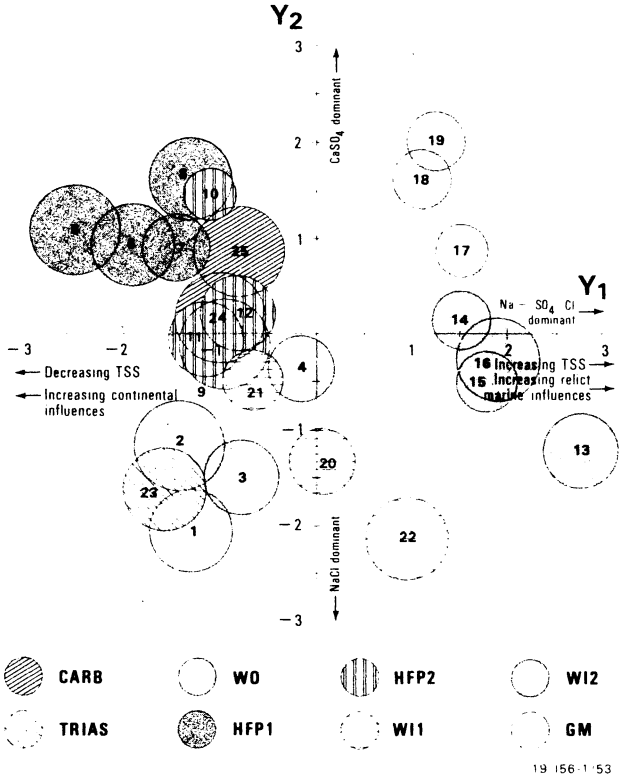

Record 1987/23

FIG 41. Canonical variate plot showing salinity and facies variations of 25 subgroups of upper Hunter Valley groundwaters. Based on 6 $\log_{10}$- transformed variables. Ninety-five per cent confidence circles shown.

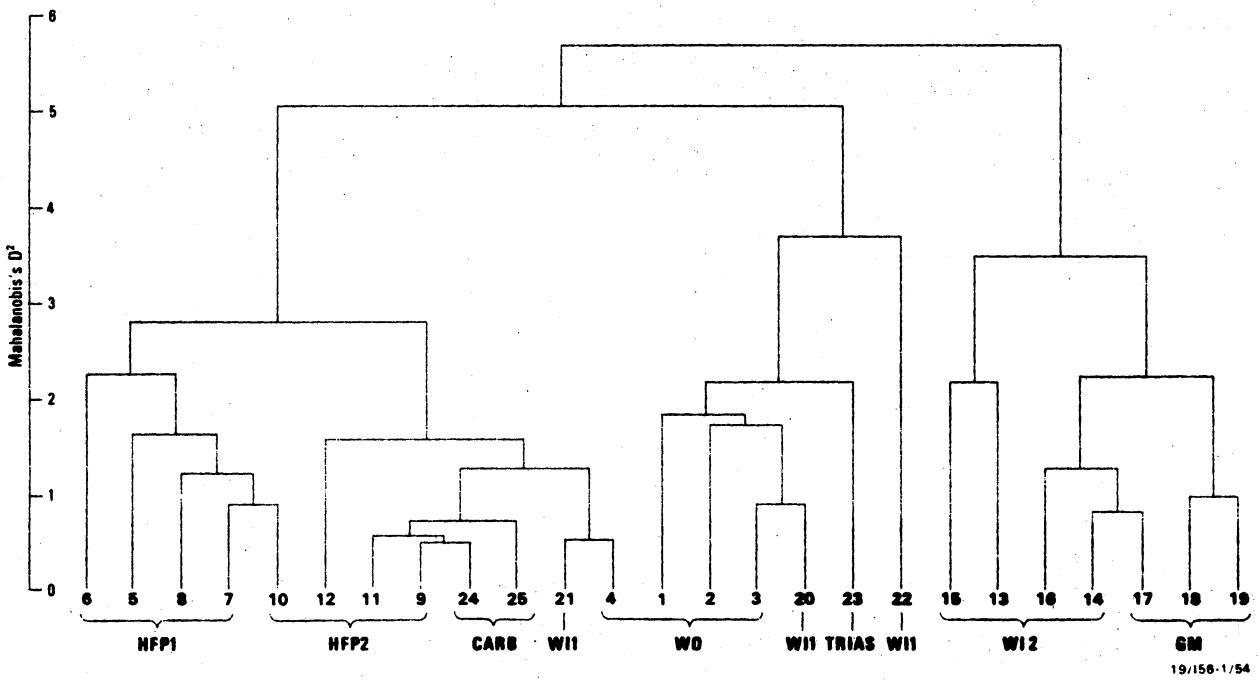

Record 1987/23

FIG 42. Complete linkage dendrogram of 25 subgroups of upper Hunter Valley groundwaters based on 6 $\log_{10}$- transformed variables

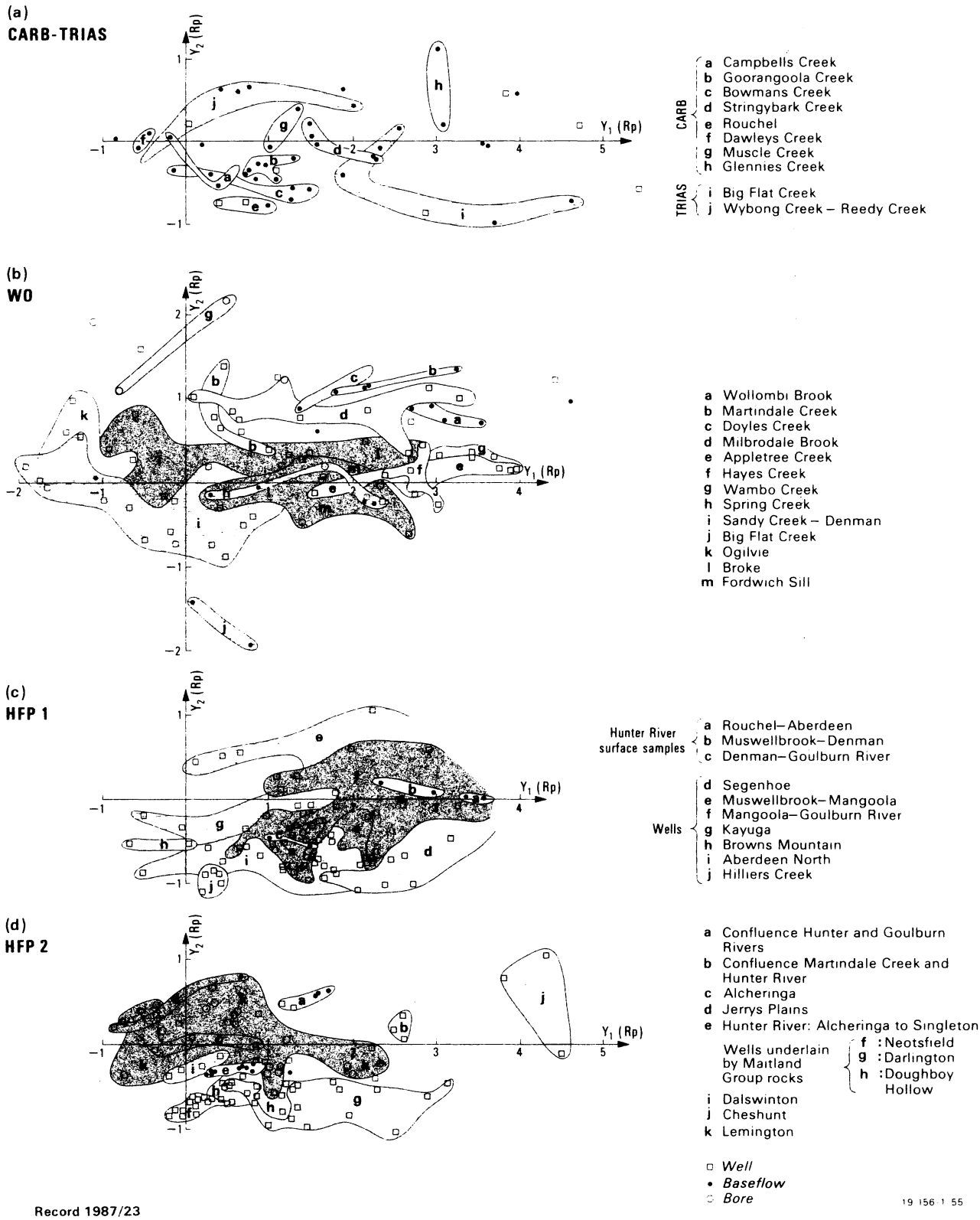

Record 1987/23

FIG 43a CARB-TRIAS)
43b WO)
43c HFP1)
43d HFP2)

Clustering by principal component scores of salinity and facies variations for 670 individuals of upper Hunter Valley groundwaters. Based on 6 $\log_{10}$- transformed variables. Principal components from pooled correlation matrix

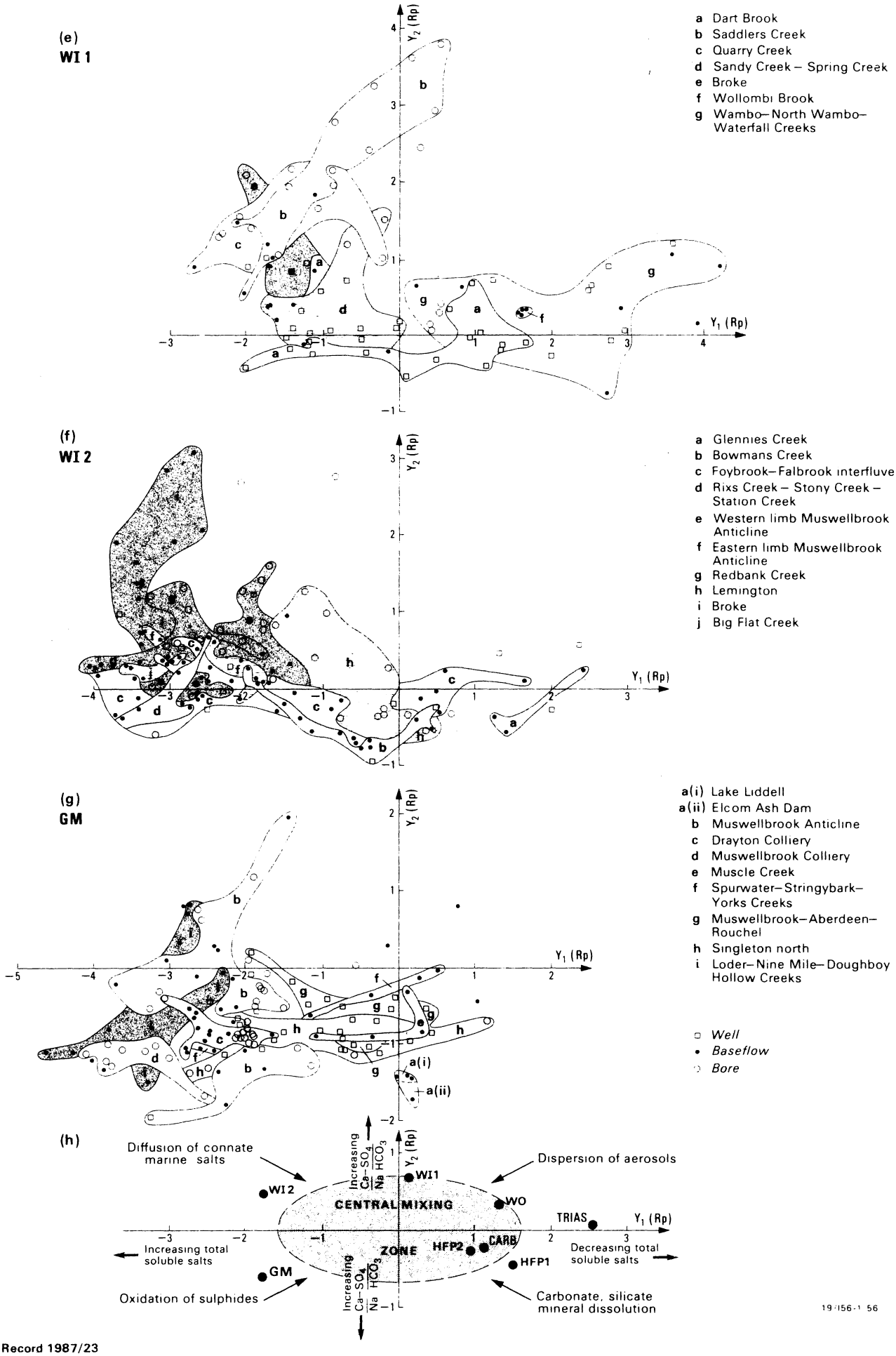

Record 1987/23

FIG 43e WI1) Clustering by principal component scores of salinity and facies
43f WI2) variations for 670 individuals of upper Hunter Valley ground-
43g GM) waters. Based on 6 $\log_{10}$ transformed variables. Principal components from pooled correlation matrix

43h Hydrochemical processes represented by principal component scores. Mean scores of hydrochemical provinces shown.

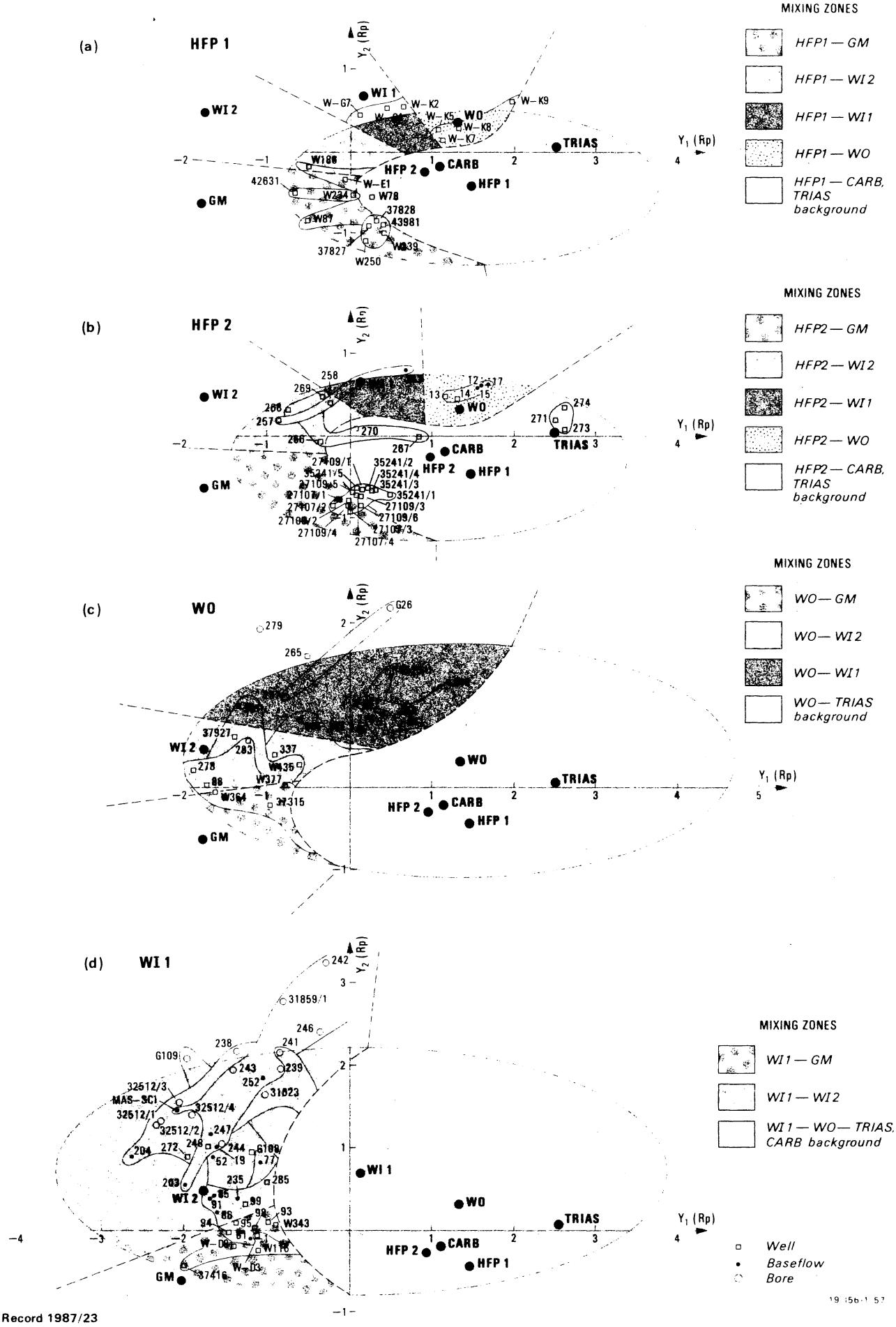

Record 1987/23

FIG 44a HFP1) Discrimination of zones of hydrodynamic mixing of Upper Hunter
44b HFP2) Valley groundwaters by principal component scores. Based on
44c WO) 6 $\log_{10}$- transformed variables measured on 670 individuals.
44d WI1) Principal components from pooled correlation matrix. Mean scores of hydrochemical provinces shown

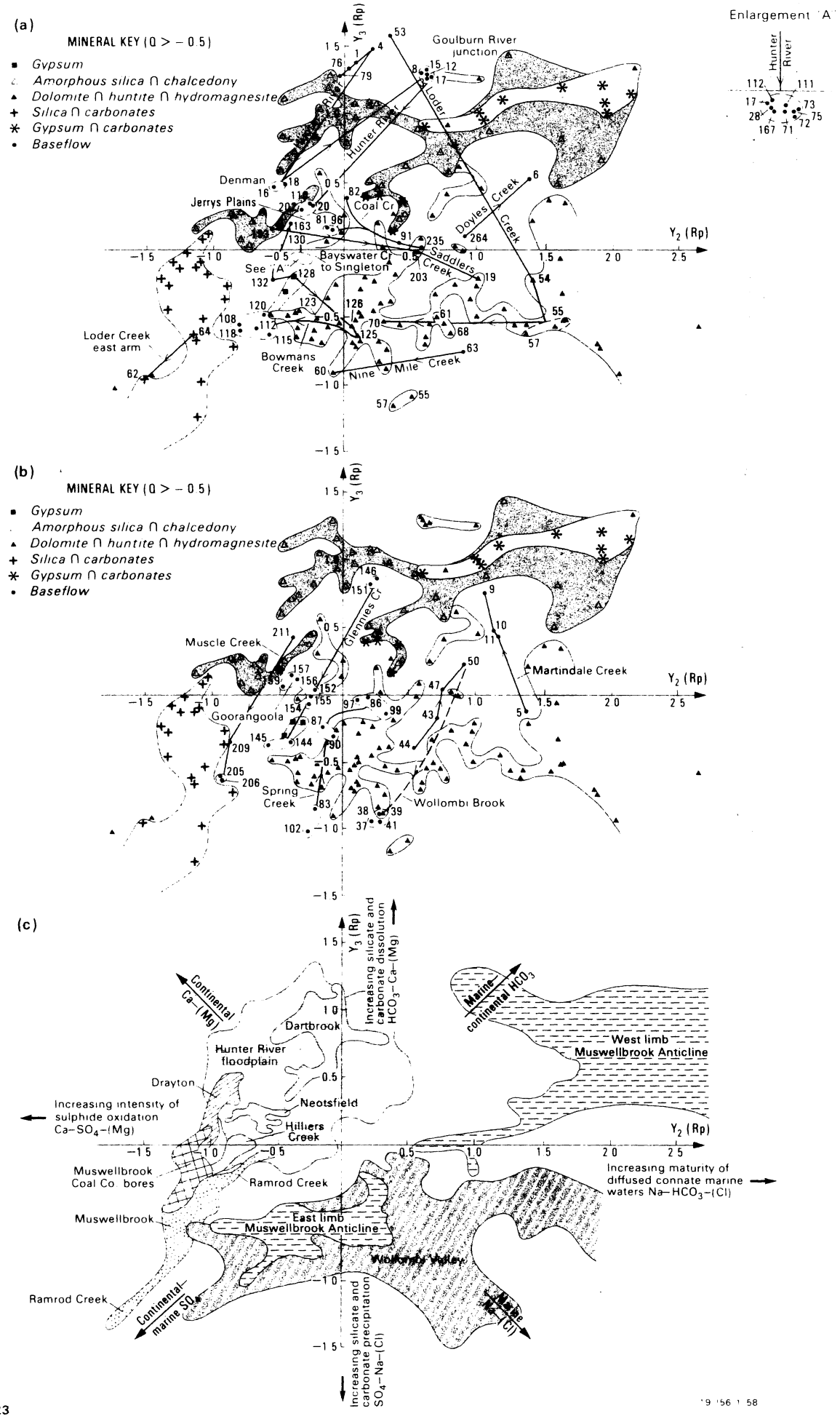

FIG 45a) Hydrochemical trends by principal component scores of baseflow waters in
45b) some upper Hunter Valley streams. Domains whose waters have reached or exceeded equilibrium with respect to certain minerals shown

FIG 45c Clustering by second and third principal component scores of facies variations for 670 samples of upper Hunter Valley groundwaters. Clusters enclose at least 80% of scores for the hydrochemical subgroup shown

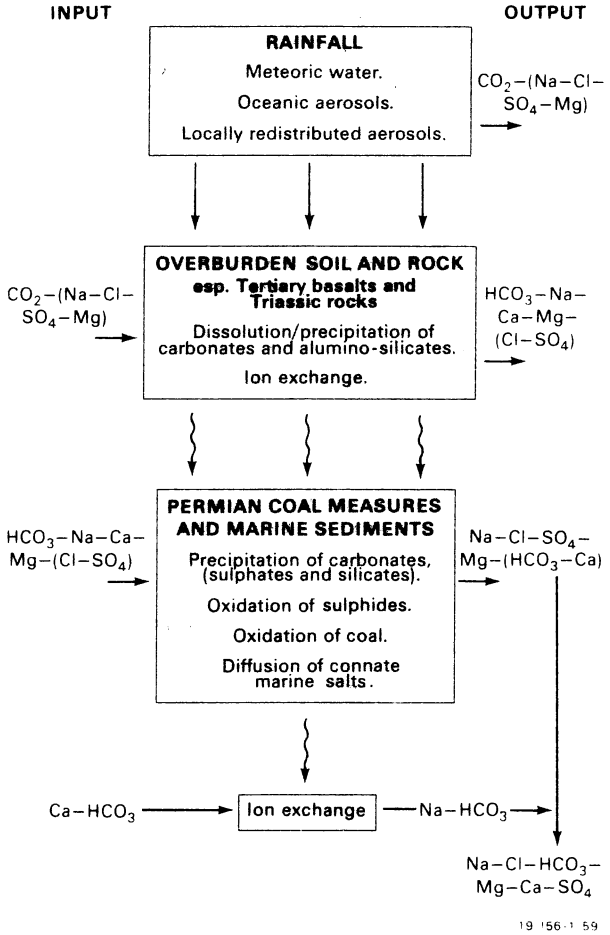

Record 1987/23

FIG 46. Sources of major ions in groundwaters of the upper Hunter River valley

Plate 1

GEOLOGY OF THE UPPER HUNTER RIVER VALLEY

NEW SOUTH WALES

SCALE 1:100000

1 0 1 2 3 4 5 6 7 8 9 10 Kilometres

Transverse Mercator Projection

Published by the Bureau of Mineral Resources, Geology and Geophysics, Department of Resources and Energy.
Base map compiled by the Bureau of Mineral Resources, from 1:25 000 scale maps supplied by the Central Mapping Authority

Geology after Rasmus P.L., Rose D.M. and Rose G. 1969 — Singleton 1:250 000 geological series, SI 56-1 (first edition), NSW Department of Mines, Sydney. Reproduced with permission of the Director, NSW Geological Survey
Compiled 1982-1984 by J.R. Kellett, BMR;
B.G. Williams, J.K. Ward, CSIRO
Cartography by A.J. Retter, P.J. Corbett, J.A. Gallagher
Printed by Mercury-Walch, Hobart, Australia

INDEX TO 1:100 000 MAPS
1:250 000 maps shown in grey

CURLEWIS 8935	TAMWORTH 9035	NUNDLE 9135	YARROWITCH 9235	COWARRAL HASTINGS 9335	KEMPSEY 9435	COROGORO POINT 9535
BLACKVILLE 8934	MURRU-RUNDI SH 56-13 9034	ELLERSTON 9134	UPPER MANNING 9234	WINGHAM SH 56-14 9334	CAMDEN HAVEN 9434	
MERRIWA 8933	MUSWELLBROOK SINGLETON 9033	CAMBERWELL 9133	DUNGOG 9233	BULAHDELAH NEWCASTLE 9333		
MOUNT POMINY 8932	HOWES VALLEY SI 56-1 9032	CESSNOCK 9132	NEWCASTLE 9232	SI 56-2 PORT STEPHENS 9332		
WALLERAWANG 8931	ST ALBANS SYDNEY 9031	GOSFORD 9131	LAKE MACQUARIE 9231			
KATOOMBA 8930	PENRITH SI 56-5 9030	SYDNEY 9130				

MAP LOCALITY

QUATERNARY		Qa	Gravel, sand, silt, clay
TERTIARY		Tv	Olivine basalt, dolerite sills
EARLY TRIASSIC	NARRABEEN GROUP	Rn	Sandstone, shale, fanglomerate
LATE PERMIAN	SINGLETON SUPERGROUP — WOLLOMBI COAL MEASURES	Psl	Conglomerate, sandstone, tuff, claystone, coal seams
	SINGLETON SUPERGROUP — WITTINGHAM COAL MEASURES	Psw	Shale, sandstone, siltstone, conglomerate, coal seams
	MAITLAND GROUP — Mulbring Siltstone	Pmm	Siltstone, shale, sandstone
	MAITLAND GROUP — Muree Sandstone	Pmms	Sandstone and conglomerate
	MAITLAND GROUP — Branxton Formation	Pmb	Sandstone, conglomerate, siltstone
EARLY PERMIAN	GRETA COAL MEASURES	Pg	Sandstone, siltstone, shale, coal seams, rhyolite
	DALWOOD GROUP	Pd	Breccia, basalt, shale, mudstone
CARBONIFEROUS	Undifferentiated	Cu	Tuff, conglomerate, tillite, varved shale
	Gilmore Volcanics	Clg	Tuff, conglomerate, sandstone
	Wallaringa Formation	Clwa	Conglomerate, tuff, sandstone

- Geological boundary
- Fault
- Thrust-fault, triangle on upthrow side, indicates direction of dip
- Anticline
- Syncline
- Monocline

Where location of boundaries, faults and folds is approximate, line is broken; where inferred, queried; where concealed, boundaries and folds are dotted, faults are shown by short dashes

- Road
- Built-up area
- Extent of open cut mine
- Open cut mine
- Dam wall
- 200 — Contour with value; 50 metre contour interval

Plate 2

HYDROCHEMICAL PROVINCES AND SAMPLING LOCATIONS OF THE UPPER HUNTER RIVER VALLEY

NEW SOUTH WALES

SCALE 1:100000

1 0 1 2 3 4 5 6 7 8 9 10 Kilometres

Transverse Mercator Projection

Published by the Bureau of Mineral Resources, Geology and Geophysics, Department of Resources and Energy.
Base map compiled by the Bureau of Mineral Resources, from 1:25 000 scale maps supplied by the Central Mapping Authority.

Hydrogeochemistry August 1982 by J.R. Kellett, BMR; B.G. Williams, J.K. Ward, CSIRO
Compiled 1982-1984 by J.R. Kellett, B.G. Williams, J.K. Ward
Cartography by A.J. Retter, P.J. Corbett, J.A. Gallagher
Printed by Mercury-Walch, Hobart, Australia

INDEX TO 1:100 000 MAPS
1:250 000 maps shown in grey

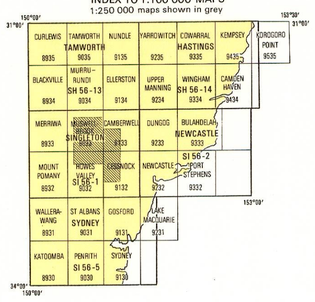

MAP LOCALITY

HYDROCHEMICAL PROVINCES

- **HFP 1** — *Alluvium of the upper section of the Hunter River floodplain between the Glenbawn Dam in the north and the Goulburn River confluence*
- **HFP 2** — *Alluvium of the lower part of the Hunter River floodplain between the Goulburn River confluence and Singleton*
- **CARB** — *Carboniferous volcaniclastics and glacigene sediments of the southern New England Fold Belt*
- **TRIAS** — *Early Triassic conglomerates, sandstones, and shales, overlain in places by Tertiary basalts*
- **WO** — *Interbedded coal seams and continental sediments of the Wollombi Coal Measures*
- **WI 1** — *Upper Wittingham Coal Measures west of the Muswellbrook Anticline in the north, and proximal to the Triassic escarpment in the south*
- **WI 2** — *Lower Wittingham Coal Measures west of the Muswellbrook Anticline in the north, and between the anticline and the Maitland Group rocks in the south*
- **GM** — *Interbedded coal seams and continental sediments of the Greta Coal Measures and marine sediments of the Maitland and Dalwood Groups*

Hydrochemical province boundary
Fault
Road
Built-up area
Extent of open cut mine
Open cut mine
Dam wall
200 *Contour with value; 50 metre contour interval*

SAMPLE SITES

- ○ *Surface (includes bed underflow)*
- □ *Well in alluvium*
- ◕ *Fractured rock bore*
- ● *Probe (Williamson, 1958)*
- ⌇ *Spring*

Sample number

Numbers **1** to **340** sampled and analysed by BMR and CSIRO

Five digit numbers are from boremaster data base of NSW Water Resources Commission

The prefix "**G**" denotes analyses from GRIFFIN, R.J., 1960 — The groundwater resources of the Wollombi Brook catchment area. NSW Department of Mines Technical Report 8

The prefix "**W**" denotes analyses from WILLIAMSON, W.H., 1958 — Groundwater resources of the Upper Hunter Valley NSW NSW Government Printer, Sydney

Several leading alphabetical characters denote data from the following Environmental Impact Statements:
MAN — Mount Arthur North (Sinclair Knight, 1981)
MAS — Mount Arthur South (Sinclair Knight, 1982)
DR — Drayton (Dames and Moore, 1980)
GL — Glendell (1982)
BLH — Black Hill (Mount Sugarloaf), (Sinclair Knight, 1983)
BBC — Buchanan Lemington (Dames and Moore, 1982)
UC — United (Warkworth), (Dames and Moore, 1981)